THE ROLE OF BIOACTIVE LIPIDS IN PAIN AND INFLAMMATION

Amy Wong, MPharm.

Thesis submitted to the University of Nottingham
for the degree of Doctor of Philosophy

April 2012

Abstract

Bioactive lipids or lipids that activate specific signalling pathways are involved in the regulation and maintenance of normal bodily functions. Furthermore, bioactive lipid targets have been implicated in a number of conditions such as cancer, asthma and arthritis, all of which contain an inflammatory element. Additionally, a number of bioactive lipids are also known to target several different types of receptors. These include the cannabinoid receptors, peroxisome proliferator activated receptor alpha (PPARα) and transient receptor potential vanilloid-1 (TRPV1) ion channels. The assessment of bioactive lipid levels in biological systems is important for understanding their role in cell function and pathological events.

The aims of this thesis were to develop an analytical method that allows the simultaneous identification and measurement of lipid mediators involved in inflammatory responses, including cyclooxygenase, lipoxygenase and cytochrome P450 metabolites, along with the endocannabinoids to determine the role of bioactive lipids in models of acute and chronic inflammatory pain.

A validated liquid chromatography tandem mass spectrometry (LC-MS/MS) method that allows the simultaneous identification and measurement of 42 bioactive lipids was developed, capable of measuring COX metabolites; PGD_2/PGE_2, TXB_2, LOX metabolites; 5-, 12-, 15-HETE, HODEs, oxoODEs, CYP metabolites; 8- and 11-HETE, EETs and the endocannabinoids; AEA and 2-AG and endocannabinoid-like compounds PEA and OEA. Levels of these analytes were quantified in rat hindpaw, dorsal root ganglia, knee joint, plasma, spinal cord and brain. This LC-MS/MS method was then used to investigate how levels of these bioactive lipids were altered in inflammation and pain.

Experiments in this thesis using a PPARα competitive binding assay showed that 8-HETE and PEA bind to PPARα, along with other lipids such as fatty acids and EETs. Levels of PPARα ligands were altered in the carrageenan model of inflammatory pain, suggesting that changes in

bioactive lipid metabolism may influence the contribution of PPARα in inflammatory pain states. Additionally, in the same model of inflammatory pain, levels of TRPV1 ligands were altered, supporting the known role of TRPV1 in inflammatory pain states. Inhibition of 15-lipoxygenase or blockade of the metabolites resulted in attenuation of hyperalgesia, which was supported by alterations in bioactive lipid levels *in vitro* but not *in vivo*. The role of bioactive lipids in a rat model of osteoarthritis was also investigated. Levels of TRPV1 ligands were altered in this model of osteoarthritis, accompanied by the time-dependent development of pain behaviour, supporting a contribution of TRPV1 to OA-induced pain.

In conclusion, the development of a novel LC-MS/MS analytical method capable of measuring a large number of bioactive lipids *in vitro* and *in vivo*, have provided novel findings to support the involvement of these lipids in inflammation and pain. Overall, these data provide evidence for the involvement of PPARα and TRPV1 ligands in inflammatory pain states.

Publications

SAGAR, D. R., GAW, A. G., OKINE, B. N., WOODHAMS, S. G., WONG, A., KENDALL, D. A. & CHAPMAN, V. 2009. Dynamic regulation of the endocannabinoid system: implications for analgesia. *Molecular Pain,* **5**, 59.

Declaration

All of the experiments and analysis detailed within this thesis were carried out by myself, unless otherwise stated. Initial method development was aided by Dr Catharine Ortori. Other collaborators are acknowledged in appropriate chapters.

Acknowledgements

I would firstly like to thank my supervisors Professor David Barrett, Professor Victoria Chapman and Professor David Kendall for the support and guidance throughout the PhD. I would also like to thank Dr Andrew Bennett for the support and guidance in the PPARα assays. I would like to thank Cath for her help throughout method development, we got there in the end! I would also like to thank everyone in CAB and Chapman groups for all their help, particularly James and Devi for supervision and support. I would like to thank Paul Millns for helping with numerous hours of tissue collection. Most of all, I would like to thank my family and my husband-to-be, Josh for all the love and support you have given me over the years, I could not have achieved this without you! I really appreciate the encouragement, middle-of-the-night lab trips and good food, it's been an emotional roller coaster! Finally, I would like to thank the BBSRC and the University of Nottingham for my funding.

Abbreviations

2-(14,15-EET)-G	2-(14,15-epoxyeicosatrienoyl) glycerol
2-AG	2-arachidonoyl glycerol
5-HT	5-hydroxytryptamine
5,6-EET-EA	5,6-epoxyeicosatrienoyl-ethanolamide
AA	Arachidonic acid
AEA	N-arachidonoyl ethanolamide
anti-GST	Anti-glutathione-s-transferase
APC	Allophycocyanin
APCI	Atmospheric pressure chemical ionisation
AraGly	N-arachidonoyl glycine
BDNF	Brain derived neurotrophic factor
cAMP	Cyclic adenosine monophosphate
CB	Cannabinoid receptor
CFA	Complete Freund's adjuvant
CGRP	Calcitonin gene-related peptide
CNS	Central nervous system
COX	Cyclooxygenase
CYP	Cytochrome P450 epoxygenase
DAGLα	Diacylglycerol lipase-alpha
DHET	Dihydroxyeicosatrienoic acid
DMSO	Dimethyl sulfoxide
DNA	Deoxyribonucleic acid
DRG	Dorsal root ganglia
DTT	Dithiothreitol
EET	Epoxyeicosatrienoic acid
ESI	Electrospray ionisation
FAAH	Fatty acid amide hydrolase
FLAP	5-lipoxygenase activating protein
fMRI	Functional magnetic resonance imaging

GABA	Gamma-aminobutyric acid
GC-MS	Gas chromatography mass spectrometry
GI	Gastrointestinal
GIRK	G-protein sensitive inward rectifying potassium
HETE	Hydroxyeicosatetraenoic acid
HODE	Hydroxyoctadecadienoic acid
HPETE	Hydroperoxyeicosatetraenoic acid
HPLC	High performance liquid chromatography
ICAM-1	Intercellular adhesion molecule-1
IFN-γ	Interferon-gamma
IκB-α	I kappa B-alpha
IL	Interleukin
iNOS	Inducible nitric oxide synthase
LA	Linoleic acid
LBD	Ligand binding domain
LC-MS/MS	Liquid chomatography tandem mass spectrometry
LOD	Limit of detection
LOQ	Limit of quantification
LOX	Lipoxygenase
LT	Leukotriene
LTD	Long-term synaptic depression
MAGL	Monoacyl glycerol lipase
MIA	Monoiodoacetate
MRM	Multiple reaction monitoring
mRNA	Messenger ribonucleic acid
NADA	N-arachidonoyl-dopamine
NAEs	N-acyl ethanolamines
NAPE-PLD	N-acyl phosphatidylethanolamine phospholipase D
NF-κB	Nuclear factor-kappa-B
NGF	Nerve growth factor
NMDA	N-methyl-D-aspartate

NSAIDs	Non-steroidal anti-inflammatory drugs
OA	Osteoarthritis
OEA	N-oleoyl ethanolamide
OxoODE	Oxooctadecadienoic acid
PAF	Platelet activating factor
PAG	Periaqueductal grey
PCA	Principal component analysis
PEA	N-palmitoyl ethanolamide
PG	Prostaglandin
PKA	Protein kinase A
PKC	Protein kinase C
PLA_2	Phospholipase A_2
PO	Post-operative
PPARα	Peroxisome proliferator activated receptor-alpha
QST	Quantitative sensory testing
RVM	Rostral ventromedial medulla
RXR	9-*cis* retinoid X receptor
SPE	Solid phase extraction
THC	Δ9-tetrahydrocannabinol
TNF-α	Tumour necrosis factor-α
TR-FRET	Time-resolved fluorescence resonance energy transfer
TRPV1	Transient receptor potential vanilloid-1
TX	Thromboxane
VCAM-1	Vascular cell adhesion molecule-1
WT	Wild-type

TABLE OF CONTENTS

Chapter 1.

General Introduction

1. General Introduction

1.1 Inflammation

Inflammation is a term used to describe a series of responses of vascularised tissues of the body to injury (Ratnoff 1971, Larsen and Henson 1983). The regulation of inflammation is a highly complex biological process that involves many receptors, cells and molecules and the specific importance of lipid molecules is widely recognised. The release of inflammatory mediators changes in response to tissue injury or insult, and is mediated by distinct mechanisms such as vasodilatation, increased capillary permeability and infiltration of immune cells (Chopade and Mulla 2010). Macrophages, neutrophils and dendritic cells are the main sources of eicosanoids, which target local receptors. These regulate cytokine production, cell proliferation and migration, antibody formation and other components of the inflammatory process (Harizi et al 2008, Mbvundula et al 2004). Persistent immune activation can result in chronic inflammation, which has pathological consequences.

1.1.1 Acute inflammatory response

Inflammation is characterised by the movement of serum proteins and inflammatory cells from the blood to the extravascular tissue, which is regulated by the sequential release of vasoactive and chemotactic mediators that contribute to the cardinal signs of inflammation, i.e. heat, redness, swelling, pain and loss of function (Lawrence et al 2002)(Figure 1).

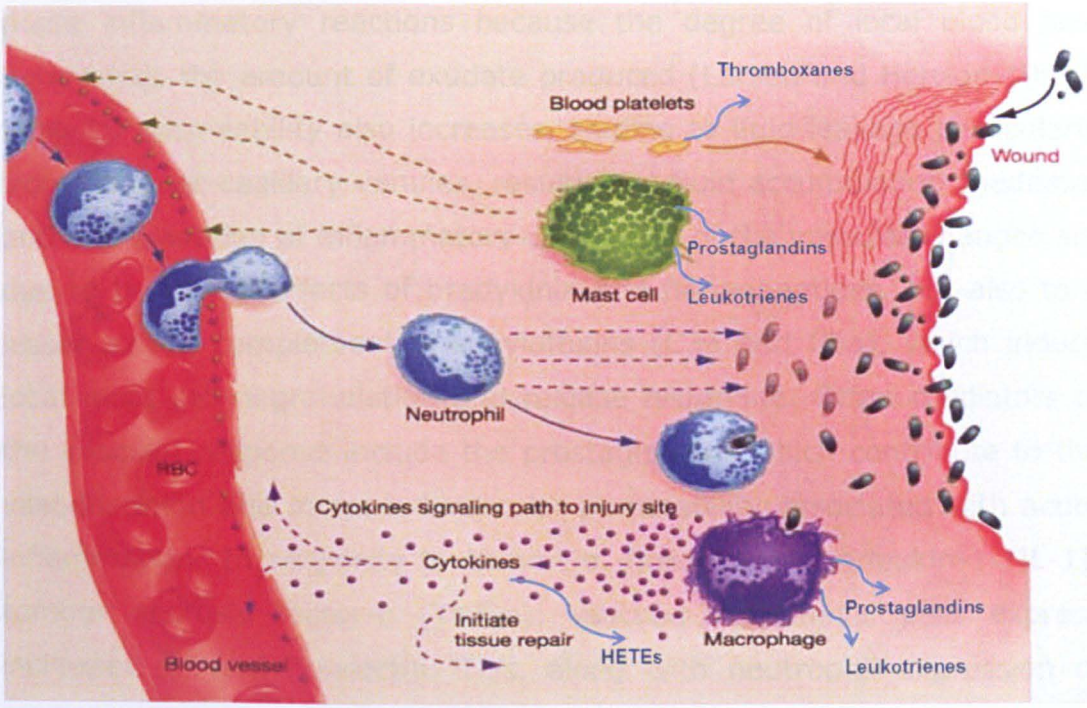

Figure 1. Inflammation is an important biological process, where the body initiates a protective response following injury through physical damage or infection. This image illustrates the fundamental elements of this process. When an injury occurs, neutrophils, mast cells and macrophages are recruited to the site of injury, releasing inflammatory mediators. Eicosanoids such as prostaglandins, leukotrienes and thromboxanes are released to facilitate this process as are HETEs or hydroxyeicosatetraenoic acids, which are released through the action of cytokines. Overall, inflammation is a highly complex process that involves many bioactive lipids *(Modified version of an image taken from www.wdict.net)*.

Increased vascular diameter, increased flow and permeability are key elements in inflammation, which allow the maximum opportunity for recruitment of inflammatory cells and plasma proteins to the site of injury. This results in initiation or perpetuation of the response, followed ultimately by resolution of the process (Ryan and Majno 1977, Wilhelm 1973).

1.1.2 Vascular events

Within minutes of tissue injury, there is an increase in vasodilatation resulting in an increase in the volume of blood in the area, accompanied by a reduction in the flow of blood. This increase in blood volume contributes to the heat and redness of the tissue. Vasodilatation is generally considered to be of central importance in the development of

acute inflammatory reactions because the degree of local blood flow determines the amount of exudate produced (Larsen and Henson 1983). Vascular permeability also increases, leading to fluid leakage particularly from the post-capillary venules, resulting in fluid accumulation (oedema) and extravasation of inflammatory cells. Most of the vascular changes are due to the direct effects of bradykinin and fibrinopeptides, but also to a lesser extent complement anaphylatoxins (C3a and C5a), which induce local mast cell degranulation and release histamine. Other mediators of the vascular response include the prostaglandins which contribute to the vasodilatation and increased vascular permeability associated with acute inflammation. In response to thrombin, histamine, interleukin-1 (IL-1), tumour necrosis factor-α (TNF-α), vascular endothelial cells express increased E- and P-selectin. This, along with neutrophil expression of mucins, enables neutrophil binding and attachment to the endothelium, allowing initiation of cellular events (Gabay and Kushner 1999).

1.1.3 Cellular events

In acute inflammation, the predominant infiltrating cell type is often the neutrophil, produced in the bone marrow. Within hours of the onset of vascular events, neutrophils adhere to endothelial cells and migrate out of the blood into the tissue (Figure 1), where infiltration usually peaks within the first 4 hours of an inflammatory response (Weksler and Coupal 1973). Neutrophils phagocytose invading pathogens and release macrophage inflammatory proteins and chemokines that attract macrophages to the site of inflammation (Figure 1). These mononuclear cells arrive after the first 4 hours following peak neutrophil infiltration, and reach a sustained peak around 18 to 24 hours (Weksler and Coupal 1973). Once activated, macrophages exhibit increased phagocytosis and release of cytokines and other mediators that contribute to the inflammatory response. These include IL-1, IL-6 and TNF-α, which act locally to increase vascular permeability, as described earlier. IL-1 also induces intercellular adhesion molecules (ICAM-1) and vascular cell adhesion molecule-1 (VCAM-1) expression, enabling binding to integrins on monocytes and lymphocytes and assisting in extravasation through

the vessel walls (Imhof and Aurrand-Lions 2004). IL-1 and TNF-α also activate macrophages and endothelial cells to produce chemokines, that contribute to the influx of inflammatory cells or chemotaxis. Additionally, TNF-α and interferon-γ (IFN-γ), activate macrophages and neutrophils to promote phagocytosis and lytic enzyme release. Cytokine release results in the influx of lymphocytes, neutrophils, monocytes, eosinophils, basophils and mast cells to the site of inflammation. Accumulation and activation of macrophages also induces a chronic inflammatory response. Cytokines, namely TNF-α and IFN-γ, released by chronically activated macrophages, NK cells and T-cells, also stimulate fibroblast proliferation and collagen production. This, in turn, stimulates fibrosis and wound healing, which can interfere with normal tissue function (Gabay and Kushner 1999, Larsen and Henson 1983). Thus, inflammation is a highly complex process and only the basic elements of these series of events are described. In addition to the vascular and cellular events of inflammation, pain, is a key component of the inflammatory process involving many complex mechanisms, and these are described in more detail.

1.2 Pain

A generally accepted definition of pain is that it is 'an unpleasant sensory and emotional experience associated with actual or potential tissue damage or described in terms of such damage' – International Association for the Study of Pain. There are several distinct types of pain that exist: nociceptive, inflammatory, neuropathic and functional as depicted in Figure 2 (Merskey 1999, Woolf 2004).

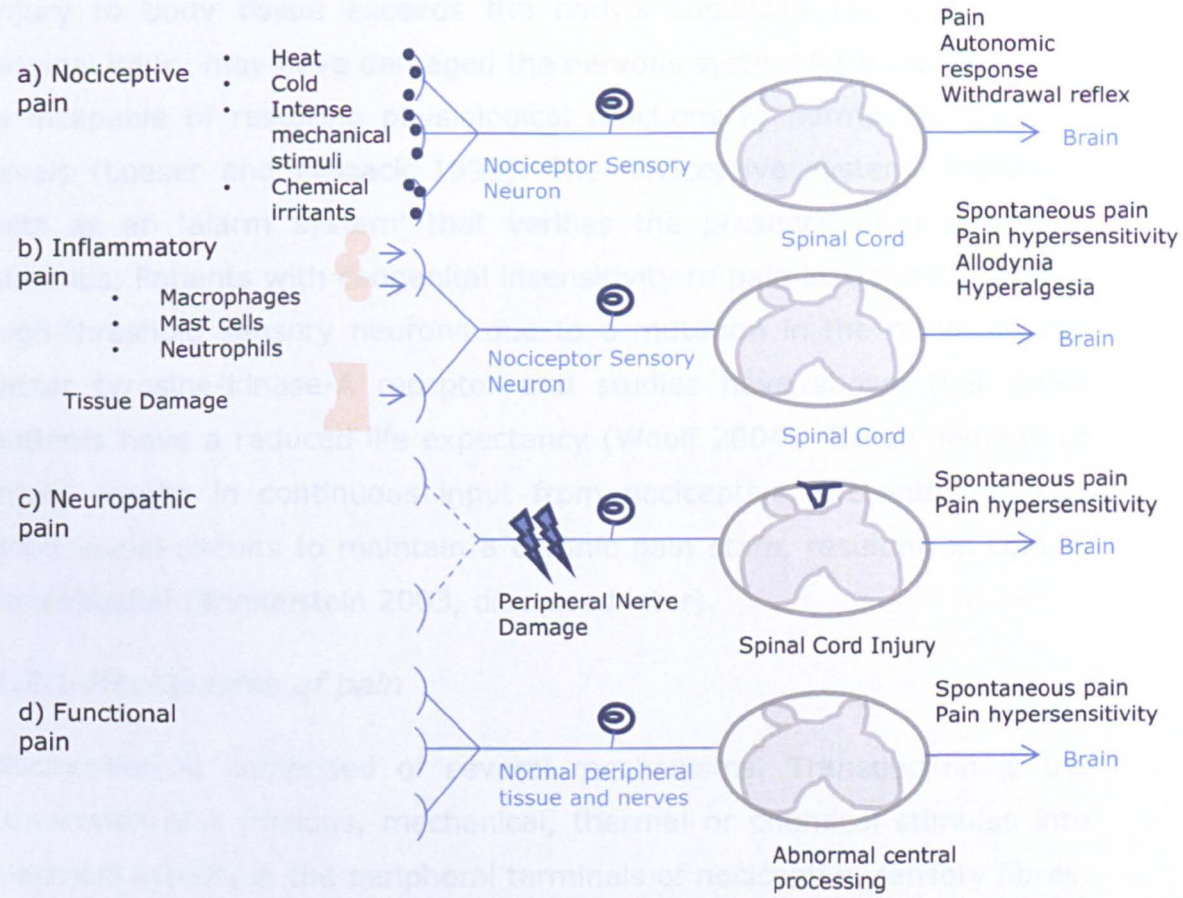

Figure 2. Schematic of the four distinct types of pain (Woolf 2004).

Nociceptive pain is a physiological, transient pain in response to a noxious stimulus. The nociceptive system extends from the periphery through to the spinal cord, brain stem and thalamus and to the cerebral cortex. The sensation of pain is perceived when nociceptive transducers are activated in the skin or other tissues in the body, even in the absence of tissue damage (Loeser and Melzack 1999, Woolf 2004). The function of such pain is to protect the body from physical damage by the environment or from stress to body tissues and is related to the speed of onset and offset of stimulation (Loeser and Melzack 1999).

Acute pain arises as a result of substantial injury to tissue and subsequent activation of nociceptive transducers at the site of injury. The body's reparative mechanisms are not overwhelmed by such an injury and the process of healing occurs. Chronic pain may occur when the

injury to body tissue exceeds the body's capability for healing. The original injury may have damaged the nervous system such that the body is incapable of restoring physiological functions to normal homeostatic levels (Loeser and Melzack 1999). The nociceptive system, therefore, acts as an 'alarm system' that verifies the presence of a damaging stimulus. Patients with congenital insensitivity to pain lose the function of high-threshold sensory neurons due to a mutation in the nerve growth factor tyrosine-kinase-A receptor and studies have shown that these patients have a reduced life expectancy (Woolf 2004). Tissue damage or injury results in continuous input from nociceptive afferents that can drive spinal circuits to maintain a chronic pain state, resulting in central sensitisation (Winkelstein 2003, discussed later).

1.2.1 Mechanisms of pain

Nociception is comprised of several mechanisms. Transduction is the conversion of a noxious, mechanical, thermal or chemical stimulus into electrical activity in the peripheral terminals of nociceptive sensory fibres. Specific receptor ion channels expressed by nociceptors such as transient receptor potential vanilloid-1 (TRPV1), along with others, mediate this process. Conduction is the transfer of action potentials along axons from the peripheral terminals to the central terminals of nociceptors in the central nervous system and transmission is the process of synaptic transfer and modulation of an input from one neuron to the next (Woolf 2004, Cho and Valtschanoff 2008).

Nociceptors are a specialised subset of primary sensory neurons that respond to intense stimuli. They consist of fibres innervating regions of the head and body for which cell bodies are located in the trigeminal and dorsal root ganglia (DRG). Myelinated Aβ-fibres are sensory fibres which are rapid conducting and have large diameter (>10 μm) cell bodies. These fibres are involved in the detection of innocuous stimuli applied to the skin, muscle and joints. The majority of nociceptors have small (<2 μm) and medium (<5 μm) diameter cell bodies, and include the unmyelinated slow conducting C-fibres and thinly myelinated more

rapidly conducting Aδ fibres. These fibres are involved in mediating the delayed, diffuse, dull pain and rapid, sharp, acute pain evoked by noxious stimuli, respectively (Purves et al 2004, Koltzenburg et al 1994). Most C-fibre nociceptors are polymodal responding to mechanical, chemical and noxious thermal stimuli (Schmidt et al 1995). Aδ nociceptors respond to intense mechanical and thermal stimuli. Some nociceptors are difficult to identify and are called 'silent' or 'sleeping' nociceptors, only responding when sensitised by tissue injury (Furst 1999, Julius and Basbaum 2001).

There are two main mechanisms that contribute to post-injury pain hypersensitivity; these are peripheral and central sensitisation.

1.2.2 Peripheral sensitisation

Changes to the chemical environment of the peripheral nerve terminals of nociceptors can be precipitated by injury and/or inflammation of tissue. Inflammatory mediators such as prostaglandins, nitric oxide, excitatory amino acids, bradykinin, histamine and substance P, induce inflammation and oedema which contribute to the healing process. However, the action of these mediators also sensitises nociceptors and new nociceptors are recruited, further enhancing pain (Furst 1999, Woolf 2004, Winkelstein 2003). A cascade of events, which ultimately lead to the increased sensitivity, and excitability of the nociceptive terminal is known as peripheral sensitisation. Damaged cells release intracellular contents such as adenosine triphosphate into the extracellular space which activates ligand-gated $P2X_3$ receptors expressed by the primary afferent nociceptors. Cytokines, chemokines and growth factors released from the site of injury either activate nociceptive terminals directly to produce pain (nociceptive activators) or sensitise the terminals (hypersensitivity) to subsequent stimuli (nociceptive sensitisers). Prostaglandin E_2 and nerve growth factor (NGF) also sensitise the terminals activating the nociceptors directly. Following binding to its receptor, prostaglandin E_2 activates adenylyl cyclase to increase levels of cyclic adenosine monophosphate which, in turn, activates cyclic adenosine monophosphate-dependent protein kinase A (PKA). Calcium is released

from microsomal stores in the terminals and subsequently activates protein kinase C (PKC). Both kinases contribute to the phosphorylation of proteins, significantly altering the activity of receptors, ion channels, membrane excitability and action potential firing (Woolf 2004, Winkelstein 2003, Ji et al 2003). The primary afferents terminate in the dorsal horn of the spinal cord and transfer information to the spinal neurons via synaptic transmission. A wide range of transmitters are released including the neuropeptides substance P, CGRP etc and the excitatory amino acid glutamate which mediate the postsynaptic response, which is relayed to the supraspinal sites via the ascending pathways (Winkelstein 2003).

1.2.3 Pain Pathways

The manifestation and modulation of pain are controlled via ascending and descending pathways. In mammals, the 2 major ascending pain pathways are the spinothalamic tract, which encodes the sensory discriminatory aspect of pain, and the spinoparabrachial tract, which encodes the affective (emotional) aspects of pain (Rea et al 2007, Millan 2002). Both these pain pathways are shown in Figure 3 (Hunt and Mantyh 2001).

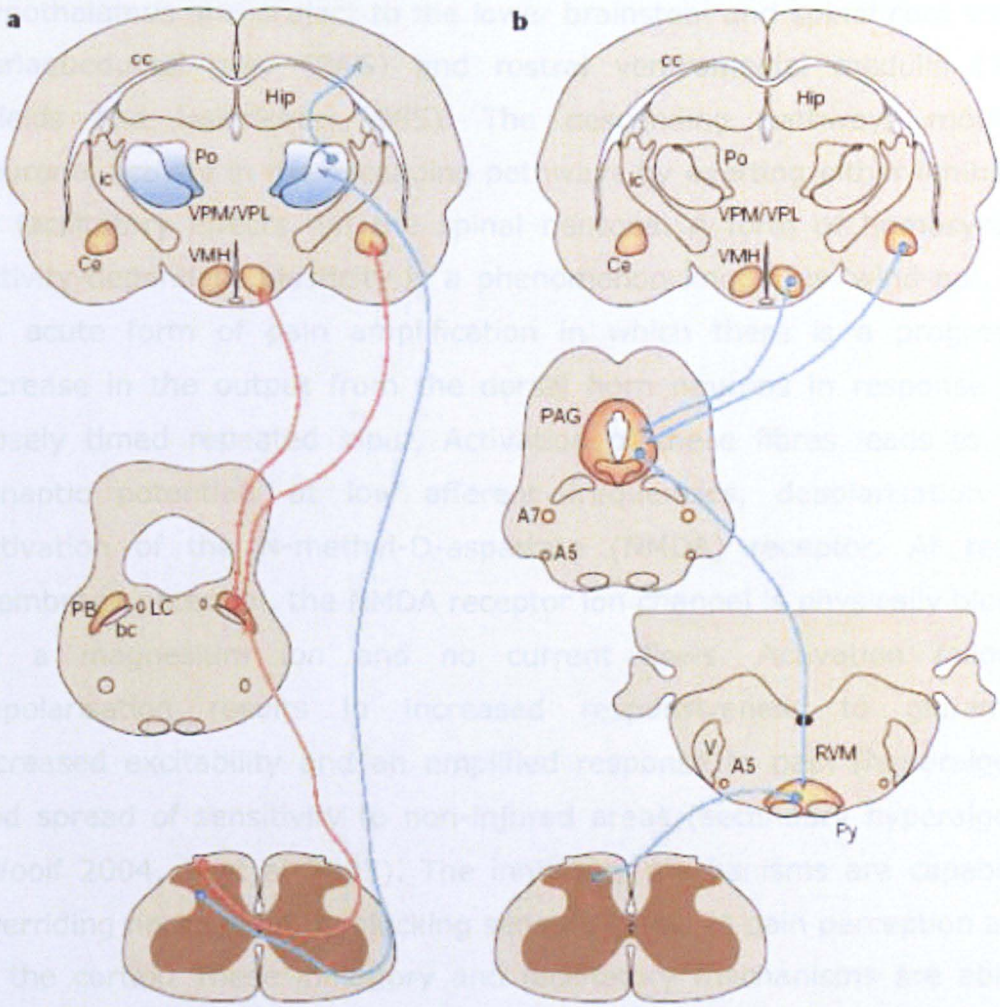

Figure 3. Schematic detailing the main ascending and descending pathways. Spinoparabrachial pathway (red), Spinothalamic pathway (blue), Abbreviations are as follows: A, adrenergic nucleus; bc, brachium conjunctivum; cc, corpus callosum; Ce, central nucleus of the amygdala; Hip, hippocampus; ic, internal capsule; LC, locus coeruleus; PAG, periaqueductal grey; PB, parabrachial area; Po, posterior group of thalamic nuclei; Py, pyramidal tract; RVM, rostroventral medulla; V, ventricle; VMH, ventral medial nucleus of the hypothalamus; VPL, ventral posteriolateral nucleus of the thalamus; VPM; ventral posteriomedial nucleus of the thalamus (Rea et al 2007).

Neurons in the ascending pain pathways receive inputs from peripheral primary afferent fibres and project from the dorsal horn of the spinal cord to several supraspinal sites. This information is projected to parts of the thalamus involved in nociceptive processing, such as the ventral posteriolateral and posteriomedial nucleus of the thalamus, and received in the somatosensory cortex (regulation of pain perception) (Rea et al 2007).

The descending inhibitory pathways originate from the amygdala and hypothalamus and project to the lower brainstem and spinal cord via the periaqueductal grey (PAG) and rostral ventromedial medulla (RVM) (Fields and Heinricher 1985). The descending pathways modulate neuronal activity in the ascending pathways by exerting either inhibitory, or facilitatory effects, on the spinal neurons. A form of homosynaptic activity-dependent plasticity is a phenomenon known as 'wind-up'. It is an acute form of pain amplification in which there is a progressive increase in the output from the dorsal horn neurons in response to a closely timed repeated input. Activation of these fibres leads to slow synaptic potentials at low afferent frequencies, depolarisation and activation of the N-methyl-D-aspartate (NMDA) receptor. At resting membrane potential, the NMDA receptor ion channel is physically blocked by a magnesium ion and no current flows. Activation following depolarisation results in increased responsiveness to glutamate, increased excitability and an amplified response to pain (hyperalgesia) and spread of sensitivity to non-injured areas (secondary hyperalgesia) (Woolf 2004, Ji et al 2003). The inhibitory mechanisms are capable of overriding nociception by blocking sensory inflow to pain perception areas in the cortex. These inhibitory and facilitatory mechanisms are able to provide additional modulation of the spinal processing of noxious inputs (Woolf 2004, Winkelstein 2003).

1.2.4 Central Sensitisation

Tissue damage or injury is associated with an increased neuronal excitability in the spinal cord which manifests as increased magnitude of responses, decreased activation thresholds and the expansion of the receptor fields of neurons. This continuous input from nociceptive afferents can drive spinal circuits to maintain a chronic pain state, resulting in central sensitisation (Winkelstein 2003). Intense peripheral noxious stimulation increases the frequency and duration of action potentials. High frequency action potentials lead to the release of neuropeptides such as substance P and glutamate from nociceptor central terminals in the spinal cord (Kidd and Urban 2001) and act on G protein

coupled receptors (GPCRs) to produce slow, persistent synaptic currents. The release of the neuropeptide, brain-derived neurotrophic factor (BDNF), acts on tyrosine receptor kinase B (TrkB) to modify membrane excitability. This along with glutamate activation of the NMDA ion channel receptor leads to activity-dependent plasticity (Woolf 2004). Activity-dependent plasticity is a result of increases in synaptic efficacy characteristic of central sensitisation. Central sensitisation persists even if the stimulus is only sustained at low levels. In the case of neuropathic pain, central sensitisation is prolonged due to ongoing ectopic activity arising from sensory fibres in the injured nerve (Woolf 2004, Winkelstein 2003, Ji et al 2003, Zimmermann 2001).

The main focus of this thesis are the lipid mediators involved in the inflammatory pain response, their synthesis and metabolism, function, and potential molecular targets and is described in more detail.

1.3 Lipid mediators of the inflammatory response

A number of mediators including histamine, bradykinin, cytokines, chemokines and eicosanoids are involved in the regulation of blood flow, vascular permeability and cell infiltration. In particular, the bioactive lipids are implicated in many areas of inflammatory pain research, as they contribute to the initiation and resolution of inflammation. These are a complex group of fatty acid-derived lipids consisting of the prostaglandins, thromboxanes, leukotrienes, endocannabinoids and many more. The metabolism and function of these lipids are described in more detail later.

1.3.1 Bioactive lipids

Bioactive lipids or lipids that activate specific signalling pathways are involved in the regulation and maintenance of normal bodily functions. The synthetic, metabolic and signalling pathways for bioactive lipids are activated in response to the multicellular signalling status of the environment, allowing cells to respond appropriately (Evans and Hutchinson 2010). Bioactive lipid targets are important in a number of

conditions such as cancer, asthma and arthritis, which all have an inflammatory element. Interestingly, a number of bioactive lipids measured are known to target several different receptor groups. These include G protein-coupled receptors such as the cannabinoid receptors or peroxisome proliferator-activated receptor alpha (PPARα), and TRPV1 ion channels.

1.3.1.1 Cannabinoid receptors

Since the discovery of Δ^9-tetrahydrocannabinol (THC) as the psychoactive component of cannabis and its properties, there has been interest in the potential therapeutic applications of cannabis-like molecules (Freund 2003, Pertwee 2008). The analgesic properties of the cannabinoids are well known, and are now explicable by the existence of the cannabinoid signalling system (Rice et al 2002). Research based on radioligand binding techniques and complementary DNA-encoding resulted in the cloning of the first cannabinoid receptor from rat brain, a GPCR now known as CB1 (Matsuda et al 1990, Herkenham et al 1991). Subsequently, a peripherally located cannabinoid GPCR, now termed CB2, was cloned from human pro-myelocytic leukaemia HL-60 cells (Bouaboula et al 1993, Jonsson et al 2006). CB1 receptors are the most abundant GPCRs in the central nervous system, but are also found in peripheral tissues including endothelial cells and adipose tissue (Galiegue et al 1995). CB2 receptors are expressed in cells of immune origin including the spleen, monocytes and B and T cells (Daaka et al 1995, Hohmann and Suplita 2006, Pacher et al 2006). CB2 receptors have also been identified in the brain, endocrine pancreas and in bone (Galiegue et al 1995, Pacher et al 2006). The distribution of CB1 receptors in the brain has been studied using techniques such as immunohistochemistry and receptor autoradiography. Cannabinoid receptors are frequently found localised on nerve endings conforming to the theory that they are presynaptic modulators of neurotransmitter release (Ahluwalia et al 2000). They are densely populated in the periaqueductal grey (PAG) and the rostal ventromedial medulla (RVM), areas of the brain relating to descending pain modulation (Walker and Huang 2002, Fox and Bevan

2005, Rice et al 2002). Other areas where CB1 receptors have been found include the amygdala, hypothalamus, thalamus and parabrachial nucleus and brainstem (Finn and Chapman 2004), which reflect the importance of the cannabinoid system in motor control, memory processing and pain modulation (Grotenhermen 2005). CB1 receptor density in the brainstem, however, is low, which explains the low toxicity of the cannabinoids, such as lack of respiratory depression, which is often seen with the opioids (Grotenhermen 2005). CB2 receptors are expressed in the brainstem (Van Sickle et al 2005), thalamus (Gong et al 2006) and cerebellum (Ashton et al 2006) of naïve rats but their roles are still uncertain. High concentrations of cannabinoid receptors are also found in the superficial layers of the spinal dorsal horn and the dorsal root ganglion from where they are transported to peripheral and central primary afferent neuron terminals (Walker and Huang 2002, Rice et al 2002, Jhaveri et al 2008a).

Endogenous ligands of the cannabinoid receptors are known as endocannabinoids. These include N-arachidonoyl ethanolamide (AEA), 2-arachidonoyl glycerol (2-AG) and N-arachidonoyl-dopamine (NADA). AEA has been shown to have intermediate (sub μM) potency at CB1 and CB2 receptors (Felder et al 1995, Slipetz et al 1995, Sugiura et al 1999), compared to 2-AG, which has high (sub nM) potency for CB1 and CB2 receptors (Sugiura et al 1999, Mechoulam et al 1995). NADA has intermediate potency for only CB1 (Bisogno et al 2000). Endocannabinoids are synthesised and released from postsynaptic neurons and activate presynaptic CB1 receptors to modulate neuronal synapses, an example of retrograde signalling. Endocannabinoids also reduce the release of neurotransmitters including glutamate and GABA (Furst 1999, Hohmann and Suplita 2006). Once released, the endocannabinoids activate cannabinoid receptors on neighbouring cells. Cannabinoid receptors have been found to be functionally coupled to several intracellular signalling mechanisms including inhibition of adenylyl cyclase activity and voltage-gated calcium channels. They also activate G protein-sensitive inward rectifying potassium (GIRK) channels, causing

hyperpolarisation, and are rapidly inactivated by transmembrane transport and enzymatic hydrolysis (Freund et al 2003, Rang et al 2003, Di Marzo et al 2004).

A number of related endogenous lipids with endocannabinoid-like activity have been detected. These include N-oleoyl ethanolamide (OEA), N-palmitoyl ethanolamide (PEA) and N-arachidonoyl glycine (AraGly) (Hohmann and Suplita 2006, Randall and Kendall 1998). PEA does not bind to CB1 or CB2 with high affinity, but is thought to enhance the effect of anandamide (AEA) via an unknown mechanism, possibly interference with its catabolism (Vandevoorde et al 2003, Sheskin et al 1997). OEA and AraGly also lack affinity for CB1 and CB2 receptors (Sheskin et al 1997, Lin et al 1998, Sipe et al 2005). AEA and 2-AG, along with the endocannabinoid-like compounds PEA and OEA have been implicated in inflammation and pain. PEA has anti-inflammatory properties (for a review see Schmid et al 1990). Oral administration of PEA produced a reduction in substance-P mast cell degranulation and extravasation, as well as an attenuation of carrageenan-induced hyperalgesia and oedema (Mazzari et al 1996). For comprehensive reviews on endocannabinoids and inflammatory hyperalgesia see Sagar et al 2009, De Petrocellis et al 2000. In addition, PEA has been shown to activate peroxisome proliferator activated receptor alpha (PPARα), and it has been suggested that this contributes to the anti-inflammatory properties of this lipid (Sun et al 2007).

1.3.1.2 PPAR receptors

Peroxisome proliferator activated receptors are ligand-activated transcription factors that belong to the nuclear receptor superfamily and are reported to regulate gene transcription (Desvergne and Wahli 1999). Different PPAR genes have been identified and divided into subgroups, alpha, beta/delta and gamma (α, β/δ and γ). Each subgroup displays distinct tissue (Braissant et al 1996, Auboeuf et al 1997, Cullingford et al 1998, Granneman et al 1998) and developmental (Braissant and Wahli

1998) expression patterns; however, the focus of the experiments described in this thesis is on the PPARα (see Chapter 3).

Each PPAR receptor has a N-terminal 'A/B' domain that has a ligand-dependent activation function, a 'C' domain encoding the DNA binding region of the receptor, followed by a 'D' or hinge region. The C-terminal 'E/F' ligand binding domain contains the ligand-dependent activation function 2, important for heterodimerisation (Escher and Wahli 2000). Dimerisation is essential for the activity of the PPARs, which is similar to the majority of receptors in the nuclear superfamily. They heterodimerise with the 9-*cis* retinoid X receptor (RXR), forming a complex that is able to bind to the PPAR response elements located in the promoter of PPAR target genes (under PPAR transcriptional control) (Dowell et al 1999, Ijpenberg et al 1997). The consequence of the interaction of the activated heterodimer with the promoter is stimulation of target gene transcription that is implicated in various functions such as lipid metabolism and inflammation control (Michalik and Wahli 1999).

PPARα receptors are expressed in rats, mice and humans; the rat and mouse PPARα proteins share 92% identity with the human receptor (Schmidt et al 1992, Borel et al 2008). Expression of PPARα protein has been reported in different areas of the gastrointestinal tract, liver, heart, adipose tissue and brain in humans (Huin et al 2000, Auboeuf et al 1997, Bunger et al 2007) and in rodents (Beck et al 1992, Braissant et al 1996, Bunger et al 2007). In the brain, expression of PPARα is highest in the brain stem and cerebral cortex, although it is also found in many regions including the hippocampus (Gofflot et al 2007). In the spinal cord, PPARα expression was also found to be lower in the grey matter compared to white matter and high expression of PPARα was found in astrocytes (Benani et al 2003a, Benani et al 2003b). Expression of PPARα is necessary for the development of inflammation; mice deficient in this receptor demonstrated an exacerbated inflammatory response to lipopolysaccharide stimulation (Delerive et al 1999)(See Chapter 3 for details on PPARα and inflammation).

Last but not least, another important receptor target of bioactive lipids are the transient receptor potential vanilloid 1 (TRPV1) receptors. In addition, this completes the set of superfamilies of receptors at which the cannabinoids act (GPCRs, nuclear receptors and ion channels).

1.3.1.3 TRPV1 receptors

Transient receptor potential vanilloid 1 (TRPV1) receptors are ligand-gated, non-selective cation channels and the first subtype of the TRP family, to be discovered (Caterina et al 1997, Dhaka et al 2006). There are at least 28 different TRP subunits that have been identified in mammals, further divided into six subfamilies, of which the vanilloid TRPs are one (Clapham 2003, Moran et al 2004). The primary structure of the TRP channels consists of six transmembrane segments with a pore domain between transmembrane segments 5 and 6 and with both the C- and N- termini located intracellularly (Doyle et al 1996, Clapham et al 2005). TRP channels are tetramers of four subunits, which are opened or closed by conformational changes in the channel protein (Voets et al 2004, Bandell et al 2007). In general, TRP channels are only weakly sensitive to depolarisation, but open in response to activation of the channel protein (Clapham et al 2005). TRPV1 channels are activated by different stimuli such as heat (>43 °C) (Caterina et al 1997), capsaicin (Hwang et al 2000), AEA (Smart et al 2000) and low pH (Tominaga et al 1998). Activation involves increased membrane permeability to cations, including sodium, but mainly calcium in the case of TRPV1 (Wood et al 1988, Caterina et al 1997, Caterina and Julius 2001).

TRPV1 is mainly found in small- to medium-diameter neurons of primary sensory neurons (dorsal root ganglia, trigeminal ganglia and sympathetic ganglia), which explains the selectivity of capsaicin for these neurons (Szallasi and Blumberg 1999, Vay et al 2012). TRPV1 has also been shown to be expressed on the terminals of primary afferent sensory nerve fibres A and C, in addition to being present in the brain, including areas involved in nociceptive transmission (Mezey et al 2000, Toth et al 2005). Areas of the brain in which TRPV1 expression has been found

include the cortex, amygdala, striatum, hippocampus and hypothalamus (Mezey et al 2000). In addition, fibres of the primary sensory neurons innervate virtually all tissues of the body including bone, internal organs and the vascular system. However, TRPV1 has been shown to be more prevalent in visceral then somatic afferent nerves (Robinson et al 2004, Brierley et al 2005, Hwang et al 2005, Christianson et al 2006). Furthermore, it is known that TRPV1 expression is important for the development of inflammatory hyperalgesia (Caterina et al 2000) and that expression is up-regulated under inflammatory conditions (Ji et al 2002)(See Chapter 4 for details on TRPV1 and inflammatory hyperalgesia).

Sensitisation of the TRPV1 channel is known to occur and several mechanisms have been suggested. Phosphorylation of the ion channel by PKA, PKC and other kinases plays an important role in the regulation of TRPV1 receptor activity (Zhang and McNaughton 2006, Bhave et al 2003, Vellani et al 2001). Phosphorylation by PKA increases TRPV1 receptor responses to lipid activators such as AEA and PGE_2 (Lopshire and Nicol 1998, Schnizler et al 2008). Mice deficient in a regulatory subunit of PKA exhibit reduced PGE_2 and formalin-induced inflammatory hypersensitivity (Malmberg et al 1997), demonstrating the importance of PKA phosphorylation in TRPV1-mediated inflammation. Increased TRPV1 activity by bradykinin, nerve growth factor, prostaglandins and AEA via PKC-mediated hydrolysis of phosphatidylinositol-4,5-bisphosphate is another mechanism of TRPV1 sensitisation (Caterina et al 1997, Tominaga et al 1998, Prescott and Julius 2003), and altering the threshold of receptor activation. In addition, the rapid recruitment of an intracellular pool of TRPV1 to the cell membrane also enhances ligand responses, a process that involves phosphoinositide 3-kinase and Src kinase (Stein et al 2006, Zhang et al 2005). Dephosphorylation of TRPV1 by protein phosphatases promotes desensitisation of the receptor and is a mechanism of inhibitory regulation (Mohapatra and Nau 2005). There are also stimulus-dependent differences in TRPV1 desensitisation; capsaicin depends on extracellular calcium for desensitisation, whereas

heat does not (Bandell et al 2007). It appears that the activation/desensitisation state of the channel is dependent on the dynamic balance between phosphorylation and dephosphorylation (Mohapatra and Nau 2005). In addition to having multiple receptor targets, bioactive lipid metabolism and function is also complex and this is described in more detail.

1.3.2 Metabolic pathways of the bioactive lipids

Eicosanoids are synthesised mainly from arachidonic acid (AA), which is released from membrane phospholipid stores through the activity of several phospholipase enzymes, predominantly phospholipase A_2 (PLA_2). PLA_2 is activated by several cellular agonists including IL-8 and platelet activating factor (PAF), phagocytic particles and microorganisms (Piper and Vane 1971). Once in the cytosol, AA can then be further metabolised by three enzymatic pathways: cyclooxygenases (COXs), lipoxygenases (LOXs) and cytochrome P450 epoxygenases (CYPs); see, Figure 4 (Samuelsson et al 1987, Serhan et al 1984, Capdevila et al 1990).

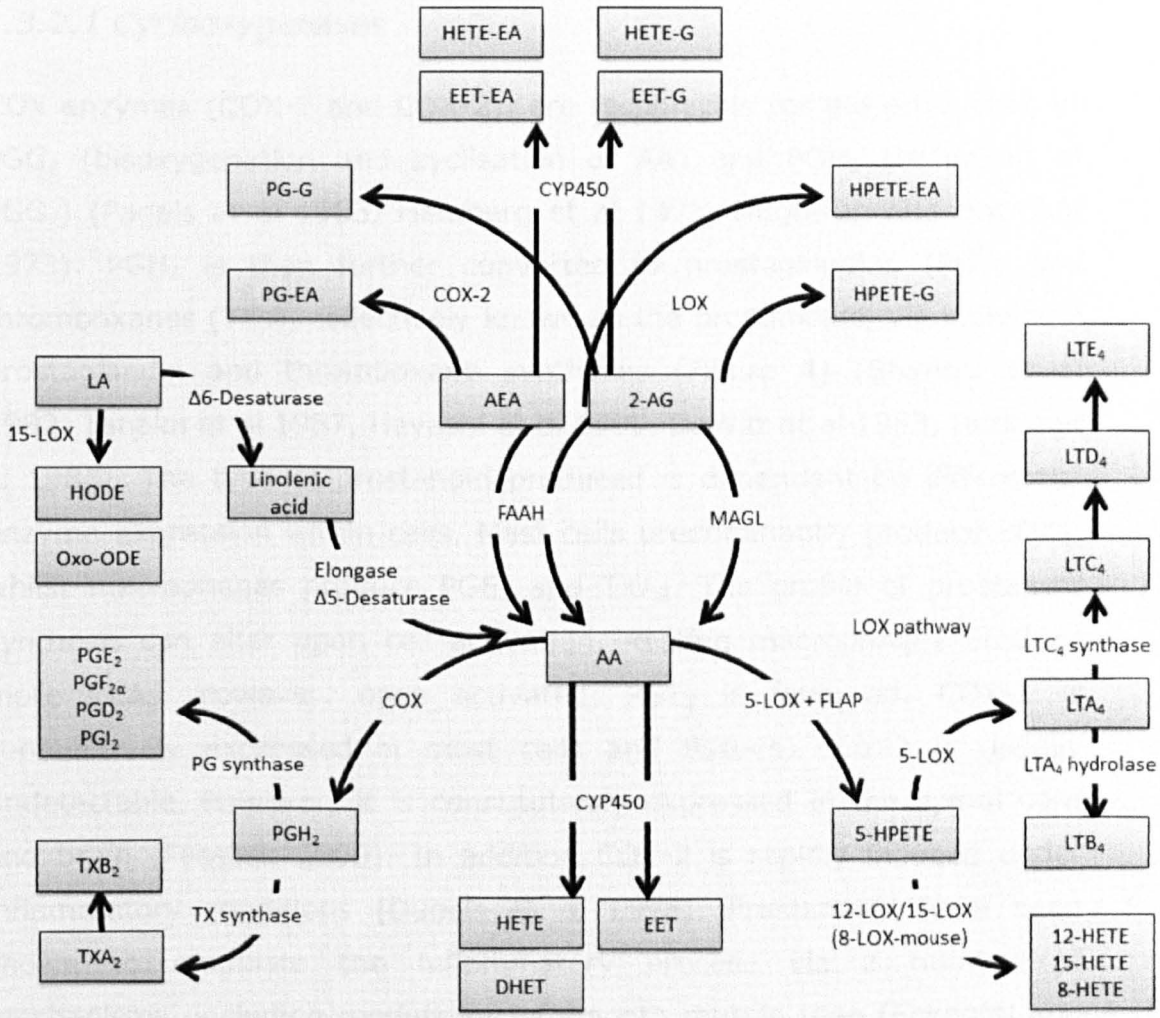

Analyte groups	COX	LOX	CYP450	ECs
Metabolites	PGs, TXs, PG-EAs, PG-Gs	LTs, HODEs, oxo-ODEs, HPETEs, HETEs	HETEs, EETs, DHETs, HETE-EAs, HETE-Gs, EET-EAs, EET-Gs	AEA, OEA, PEA, 2-AG, AraGly, NADA

Figure 4. Metabolic pathways of bioactive lipids analysed with this LC-MS/MS method. Lipid abbreviations: DHET - dihydroxyeicosatrienoic acids, EET - epoxyeicosatrienoic acid, HETE - hydroxyeicosatetraenoic acid, HPETE - hydroperoxyeicosatetraenoic acid, AEA - N-arachidonoyl ethanolamide, 2-AG - 2-arachidonoyl glycerol, EA – ethanolamide, G – glycerol, LA – linoleic acid, HODE - hydroxyoctadecadienoic acid, OxoODE - oxooctadecadienoic acid, PG – prostaglandin, TX – thromboxane, AA – arachidonic acid, LT – leukotriene. Enzyme abbreviations: COX – cyclooxygenase, CYP450 – cytochrome P450, LOX – lipoxygenase, FAAH – fatty acid amide hydrolase, MAGL – monoacyl glycerol lipase, FLAP – five lipoxygenase (5-LOX) activating protein.

1.3.2.1 Cyclooxygenases

COX enzymes (COX-1 and COX-2), are responsible for the production of PGG_2 (bisoxygenation and cyclisation of AA) and PGH_2 (reduction of PGG_2) (Pagels et al 1983, Hamberg et al 1973, Nugteren and Hazelhof 1973). PGH_2 is then further converted to prostaglandins (PGs) and thromboxanes (TXs), collectively known as the prostanoids, via individual prostaglandin and thromboxane synthases (Figure 4) (Shimizu et al 1982, Tanaka et al 1987, Hayashi et al 1989, DeWitt et al 1983, Ullrich et al 1983). The type of prostanoid produced is dependent on differential enzyme expression within cells. Mast cells predominantly produce PGD_2, whilst macrophages produce PGE_2 and TXA_2. The profile of prostanoid synthesis can alter upon cell activation. Resting macrophages produce more TXA_2; however, once activated, PGE_2 is favoured. COX-1 is constitutively expressed in most cells and tissues, COX-2 is usually undetectable, however, it is constitutively expressed in the spinal cord and brain (Fosslien 2000). In addition COX-2 is rapidly induced under inflammatory conditions (Dubois et al 1998). Prostanoids have been shown to modulate the inflammatory process via a number of mechanisms, including modulation of smooth muscle tone (Eckenfel and Vane 1972, Ferreira et al 1972, Main 1964), vascular permeability (Williams 1979, Williams and Jose 1981), hyperalgesia (Ferreira et al 1978), fever (Feldberg and Gupta 1973, Feldberg and Saxena 1971, Milton and Wendlandt 1971) and platelet aggregation (Moncada et al 1976). They exert their biological effects by binding to specific cell surface receptors that have been characterised in mice and humans. These include PGD_2 receptors; DP1, DP2, PGE_2 receptors; EP1, EP2, EP3, EP4, $PGF_{2\alpha}$ receptor; FP, PGI_2 receptor; IP and the TXA_2 receptor; TP (Hirai et al 2001, Monneret et al 2001, Xue et al 2005). PGE_2 and PGI_2 are the predominant pro-inflammatory prostanoids and both increase vascular permeability, particularly in the presence of histamine, bradykinin, 5-HT (Hata and Breyer 2004, Higgs et al 1978, Komoriya et al 1978, Lewis et al 1975, Moncada et al 1973, Williams and Morley 1973) and enhance vasodilatation and oedema (Kaley et al 1985). PGE_2

is the most potent pyretic agent, with elevated concentrations found in cerebrospinal fluid taken from patients with bacterial or viral infections (Saxena et al 1979). PGI_2 and PGE_2 also cause peripheral and central hyperalgesia when bound to IP and EP1, EP3 and EP4 receptors respectively and achieves this by reducing nociceptor sensory neuron threshold to stimulation (Ferreira et al 1972, Ferreira et al 1978, Ahmadi et al 2002, Lin et al 2006, McAdam et al 2000, Moriyama et al 2005, Murata et al 1997, Reinold et al 2005, Ueno et al 2001). In addition to pro-inflammatory properties, some prostanoids also exert immunosuppressive effects through up-regulation of intracellular cyclic adenosine monophosphate (cAMP) (Aronoff et al 2006, Luo et al 2004, van der Pouw Kraan et al 1995). The ability of inflammatory leukocytes to phagocytose and kill microorganisms is reduced by the action of PGE_2 and PGI_2 (Aronoff et al 2004, Rossi et al 1998, Serezani et al 2007, Weinberg et al 1985), which also inhibit the production of downstream inflammatory mediators (Kunkel et al 1988, Takayama et al 2002, van der Pouw Kraan et al 1996, Xu et al 2008) and enhance the production of IL-6 and IL-10 (Harizi et al 2002, Hinson et al 1996). PGE_2 has also been shown to induce transcription of enzymes required for the generation of potent pro-resolution lipid mediators such as resolvins and protectins (Marcheselli et al 2003, Serhan et al 2000, Serhan et al 2002).

1.3.2.2 Lipoxygenase

The LOX pathways consist of 5-LOX, 12-LOX and 15-LOX enzymes found in leukocytes, platelets and endothelial cells respectively (Lewis et al 1980). An 8-LOX enzyme has been shown to produce 8-HETE in mouse skin (Gschwendt et al 1986) and, recently, in human skin (Rhodes et al 2009). Unlike COX, 5-LOX only becomes functional following cell activation via increases in intracellular calcium (Rouzer and Samuelsson 1985, Ochi et al 1983) or by phosphorylation independent of calcium changes (Werz et al 2002). The LOX enzyme pathway is responsible for the production of leukotrienes (LTs), HPETEs (hydroperoxyeicosatetraenoic acids) and HETEs (hydroxyeicosatetraenoic acids) (Figure 4). Following activation, AA is converted into 5-HPETE via

5-LOX-activating protein (FLAP) and this intermediate is then rapidly reduced to 5-HETE (Figure 4). 5-HPETE can also be converted to LTA_4, an unstable 5,6-epoxide containing a conjugated triene, which is metabolised either via LTA_4 hydrolase to LTB_4 (Funk 2001, Minami et al 1987) or via γ-glutamyl-S-transferase to LTC_4 (Hammarstrom et al 1985). Subsequently, 5-HETE, LTB_4 and LTC_4 are thought to be exported from the cell (Lam et al 1990, Leier et al 1994), where LTC_4 is metabolised by γ-glutamyl transpeptidase to LTD_4 and further modified by cysteinyl glycinase to LTE_4 (Rouzer and Samuelsson 1985). Collectively, LTC_4, LTD_4 and LTE_4 are termed the cysteinyl leukotrienes (Okubo et al 2010). LTs act via specific receptors; B leukotriene receptor 1 and 2 (BLT1 and BLT2) and cysteinyl leukotriene receptor 1 and 2 (cysLT1 and cysLT2) located on the plasma membrane of structural and inflammatory cells (Tager et al 2003, Lynch et al 1999). Ligand binding to the receptors results in increased intracellular calcium and blocks cAMP formation, altering cellular activities such as motility and transcriptional activation (Lynch et al 1999). BLT1, a high affinity receptor for LTB_4, has chemo-attractant and pro-inflammatory properties (Tager et al 2003), whereas LTB_4 activation of PPARα has been shown to be anti-inflammatory *in vitro* and in a mouse model of inflammation (Devchand et al 1996, Krey et al 1997, Lin et al 1999). LTs act primarily as pro-inflammatory lipid mediators, generated primarily by neutrophils, macrophages and mast cells at the site of inflammation (Tager et al 2003). LTB_4 works by attracting and activating inflammatory cells such as neutrophils and leukocytes (Tager et al 2003, Borgeat and Naccache 1990, Ott et al 2003), whereas LTD_4 mainly targets eosinophils (Woodward et al 1991). The cysteinyl LTs increase vascular permeability and plasma leakage, contributing to oedema formation (Bjork et al 1982, Orange et al 1969, Svensjo 1978). 5-HETE, a 5-LOX metabolite, has also been shown to be pro-inflammatory. This lipoxygenase product of leukocytes promotes neutrophil and eosinophil chemotaxis and is elevated under inflammatory conditions (Goetzl et al 1982). 12-HETE is also pro-inflammatory and is a potent keratinocyte-derived chemoattractant, shown in vitro to attract neutrophils and lymphocytes

(Bacon et al 1988, Dowd et al 1985). 15-HETE has also been shown to have pro-inflammatory properties, causing chemotaxis of inflammatory cells into the lumen in the airways (Johnson et al 1985). However, the 12/15 LOX pathway has been shown to be highly complex in the regulation of inflammation (See Kuhn and O'Donnell 2006 for a comprehensive review).

1.3.2.3 Cytochrome P450

Cytochrome P450 (CYPs) are membrane-bound, haem-containing enzymes found in the liver, brain, kidneys and heart (Nelson et al 1996, Scarborough et al 1999). Particular CYPs catalyses AA to produce HETEs along with epoxyeicosatrienoic acids (EETs) and dihydroxyeicosatrienoic acids (DHETs) (Figure 4) (Roman 2002). In the vascular endothelium, AA is metabolised by CYP epoxygenase to the EETs, which are then converted by soluble epoxide hydrolase to the DHETs (Roman 2002, Zhang et al 2001). In vascular smooth muscle, AA is converted by CYP hydrolases to 20-HETE (Wang et al 1999). In inflammation, EETs are converted via CYPs 2C8, 2C9 and 2J2 and block the adhesion of neutrophils and eosinophils to the vascular wall, by suppressing VCAM-1 and E-selectin expression (Fleming 2007, Node et al 1999). EETs have been suggested to modulate the NF-κB pathway and, as a consequence, may prevent expression of various cytokine-induced pro-inflammatory enzymes including COX-2 (Inceoglu et al 2007, Inceoglu et al 2008). In addition, EETs have been shown to display hyperalgesic actions in models of inflammatory pain (Inceoglu et al 2006, Inceoglu et al 2007, Inceoglu et al 2008). Recently, it has been suggested that the anti-inflammatory properties of the EETs are due to binding to a monocytic cell-surface receptor, an 'EET receptor', coupled to G proteins (Behm et al 2009). In terms of the HETEs, 16-HETE has also been shown to prevent leukocyte adhesion to the endothelium and suppress production of pro-inflammatory LTs in rabbits (Bednar et al 2000). 8- and 11-HETE are potent neutrophil chemoattractants *in vitro* and in *in vivo* experimental models (Goetzl et al 1980a, Goetzl et al 1980b). However, their

derivation is uncertain and is thought to be from a combination of CYP, LOX and non-enzymatic oxidation pathways (Kuhn and O'Donnell 2006).

Eicosanoid production has been shown to increase following inflammation; however, the different metabolites of AA can be pro-inflammatory (e.g. LTs, PGs) and anti-inflammatory (e.g. PGs, EETs and HETEs) (Harizi et al 2008, Funk 2001, Bednar et al 2000, Fleming 2007), suggesting that the changes in pro-inflammatory and anti-inflammatory lipids are part of a dynamic process.

These COX, LOX and CYP pathways are also involved in the metabolism of other bioactive lipids involved in inflammation and pain, such as the endocannabinoids, AEA and 2-AG (Figure 4).

1.3.2.4 Other bioactive lipids involved in inflammation and pain

Other bioactive lipids that either promote or attenuate the inflammatory process include the polyunsaturated fatty acids, such as linoleic acid (LA) and the endocannabinoids and endocannabinoid-like compounds described. LA is a precursor of AA and can only be obtained from plant material in the diet. It is a key source for AA and, therefore, in eicosanoid synthesis (Chopade and Mulla 2010, Tapiero et al 2002). LA also generates hydroxyoctadecadienoic acids (HODEs), which are oxidised to oxooctadecadienoic acids (oxoODEs). These are generated through the action of 15-LOX and have been shown to be anti- and pro-inflammatory (See Chapter 4 for details, Vangaveti et al 2010).

1.3.3 Interaction of the bioactive lipids with different receptor systems

As mentioned previously, a number of bioactive lipids target several different receptor groups. These include cannabinoid receptors, PPARs (Harizi et al 2008) and TRPV1. These receptor groups are implicated in inflammation and pain; for example, PPARα (See Chapter 3) and TRPV1 (See Chapter 4). Several of these lipids, including AA, 5-HETE, 12-HETE, 15-HETE, 5-HPETE, 12-HPETE, 9-HODE, 13-HODE, 9-oxoODE, 13-oxoODE are agonists of TRPV1 receptors (Meves et al 2008, Patwardhan

et al 2009, Patwardhan et al 2010, Fowler 2007). PPARα activators include endogenous lipids such as 8-HETE, 20-HETE, 5,6-EET, 8,9-EET, 11,12-EET, 14,15-EET, 9-HODE, 13-HODE, LA, AA and LTB_4 (Yu et al 1995, Devchand et al 1996, Kliewer et al 1997, Delerive et al 2000, Cowart et al 2002). In addition to activating the cannabinoid receptors, the endocannabinoid AEA is also a PPARα agonist (Sun et al 2007), along with the endocannabinoid-like compounds OEA and PEA (Fu et al 2003, LoVerme et al 2005, Sun et al 2007, Moraes et al 2006). AEA and another endocannabinoid, NADA, also activate TRPV1 receptors (Huang et al 2002). The COX metabolites of AEA, the prostaglandin ethanolamides PGD_2-EA, PGE_2-EA and $PGF_{2\alpha}$-EA, are also agonists of the cannabinoid receptors (Matias et al 2004, Fowler 2007), as are the CYP metabolites of AEA and 2-AG, 5,6-epoxyeicosatrienoyl-ethanolamide (5,6-EET-EA) and 2-(14,15-epoxyeicosatrienoyl) glycerol (2-(14,15-EET)-G) respectively. 5,6-EET-EA has been shown to activate CB2 receptors (Snider et al 2009) and 2-(14,15-EET)-G activates both CB1 and CB2 receptors (Figure 4). The biological actions of some of these lipids are summarised in Table 1 (See Appendices for chemical structures).

Table 1. Receptor targets of the bioactive lipids of interest and evidence in inflammatory pain models

Chemical name	Synonym	CB_1	CB_2	$TRPV_1$	PPAR-α	Action in inflammatory pain models
Prostaglandin D_2 ethanolamide	PGD_2-EA	weak agonist	weak agonist			Yet to be shown (Matias et al 2004, Fowler et al 2007)
Prostaglandin E_1 ethanolamide	PGE_1-EA					Yet to be shown
Prostaglandin E_2 ethanolamide	PGE_2-EA		weak agonist			Yet to be shown (Matias et al 2004, Fowler et al 2007)
Prostaglandin $F_{2\alpha}$ ethanolamide	$PGF_2\alpha$-EA	agonist		weak agonist		Pro-inflammatory, produces allodynia following administration (Matias et al 2004, Minami et al 2001, Minami et al 1992, Fowler et al 2007)
5,6-epoxyeicosatrienamide	5,6-EET-EA		agonist			Yet to be shown (Snider et al 2009)
2-(14,15-epoxyeicosatrienoyl) glycerol	14,15-EET-G	agonist	Agonist			Yet to be shown (Chen et al 2008)
5-hydroperoxyeicosatetraenoic acid	5-HPETE			agonist		Yet to be shown (Hwang et al 2000)
12-hydroperoxyeicosatetraenoic acid	12-HPETE			agonist		Yet to be shown (Kim et al 2008, Hwang et al 2000)
5,6- dihydroxyeicosatrienoic acid	5,6-DHET					Yet to be shown, but DHETs thought to be pro-inflammatory (Inceoglu et al 2006)
8,9- dihydroxyeicosatrienoic acid	8,9-DHET					Yet to be shown, but DHETs thought to be pro-inflammatory (Inceoglu et al 2006)

Chemical name	Synonym	CB_1	CB_2	$TRPV_1$	PPAR-α	Action in inflammatory pain models
11,12- dihydroxyeicosatrienoic acid	11,12-DHET					Yet to be shown, but DHETs thought to be pro-inflammatory (Inceoglu et al 2006)
14,15- dihydroxyeicosatrienoic acid	14,15-DHET					Yet to be shown, but DHETs thought to be pro-inflammatory (Inceoglu et al 2006)
5- hydroxyeicosatetraenoic acid	5-HETE			agonist		Yet to be shown, thought to be pro-inflammatory (Goetzl et al 1982, Ross et al 2003, Hwang et al 2000)
8- hydroxyeicosatetraenoic acid	8-HETE				agonist	Yet to be shown, thought to be pro-inflammatory (Goetzl et al 1980a, Goetzl et al 1980b, Krey et al 1997, Funk 2001)
9- hydroxyeicosatetraenoic acid	9-HETE					Yet to be shown
11- hydroxyeicosatetraenoic acid	11-HETE					Yet to be shown, thought to be pro-inflammatory (Goetzl et al 1980a, Goetzl et al 1980b)
12- hydroxyeicosatetraenoic acid	12-HETE			agonist		Yet to be shown, thought to be pro-inflammatory (Bacon et al 1988, Dowd et al 1985, Kim et al 2008)
15- hydroxyeicosatetraenoic acid	15-HETE			agonist		Yet to be shown, thought to be pro-inflammatory (Johnson et al 1985, Hwang et al 2000)
16- hydroxyeicosatetraenoic acid	16-HETE					Yet to be shown, thought to be anti-inflammatory (Bednar et al 2000)
19- hydroxyeicosatetraenoic acid	19-HETE					Yet to be shown
20- hydroxyeicosatetraenoic acid	20-HETE				agonist	Yet to be shown (Cowart et al 2002)
5,6- epoxyeicosatrienoic acid	5,6-EET				agonist	↑ EET levels through soluble epoxide hydrolase (sEH) inhibition attenuated thermal hyperalgesia in inflammatory model (LPS model) (Cowart et al 2002, Inceoglu et al 2006)

Chemical name	Synonym	CB_1	CB_2	$TRPV_1$	PPAR-α	Action in inflammatory pain models
8,9- epoxyeicosatrienoic acid	8,9-EET				agonist	↑ EET levels through soluble epoxide hydrolase (sEH) inhibition attenuated thermal hyperalgesia in inflammatory model (LPS model) (Cowart et al 2002, Inceoglu et al 2006)
11,12- epoxyeicosatrienoic acid	11,12-EET				agonist	↑ EET levels through soluble epoxide hydrolase (sEH) inhibition attenuated thermal hyperalgesia in inflammatory model (LPS model) (Cowart et al 2002, Inceoglu et al 2006)
14,15- epoxyeicosatrienoic acid	14,15-EET				agonist	↑ EET levels through soluble epoxide hydrolase (sEH) inhibition attenuated thermal hyperalgesia in inflammatory model (LPS model) (Cowart et al 2002, Inceoglu et al 2006)
N-arachidonoyl ethanolamide	AEA	partial agonist	Agonist	agonist	agonist	↓AEA in rat paw tissue (Carrageenan model), no change in rat paw tissue (Formalin model)(Sagar et al 2009)
N-oleoyl ethanolamide	OEA			agonist	agonist	No change in levels in rat paw tissue (Carrageenan model)(Sagar et al 2009)
N-palmitoyl ethanolamide	PEA				agonist	↓PEA in rat paw tissue (Carrageenan model), no change in rat paw tissue (Formalin model)(Sagar et al 2009)
2-arachidonoyl glycerol	2-AG	agonist	Agonist			↓2-AG in rat paw tissue (Carrageenan model), no change in rat paw tissue (Formalin model)(Sagar et al 2009)
N-arachidonoyl dopamine	NADA	agonist		agonist		Yet to be shown (Bisogno et al 2000, Huang et al 2002). Intraplantar injection of the higher dose of NADA (5 μg/50 μL) significantly inhibited innocuous mechanically evoked responses of dorsal horn neurons compared to vehicle (Sagar et al 2004).
N-arachidonoyl glycine	AraGly					AraGly reduces allodynia and hyperalgesia in Freund's complete adjuvant-induced model of inflammatory pain in rats (Succar et al 2007)
Leukotriene-B_4	LTB_4				agonist	LTB_4 produces hyperalgesia in humans (Bisgaard and Kristensen 1985, Devchand et al 1996, Krey et al 1997)
Leukotriene-E_4	LTE_4					Yet to be shown, thought to be pro-inflammatory (Bjork et al 1982, Orange et al 1969, Svensjo 1978)

Chemical name	Synonym	CB_1	CB_2	$TRPV_1$	PPAR-α	Action in inflammatory pain models
Thromboxane-B_2	TXB_2					Yet to be shown, thought to be pro-inflammatory (Kitchen et al 1978)
Prostaglandin D_2	PGD_2					Yet to be shown, thought to be pro-inflammatory (Hirai et al 2001)
Prostaglandin E_2	PGE_2					Yet to be shown, thought to be pro-inflammatory (Kitchen et al 1978)
Arachidonic acid	AA			agonist	agonist	Yet to be shown (Meves et al 2008)
Linoleic acid	LA					Yet to be shown, conjugated linoleic acid thought to be anti-inflammatory (Yu et al 2002)
9-hydroxyoctadecadienoic acid	9-HODE			agonist	agonist	9, 13-HODE, 9- and 13-oxoODE produced behavioural pain responses following peripheral and spinal administration (Patwardhan et al 2010, Patwardhan et al 2010)
13-hydroxyoctadecadienoic acid	13-HODE			agonist	agonist	9, 13-HODE, 9- and 13-oxoODE produced behavioural pain responses following peripheral and spinal administration (Patwardhan et al 2010, Patwardhan et al 2010)
9-oxooctadecadienoic acid	9-oxoODE			agonist		9, 13-HODE, 9- and 13-oxoODE produced behavioural pain responses following peripheral and spinal administration (Patwardhan et al 2010, Patwardhan et al 2010)
13-oxooctadecadienoic acid	13-oxoODE			agonist		9, 13-HODE, 9- and 13-oxoODE produced behavioural pain responses following peripheral and spinal administration (Patwardhan et al 2010, Patwardhan et al 2010)

There is evidence for the interaction of the cannabinoid, PPARα and TRPV1 receptor systems in inflammatory hyperalgesia, which is briefly described below. A number of bioactive lipids such as AEA and OEA, are activators of all these receptor systems. Attenuation of inflammatory hyperalgesia has been shown in the carrageenan model following inhibition of catabolic enzymes, fatty acid amide hydrolase (FAAH) and COX-2, and these effects were blocked by the PPARα antagonist GW6741 but not a PPARγ antagonist, suggesting that the effects observed were PPARα-mediated (Jhaveri et al 2008b). Other research groups have shown that PEA causes PPARα-mediated effects in several animal models of pain behaviour (LoVerme et al 2006, D'Agostino et al 2009). Studies have also demonstrated the involvement of CB1, TRPV1 and PPARα in the hyperalgesic effects of PEA (Costa et al 2008). Furthermore, the synthetic CB1/CB2 agonist, WIN55212-2, binds to and increases the transcriptional activity of PPARα, indicating cannabinoid modulation of this nuclear receptor system (Sun et al 2006). Cannabinoid receptors and TRPV1 channels have been shown to be co-expressed in dorsal root ganglia (Ahluwalia et al 2000) and to be functionally active (Ahluwalia et al 2003). Cannabinoid receptors also have the ability to both enhance and attenuate TRPV1-mediated actions (Hermann et al 2003, Millns et al 2001). NADA has been shown to activate cannabinoid and TRPV1 channels (Huang et al 2002). Intraplantar injection of a high dose of NADA (5 μg/50 μL) significantly inhibited innocuous mechanically evoked responses of dorsal horn neurons compared to vehicle (Sagar et al 2004). These effects were blocked by intraplantar injection of rimonabant, a CB1 receptor antagonist. Furthermore, noxious-evoked responses of dorsal horn neurons were also significantly inhibited by NADA (5 μg/50 μL), and these effects were blocked by intraplantar injection of a TRPV1 antagonist, iodo-resiniferatoxin (Sagar et al 2004), again demonstrating an interaction between the cannabinoid and TRPV1 receptor systems.

1.4 Animal models of inflammatory pain

Experiments involving human subjects are ethically-challenging and the perception of pain can also be subjective; therefore, many animal models of inflammatory pain have been devised for this area of research (Kidd and Urban 2001). Animal models of inflammatory pain have been widely used to study the mechanisms of tissue injury-induced persistent pain and to investigate the anti-inflammatory and analgesic actions of novel or existing compounds. Studies conducted in animals can give an insight into certain aspects of human pain under inflammatory conditions and can lead to improved pain management or the discovery of novel treatments for patients. Although animal models of inflammatory pain do not simulate every aspect of chronic pain, they do model key features of human inflammatory pain. A variety of inflammatory agents and irritants have been used to produce tissue injury, inflammation and hyperalgesia in subcutaneous tissues, joints and muscles. These include complete Freund's adjuvant (CFA), carrageenan, formalin, capsaicin, lipopolysaccharide, mustard oil, acidic saline, inflammatory cytokines and sodium urate crystals (Mogil 2009, Kidd and Urban 2001, Chapman et al 1985). The carrageenan inflammatory pain model is described in more detail in Chapter 3.

1.5 Current analgesic treatments for inflammatory pain

Paracetamol is used in the treatment of mild to moderate pain. Non-steroidal anti-inflammatory drugs (NSAIDs) include aspirin, ibuprofen, naproxen and diclofenac are anti-inflammatory and analgesic treatments for mild to moderate pain. Non-selective inhibition of COX is considered to be the main mechanism of action of these drugs (Rainsford 2007), preventing the production of pro-inflammatory and pro-nociceptive prostanoids (See cyclooxygenase section). Adverse effects include gastrointestinal (GI) bleeding and ulceration, with long-term use leading to gastrointestinal damage and renal irritation (Koeberle and Werz 2009, Scott et al 2000). These GI side effects are a consequence of COX-1 inhibition, which is involved in the production of GI-protective

prostaglandins (Chan et al 1995). These adverse effects lead to the development of the selective COX-2 inhibitors, celecoxib and rofecoxib. However, both these drugs were shown to have adverse cardiovascular effects and were withdrawn from sale (Brophy 2005, Burnier 2005). Analgesics such as opioids, may be used for treatment of moderate to severe pain, due to the relative lack of effectiveness and side effects associated with the long-term use of NSAIDs (Scott et al 2000). These include codeine, morphine, fentanyl and oxycodone; however, many adverse effects such as nausea, constipation, respiratory depression and tolerance can limit their use (Labianca et al 2012). It is, therefore, necessary to develop novel drugs for the treatment of inflammatory pain, potentially involving novel anti-inflammatory and anti-nociceptive targets, including specific lipids and/or receptors. Evidence for the anti-inflammatory effects of PPARα ligands has emerged (See Chapter 3 for details), along with TRPV1 receptor antagonism and TRPV1 ligands (See Chapter 4 for details). However, a substantial amount of work remains to be done to fully understand the roles of the different receptor systems involved in inflammatory pain mechanisms. In order for this to be achieved, quantification of a large number of bioactive lipids in tissues involved in inflammation and pain processing is necessary.

1.6 Analytical methodology for the identification and quantification of bioactive lipids

Metabolomics has been defined as the systematic study and quantitative measurement of either the unique chemical fingerprints that specific cellular processes leave behind or the total biochemical complement of a cell or a particular organ (Fiehn 2002, Daviss 2005). However, as the field of global metabolite profiling has developed, this distinction has become blurred and the use of terms is now usually based on personal preference (For a review, see Lindon and Nicholson 2008). In general, analytical strategies are applied to collect targeted or untargeted analytical data to investigate the patterns and concentrations of low molecular weight lipids in biofluids, cells or tissues. An ideal analytical method would involve little or no sample preparation, providing direct

analysis of the samples, rapidly and at the same time being highly and equally sensitive to all lipids present in samples and be robust and reproducible (Lenz and Wilson 2007). However, unsurprisingly, no such method providing all these desired properties currently exists.

Lipidomics is defined as the systems-level analysis and characterisation of lipids and their interacting moieties (Wenk 2005), and is a relatively young field of biomedical research. The importance of lipidomics is now widely recognised and is reflected by international initiatives that aim at investigating lipid function in physiology and disease (Wenk 2005). An example of this, is the LIPID MAPS initiative, a consortium with the mission to comprehensively measure all of the lipids in a human macrophage cell line. Lipids involved in signalling are not very abundant in resting conditions but may accumulate dramatically upon stimulation of a cell (Wenk 2005). The protein machinery responsible for such changes can be a single enzyme or a set of enzymes working in sync. The levels of these enzymes might well be relatively constant, which makes it difficult to detect such cases by expression profiling or the measurement of protein levels. In fact, it could be proposed that even enzymatic activities might change only moderately in different functional states of the cell. Careful inspection of the lipid metabolites involved will help to pinpoint underlying metabolic pathways in such events. Such information can now be determined with high precision analytical methodologies including gas chromatography mass spectrometry (GC-MS) and liquid chromatography mass spectrometry (LC-MS). A disadvantage of early mass spectrometry was fragmentation of the lipid analyte during ionisation, making assignments of free fatty acids, backbones and headgroups a difficult task. This and the high chemical backgrounds observed in early studies with fast-atom bombardment and chemical ionisation were further disadvantages, in particular for the analysis of complex lipid mixtures (Wenk 2005). However, over time, methodology and techniques for measuring lipid species have improved and these developments in methodology are supported by the more widespread availability of reagents and tools, such as synthetic lipid standards. These

developments highlight the importance of high quality analytical methods in lipid research.

1.6.1 Analytical methodologies

GC-MS is commonly used for identification and quantification of trace compounds in complex sample mixtures. It is most advantageous for analysis of trace amounts of organically extractable, non-polar, volatile compounds because the analyte is required to be in the gas phase and also applies to mass spectrometry analysis. GC-MS provides a powerful tool with strengths resulting from its sensitivity and metabolite identification potential but also weaknesses due to its poor ability to analyse large and/or non-volatile molecules without prior derivatisation (Muccio and Stella 2008, Prakash et al 2007). Sample preparation can often be time-consuming and labour-intensive (Fiehn et al 2000, Kanani et al 2008, Strehmel et al 2008). However, because the majority of the metabolites encountered in biological samples are not volatile and due to the need to obtain the maximum possible coverage of the metabolome, profiling by LC–MS is usually favoured (Theodoridis et al 2008).

LC-MS has become a favoured method among researchers for bioactive lipid analysis due to the improved speed, sensitivity and specificity and also enhanced resolution, especially seen with the LC-tandem MS (LC-MS/MS). High performance liquid chromatography (HPLC) coupled to MS requires less sample 'clean-up' and there is no need for chemical derivatisation or exposure to excessive heat and sample throughput is generally greater than with GC-MS. An effective ion source to convert the solution of molecules from the liquid phase to the gas phase is important in LC-MS. The most common vaporisation techniques used are electrospray ionisation (ESI) and atmospheric pressure chemical ionisation (APCI) (McMaster 2005, Prakash et al 2007).

Currently, ESI is the method of choice in LC-MS, because it produces a large number of ions via charge exchange in solution (Sana et al 2008). APCI on the other hand produces ions by charge exchange in the gas phase and may provide a wider dynamic range (Want et al 2005), lower

signal intensities, background noise and in-source fragmentation compared to ESI (Aharoni et al 2002). ESI-MS was also found to show excellent reproducibility of results from the same samples (Aharoni et al 2002). Baseline noise can be a problem with low abundance species like the bioactive lipids of interest and tandem mass spectrometric analysis is able to reduce this problem and simplify the spectrum (Han and Gross 2005).

1.6.2 Measurement of bioactive lipids

Various analytical techniques have been employed for investigating bioactive lipids in biological samples. The low abundance of these compounds means they are usually quantified by isotope dilution assays using mass spectrometry coupled to either LC or GC as discussed (Hardison et al 2006). Mass spectrometry allows a complex mixture to be analysed for trace amounts of a particular compound and this technique can be used to confirm the presence of a compound based on the precise mass of compounds and a fragment ion spectrum can also be generated to help determine the structure of an unknown molecule (McMaster 2005, Prakash et al 2007).

Many analytical LC-MS/MS methods utilise targeted lipidomics, and measure the eicosanoids (Blewett et al 2008, Kortz et al 2009, Yue et al 2007, Yoshida et al 2008, Zhang et al 2007) or the endocannabinoids (Zhang et al 2010, Balvers et al 2006, Chen et al 2009, Palandra et al 2009, Richardson et al 2007) separately (See Chapter 2 for details). However to date, a targeted analytical method that is able to identify and quantify both these lipid classes within the same method still remains to be developed. This would enable maximum coverage of the metabolome, in this case the lipid mediators involved in the inflammatory process. A major advantage of such lipidomics-based discovery is that, together with our relatively good understanding of many biosynthetic and metabolic pathways, it will lead to further clarification of the involvement of these pathways and enzymes in this area of research. The development of an analytical method that is able to identify and quantify a large number of

bioactive lipid mediators in the inflammatory process, combined with pharmacological studies evaluating the effects of these lipids in inflammation and hyperalgesia may address any unexplained questions in this area of research.

1.7 General Aims and Objectives

The aim of the thesis is to develop a sensitive, robust and reproducible LC-MS/MS method for the simultaneous measurement of bioactive lipids discussed in this chapter and to apply this method to understand better the role of these bioactive lipids in inflammation and pain.

The specific objectives were:

- To develop an LC-MS/MS method capable of simultaneously measuring bioactive lipids including eicosanoids
- To determine whether levels of these bioactive lipids are altered in a model of acute inflammatory pain
- To determine the potential role of these bioactive lipids in different receptor-mediated pathways such as PPARα and TRPV1
- To determine whether levels of these bioactive lipids are altered in a model of chronic joint pain

Chapter 2.

Development of an LC/MS-MS analytical method to identify and quantify levels of bioactive lipids in different tissues.

2. Development of an LC/MS-MS analytical method to identify and quantify levels of bioactive lipids in different tissues.

2.1 Introduction

Liquid chromatography tandem mass spectrometry (LC-MS/MS) has played an important role in lipidomics since its introduction. LC-MS/MS has led to major breakthroughs in the field of quantitative bioanalysis since the 1990s due to inherent specificity, sensitivity and speed (Xu et al 2007).

There are a number of factors in LC-MS/MS method development that bioanalysts would consider to be of prime importance including sample preparation, chromatographic separation and mass spectrometry conditions. Bioanalysts must also take into account and reduce matrix effects, which can have a considerable effect on the way the analysis is conducted and the quality of the results obtained (see later). After an analytical method has been optimised in terms of LC mobile phase, mass spectrometric parameters and chromatographic peak efficiency, there is little a bioanalyst can do to further optimise sensitivity (Jemal 2000).

2.1.1 Validation

The next process following extensive method development involves a full validation of the analytical methodology. Validation of a method is the accepted way to ensure confidence in bioanalytical data, where the procedure is designed to assess the performance of the method in a biological matrix. There are few analytical methodologies that are fully validated according to these guidelines, many of which are industry-based. This can be an intensive and extensive process, particularly if the methodology involves a large number of analytes.

Validation comprises several elements; accuracy, precision, linearity, recovery and ion suppression. Guidelines are set by the Food and Drug Administration (FDA 2001 Guidance for Industry-Bioanalytical method

validation-November 2010), which generally applies to bioanalytical procedures such as GC, HPLC and combined GC and HPLC mass spectrometric procedures GC-MS, GC-MS/MS, LC-MS and LC-MS/MS. These procedures are performed for quantitative determination of drug and/or metabolites in biological matrices including blood, serum and plasma (FDA 2001 Guidance for Industry-Bioanalytical method validation-November 2010). The *accuracy* of an analytical method describes the closeness of mean test results obtained by the method to the concentration of the analyte. The mean value should be within 15% of the actual value (concentration chosen) except at the lower limit of quantification (LLOQ), where it should not deviate by more than 20%. The deviation of the mean from the true value serves as a measure for accuracy. The *precision* of an analytical method describes the closeness of individual measures of an analyte when the procedure is repeatedly applied to multiple aliquots of a single homogenous volume of biological matrix. This is further divided into inter- and intra- batch precision. The precision should not exceed 15% of the coefficient of variation (CV) except for the LLOQ, where it should not exceed 20% of the CV (FDA 2001 Guidance for Industry-Bioanalytical method validation-November 2010). Linearity is determined by a standard calibration curve (relationship between instrument response and known concentrations of the analyte), where standard concentrations are chosen based on the concentration range expected in a particular study. Recovery is the detector response obtained from an amount of the analyte added to and extracted from the biological matrix, compared to the detector response obtained for the true concentration of a pure standard. Quantitative analysis with electrospray ionisation (ESI) or atmospheric pressure chemical ionisation (APCI) can be substantially affected by the occurrence of ion-suppression or –enhancement, otherwise known as matrix effects. This phenomenon is caused by the presence of a matrix or other interferences in the sample and is responsible for poor and unreliable data in a quantitative assay. Matrix effects can also affect the reproducibility, linearity and accuracy of the method (Trufelli et al 2011).

It is important to consider all these factors during the method development process.

2.1.2 LC-MS/MS analysis of bioactive lipids

Biological processes such as inflammation and pain, which involve lipid mediators are complex events and often include significant regional changes in the levels of many lipid species. To fully understand these biochemical events it is now appreciated that measurement of changes in the profile of these bioactive lipids is essential. Although LC-MS/MS methods have been developed for bioactive lipids such as Buczynski et al 2010, who utilise the resources of the Lipid Maps database mentioned earlier (Lipid Maps-Nature Lipidomics Gateway, February 2010). It is often the case that the methods have been limited to a relatively small number of lipids or for a specific type of tissue. Structural similarity and isomerisation are a challenge and this has been addressed in a number of papers (Masoodi et 2010, Jiang et al 2004). However although the majority of lipid analysis by LC-MS/MS is in negative ionisation mode, a significant number of modified bioactive lipids have to be identified in positive mode. The endocannabinoids (altered in inflammatory pain models) (Sagar et al 2009, Mbvundula et al 2004) are an example of this, where these lipids and structurally-related species do not ionise well in negative ion mode. A number of LC-MS/MS profiling methods have been published (Table 1).

Table 1. Current literature on the lipid profiling of the eicosanoids or endocannabinoids in different tissues and species.

Reference	Analytical Method	Ionisation mode	Type of lipids analysed	Tissues analysed
De Grauw et al 2011	LC-MS/MS	Negative ESI mode	Eicosanoids	Equine synovial fluid
Ferreiro-Vera et al 2011	SPE-LC-MS/MS	Negative ESI mode	Eicosanoids	Human serum, bone marrow, mesenchymal cell cultures
Buczynski et al 2010	LC-MS/MS and GC-MS/MS	One method in negative and one method in positive ESI mode	Eicosanoids and endocannabinoids	Rat cerebral spinal fluid and spinal cord
Kortz et al 2009	SPE-LC-MS/MS	Negative ESI mode	Eicosanoids	Human plasma
Lundstrom et al 2009	RP-HPLC-MS/MS	Negative ESI mode	Eicosanoids	Human bronchoalveolar lavage fluid
Richardson et al 2007	LC-MS/MS	Positive ESI mode	Endocannabinoids	Rat brain regions
Masoodi et al 2008	LC-MS/MS	Negative ESI mode	Eicosanoids	Rat brain, liver and plasma
Yang et al 2006	RP-HPLC-MS/MS	Negative ESI mode	Eicosanoids	Mouse xenograft tumour model, hamster squamous cell carcinoma model, mouse prostatic lobes

Although a number of LC-MS/MS methods have been published to date (Table 1), focussing on a large proportion of the lipid cascade, there is not yet a method available that incorporates negative to positive ionisation mode switching for quantification of bioactive lipids in both ionisation modes. The main difficulty that a bioanalyst has to overcome is the difference in mass spectrometry ionisation modes. Eicosanoids are readily ionised in negative ionisation mode (mainly acid based molecules), whereas the endocannabinoids are better ionised in positive ionisation mode (some are nitrogen containing molecules). This would enable maximum coverage of the inflammatory lipidome, in this case the

lipid mediators involved in the inflammatory process. Currently, the utilisation of ion sources capable of fast switching between ionisation modes is not common. This is due to the loss of sensitivity that is incurred as a result of the switching process and, also, because the capacity for polarity switching in older machines is often poor. In such cases, the samples are first analysed in positive mode and then re-analysed in negative mode to overcome this. However, this doubles analysis time and may not be suitable for samples of poor stability or those prone to degradation. Triple quadrupole mass spectrometers can provide automatic polarity switching and, hence, enable reduced analysis time, but by sacrificing some sensitivity. However, even with these instruments, there are still many chromatography-based challenges that need to be overcome for the methodology to succeed and is discussed later.

Many analytical LC-MS/MS methods measure the eicosanoids (Blewett et al 2008, Yue et al 2007, Yoshida et al 2008,, Zhang et al 2007, Nithipatikom et al 2001) or the endocannabinoids (Zhang et al 2010, Balvers et al 2006, Chen et al 2009) separately, however there are very few LC-MS/MS methods that provide a full lipid profile of important inflammatory mediators and when this occurs, it is usually achieved with two or more different methods (Buczynski et al 2010). Lipid profiling of a large number of eicosanoids have previously been achieved in rat spinal cord (Buczynski et al 2010) and rat brain, liver and plasma have been used in the validation of a profiling method (Masoodi et al 2008). The majority of LC-MS/MS methods focus on a selective small group of lipids and validated methods often use human plasma as the biological tissue of interest.

Profiling of these bioactive lipids involve many difficulties as many eicosanoids have very similar or even identical (isomeric) chemical structures and therefore a single *m/z* transition may not be as specific to individual compounds as desired (De Grauw et al 2011). Another challenge is the analytical determination of a large number of bioactive lipids in a single biospecimen, often necessary to fully characterise the

relevant biochemical processes. These bioactive lipids are all produced under related cascades of biochemical signalling events and the lipid species produced are often enzymatically linked to one another. An analytical method that can incorporate all these lipids in a single analytical assay would be ideal to determine all relevant lipids involved in a particular biological process. An analytical method which is highly selective and able to distinguish between similar structures and has sufficiently high sensitivity to be able to detect small amounts in biological tissue is therefore required.

2.1.3 LC-MS/MS analysis of bioactive lipids in different tissues

Numerous analytical methods have also identified and quantified the eicosanoids and endocannabinoids in different tissues (Table 2 and 3). As mentioned previously, the majority of the methods in the literature only measure a selective number of lipids in the different tissues, which may be due to the reasons discussed earlier. An overview of current literature on the separation and quantification of eicosanoids (Table 2) and endocannabinoids and endocannabinoid-like compounds (Table 3) in different species and tissues were presented.

Table 2a. Current literature on the identification and quantification of eicosanoids (-ve ionisation mode) in different tissues and species.

EICOSANOIDS		Analytical Conditions	Extraction Method	Analyte Summary	References
Rat	Spinal Cord	A: ACN:H_2O:acetic acid, B:ACN:isopropyl alcohol. C18 SPE-LC-MS/MS	Extraction with SPE (Phenomenex Strata-X) with 10% MeOH	Eicosanoid profiling	Buczynski et al 2010
	Trigeminal Neurons	A:H_2O, B:ACN, both with 0.002% acetic acid. C18 ESI-LC-MS/MS	Extraction with MeOH	8 eicosanoids detected including EETs, HETEs and DHETs	Iliff et al 2010
	Brain	A:MeOH:H_2O, B:ACN:H_2O, both with acetic acid. C18 ESI-LC-MS/MS	Extraction with SPE (Phenomenex Strata-X) with <15% MeOH	Eicosanoid profiling	Masoodi et al 2008
	Brain	A:Acetic acid buffered with NH_4OH, B:ACN:MeOH. C18 ESI-LC-MS/MS	Extraction with SPE (Phenomenex Strata-X) with <15% MeOH	Eicosanoid mediators of arachidonic acid and docosahexaenoic acid	Farias et al 2008
	Brain	A:H_2O, B:ACN, both with 0.1% formic acid. C18 ESI-LC-MS/MS	Extraction with SPE (Oasis HLB) with <15% MeOH	Eicosanoid profiling	Yue et al 2007
	Brain	A:H_20, B:MeCN:formic acid (100:0.1), C:H_2O:formic acid (100:0.1), D:MeOH:formic acid(100:0.2). C18 ESI-LC-MS/MS	Extraction with SPE (Oasis HLB) with <15% MeOH	Eicosanoid profiling	Yoshikawa et al 2006
	Kidney	A:ACN, B:H_2O, both with 0.1% formic acid. C18 ESI-LC-MS/MS	Extraction with SPE (Oasis HLB) with 10% MeOH (with formic acid and ethyl acetate)	Profiling of 23 eicosanoids	Blewett et al 2008
	Liver	A:MeOH:H_2O, B:ACN:H_2O, both with acetic acid. C18 ESI-LC-MS/MS	Extraction with SPE (Phenomenex Strata-X) with <15% MeOH	Eicosanoid profiling	Masoodi et al 2008

Table 2b. Current literature on the identification and quantification of eicosanoids (-ve ionisation mode) in different tissues and species.

EICOSANOIDS		Analytical Conditions	Extraction Method	Analyte Summary	References
Rat	Serum	A:10mM ammonium formate in H_2O, B:ACN with 0.1% formic acid. C18 ESI-LC-MS/MS	Extracted with ACN	6 eicosanoids including AA, PGD2 and LTB4	Bai et al 2010
	Plasma	A:MeOH: H_2O, B:ACN:H_2O, both with acetic acid. C18 ESI-LC-MS/MS	Extraction with SPE (Phenomenex Strata-X) with <15% MeOH	Eicosanoid profiling	Masoodi et al 2008
Mouse	Spinal Cord	A: H_2O, B:MeCN:formic acid (100:0.1), C: H_2O:formic acid (100:0.1), D:MeOH:formic acid (100:0.2). C18 ESI-LC-MS/MS	Extraction with SPE (Oasis HLB) with <15% MeOH	Eicosanoid profiling	Kihara et al 2009
	Brain	A: H_2O, B:ACN, both with 0.1% formic acid. C18 ESI-LC-MS/MS	Washed with hexane and formic acid, then extracted with chloroform	Prostaglandins	Brose et al 2011
	Brain	A: H_2O, B:ACN, both with 0.1% formic acid. C18 RP-ESI-LC-MS/MS	Extraction with ACN	EETs	Marowsky et al 2009
Human	Synovial Fluid	A: H_2O:ACN:acetic acid (70:30:0.02), B: ACN-isopropyl alcohol (50:50). C18 ESI-LC-MS/MS	Extraction with MeOH:EtOH:H_2O (2:1:1)	Eicosanoid profiling	Blaho et al 2009
	Uterine Tissue	A:0.05% formic acid in H_2O, B:MeOH:ACN (20:80). C18 ESI-LC-MS/MS	Extraction with SPE (Phenomenex Strata-X) with 25% EtOH	13 eicosanoids including HETEs and EETs	Zhang et al 2007
	Liver	A:2mM ammonium acetate in H_2O, B:MeOH:ACN (5:95) C18 ESI-LC-MS/MS	Extraction with chloroform:ethyl acetate (4:1)	10 eicosanoids including HETEs and HODEs	Yoshida et al 2008

Table 2c. Current literature on the identification and quantification of eicosanoids (-ve ionisation mode) in different tissues and species.

EICOSANOIDS		**Analytical Conditions**	**Extraction Method**	**Analyte Summary**	**References**
Human	Plasma	Isocratic gradient of ACN/ H_2O /MeOH/acetic acid (75:15:10:0.05). C18 ESI-LC-MS/MS	Extraction with $CHCl_3/CH_3OH$ (2:1)	5 eicosanoids, including EETs, 20-HETE	Minuz et al 2008
	Plasma	A:2mM ammonium acetate in H_2O, B:MeOH:ACN (5:95) C18 ESI-LC-MS/MS	Extraction with chloroform:ethyl acetate (4:1)	10 eicosanoids including HETEs and HODEs	Yoshida et al 2008
	Plasma	A:1mmol/L formic acid in H_2O, B:ACN. Inertsil ODS-3 LC column, LC-MS/MS	Extraction by C18 SPE (Bond Elut) with ethyl acetate, MeOH, H_2O and 1% acetic acid	Prostaglandins	Komaba et al 2009
	Urine	A: H_2O, B:ACN, both with 0.1% formic acid. C18 ESI-LC-MS/MS	Extraction with C18 SPE (Sep-Pack) with ethyl acetate	15 eicosanoids including HETEs, EETs and 13-HODE	Martin-Venegas et al 2011
	Urine	Isocratic gradient of ACN / H_2O / MeOH/acetic acid (75:15:10:0.05). C18 ESI-LC-MS/MS	Extraction with $CHCl_3/CH_3OH$ (2:1)	5 eicosanoids, including EETs, 20-HETE	Minuz et al 2008

Table 3a. Current literature on the identification and quantification of endocannabinoids (+ve ionisation mode) in different tissues and species.

ENDOCANNABINOIDS		Analytical Conditions	Extraction Method	Analyte Summary	References
Rat	Hindpaw	A: H_2O, B:ACN, both with 1g/L ammonium acetate and 0.1% formic acid. C8 ESI-LC-MS/MS	Extraction with ethyl acetate/hexane (9:1)	Endocannabinoids and endocannabinoid-like compounds 2-AG, AEA, OEA and PEA.	Jhaveri et al 2008
	Hindpaw	A: H_2O, B:MeOH. C18 ESI-LC-MS/MS	Extraction with chloroform:H_2O (2:1)	Endocannabinoids 2-AG and AEA	Guindon et al 2011
	Spinal Cord	A: ACN: H_2O:acetic acid, B:ACN:isopropyl alcohol. C8 RP-LC-MS/MS	Extraction with SPE (Phenomenex Strata-X) with 10% MeOH	Ethanolamine profiling	Buczynski et al 2010
	Spinal Cord	A: H_2O, B:ACN, both with 1g/L ammonium acetate and 0.1% formic acid. C8 ESI-LC-MS/MS	Extraction with ethyl acetate/hexane (9:1)	Endocannabinoids and endocannabinoid-like compounds 2-AG, AEA, OEA and PEA.	Staniaszek et al 2010
	DRGs	Isocratic gradient of H_2O /MeOH with 0.005% acetic acid and 1mM ammonium acetate. C18-RP-APCI-LC-MS/MS	Extraction with ACN	Endocannabinoids 2-AG and AEA	Mitrirattanakul et al 2006
	Brain	A: 5% methanol in H_2O, B:MeOH, both with 1mM ammonium acetate and 0.1% acetic acid. C18 ESI-LC-MS/MS	Extraction with ACN	3 endocannabinoids	Chen et al 2009
	Brain	A:ACN, B: H_2O, both with 0.1% formic acid. C18 ESI-LC-MS/MS	Homogenised with MeOH, followed by extraction with chloroform	Endocannabinoids 2-AG and AEA	Malinen et al 2009

Table 3b. Current literature on the identification and quantification of endocannabinoids (+ve ionisation mode) in different tissues and species.

ENDOCANNABINOIDS		Analytical Conditions	Extraction Method	Analyte Summary	References
Rat	Brain	A: H_2O, B:ACN, both with 0.05% formic acid. C18 ESI-LC-MS/MS	Extraction with chloroform:MeOH (2:1)	Endocannabinoids and endocannabinoid-like compounds 2-AG, AEA, OEA and PEA.	Artmann et al 2008
	Brain	A: H_2O, B:MeOH, both with 10mM ammonium acetate. C18 micro ESI-micro LC-MS/MS	Extraction with customised microSPE (Spark Holland) with MeOH/H_2O	Endocannabinoids 2-AG and AEA	Bequet et al 2007
	Brain	A: H_2O, B:ACN, both with 1g/L ammonium acetate and 0.1% formic acid. C8 ESI-LC-MS/MS	Extraction with ethyl acetate/hexane (9:1)	Endocannabinoids and endocannabinoid-like compounds 2-AG, AEA, OEA and PEA.	Richardson et al 2007
	Brain	A:10mM ammonium acetate, B:MeOH. Zorbax SB-CN APCI-LC-MS/MS	Extraction with chloroform:MeOH (2:1)	Profiling of ethanolamine and glycerol products from different fatty acids	Williams et al 2007
	Brain	Isocratic gradient of H_2O /MeOH with 0.005% acetic acid and 1mM ammonium acetate. C18 ESI-LC-MS/MS	Extraction with ACN	Endocannabinoids 2-AG and AEA	Mitrirattanakul et al 2007
	Brain	TraceDSQ equipped with Rtx-5MS column. GC/Chemical ionisation MS	Extraction with chloroform:H_2O, followed by C18 SPE (Bond Elut) with MeOH	Endocannabinoids 2-AG and AEA	Hardison et al 2006

Table 3c. Current literature on the identification and quantification of endocannabinoids (+ve ionisation mode) in different tissues and species.

ENDOCANNABINOIDS		**Analytical Conditions**	**Extraction Method**	**Analyte Summary**	**References**
Rat	Plasma	A:2mM ammonium acetate, B:ACN, both with 0.1% formic acid. C18 UPLC-MS/MS	Extraction with SPE (Oasis HLB) with MeOH:H_2O	Endocannabinoid AEA and endocannabinoid-like compounds PEA and OEA	Fonseca et al 2010
Mouse	Brain	Ethanolamines derivatised to TMS-ethers and analysed by GC-MS	Extraction with chloroform, isopropanol and H_2O	Ethanolamines	Kilaru et al 2010
	Brain	A: H_2O, B:MeOH:H2O (9:1), both with 70µM silver acetate. C8 ESI LC-MS/MS	Extraction with C18 SPE (Bond Elut) with MeOH/H_2O	Endocannabinoids including 2-AG and AEA	Placzek et al 2010
Human	Brain	Isocratic gradient with H_2O /ACN/formic acid (33:67:0.1). C18 ESI LC-MS/MS	Extraction with chloroform:H_2O, followed by C18 SPE (Bond Elut) with MeOH	Endocannabinoids AEA, NADA and 2-AG and endocannabinoid-like compounds PEA and OEA	Lehtonen et al 2011
Human	Plasma	A: H_2O, B:MeOH, both with 0.2% acetic acid. C18 ESI LC-MS/MS	Extraction with ACN	2-AG, 1-AG and AA	Zhang et al 2010
	Plasma	A: H_2O, B:ACN, both with 1g/L ammonium acetate and 0.1% formic acid. C8 ESI-LC-MS/MS	Extraction with ethyl acetate/hexane (9:1)	Endocannabinoids AEA and 2-AG, endocannabinoid-like compounds OEA and PEA	Jean-Gilles et al 2009
	Plasma	A:ACN, H_2O, both with 0.1% formic acid. XTerra column. LC-MS/MS.	Extraction with heptane/ethyl acetate (1:1)	Endocannabinoids AEA, NADA and 2-AG	Thomas et al 2009

Table 3d. Current literature on the identification and quantification of endocannabinoids (+ve ionisation mode) in different tissues and species.

ENDOCANNABINOIDS		Analytical Conditions	Extraction Method	Analyte Summary	References
Human	Plasma	A:H_2O:MeOH (95:5), B:MeOH, both with 1g/L ammonium acetate and 0.1% formic acid. C8 ESI-LC-MS/MS	Extraction by C8 SPE (Bond Elut) with ACN	Endocannabinoids AEA and NADA, including endocannabinoid-like compounds PEA and OEA	Balvers et al 2009
	Plasma	A: H_2O, B:ACN, both with 1g/L ammonium acetate and 0.1% formic acid. C8 ESI-LC-MS/MS	Extraction with ethyl acetate/hexane (9:1)	Endocannabinoids and endocannabinoid-like compounds 2-AG, AEA, OEA and PEA	Jhaveri et al 2008

A large proportion of the current literature reviewed here utilised C18-ESI-LC-MS/MS methodology for eicosanoid analysis, whereas C8- and C18-ESI-LC-MS/MS methodology was employed for endocannabinoid analysis. The analytical conditions were also very similar for both these lipid classes reviewed, with the majority having used methanol or acetonitrile along with acetic or formic acid and their salts, including ammonium salts to control the pH of mobiles phases (Bai et al 2010, Fonseca et al 2010, Yoshida et al 2008, Mitrirattanakul et al 2007, Williams et al 2007). Extraction methods on the other hand, were more variable, with some methods having used solid phase extraction (SPE)(Buczynski et al 2010, Masoodi et al 2008, Farias et al 2008, Richardson et al 2007). SPE was found to increase MS specificity and sensitivity and also prolong HPLC column life (Richardson et al 2007). It is a useful technique when large amounts of tissue (>200mg) are used by preventing HPLC overload and for sample clean-up, however when small tissue weights are involved (<70mg) this can interfere with analyte recovery (Poole 2003).

A number of the eicosanoids were shown to be unstable to oxidation (Iliff et al 2010, Blewett et al 2008). 5,6-epoxyeicosatrienoic acid (5,6-EET) was initially undetectable in trigeminal ganglion neurons, but the spontaneous oxidative breakdown product of 5,6-EET, 5,6-dihydroxyeicosatrienoic acid (5,6-DHET) was detectable, however this issue was resolved through sample collection and storage modifications (Iliff et al 2010). The lipoxygenase metabolites, leukotriene C_4 (LTC_4) and leukotriene D_4 (LTD_4) are also inherently unstable *in vivo* and *ex vivo*. *In vivo*, peptidase enzymes catalyse the cleavage of amino acid residues on LTC_4 and LTD_4 and *ex vivo*, autooxidative degradation occurs (Blewett et al 2008). Therefore, some methods may include an antioxidant, which is normally added during sample extraction to minimise formation of oxidation products prior to analysis. These include butylhydroxytoluene (Blewett et al 2008, Yoshida et al 2008, Zhang et al 2007) and triphenylphosphine (Minuz et al 2008).

The majority of the methods listed in Table 2 and 3 focus on singular pathways or phases of the inflammatory response, which increase our knowledge of the inherent potential of certain molecules. However, this provides an incomplete picture and gives the impression that some lipids function in isolation. In reality, this is more complex and are likely to be governed by upstream mediators, which in turn, regulate other metabolites to produce the overall outcome of inflammatory responses. Ideally, an analytical method that can measure a large proportion of the inflammatory cascade and fully characterise this biochemical process is therefore needed. However, another difficulty in analytical method development is that a number of compounds that are biologically active *in vivo* are not readily available as commercial standards. These include 15-hydroperoxyeicosatetraenoyl glycerol (15-HPETE-G), a peroxisome proliferator activated receptor alpha (PPARα) agonist (Vandevoorde 2007) and 2-(11,12-epoxyeicosatrienoyl)-glycerol (11,12-EET-G), a cannabinoid receptor-1 (CB1) and cannabinoid receptor-2 (CB2) agonist (Chen et al 2008). Experiments involving these compounds could be conducted if the compounds were either synthesised (Chen et al 2008) or through qualitative analysis (Blewett et al 2008, Yue et al 2007). Therefore, in order to develop an analytical method that can achieve this, it would involve overcoming the challenges in method development as discussed earlier. The ability to measure and investigate all relevant bioactive lipids in the same methodology would aid our understanding of this complex system and to be able to fully appreciate what is happening *in vivo*.

2.1.4 Aims and Objectives

- To develop and validate an LC/MS-MS analytical method that can simultaneously measure a wide range of bioactive lipids including eicosanoids and endocannabinoids
- To measure and determine the levels of these bioactive lipids in different biological tissues in the rat
- To compare the distribution of measured lipids between the different biological tissues

2.2 Materials and Methods

2.2.1 Chemicals

Acetonitrile, ammonium hydroxide, ethanol, ethyl acetate, hexane, formic acid and methanol were all purchased from Fisher Scientific (Loughborough, UK). All solvents were HPLC grade and far UV grade acetonitrile was also used. Prostaglandin D_2 ethanolamide (PGD_2-EA), prostaglandin E_1 ethanolamide (PGE_1-EA), prostaglandin E_2 ethanolamide (PGE_2-EA), prostaglandin $F_{2\alpha}$ ethanolamide ($PGF_{2\alpha}$-EA), 5,6-dihydroxyeicosatrienoic acid (5,6-DHET), 8,9-dihydroxyeicosatrienoic acid (8,9-DHET), 11,12-dihydroxyeicosatrienoic acid (11,12-DHET), 14,15-dihydroxyeicosatrienoic acid (14,15-DHET), 8,15-dihydroxyeicosatetraenoic acid (8,15-DiHETE), 9-hydroxyeicosatetraenoic acid (9-HETE), 11-hydroxyeicosatetraenoic acid (11-HETE), 12-hydroxyeicosatetraenoic acid (12-HETE), 15-hydroxyeicosatetraenoic acid (15-HETE), 16-hydroxyeicosatetraenoic acid (16-HETE), 19-hydroxyeicosatetraenoic acid (19-HETE), 20-hydroxyeicosatetraenoic acid (20-HETE), arachidonic acid (AA), linoleic acid (LA), 5-hydroperoxyeicosatetraenoic acid (5-HPETE), 9-hydroxyoctadecadienoic acid (9-HODE), 13-hydroxyoctadecadienoic acid (13-HODE), 9-oxooctadecadienoic acid (9-oxoODE), 13-oxooctadecadienoic acid (13-oxoODE), leukotriene-B_4 (LTB_4), leukotriene-E_4 (LTE_4), prostaglandin D_2

(PGD_2), prostaglandin E_2 (PGE_2), thromboxane-B_2 (TXB_2) N-arachidonoyl ethanolamide (AEA), 2-arachidonoyl glycerol (2-AG), N-palmitoyl ethanolamide (PEA), N-oleoyl ethanolamide (OEA), N-arachidonoyl dopamine (NADA), N-arachidonoyl glycine (AraGly), 5,6-epoxyeicosatrienamide (5,6-EET-EA), 2-(14,15-epoxyeicosatrienoyl)-glycerol (14,15-EET-G), arachidonic acid-d8 (AA-d8), prostaglandin D_2-d4 (PGD_2-d4), prostaglandin $F_{2\alpha}$ ethanolamide-d4 ($PGF_{2\alpha}$-EA-d4), N-arachidonoyl ethanolamide-d8 (AEA-d8) and 2-arachidonoyl glycerol-d8 (2-AG-d8) were purchased from Cambridge Bioscience (Cambridge, UK). 5-hydroxyeicosatetraenoic acid (5-HETE), 8-hydroxyeicosatetraenoic acid (8-HETE), 5,6-epoxyeicosatrienoic acid (5,6-EET), 8,9-epoxyeicosatrienoic acid (8,9-EET), 11,12-epoxyeicosatrienoic acid (11,12-EET), 14,15-epoxyeicosatrienoic acid (14,15-EET), 12-hydroperoxyeicosatetraenoic acid (12-HPETE) and 15-hydroxyeicosatetraenoic acid-d8 (15-HETE-d8) were all purchased from Biomol International (Exeter, UK). HPLC grade water (ELGA Ltd. High Wycombe, UK) was used in all experiments.

2.2.2 Preparation of standards

All stock solutions of each compound were prepared in ethanol, except for 2-AG and 2-AG-d8 which is known to be more stable in acetonitrile and is therefore diluted in this solvent. All stock solutions were stored at -80°C. Serial dilutions of these compounds were used for calibration and stored for no longer than two weeks, comparison of each LC-MS/MS analysis showed no evidence of degradation in these conditions.

2.2.3 Tissue Collection

Male Sprague-Dawley rats (250-300 g, Charles River Laboratories) were used and all experiments were conducted in accordance with the UK Home Office regulations. Animals were killed by stunning and decapitation followed by rapid dissection by Professor David Kendall, Professor Vicky Chapman and Paul Millns and transferred into liquid nitrogen. Tissues were stored immediately at -80 °C until analysis.

2.2.4 Sample Extraction

Tissue samples from brain (100-700mg), spinal cord (20-50mg), and dorsal root ganglia (DRGs, ≈ 10mg were weighed and then homogenised with hand-held pestles in glass tubes and 1 mL ELGA water. Internal standards (100 µL of 2-AG-d8 (10 µM) and 15 µL of AEA-d8 (28 nM), 10 µL of PGF2a-EA-d4 (2.49 µM), 10 µL of AA-d8 (100 nM), 10 µL of PGD2-d4 (1 µM), 10 µL of 15-HETE-d8 (7.6 µM)) were added to each sample or blank sample (0.2 ml water), along with 10 µL (0.005g in 1mL of ethanol) of an antioxidant butylhydroxytoluene (BHT). For each sample 2.5 mL of ethyl acetate: hexane (9:1 v/v) was used to extract the compounds from the tissue, followed by a slow vortex stage (10 min) and centrifuged (3200 g, 4°C) for 15 min. The supernatants were transferred to glass tubes, the procedure repeated and the supernatants pooled and evaporated under nitrogen. The samples were then reconstituted in 200 µL of acetonitrile:water (50:50 v/v) and analysed immediately.

Paw tissue (40-80mg) was weighed and homogenised in glass tubes and 1 mL ELGA water. Internal standards were added and the procedure followed as for brain tissue. The samples were then left to shake for one hour on a flat-bed shaker to allow for slow partitioning of lipids and centrifuged (3200 g, 4°C) for 15 min. The supernatants were transferred to glass tubes, the procedure repeated replacing the one hour shaking with a 10 min slow vortex stage and the supernatants pooled and evaporated under nitrogen. The samples were then reconstituted in 200 µL of acetonitrile:water (50:50 v/v) and analysed immediately.

Knee joints were weighed (400-600mg) and crushed with surgical pliers in glass tubes and 1 mL ELGA water. Internal standards were added and the procedure followed as for paw tissue.

Plasma samples (≈1mL) were thawed and 0.4 mL added to 2.5 mL of ethyl acetate: hexane (9:1 v/v) per sample, followed by 1 mL ELGA water. Internal standards were added and the procedure followed as for brain tissue.

2.2.5 LC-MS/MS Method

The majority of the initial method development was carried out using the Quattro Ultima mass spectrometer (Waters Micromass, Manchester, UK) coupled to an Agilent 1100 LC system (Agilent Technologies, Waldbron, Germany). The methodology was later transferred onto the Applied Biosystem MDS SCIEX 4000 Q-Trap hybrid triple-quadrupole–linear ion trap mass spectrometer (Applied Biosystem, Foster City, CA, USA) used in conjunction with a Shimadzu series 10AD VP LC system (Shimadzu, Columbia, MD, USA). Analytes were separated chromatographically using a complex gradient that was systematically optimised to provide separation of two different types of lipid; ones containing a carboxylic acid group and ones that did not (Table 4).

Table 4. Detailed final gradient applied for this LC-MS/MS method.

Time (min)	Pump A (%)	Pump B (%)	Pump C (%)	Total Flow (mL/min)
0.00	55	45	0	0.2
5.25	55	45	0	0.2
7.50	50	50	0	0.2
7.60	50	50	0	0.3
13.50	30	70	0	0.3
13.60	30	70	0	0.25
18.00	0	100	0	0.25
20.00	0	100	0	0.25
20.10	55	45	0	0.25
22.50	0	0	100	0.3
26.00	55	45	0	0.2
26.10	55	45	0	0.2
29.00	55	45	0	0.2
30.00	STOP			

At 22.5 minutes the system controller is switched from event 0 to event 2, this allows 100% of pump C to pass through and wash the column. At 26 minutes, it switches back from event 2 to event 0, allowing 45% B to pass through at 0.2mL/min allowing the column to equilibrate back to initial conditions. This gradient was the final version following completion of method development, which, along with mass spectrometry conditions, took over 12 months to complete.

Mobile phase A consisted of 0.05% formic acid in water, pH adjusted with dilute ammonium hydroxide, whilst mobile phase B was methanol: acetonitrile (20:80 v/v) and mobile phase C was 100 % acetonitrile. A Phenomenex Luna C18 (150 x 2.0 mm, 3 µm I.D.) column fitted with a

guard column was used and the autosampler temperature was maintained at 4°C throughout analysis. During method development different LC conditions were investigated and will be discussed in this chapter.

Multiple reaction monitoring (MRM) of individual compounds in negative and positive mode using specific precursor and product mass-to-charge (*m/z*) ratios allowed simultaneous measurement of 42 compounds in the same method along with 6 internal standards. MS conditions were carefully optimised using product ion scans to optimise the product ions used for the MRM transitions to allow simultaneous measurement of similar lipids. Source parameters, declustering potential, collision energy and collision cell exit potential were optimised by direct infusion or injection to maximise sensitivity (Table 5).

Analyte	Retention Time (min)	Q1 mass	Q3 mass	DP (V)	CE (V)	CXP (V)
PGD_2	1.9	351.22	271.21	-40	-25	-20.00
PGE_2	1.9	351.22	271.21	-50	-25	-15.00
TXB_2	1.9	369.23	169.09	-50	-25	-10.00
PGE_1-EA	3.7	396.28	360.20	-55	-15	-10.00
$PGF_{2\alpha}$-EA	3.7	396.28	334.21	-70	-25	-10.00
8,15-DIHETE	4.1	335.23	127.20	-60	-30	-10.00
PGE_2-EA	4.3	394.26	358.24	-70	-17	-10.00
PGD_2-EA	4.4	394.26	203.12	-55	-34	-15.00
14,15-DHET	5.0	337.25	207.15	-75	-25	-3.24
LTB_4	5.6	335.23	335.23	-60	-15	-15.00
LTE_4	-	438.23	438.23	-50	-12	-10.00
11,12-DHET	6.0	337.25	167.11	-70	-26	-10.90
19-HETE	6.7	319.24	275.20	-85	-27	-7.23
20-HETE	7.2	319.24	289.22	-67	-30	-6.27
13-HODE	8.3	295.23	195.14	-60	-28	-10.00
16-HETE	8.0	319.24	233.15	-65	-20	-3.91
8,9-DHET	8.3	337.25	127.11	-74	-28	-8.41
9-HODE	9.1	295.23	171.10	-60	-30	-10.00
13-oxoODE	9.7	293.21	113.10	-75	-28	-8.00
15-HETE	9.7	319.24	219.14	-65	-18	-3.78
14,15-EET	11.6	319.24	219.14	-72	-15	-3.50
9-oxoODE	10.1	293.21	185.12	-85	-28	-12.00
5,6-DHET	10.4	337.25	145.06	-71	-26	-10.02
11-HETE	10.8	319.24	167.11	-85	-23	-2.01
11,12-EET	12.8	319.24	167.11	-65	-21	-7.89
12-HETE	11.1	319.24	179.11	-70	-21	-3.00
8-HETE	11.7	319.24	155.07	-65	-20	-9.89
8,9-EET	13.4	319.24	155.08	-72	-17	-9.74
9-HETE	11.9	319.24	123.00	-70	-23	-6.60
12-HPETE	12.1	317.23	153.10	-80	-24	-10.75
5-HETE	13.1	319.24	115.04	-64	-20	-7.00
5-HPETE	13.9	317.23	203.18	-75	-30	-12.00
5,6-EET	13.9	319.24	191.18	-70	-16	-13.60
ARAGLY	16.3	360.25	74.02	-60	-45	-10.00
LA	17.8	279.23	279.23	-60	-15	-7.00
AA	18.0	303.23	259.00	-80	-20	-15.00
14,15-EET-G	18.9	395.27	285.21	80	23	10.02
5,6-EET-EA	19.1	364.28	62.06	90	40	9.00
AEA	20.7	348.28	62.06	25	30	8.56
NADA	21.0	440.31	137.06	25	33	23.98
2-AG	21.1	379.28	287.22	88	22	4.90
PEA	21.6	300.28	62.06	25	30	9.22
OEA	21.9	326.30	62.06	25	32	8.19
AEA-d8*	20.6	356.33	63.03	80	45	15.00
2-AG-d8*	21.0	387.33	95.11	70	61	7.08
PGD_2-d4*	1.9	355.24	193.15	-45	-29	-10.00
$PGF_{2\alpha}$-EA-d4*	3.7	400.26	338.24	-70	-23	-10.00
15-HETE-d8*	9.5	327.29	226.25	-67	-20	-3.97
AA-d8*	17.8	311.28	267.29	-50	-20	-10.00

Table 5. Mass spectrometer values for all compounds where the product ions, declustering potential, collision energy and collision exit potential were optimised increased sensitivity. The internal standards are denoted with *

Quantification was performed using Analyst 1.4.1 (Applied Biosystems, Foster City, CA, USA). Identification of each compound in biological tissue was confirmed by LC retention times of each standard and precursor and product ion *m/z* ratios. Integration of each analyte was conducted to obtain peak areas and imported into Microsoft Excel for further data processing.

2.2.6 Data Analysis

Data were quantified and presented using Microsoft Excel 2010 and Prism (version 5.01; GraphPad, USA), and are expressed as mean ± SEM. Outliers greater than twice the standard deviation were excluded, which usually involved one or two samples in each batch analysed.

Principal component analysis (PCA) was used for further data processing. PCA, a multivariate data analysis technique was used to identify and detect similarities and differences between datasets, which were translated into distances and can be easily visualised (See references in Witkamp 2005). Datasets for n variables are displayed as vectors in an n-dimensional space and PCA was developed for statistical analysis of high dimensional data (small number of objects and a large number of variables). Any observed clustering of samples resulting from PCA provides strong evidence for statistically significant differences between or among datasets (Witkamp 2005). PCA was performed by importing the levels of each individual lipid measured from different tissue types from Microsoft Excel into the SIMCA-P software package (Version 11, Umetrics AB, Umea, Sweden). The data were reduced to two latent variables (or principle components) that will describe the maximum variation within the data (Law et al 2008) to create a two-component model expressed as scores and loadings plots. The principle components obtained from the scores highlighted clusters, trends and outliers within the dataset.

2.2.7 Validation

The majority of the analytes are found endogenously and there is no appropriate 'blank' matrix available for the validation. Therefore all the

analytes were spiked into rat brain tissue as a standard biological matrix to determine the accuracy, precision, recovery and ion suppression of the method. The rat brain tissue was frozen with liquid nitrogen and homogenised in a pestle and mortar, before distributing into approximately 100 mg aliquots. This was conducted to ensure that the background concentrations of all the endogenous analytes were equal between the replicate brain tissue sample aliquots used for validation. These endogenous concentrations of analytes were accounted for in all subsequent validation calculations.

Seven-point calibration curves spiked into rat brain tissue were used for each of the thirty analytes at concentrations of 0.01, 0.025, 0.05, 0.1, 0.5, 2 and 5 nmol/g. 2-AG was spiked at concentrations of 0.1, 0.25, 0.5, 1, 5, 20 and 50 nmol/g to account for the high endogenous levels of this analyte in rat brain. These spiked validation samples were then extracted following the method described in the sample extraction section for brain tissue. Linearity was calculated using the peak area of each analyte expressed as a ratio to the peak area of the internal standard. This was chosen based on structural similarities and these calibration lines were also used to determine slope, intercept and the regression coefficient.

Accuracy and precision values for intraday (n=5) and interday (n=4) were determined using rat brain tissue, spiked with each analyte added at concentrations of 0.02 (low), 0.2 (medium) and 0.8 (high) nmol/g. 2-AG was spiked in at concentrations of 0.2, 2 and 8 nmol/g, reflecting its much higher endogenous concentration.

Accuracy and precision values were calculated from the relative standard deviation (RSD) of the replicates. Accuracy values were determined as a ratio of the measured levels of each analyte to the expected concentration. An RSD of 15% was considered acceptable for the accuracy and precision values of each analyte for each concentration. The lower limit of quantification (LLOQ) was defined as the concentration at which the RSD of the analyte was found to be 20% or more. The limit of

detection (LOD) is defined as the concentration at which the signal to noise ratio is greater than 3:1.

Recovery values were calculated by comparing the peak area of each analyte at all three concentrations with the peak area of 100% standard. The endogenous levels of the analytes were taken into account when necessary for the calculations.

Ion suppression values were calculated by spiking the analytes at the end of the extraction process to rat brain extracts. This was calculated by comparing the peak area of each analyte to 100% standard.

2.2.8 Measurement of lipids in rat tissues

Male Sprague-Dawley rats (340-450 g, Charles River Laboratories) were used and these experiments were conducted in accordance with the UK Home Office regulations. Animals were killed by stunning and decapitation and the blood collected by Professor David Kendall followed by rapid dissection of the spinal cord by Professor Vicky Chapman. The brain divided into frontal cortex, midbrain, hippocampus, rest of cortex and rest of brain regions were rapidly dissected by Professor David Kendall, the DRGs by Paul Millns, whilst I removed the knee joints. All tissue samples were transferred into liquid nitrogen immediately and the blood was centrifuged for separation and the plasma collected and frozen. All samples were stored immediately at -80 ^{o}C until analysis. Individual tissue samples were extracted following the different extraction procedures described in the sample extraction methods section.

2.3 Results and Discussion

2.3.1 Development and optimisation of analytical method

The incorporation of important inflammatory mediators alongside the endocannabinoids forms the rationale behind the development of this method. Previously it has been necessary to use separate methods for this purpose in our group (Richardson et al 2007, Zhang et al 2007). Addition of further eicosanoids to the method since the validation has resulted in a targeted analytical LC-MS/MS method of 42 compounds, which includes 6 internal standards (See Materials and Methods). 30 compounds within this method have been fully validated and discussed later in the chapter. The different bioactive lipids have been combined into different groups according to the major route of synthesis or biological class (Table 6) to facilitate discussion of the validation and tissue distribution results.

Table 6. Analyte groups of the bioactive lipids analysed with this LC-MS/MS method.

Analyte groups	**COX**	**LOX**	**CYP450**	**ECs**
Metabolites	PGs, TXs, PG-EAs, PG-Gs	LTs, HODEs, oxoODEs, HPETEs, HETEs	HETEs, EETs, DHETs, HETE-EAs, HETE-Gs, EET-EAs, EET-Gs	AEA, OEA, PEA, 2-AG, AraGly, NADA

Lipid abbreviations: EET - epoxyeicosatrienoic acid, HETE - hydroxyeicosatetraenoic acid, HPETE - hydroperoxyeicosatetraenoic acid, AEA - N-arachidonoyl ethanolamide, 2-AG - 2-arachidonoyl glycerol, PEA - palmitoyl ethanolamide, OEA - oleoyl ethanolamide, AraGly - arachidonoyl glycine, NADA-N-arachidonoyl dopamine, EA - ethanolamide, G - glycerol, LA - linoleic acid, HODE - hydroxyoctadecadienoic acid, oxoODE - oxooctadecadienoic acid, PG - prostaglandin, TX - thromboxane, DHET - dihydroxyeicosatrienoic acid, LT - leukotriene, ECs-endocannabinoids. Enzyme abbreviations: COX - cyclooxygenase, CYP450 - cytochrome P450, LOX - lipoxygenase.

Profiling of both the endocannabinoids and eicosanoids within the same LC-MS/MS method was a difficult process due to the structural

differences between these two sets of compounds. In particular quantitative methodologies of this type require versatility, high sensitivity, selectivity and reproducibility, due to the small amounts detectable in different tissue types. This is also true for separation within the eicosanoids where the structural similarities between the HETEs, EETs and DHETs have been challenging with regards to selectivity (Figure 1).

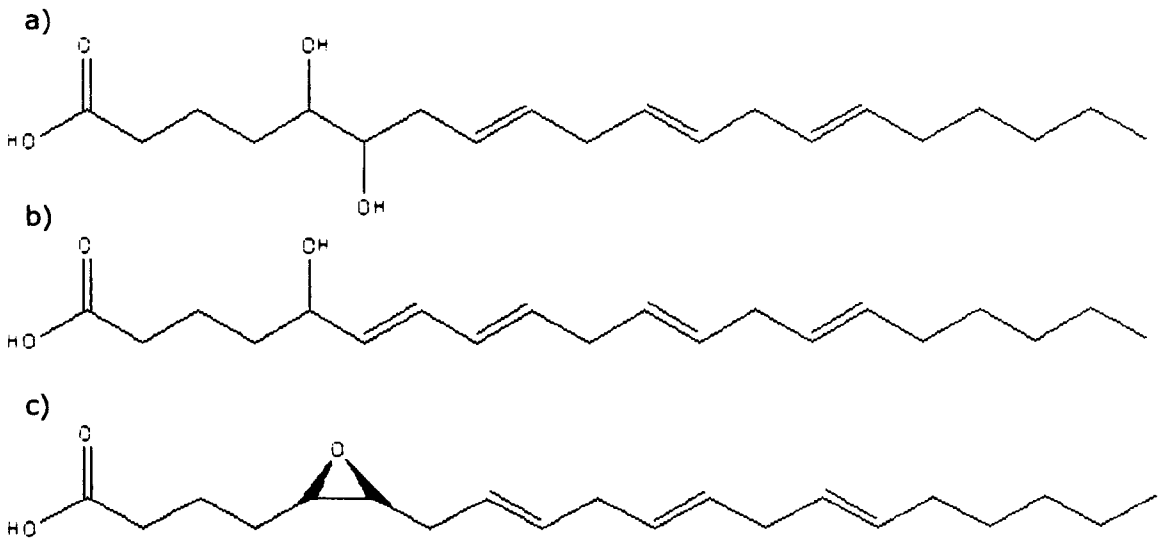

Figure 1. Structures of a) 5,6-DHET, b) 5-HETE and c) 5,6-EET.

These structural complications require careful fine-tuning of LC and MS conditions and are discussed in detail in this chapter.

2.3.1.1 Investigating the effects of temperature and pH on eicosanoid and endocannabinoid retention time

The main factor for optimisation of the method was to allow simultaneous identification and detection of a large number of analytes in negative and positive mode. Significant factors that may alter the separation between the two groups of compounds are temperature and pH. Retention time variation with pH and temperature of the eicosanoids, which have an ionisable carboxylic acid group, was investigated (Figure 2). The initial pH of mobile phase A was measured to be 2.6 and increases in pH from this point were considered. Retention time was shown to decrease as pH increased (Figure 2a), with the greatest difference observed between pH

4 and pH 5, possibly around the pK_a of this group of lipids. Fatty acids with a carboxylic group, such as the eicosanoids are classed as weak acids and short-chain fatty acids have a pK_a typically around 4 and 5 (Kanicky and Shah 2002). There was little change in the retention time of the endocannabinoids with pH (data not shown), as expected, due to absence of a –COOH group, with the exception of arachidonoyl glycine, the only endocannabinoid with a -COOH group that followed the eicosanoid trend (data not shown).

Analysis of the compounds under the same conditions other than temperature change found that a temperature decrease at pH 7.1 from 50 °C to 30 °C had minimal effects on the retention time of the eicosanoids (Figure 2b) and endocannabinoids (data not shown). All other pH values were also investigated (pH 2.6-8.6) between 50°C to 30°C and the results indicated that temperature had little effect (data not shown).

a)

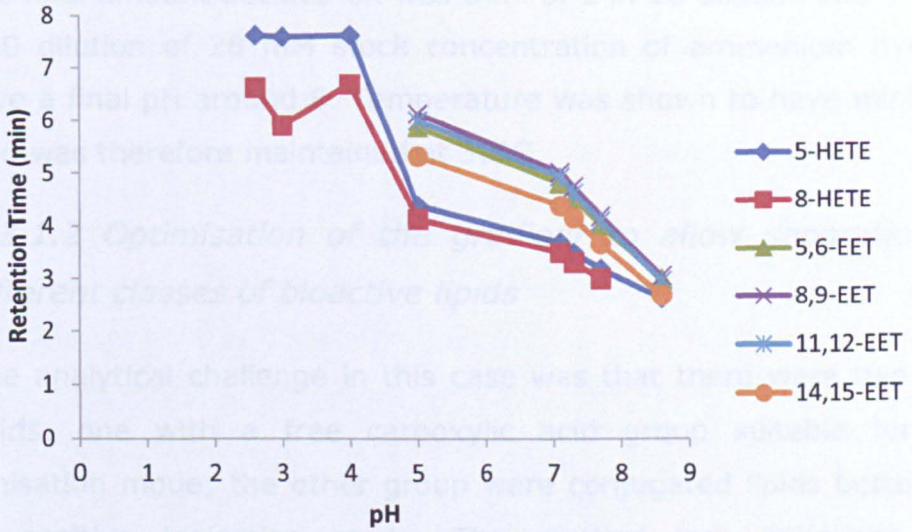

b)

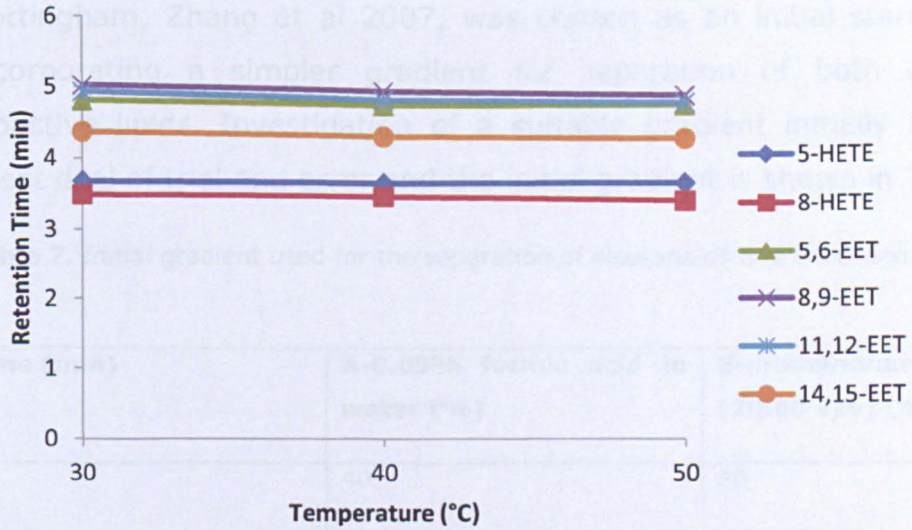

Figure 2. Retention time variation of the eicosanoids against a) pH at 30°C and b) temperature at pH 7.1, according to the gradient and conditions in Table 7.

Separation was achieved by optimising the pH of the mobile phase A to alter the retention times of the eicosanoids that contained an ionisable carboxylic acid group, thereby decreasing the retention time of these analytes. This allowed time for switching mass spectrometry ionisation modes to detect for the endocannabinoids in positive ion mode. pH was

adjusted initially by adding ammonium hydroxide to the desired pH and the final amount decided on was 6 ml of 1 in 10 dilution and 6 mL of 1 in 100 dilution of 28 mM stock concentration of ammonium hydroxide to give a final pH around 8. Temperature was shown to have minimal effect and was therefore maintained at 30°C.

2.3.1.2 Optimisation of the gradient to allow separation of two different classes of bioactive lipids

The analytical challenge in this case was that there were two groups of lipids, one with a free carboxylic acid group suitable for negative ionisation mode; the other group were conjugated lipids better detected in positive ionisation mode. The method was optimised to allow simultaneous identification and detection of these two groups of lipid mediators. One method originally developed at the University of Nottingham, Zhang et al 2007, was chosen as an initial starting point, incorporating a simpler gradient for separation of both classes of bioactive lipids. Investigation of a suitable gradient initially involved a great deal of trial and error and the initial gradient is shown in Table 7.

Table 7. Initial gradient used for the separation of eicosanoids and endocannabinoids

Time (min)	**A-0.05% formic acid in water (%)**	**B-methanol:acetonitrile (20:80 v/v) (%)**
0	40	60
18	0	100
25	0	100
25.1	40	60
31	40	60

The same method was used to analyse a 100 µM stock solution of the endocannabinoids to investigate whether any of these compounds would be detectable in negative mode. Even at this high concentration, none of

the endocannabinoids gave a response in negative ion mode, hence confirming that it was essential to use electrospray positive ion mode for these compounds (data not shown). Analysis was repeated using positive mode, which produced effective detection of the compounds using the conditions of the eicosanoid LC-MS/MS method and the initial gradient.

The next step was to alter the gradient and improve the chromatography of both sets of compounds, to optimise run time and separate the compounds further to avoid co-elution. Initial conditions were increased to a higher percentage of organic solvent, 65% and 70%, which decreased the elution time of both sets of compounds by almost 5 min, minimising run time. 15 different gradients were compared, which involved altering the initial percentage of mobile phase B and extending the time that mobile phase B was maintained at a lower percentage. This was chosen to extend the elution time of the endocannabinoids and to increase the time interval between eicosanoid and endocannabinoid elution. Further alterations to the gradient were made by altering the length of time held at 80% organic, as this was found to be the starting organic percentage for endocannabinoid elution. All gradients were tested with initial starting conditions of 65% and 70% mobile phase B. However, there was still a degree of overlap between the last eicosanoid and the first endocannabinoid, so a shallower gradient was required. Further analysis found that the elution of the eicosanoids was around 70%, so this was held for a further 11 min. AEA elution was also found to be around 75% B and therefore this was held for around 7 min to give the final gradient (Table 8). Comparison of the initial gradient (Table 7) and the final gradient (Table 8), found that the compounds eluted much earlier in the run, however the separation was still not apparent.

Table 8. Last gradient used for the separation of eicosanoids and endocannabinoids, which was further optimised following the addition of prostaglandins, leukotrienes, HODEs and oxoODEs, as discussed later.

Time (min)	A-0.05% formic acid in water (%)	B-methanol:acetonitrile (20:80 v/v) (%)
0	30	70
11	30	70
18	25	75
25	0	100
25.1	30	70
31	30	70

Following the addition of new lipid mediators to the method, the gradient was further optimised to allow incorporation of these compounds. The percentage of mobile phase B was decreased to 45% to allow better separation of the early eluting compounds such as PGD_2/PGE_2 and TXB_2, where the chromatography was extremely poor at the higher 70% organic phase. To further delay the elution time and therefore improve separation of the 35 analytes detected in negative mode, the gradient was modified to increase from 45% to 50% organic at 7.50 min (Table 3) before increasing to 70% at 13.50 min. The modifications to the flow rate from 0.2 mL/min starting flow rate up to 0.25 mL/min and 0.3 mL/min was also optimised to alter elution time of some of the analytes. Thereby increasing the gap between the last analyte in negative mode and the first analyte in positive mode and extending time for switching modes. The final gradient is a mixture of fine tuning between the length of time and percentage of organic phase coupled to the speed of the flow rate. The negative to positive mode switch is around 18.50 min and during this time the gradient was increased from 70% to 100% organic. This enabled the elution of the endocannabinoids and the two metabolites, 5,6-EET-EA and 14,15-EET-G, which were established during the initial gradient

development stage. At 22.50 min, a third pump C was used to introduce 100% acetonitrile as a mobile phase. The reason for this extra step was to ensure a complete column wash at the end of each run to minimise carryover between injections. The difference in gradient between this new method and the original endocannabinoid method (Richardson et al 2007) was that the original method utilised 100% acetonitrile as mobile phase B which may have helped wash the column at the end of each analytical run. The mobile phase B of this new method contained methanol:acetonitrile (20:80 v/v) and this 80% acetonitrile may not be sufficient to diminish any carryover. At 22.50 min, an event triggers the valve to rotate from position 0 to position 2, this in turn allows flow from pump C only for 3.50 min. Following this, a second event triggers the valve to rotate back to position 0, with the gradient set at initial conditions and the column is re-equilibrated for the remaining 4 min of the analytical run.

Optimisation of peak shape and resolution of the HETEs and EETs were also achieved using a longer length column, changing the original 100 mm length column to a 150 mm. This was found to produce improved separation for these two groups of eicosanoids.

Chromatographic separation of the structurally similar DHETs, HETEs and EETs (Figure 1) were also achieved by a combination of this complex gradient (Table 3), timing of organic phase changes and a longer column length. Elution times based on organic phase percentage was carefully considered to enable separation of these analytes. Some of the standards purchased, namely the EETs, are racemic mixtures of the analyte. The chromatography of this method is able to separate these into two clear peaks, an example of which is shown in Figure 3.

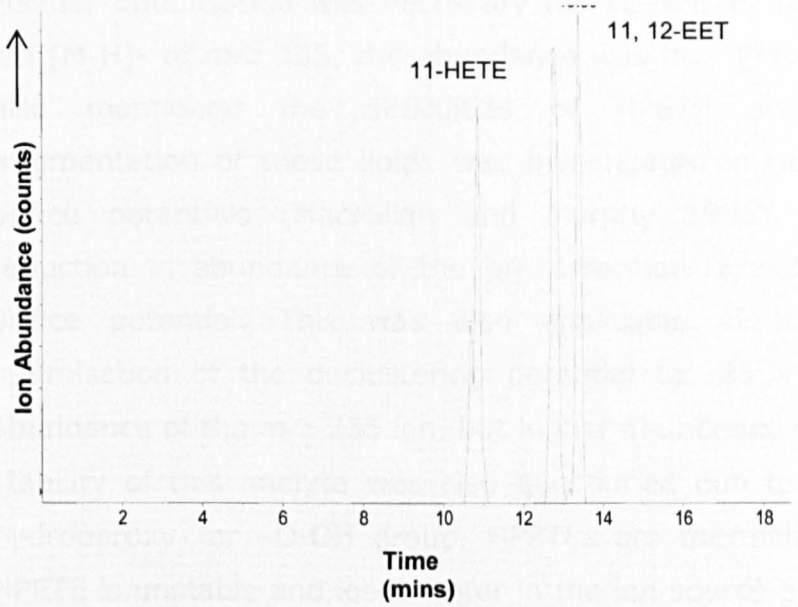

Figure 3. Separation of 11-HETE and 11,12-EET according to the final gradient in Table 4, there are clearly two distinct peaks for 11,12-EET as the standard is purchased as a racemic mixture or (±)11,12-EET.

Jiang et al have previously mentioned the existence of *cis*- and *trans*-EETs, which vary in potency in their biological actions and 5,6-*trans*-EET has been identified in erythrocytes (Jiang et al 2004). 5,6-*cis*-EET has been shown to elute first followed by 5,6-*trans*-EET (Jiang et al 2004).

2.3.1.3 Optimisation of mass spectrometry parameters

Unique product ions for each analyte were used to distinguish between analytes and to enable quantification either by retention time or MRM transition. For example, the MRM transition *m/z* 319.24-155.08 was used for detection of 8-HETE (retention time 11.5 min) and 8,9-EET (retention time 13.2 min). Detection by retention time at the same MRM transition also applied to 11-HETE and 11,12-EET and also to 15-HETE and 14,15-EET. MRM transitions used were based on previous methods (Richardson et al 2007, Zhang et al 2007), Lipid Maps database (Lipid Maps-Nature Lipidomics Gateway, February 2010) and further optimisation conducted experimentally using product ion scans. The approach of combined measurement of 1-AG and 2-AG was also adopted in this method as in previous methods (Richardson et al 2007).

Further optimisation was necessary for 12-HPETE; using the precursor ion [M-H]- of *m/z* 335, the abundance was low. Previous methods have also mentioned the difficulties of HPETE analysis, where the fragmentation of these lipids was investigated in relation to modifying orifice potentials (MacMillan and Murphy 1995). They observed a reduction in abundance of the precursor ion *m/z* 335 with increasing orifice potential. This was also applicable in this method where optimisation of the declustering potential to -85 V resulted in a low abundance of the *m/z* 335 ion, but higher abundance of the *m/z* 317. The stability of this analyte was also questioned due to the presence of a hydroperoxy- or –O-OH group. HPETEs are thermally labile and if 12-HPETE is unstable and loses water in the ion source producing a *m/z* 317 ion, this could then be monitored as the precursor ion. Therefore, product ions of this analyte were investigated and the spectra confirmed this hypothesis (Figure 4).

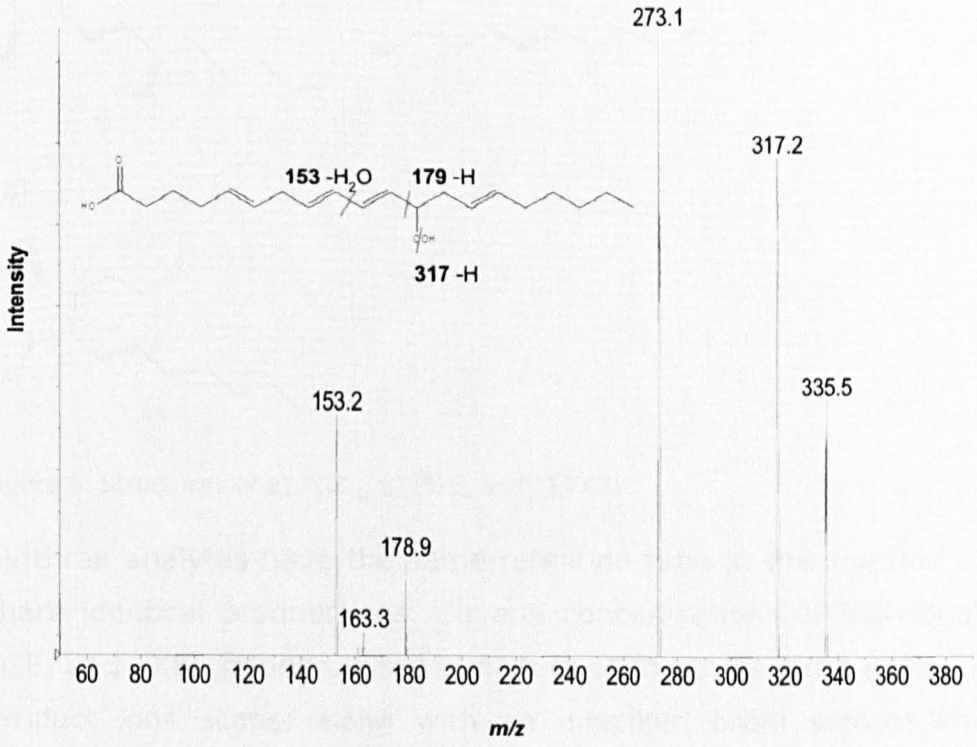

Figure 4. Product ion spectra of 12-HPETE, including the structure of this analyte, according to the mass spectrometry conditions in Table 5, *m/z* 317.23>153.10, DP -80V, CE -24V and CXP -10.75V.

The focus of optimisation work was to look for strong product ions of this analyte, so the scan was set from *m/z* 50 to *m/z* 350. The strongest product ion was *m/z* 317, the precursor ion minus water $[M\text{-}H_2O]^-$, which is a common trait in this type of lipid analysis (Garscha et al 2008, Havrilla et al 2000, MacMillan and Murphy 1995). This was followed by a product ion of *m/z* 273 which is a further loss of COO-, to give $[M\text{-}H_2O\text{-}COO]^-$, however the *m/z* 273 product ion was common to both 5-HPETE and 12-HPETE. A unique product ion of *m/z* 153 of the 12-HPETE was therefore selected for the MRM transition. The precursor ion of *m/z* 317 was also applied to 5-HPETE during the optimisation of this analyte.

Further work was also required to distinguish between PGD_2, PGE_2 and TXB_2, due to the similarities in structure (Figure 5).

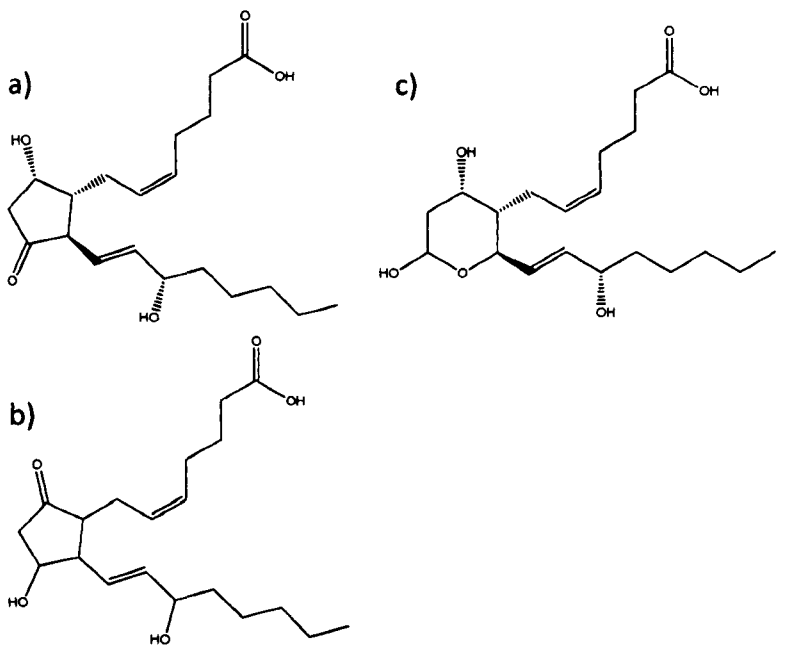

Figure 5. Structures of a) PGD_2, b) PGE_2 and c) TXB_2.

All three analytes have the same retention time in this method and also share identical product ions. Several concentrations of individual PGD_2, PGE_2 and TXB_2 standards and a mixture of the three were analysed using product ions scans, along with an unspiked brain sample known to contain these three analytes. The spectrum of the sample for each analyte was compared to the concentration most closely resembling the concentration detected in the sample. Investigation of the individual

product ion spectra of each analyte confirmed the unique product ion of *m/z* 169.09 of TXB_2 (Figure 6), which was apparent in both the sample and standard spectra.

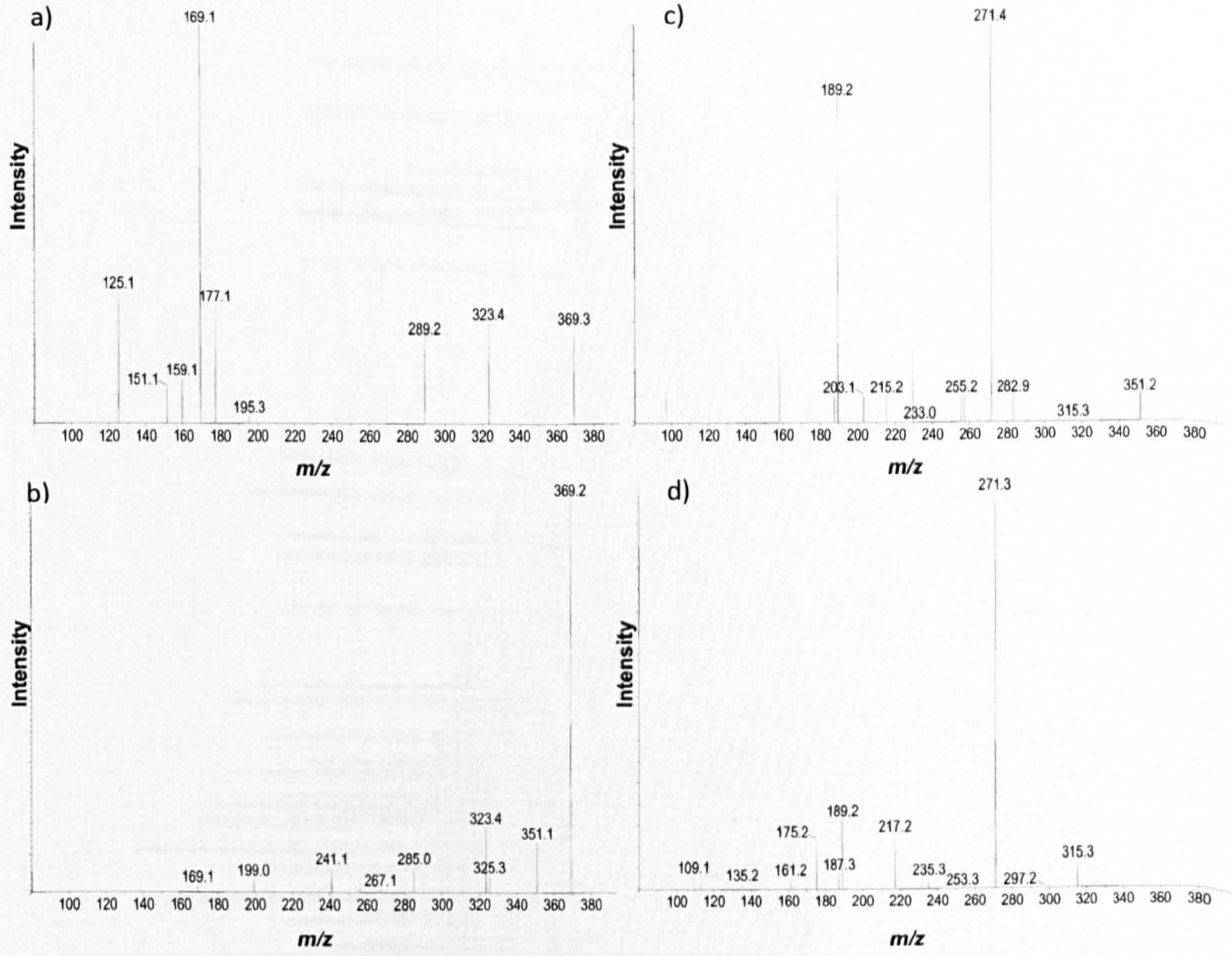

Figure 6. Product ion spectra of a) TXB_2 standard, b) TXB_2 peak in a brain sample, c) PGD_2 standard and d) PGE_2 standard according to the mass spectrometer conditions in Table 5.

Therefore the MRM transition of *m/z* 369.23>169.09 was used for detection of TXB_2. However, PGD_2 and PGE_2 have very similar product ion spectra and it was extremely difficult to find a unique product ion where the MRM transition provided a reasonable signal to noise ratio greater than four. A unique product ion of *m/z* 175.11 was found for PGE_2, but using this MRM transition of *m/z* 351.22>175.11 did not give a detectable signal where the signal to noise ratio was greater than four.

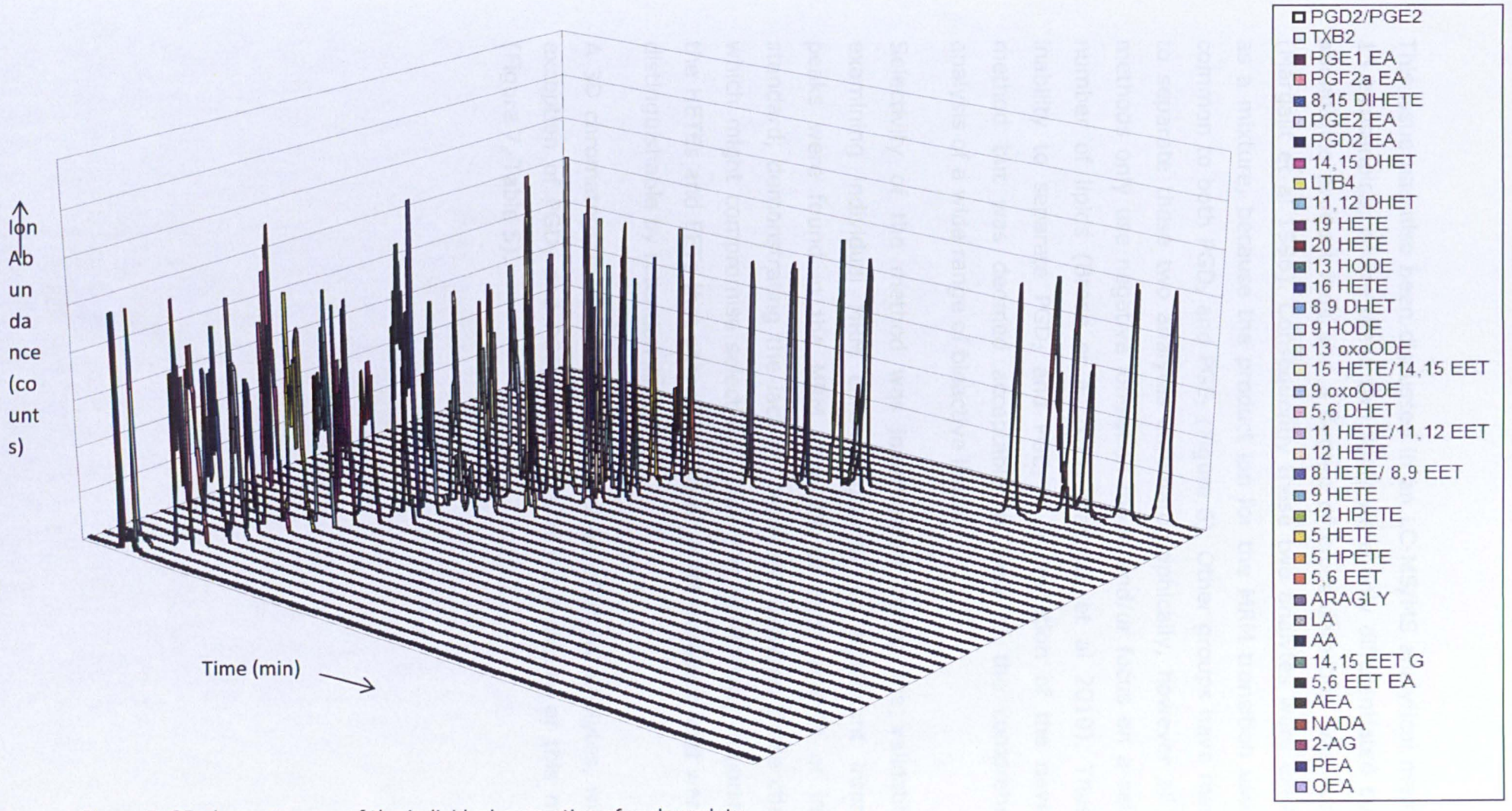

Figure 7. 3D chromatogram of the individual separation of each analyte.

This issue has also been discussed in an LC-MS/MS analytical method of 15 eicosanoids, where these two lipids were only differentiated by low-abundance product ions and a degree of cross-detection was apparent (Margalit et al 1996). Consequently these two analytes were expressed as a mixture, because the product ion for the MRM transition used was common to both PGD_2 and PGE_2 (Figure 6). Other groups have managed to separate these two analytes chromatographically, however all these methods only use negative ionisation mode and/or focus on a selective number of lipids (Brose et al 2011, Masoodi et al 2010). Thus, the inability to separate PGD_2 and PGE_2 is a limitation of the developed method but was deemed acceptable in view of the comprehensive analysis of a wide range of bioactive lipids.

Selectivity of the method was investigated during the validation by examining individual MRM chromatograms. No significant interfering peaks were found in the MRM channels of each analyte or internal standard, demonstrating the lack of 'crosstalk' between these channels which might compromise selectivity. This was particularly important for the HETEs and EETs that shared the same MRM transition and were only distinguishable by retention time.

A 3D chromatogram showing the separation of all 42 analytes, with the exception of PGD_2 and PGE_2, highlights the complexity of this method (Figure 7, Table 5).

2.3.1.4 Investigating the effects of reconstitution and injection volume on sensitivity

Initially the endocannabinoids were used as a basis for optimisation work since these were the analytes with the least solubility in polar solvents and hence any conditions would be readily suitable for the more polar eicosanoids. Firstly, reconstitution was investigated to determine whether this factor could be optimised to increase sensitivity. Reconstitution with 100% acetonitrile was found in previous work to give the best recovery of the endocannabinoids without detrimental effects on peak shape (Richardson et al 2007). Inclusion of the eicosanoids meant the possibility of introducing a more polar injection solvent such as water, specifically with a view to allowing a greater injection volume without degradation of peak shapes.

1 g of rat brain tissue was extracted following the methods described earlier. This extract was further divided into 7 replicate aliquots, labelled tubes A-G, and the contents of each tube was evaporated to dryness under nitrogen. Each tube was then reconstituted with different percentages of water, with one containing 100% acetonitrile. All the chromatograms showed good separation and detection of the endocannabinoids without losing resolution and reconstitution with the various aqueous combinations found that acetonitrile:water (50:50 v/v) gave the best total peak area value for all the endocannabinoids without loss of peak shape (Table 9).

Table 9. Total peak areas of the endocannabinoids in the reconstitution experiment, using a C18 Phenomenex Luna (100 x 2.0, 3 µm I.D) column with mobile phase A (0.05% formic acid in water) and mobile phase B (methanol:acetonitrile (20:80 v/v) according to the initial conditions in Table 7.

	Reconstitution	
Tube	**Water (%)**	**Total EC (Peak Area)**
A	0	217519
B	25	240299
C	50	259412
D	60	70372
E	70	24729
F	80	24772
G	90	31452

Increasing the percentage of aqueous above 50% decreased the peak areas as expected due to the lipophilic nature of these compounds. These results were also applicable for the eicosanoids due to the similarities in chemical structures and the more polar nature of these lipids.

Afterward, sample injection volume was investigated using acetonitrile:water (50:50 v/v). The standard injection volume used was 5 µL, however, with a higher reconstitution percentage of aqueous, the tolerable injection volume for the column was investigated. Under the same conditions, 5, 10, 15, 20 and 25 µL injection volumes were considered. Again, all injection volumes investigated showed good chromatographic separation of the endocannabinoids, with 20 and 25 µL displaying the highest signal intensity (Table 10). However, 20 µL gave the greatest peak areas for all the endocannabinoids.

Table 10. Total peak areas of the endocannabinoids in the injection volume experiment, using a C18 Phenomenex Luna (100 x 2.0, 3 µm I.D) column with mobile phase A (0.05% formic acid in water) and mobile phase B (methanol:acetonitrile (20:80 v/v) according to the initial conditions in Table 7.

Tube	Injection Volume (µL)	Total EC (Peak Area)
A	5	40152
B	10	113442
C	15	576385
D	20	1616691
E	25	1284331

The eicosanoids were also found to be detectable following the conditions and parameters of the existing LC-MS/MS method (data not shown). Optimisation of sensitivity was achieved following minor alterations to the existing method, which was applied to future development work, and the structural similarities of the endocannabinoids and eicosanoids were taken into account.

2.3.2 Validation

The validation results for this method are shown in Table 11 and it is important to note that there are few published lipid profiling methods that have provided full validation data. Values are represented as %RSD (relative standard deviation) of individual replicates and conducted according to the validation section in methods described earlier.

Table 11a. Validation table of all 30 compounds investigated, n = 6 for accuracy and precision values for low, medium and high concentrations.

Analyte	R^2	Slope	Concentration (nmol/g)	Recovery (%)	ION SUPP (%)	Intraday (n = 5) Precision (RSD%)	Intraday (n = 5) Accuracy (RSD%)	Interday (n = 4) Precision (RSD%)	Interday (n = 4) Accuracy (RSD%)
PGD_2-EA	0.993	y=1.47x+0.161	**0.02**	60 ± 3	61 ± 6	5	105	10	96
			0.2	50 ± 5	60 ± 7	9	103	9	102
			0.8	60 ± 5	74 ± 4	1	101	5	103
PGE_1-EA	0.993	y=15.2x+2.09	**0.02**	59 ± 4	50 ± 3	3	92	14	86
			0.2	60 ± 3	60 ± 7	6	114	9	108
			0.8	67 ± 4	78 ± 6	2	112	7	102
PGE_2-EA	0.993	y=1.47x+0.161	**0.02**	60 ± 3	61 ± 6	5	105	10	96
			0.2	50 ± 5	60 ± 7	9	103	9	102
			0.8	60 ± 5	74 ± 4	1	101	5	103
PGF_2a-EA	0.999	y=24.7x+1.10	**0.02**	51 ± 4	48 ± 2	5	94	13	88
			0.2	51 ± 3	54 ± 7	5	112	7	105
			0.8	57 ±3	72 ± 5	2	110	7	102
5,6-DHET	0.993	y=0.733x+0.0635	**0.02**	89 ± 9	43 ± 6	15	93	11	98
			0.2	70 ± 3	75 ± 11	6	98	10	99
			0.8	69 ± 4	87 ± 6	4	96	11	100
8,9-DHET	0.998	y=1.70x+0.136	**0.02**	83 ± 9	55 ± 4	9	96	13	88
			0.2	76 ± 3	74 ± 11	9	114	8	101
			0.8	70 ± 5	93 ± 5	4	112	9	101
11,12-DHET	0.995	y=4.43x+0.399	**0.02**	93 ± 9	56 ± 4	7	100	14	103
			0.2	77 ± 3	81 ± 11	9	111	11	100
			0.8	70 ± 5	94 ± 6	4	111	10	99
14,15-DHET	0.994	y=1.71x+0.171	**0.02**	34 ± 6	21 ± 3	8	90	14	87
			0.2	25 ± 2	23 ± 3	12	103	7	96
			0.8	26 ± 2	36 ± 2	6	109	11	104

Table 11b. Validation table of all 30 compounds investigated, n = 6 for accuracy and precision values for low, medium and high concentrations.

Analyte	R^2	Slope	Concentration (nmol/g)	Recovery (%)	ION SUPP (%)	Intraday (n = 5) Precision (RSD%)	Intraday (n = 5) Accuracy (RSD%)	Interday (n = 4) Precision (RSD%)	Interday (n = 4) Accuracy (RSD%)
12-HPETE	0.931	y=0.285x+0.0625	**0.02**	36 ± 4	72 ± 22	12	92	27	101
			0.2	24 ± 3	40 ± 8	15	103	19	111
			0.8	18 ± 2	70 ± 20	5	96	15	85
5-HETE	0.991	y=2.59x+0.266	**0.02**	69 ± 11	57 ± 3	10	94	6	100
			0.2	84 ± 8	80 ± 10	13	111	11	105
			0.8	86 ± 8	99 ± 7	8	106	14	103
8-HETE	0.998	y=3.10x+0.106	**0.02**	67 ± 19	80 ± 7	13	106	13	102
			0.2	86 ± 7	82 ± 11	8	103	8	101
			0.8	68 ± 4	99 ± 9	3	101	5	98
9-HETE	0.995	y=0.897x+0.0743	**0.02**	74 ± 21	58 ± 9	14	103	10	98
			0.2	75 ± 7	83 ± 13	7	107	7	100
			0.8	66 ± 5	99 ± 8	4	108	7	98
11-HETE	1	y=7.91x+0.0967	**0.02**	64 ± 11	63 ± 3	7	103	6	105
			0.2	83 ± 9	76 ± 9	14	107	9	103
			0.8	74 ± 4	96 ± 6	3	98	8	101
12-HETE	0.997	y=3.11x+1.75	**0.02**	87 ± 9	97 ± 7	14	106	10	105
			0.2	85 ± 2	91 ± 15	2	104	5	104
			0.8	85 ± 4	103 ± 13	5	107	5	104
15-HETE	1	y=1.90x+0.121	**0.02**	54 ± 24	78 ± 3	2	114	13	102
			0.2	91 ± 10	85 ± 11	15	98	10	98
			0.8	77 ± 5	100 ± 8	2	93	6	99
16-HETE	1	y=2.32x-0.0024	**0.02**	86 ± 9	55 ± 4	9	97	14	91
			0.2	75 ± 5	78 ± 9	9	105	9	99
			0.8	74 ± 5	100 ± 8	4	107	8	104

Table 11c. Validation table of all 30 compounds investigated, n = 6 for accuracy and precision values for low, medium and high concentrations.

Analyte	R^2	Slope	Concentration (nmol/g)	Recovery (%)	ION SUPP (%)	Intraday (n = 5) Precision (RSD%)	Intraday (n = 5) Accuracy (RSD%)	Interday (n = 4) Precision (RSD%)	Interday (n = 4) Accuracy (RSD%)
19-HETE	1	y=1.12x+0.008	**0.02**	99 ± 14		6	110	15	101
			0.2	82 ± 4	56 ± 7	9	105	7	95
			0.8	76 ± 4	74 ± 5	4	105	10	101
20-HETE	1	y=0.325x-0.0008	**0.02**	90 ± 9	54 ± 11	12	102	21	102
			0.2	69 ± 9	81 ± 13	12	99	9	100
			0.8	79 ± 6	99 ± 7	3	98	10	100
5,6-EET	1	y=1.16x+0.0144	**0.02**	103 ± 16	61 ± 12	14	99	13	92
			0.2	99 ± 4	109 ± 16	5	89	11	99
			0.8	92 ± 7	116 ± 8	10	113	14	97
8,9-EET	0.991	y=0.896x+0.0876	**0.02**	58 ± 10	46 ± 4	10	98	13	93
			0.2	72 ± 7	79 ± 9	13	105	10	104
			0.8	62 ± 4	97 ± 7	5	108	13	105
11,12-EET	0.991	y=0.742x+0.0742	**0.02**	80 ± 12	44 ± 7	11	104	11	89
			0.2	81 ± 7	68 ± 9	10	103	12	101
			0.8	79 ± 8	95 ± 9	9	112	14	99
14,15-EET	0.995	y=1.63x+0.0427	**0.02**	73 ± 3	52 ± 6	12	104	8	111
			0.2	75 ± 11	76 ± 11	11	103	7	99
			0.8	67 ± 6	110 ± 8	9	112	10	102
5-HPETE	1	y=0.399x+0.0194	**0.02**	31 ± 6	38 ± 4	11	93	14	97
			0.2	23 ± 3	35 ± 3	15	102	14	95
			0.8	25 ± 3	55 ± 4	7	103	14	101
5,6-EET-EA	0.999	y=0.166x+0.0047	**0.02**	61 ± 8	51 ± 5	10	93	13	98
			0.2	64 ± 6	68 ± 10	7	100	12	99
			0.8	70 ± 7	93 ± 7	5	94	12	101

Table 11d. Validation table of all 30 compounds investigated, n = 6 for accuracy and precision values for low, medium and high concentrations.

Analyte	R^2	Slope	Concentration (nmol/g)	Recovery (%)	ION SUPP (%)	Intraday (n = 5) Precision (RSD%)	Intraday (n = 5) Accuracy (RSD%)	Interday (n = 4) Precision (RSD%)	Interday (n = 4) Accuracy (RSD%)
14,15-EET-G	0.995	y=1.39x+0.108	**0.02**	80 ± 14	51 ± 7	13	102	13	99
			0.2	74 ± 8	70 ± 10	11	94	12	94
			0.8	66 ± 6	99 ± 9	12	107	15	103
PEA	0.999	y=2.25x+0.0495	**0.02**	75 ± 5	45 ± 2	14	105	15	103
			0.2	75 ± 10	39 ± 5	4	111	13	109
			0.8	82 ± 2	72 ± 2	12	104	10	98
OEA	0.971	y=2.71x+1.04	**0.02**	52 ± 17	62 ± 4	3	102	13	101
			0.2	67 ± 9	68 ± 6	11	108	7	97
			0.8	53 ± 6	92 ± 4	6	112	16	99
AEA	0.996	y=1.08x+0.134	**0.02**	34 ± 8	72 ± 2	15	113	4	106
			0.2	56 ± 9	78 ± 10	8	111	9	106
			0.8	58 ± 5	111 ± 8	5	103	7	101
2-AG	0.99	y=3.93x+3.79	**0.02**	54 ± 11	102 ± 6	11	95	15	100
			0.2	51 ± 6	133 ± 19	6	113	13	111
			0.8	51 ± 1	87 ± 8	12	104	11	110
NADA	0.996	y=18.1x-1.20	**0.02**	92 ± 8	45 ± 7	8	96	13	92
			0.2	66 ± 10	86 ± 15	8	100	10	104
			0.8	62 ± 4	109 ± 11	5	101	11	100

Linearity of the method was confirmed by a 7-point calibration curve of each analyte over a range of 0.01 – 5 nmol/g. The correlation coefficients (r^2) in the validation ranged from 0.9311 to 0.9999 (Table 10). Recovery values also show that this method provided good recoveries (50-103%) for the majority of the analytes for low, medium and high concentrations, although some were below 50% (18-36%). Some of the analytes validated such as 12-HPETE has been shown to be fairly unstable and consequently gave much lower recovery values (18-36%). 12-HPETE has been shown to partly dehydrate to the corresponding oxoeicosatetraenoic acid (OETE) in the heated capillary of the mass spectrometer during electrospray ionisation (Liminga and Oliw 2000, Piomelli et al 1988). The strongest product ion in our method as discussed earlier was *m/z* 317, the precursor ion of 12-HPETE minus water $[M\text{-}H_2O]^-$ and may explain the poor recovery values for this particular lipid. Calculations of recovery, particularly for the lowest validation concentrations of endocannabinoids and some eicosanoids, were impeded due to endogenous levels of these in rat brain. High endogenous background concentrations subtracted from low concentrations of spiked standard can often lead to an overestimation of recovery. The results are comparable to previous work 49-90% (De Grauw et al 2011), 67-251% (Masoodi et al 2010), 54-92% (Zhang et al 2007) and there were a greater number of validated analytes in this method compared with other published methods. The limit of quantification (LOQ) for all lipids was found to range from 0.05 to 2.5 pmol/g and comparable to other methods (Richardson et al 2007, Zhang et al 2007), however some methods express this as a ratio of signal to noise rather than a calculated value (Masoodi et al 2008).

The phenomenon of matrix effects is widely reported in LC-MS/MS (Trufelli et al 2011, Kittlaus et al 2011, Matuszewski et al 2003, King et al 2000), which can be detrimental to the sensitivity of the method. Hence, ion suppression was also investigated where 100% represented the value for the absence of a biological matrix. The results range from 20% to 110%, with the lowest concentration generating the poorest figures (Table 11). As mentioned, matrix effects can affect sensitivity and

decrease the response of an analyte, which unsurprisingly has a greater effect on the lowest concentration. Overall, the results showed that the majority of the analytes were minimally affected by the matrix. Previous work on ion suppression looked at the internal standards 15-HETE-d8 (104%) and 11,12-EET-d8 (96%) along with 8,15-diHETE (112%) and also showed that there were minimal matrix effects (Zhang et al 2007).

The accuracy and precision data for intraday (n = 5) and interday (n = 4) are shown in Table 10. The results for each analyte were within the recommended RSD of <±15% for accuracy and precision for intraday and accuracy for interday. A few values for interday precision were not within this recommended range, 12-HPETE at the low (27%) and medium (19%) concentration and 20-HETE (21%) at the low concentration. The intraday precision range was between 1.4 and 14.9% and the interday precision range was between 3.8 and 26.8%. The intraday accuracy range was between 89.2 and 114.3% and the interday precision range was between 85.2 and 111.4%.

A few of the values that were slightly higher than the recommended RSD% can be explained by the poor sensitivity of 12-HPETE and 20-HETE. Looking at the chemical structure and spectra (Figure 4 and 8), both 12-HPETE and 20-HETE have a limited number of product ions at detectable intensities. 20-HETE has been found previously to only show dissociation at higher collision energies and also this particular lipid did not exhibit a large number of structurally significant product ions like the other HETEs (Masoodi et al 2010). This finding agrees with the results seen in this method, where it was also a challenge to find a product ion with sufficient sensitivity for MRM detection.

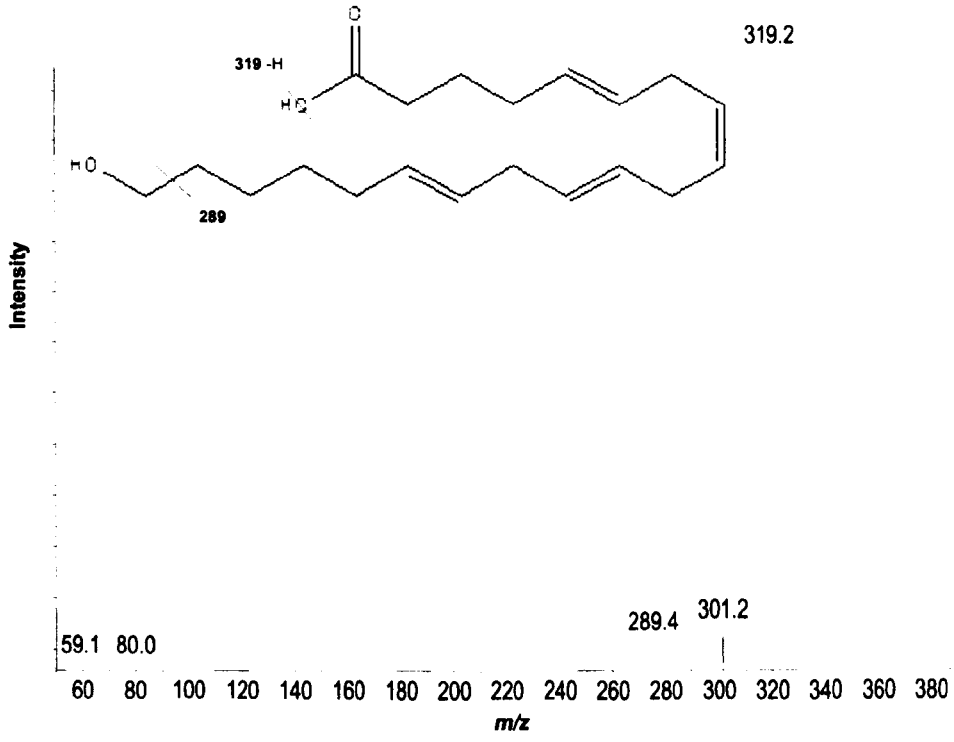

Figure 8. Product ion spectra of 20-HETE and the fragmentation of this lipid.

Both 20-HETE and 12-HPETE had reduced sensitivity compared with the other analytes, and this should be noted in view of the lack of detection of these lipids in any of the biological samples studied.

2.3.3 Measurement of bioactive lipids in rat tissues

The newly developed method was evaluated by analysing the bioactive lipid profiles of a range of rat tissues/biofluids which would be representative of studies planned for future work (included in later chapters of this thesis).

2.3.3.1 Comparison of the lipid profiles in different rat tissues

Spinal cord, dorsal root ganglia (DRGs; L3-L5), knee joint, plasma and five brain regions: frontal cortex, midbrain, hippocampus, rest of cortex and rest of brain were collected from saline treated rats according to the methods described earlier. These samples were analysed using the validated method to measure levels of bioactive lipids in different tissues. A profile of the different bioactive lipids in each type of tissue was created

to look at the overall distribution. 9-HODE was yet to be incorporated into the method at the time when this analysis was performed, therefore the data presented do not include this analyte. For convenience, the bioactive lipids have been grouped into four analyte groups related to their biosynthetic pathways, this is clearly shown earlier in this chapter in Table 6. These include the cyclooxygenase (COX), lipoxygenase (LOX), cytochrome p450 (CYP450) and endocannabinoid (EC) groups.

In the rat knee joint 5-, 11-, 12-, 15-HETE, AEA, PEA, OEA, 2-AG, AraGly, PGD_2/PGE_2, TXB_2, AA, LA, 13-HODE, 9-, 13-oxoODE were all detected (Figure 9, Table 11). The majority of the analytes measured in the tissue are from AA (90%), LA (2%) and 2-AG (5%) and have therefore been excluded to give a clearer distribution of the other analytes in the tissue (Figure 9b). Likewise in rat plasma, 5-, 11-, 12-HETE, AEA, PEA, OEA, 2-AG, AraGly, PGD_2/PGE_2, AA, LA, 13-HODE, 9- and 13-oxoODE were all detected (Table 12) with the major lipids being AA, LA and 2-AG (99%). 8-, 15-HETE, TXB_2 and AraGly were all below the limit of quantification in these samples. Again, AA and 2-AG have been excluded for reasons of clarity in all figures to provide a better distribution of all the other lipids detected (Figure 9).

The distribution of bioactive lipids in plasma and knee (Figure 9) were clearly different to the distribution of lipids found in neural tissue such as spinal cord, DRGs and brain (Figure 9). The majority of the bioactive lipid profile of knee joint and plasma were made up of LA, AA and 2-AG, whereas in neural tissue the proportion of LA is relatively small and the major lipids are AA and 2-AG (Table 12).

a)

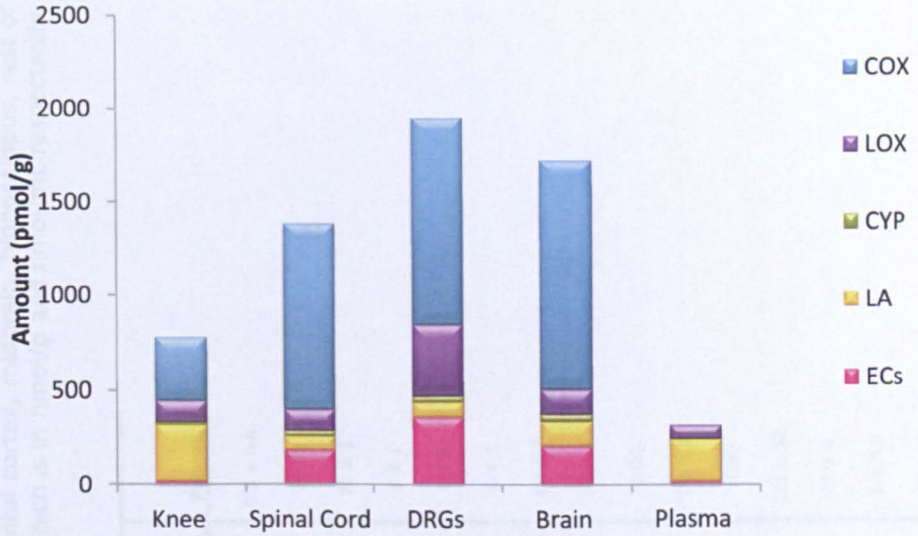

b)

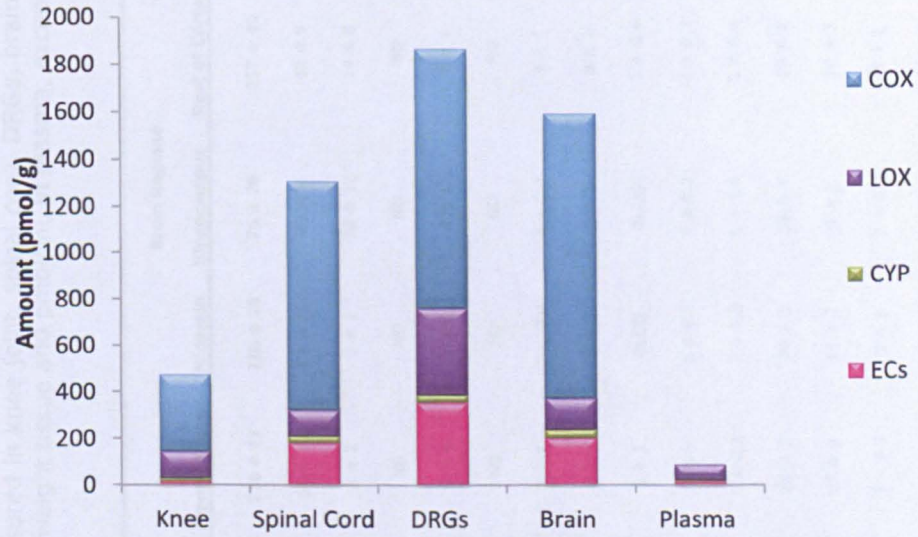

Figure 9. a) Lipid distribution of the measured analytes in knee joint, spinal cord, DRGs, brain and plasma, excluding 2-AG and AA in wet weight tissue, n=8. All values for knee, joint, spinal cord, DRGs and brain are in pmol/g and plasma in pmol/mL. b) Lipid distribution of the measured analytes in knee joint and plasma, excluding LA, 2-AG and AA.

Table 12. Levels of individual analytes measured in knee joint, spinal cord, DRGs, brain regions; frontal cortex, midbrain, hippocampus, rest of cortex, rest of brain and plasma in pmol/g in all wet weight tissue and pmol/mL in plasma, except for 2-AG, which is in nmol/g and nmol/mL respectively.

				Brain Regions					
	Knee Joint	Spinal Cord	DRGs (L3-L5)	Frontal Cortex	Midbrain	Hippocampus	Rest of Cortex	Rest of Brain	Plasma
PGD2/PGE2	282 ± 26	587±195	496 ±46	236 ± 13	128 ± 28	76 ± 28	257 ± 40	307 ± 114	0.5 ± 0.6
TXB2	48 ± 4	399±133	608 ±63	64 ± 12	61 ± 14	23 ± 8	32 ± 9	35 ± 13	BLOQ
13-HODE	21 ± 3	9 ± 3	18 ± 4	3 ± 2	3 ± 1	23 ± 12	14 ± 8	19 ± 9	23 ± 2
13-oxoODE	0.5 ± 0.1	ND	ND	ND	ND	ND	ND	ND	8 ± 1
15-HETE	23 ± 2	22 ± 6	BLOQ	6 ± 4	2 ± 1	2 ± 1	7 ± 1	7 ± 2	BLOQ
9-oxoODE	2 ± 0.3	ND	ND	ND	ND	ND	ND	ND	6 ± 1
11-HETE	8 ± 1	15 ± 3	31 ± 6	9 ± 1	3 ± 0.4	4 ± 0.2	7 ± 1	3 ± 0.5	2 ± 0.5
12-HETE	71 ± 7	82 ± 22	358 ± 68	8 ± 2	9 ± 2	6 ± 2	8 ± 2	16 ± 3	34 ± 4
8-HETE	2 ± 0.2	2 ± 1	BLOQ	2 ± 1	BLOQ	BLOQ	1 ± 0.4	0.3 ± 0.2	BLOQ
5-HETE	2 ± 0.2	11 ± 4	BLOQ	3 ± 1	1 ± 0.4	1 ± 0.2	1 ± 0.3	1 ± 0.2	2 ± 0.2
AraGly	0.3 ±0.1	1 ± 0.5	BLOQ	1 ± 0.3	1 ± 0.5	1 ± 0.4	1 ± 0.4	1 ± 0.4	BLOQ
LA	300 ± 40	74 ± 10	80 ± 19	24 ± 3	24 ± 3	19 ± 4	26 ± 3	36 ± 5	221 ± 22
AA	16 ± 1	84 ± 17	31 ± 4	15 ± 3	11 ± 2	9 ± 3	10 ± 3	8 ± 3	27 ± 4
AEA	1.4 ± 0.1	4 ± 0.5	4 ± 1	3 ± 0.3	3 ± 1	2 ± 0.4	3 ± 1	2 ± 0.5	1 ± 0.1
2-AG	1 ± 0.1	8 ± 1	1.3 ± 0.1	3 ± 0.5	6 ± 1	4 ± 0.5	3 ± 0.5	3 ± 1	48 ± 15
PEA	9 ± 2	116 ± 19	233 ± 33	23 ± 5	46 ± 7	22 ± 2	13 ± 2	20 ± 3	7 ± 0.3
OEA	4 ± 1	60 ± 9	118 ± 18	11 ± 1	23 ± 4	9 ± 1	8 ± 1	10 ± 1	6 ± 1

All values are expressed as mean ± SEM in pmol/g for tissues, except for AA and 2-AG in nmol/g, n=8. All values for plasma are in pmol/mL, except for AA in nmol/mL. All outlier values greater than 2 standard deviations from the mean were excluded, maximum of one per tissue group for each lipid measured. Some lipids were not detected (ND) in any of the samples, others were only detected in a few samples and were therefore below the limit of quantification (BLOQ).

In neural tissue, levels of several lipids found in the DRGs were very high when compared to the spinal cord and brain (Figure 9). In the DRGs, 11-, 12-HETE, AEA, PEA, OEA, 2-AG, PGD_2/PGE_2, TXB_2, AA, LA and 13-HODE were all detected (Figure 9, Table 11). This was similar to the spinal cord (Figure 9, Table 11), although AraGly along with 5-, 8- and 15-HETE were below the limit of quantification in the DRGs. In the DRGs 91% of the distribution of lipids measured consisted of AA, with 2-AG making up 4%. In the spinal cord, 5-, 8-, 11-, 12-, 15-HETE, AEA, PEA, OEA, 2-AG, AraGly, PGD_2/PGE_2, TXB_2, AA, LA and 13-HODE were all detected (Figure 9, Table 11) and consisted mainly of AA (90%) and 2-AG (8%)(both excluded). The distribution of lipids found in the spinal cord was also very similar to the brain (Figure 9). The main difference between neural tissue and the knee and plasma was the huge amounts of AA compared to LA. A reason could be because neurons are not capable of synthesis of AA from LA by elongation and desaturation, which occurs in other cells. Free AA is rapidly stored by esterification to membrane phospholipids until needed for regulation of neuronal activity (Piomelli 1994, Piomelli 1993). Once released AA can either be metabolised by COX, LOX or CYP450s to produce lipids that act within neurons to modulate the activities of ion channels, ion pumps, protein kinases and neurotransmitter uptake systems (Piomelli 1994). These three routes of AA metabolism have also been extensively described in the brain for many years (Farooqui et al 2007, Phillis et al 2006, Kauffmann et al 1997, Needleman et al 1986).

Additionally, brain tissue was subdivided into regions for analysis (See methods). 5-, 8-, 11-, 12-, 15-HETE, AEA, PEA, OEA, 2-AG, AraGly, PGD_2/PGE_2, TXB_2, AA, LA and 13-HODE were all detected in the frontal cortex, rest of cortex and the rest of brain. All of these were also detected in the midbrain and hippocampus except 8-HETE, which was below the limit of quantification (Figure 10, Table 11). In the frontal cortex AA made up 82% of the distribution, with 2-AG the remaining 16% (both excluded). This was similar for the midbrain, hippocampus, rest of cortex and rest of brain regions, where AA made up 66-76% of the distribution with 2-AG a large proportion of the remainder. The main

components of brain tissue were the fatty acids AA and LA, endocannabinoid-like compounds OEA and PEA and the COX-2 metabolites TXB_2 and PGD_2/PGE_2. PGE_2 is the main product of the COX pathway and is involved in brain maturation and the regulation of synaptic activity and plasticity (Alix et al 2008). The fatty acids as mentioned in the introduction are important instigators of many neuronal processes by production of a cascade of products via different enzymatic pathways (Table 6).

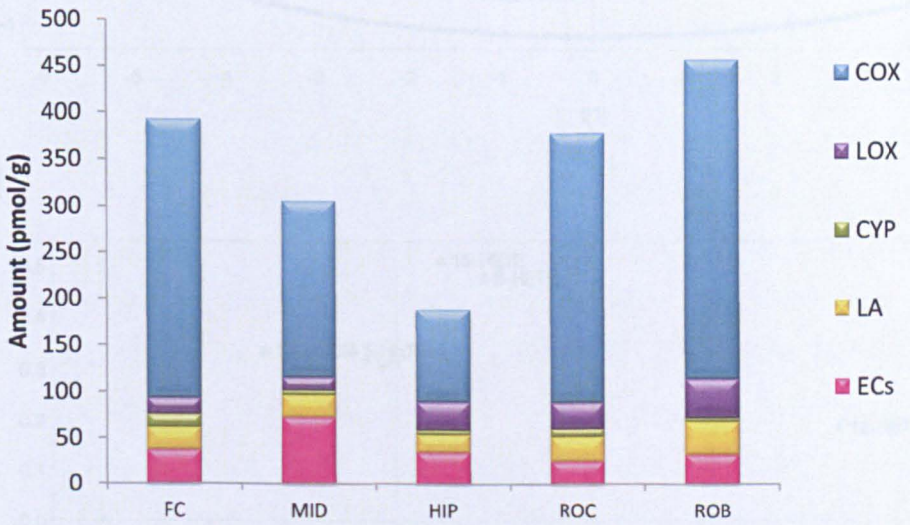

Figure 10. Lipid distribution of the measured analytes in rat brain divided into five regions; frontal cortex (FC), midbrain (MID), hippocampus (HIP), rest of cortex (ROC) and rest of brain (ROB) in pmol/g, n=8. All outlier values greater than 2 standard deviations from the mean were excluded, maximum of one per tissue group for each lipid measured.

The main difference when comparing the DRGs to spinal cord and brain are the high levels of 12-HETE. In the plasma and knee joint, high levels of the precursor LA can be found (Figure 9, Table 11), whereas in the DRGs this is not as apparent (Figure 9, Table 11).

A qualitative comparison between the different tissues was conducted using PCA (See Materials and Methods) to complement the discussion of

the differential distribution of lipids between the different tissue types (Figure 11).

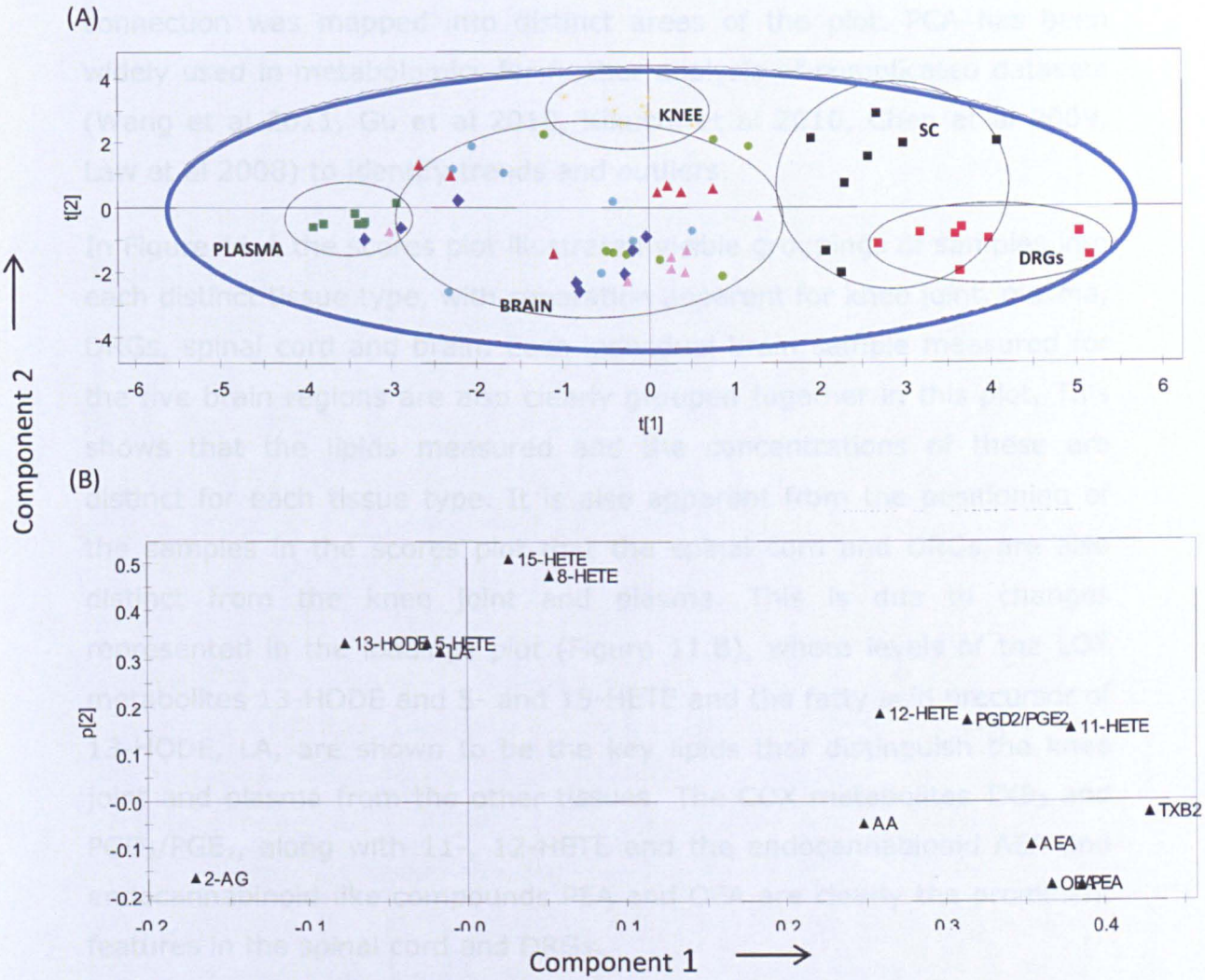

Figure 11. Individual samples were independently analysed using Principle Component Analysis (PCA) to look at variation between samples represented by (A) scores plot of a two-component PCA model of the dataset and (B) loadings plot of the same model dataset. Each sample was colour coded according to tissue type: yellow=knee joint, green=plasma, red=DRGs, black=spinal cord, lime=frontal cortex, blue=hippocampus, purple=midbrain, maroon=rest of cortex and turquoise=rest of brain. These tissue groups have been circled in black for better visualisation. Samples that fit within the 95% confidence interval are included within the blue circle.

Each individual sample represented a measured concentration of the lipid analysed (variable 1) from a tissue type (variable 2). Individual points were then mapped in the space spanned by principal components 1 and 2 and colour coded for tissue type (Figure 11) and any variance or connection was mapped into distinct areas of the plot. PCA has been widely used in metabolomics for further analysis of complicated datasets (Wang et al 2011, Gu et al 2010, Kikuchi et al 2010, Chen et al 2009, Law et al 2008) to identify trends and outliers.

In Figure 11.A the scores plot illustrated visible groupings of samples into each distinct tissue type, with separation apparent for knee joint, plasma, DRGs, spinal cord and brain. Each individual brain sample measured for the five brain regions are also clearly grouped together in this plot. This shows that the lipids measured and the concentrations of these are distinct for each tissue type. It is also apparent from the positioning of the samples in the scores plot that the spinal cord and DRGs are also distinct from the knee joint and plasma. This is due to changes represented in the loadings plot (Figure 11.B), where levels of the LOX metabolites 13-HODE and 5- and 15-HETE and the fatty acid precursor of 13-HODE, LA, are shown to be the key lipids that distinguish the knee joint and plasma from the other tissues. The COX metabolites TXB_2 and PGD_2/PGE_2, along with 11-, 12-HETE and the endocannabinoid AEA and endocannabinoid-like compounds PEA and OEA are clearly the prominent features in the spinal cord and DRGs.

2.3.3.2 Comparison of quantitative levels of the bioactive lipids in literature on rat tissues

Plasma

Profiling of bioactive lipids has previously not been reported in rat plasma, so for the first time, this work is presented in this chapter. Eicosanoids however have been profiled in human serum from obese individuals using SPE-LC-MS/MS (Ferreiro-Vera et al 2011). 12-HETE (10 ng/mL), PGE_2 (0.1 ng/mL), PGE_3 (9 ng/mL), 9-HODE (6 ng/mL) and 13-HODE (5 ng/mL) were all detected in the human serum, 5-, 8-, 11- and

15-HETE were all measured and not detected (Ferreiro-Vera et al 2011). PGD_2, AA and LA have previously been measured in rat serum and the control levels of these lipids ranged from 2-6 µg/mL, much higher compared to this method (Table 11; Bai et al 2010). A possible explanation for this could be that the method by Bai et al only managed to separate and quantify six lipids, whereas in our method there were 42 lipids. Therefore this large difference in lipid numbers may contribute to the sensitivity of the method. Also, rat serum contains lipids associated with the coagulation process and consequently the lipid composition of this biological sample is very different to plasma. AEA, PEA and OEA have also been measured in rat plasma; levels are 3.1±0.6 pmol/mL, 9.4±1.6 pmol/mL and 9.2±1.8 pmol/mL respectively (Guiffrida et al 2000). 12-HETE has previously been measured in rat plasma at levels of approximately 100 ng/mL. There are a number of LOX metabolites of LA and AA found in plasma, such as 13-HODE, 9-, 13-oxoODE and the HETEs mainly 12-HETE. 12-HETE is primarily formed from the metabolism of AA by 12-lipoxygenase (12-LOX; Hampson and Grimaldi 2002), whereas the HODEs are formed through the metabolism of LA by 15-lipoxygenase (15-LOX) and are further reduced by dehydrogenase to the oxoODEs (Vangeveti et al 2010). Lipoxgenases have been shown to be highly expressed in blood and immune cells (Hampson and Grimaldi 2002), which may account for the high levels of LOX products in plasma. Also positional specificity of enzymes may be of pathophysiological importance because lipoxygenases in the rat favour production of 12-HPETE which is further metabolised to 12-HETE, whereas in humans 15-HPETE is favoured (Kuhn and O'Donnell 2006).

Knee Joint

Prostaglandins have previously been investigated in rabbit and human synovial fluid (Alstergren and Kopp 2000, Schumacher et al 1996, Gold et al 1976) and endocannabinoids in human synovial fluid (Richardson et al 2008). However, profiling of lipids in the knee joint is yet to be investigated until now, therefore the profiling of lipids in the knee joint is novel data. A higher proportion of LOX metabolites such as 12-, 15-HETE,

13-HODE, 9- and 13-oxoODE are found in the knee joint compared to plasma, along with a greater proportion of COX-2 metabolites, PGD_2/PGE_2 and TXB_2. 9- and 13-oxoODE which are the oxidative metabolites of the HODEs are only detected in the knee joint and plasma but are not detectable in the other tissues (Table 11). The level of LA detected in the knee joint is significantly higher than the other tissues, especially when this is expressed as a ratio of AA. The majority of research investigating expression of LOX in bone is conducted in mouse models, where increased expression is shown to be detrimental to skeletal development (Almeida et al 2009, Klein et al 2004). Higher levels of the precursor may contribute to the greater levels of LOX metabolites of LA observed in the knee joint. PGD_2, PGE_2, TXB_2, 5-, 12-HETE, 9- and 13-HODE were all previously measured in the tibiotarsal joint of mice, where concentrations of LA metabolites were also several fold higher than AA metabolites (Blaho et al 2009). The importance of COX-2 in this joint and bone formation has been discussed (Blaho et al 2009, Tang et al 2006, Zhang et al 2002, Sato et al 1997), where knockout models show not only a decrease in COX metabolites but also 5-LOX metabolites, suggesting a link between these two metabolic pathways (Blaho et al 2009).

DRGs

Profiling of the bioactive lipids has previously not been conducted in the DRGs, however individual lipids have been measured, again, shown here for the first time. AEA and 2-AG have previously been detected in a dorsal root ganglia cell line (Rimmerman et al 2008), where the distribution of AEA and 2-AG in lipid rafts were investigated. Levels of AEA (26 pmol/g) and 2-AG (9 nmol/g) were also measured using LC-API-MS/MS in DRGs (Mitrirattanakul et al 2006). Levels of AEA and 2-AG in the DRGs reported previously were considerably higher than those measured with this method (Table 11), which may be due to differences in extraction methods (Mitrirattanakul et al 2006, Huang et al 1999). The eicosanoids however have not been measured in the DRGs, but the EETs have been measured in trigeminal ganglion neurons (Iliff et al 2010).

Spinal Cord

Lipid profiling in the spinal cord has previously been conducted using two separate methods; one measuring eicosanoids using GC-MS/MS and one measuring the endocannabinoids using LC-MS/MS (Buczynski et al 2010). However, a comparison of the lipid levels in the spinal cord (Table 11) found that the lipids measured were much lower than those reported previously (Buczynski et al 2010). As discussed earlier, this could be due to differences in extraction technique, therefore a direct comparison cannot be drawn. There is little information on eicosanoid levels in the spinal cord apart from work by Buczynski et al; only PGD_2 has previously been measured in mouse spinal cord (Kihara et al 2009). In terms of the endocannabinoids, 2-AG has also been detected in the rat spinal cord using a number of LC-MS/MS methods (Staniaszek et al 2010, Petrosino et al 2007, Jhaveri et al 2006, Huang et al 1999), as well as AEA (Jhaveri et al 2006). The endocannabinoid-like compounds OEA and PEA have also been measured (Jhaveri et al 2006). Again, a comparison of spinal cord lipid levels quantified with our method, found that concentrations reported previously were higher than this method. Although the concentrations discussed here were control values, there are still species differences and other study factors, alongside different methodologies that may also influence the lipid amounts detected.

Brain

Rat brain has been used as part of a full validation for an eicosanoid profiling LC-MS/MS method, however levels of these were not reported (Masoodi et al 2008). Lipid profiling in the rat brain or different regions of the rat brain has yet to be investigated. 5-, 8-, 12-, 20-HETE have previously been measured in whole rat cortex ranging from 2.6-12.14pg/mg, along with PGD_2 and PGE_2 at 1.76 and 3.97 pg/mg respectively (Yue et al 2007). As mentioned previously, 20-HETE had reduced sensitivity compared with the other analytes in our method, and that this should be noted in view of the lack of detection of 20-HETE in any of the biological samples studied. Since 20-HETE was measured in a

previous method (Yue et al 2007), where 5-, 8- and 12-HETE concentrations were also reported to be higher than those reported in our method (Table 10), this may be due to a sensitivity factor between methods. AA, PGD_2, PGE_2, TXB_2, 5- and 12-HETE were all measured in ischaemic rat brain, however PGD_2 and PGE_2 were not detected in control brains (Farias et al 2008). PGE_2 (11 ng/g) and PGD_2 (25 ng/g) were both also detected in mouse brain (Brose et al 2011). AEA, OEA, PEA, 2-AG and arachidonic acid have also been measured in the rat frontal cortex, where levels of these lipids were significantly higher than this method (Williams et al 2007). AEA and 2-AG have been measured in the prefrontal cortex and hippocampus in rats (Malinen et al 2009). The endocannabinoids 2-AG, AEA, PEA, OEA and 2-linoleoyl glycerol (2-LG) have also previously been measured in several different brain regions, where AraGly was analysed but not detected (Richardson et al 2007). Although levels of the bioactive lipids are lower in this method (Table 11) compared to those previously published (Yue et al 2007, Richardson et al 2007, Williams et al 2007), a wider range of lipids are detected and measured in our method including AraGly. A combination of LC and MS optimisation meant that AraGly is analysed in negative electrospray ionisation mode rather than positive electrospray ionisation mode as previous (Richardson et al 2007). Furthermore, it may be for this reason that levels of AraGly are detected in all five brain regions analysed using this method.

It is difficult to draw comparisons with other methods, due to the lack of detailed literature in this area and the frequent use of separate methods for individual lipids. Differences in reported absolute levels of lipids can result from many different factors, ranging from tissue collection, differences in timings, sex, ages and strain of animals to the methodology, such as differences in extraction methods and efficiencies. Evidence from previous publications along with good validation results have shown that the methodology is capable of measuring lipids in a particular tissue, yet there is limited literature to allow further comparison. This combined with differences between methodologies also

makes it extremely difficult to draw direct comparisons of lipid concentrations with other publications. However, the strength of the newly developed method is in its ability to provide a comprehensive profile of bioactive lipids from a single sample, thus providing consistent and comparable data for comparisons of different tissues or interventions.

2.4 Conclusions

The sensitive and selective LC-MS/MS method described allows comprehensive profiling of a wide range of bioactive lipids ranging from pro-inflammatory to anti-inflammatory. The use of polarity switching has enabled simultaneous analysis of a structurally diverse range of compounds and provides a more representative picture of the *in vivo* inflammatory process. This method shows that careful manipulation of factors such as pH to chromatographically separate a large range of compounds has provided a useful analytical tool for biological investigation. The key advantage of using a single method for comparative profiling studies not only eliminates the problem of comparing across different published data sets but also between different analytical methods. A wide range of samples have been analysed using this validated method which includes rat brain, spinal cord, knee joint, DRGs, plasma, hindpaw, mouse brain and colon and human plasma and colon. This has provided useful information on the distribution of lipids in different tissues, which has previously not been shown, in relation to their biological function and involvement in biological processes. As shown in subsequent chapters of this thesis, the method has been used to investigate changes in levels of bioactive lipids in different disease states and also monitored for changes in these lipids following drug treatment. Additionally the method can be used to investigate ligands of receptor targets such as TRPV1 and PPAR, to explore the significance of these targets in different disease models. Finally to conclude, this LC-MS/MS method is a valuable analytical tool that can be applied to a diverse range of tissues, disease states and biological targets in different areas of research.

Chapter 3.

Investigation of endogenous ligands for peroxisome proliferator activated receptors (PPARs)

3. Investigation of endogenous ligands for peroxisome proliferator activated receptors (PPARs)

3.1 Introduction

Peroxisome proliferator activated receptors (PPARs) have well established anti-inflammatory actions (discussed later). A number of ligands present in the body have been shown to activate PPARα (see below), but in most cases their biological contribution to PPARα activation is yet to be ascertained. In this chapter the further application of the novel validated LC-MS/MS analytical method described in Chapter 2 to measure levels of endogenous ligands for PPAR alpha (PPARα) was undertaken to investigate which of these ligands may modulate inflammatory pain responses. This included investigating the effects of carrageenan-induced inflammation on levels of PPARα ligands in the hindpaw, spinal cord and brain.

3.1.1 Identification of endogenous PPARα ligands

A number of PPARα ligands have been identified *in vitro* such as AEA, OEA, PEA, 8-HETE, 5,6-EET, 8,9-EET, 11,12-EET, 14,15-EET, arachidonic acid (AA), linoleic acid (LA), palmitic acid (AA) and oleic acid (OA). In transactivation assays, AA, LA, PA and OA have been shown to activate PPARα when assayed at 100 μM (Kliewer et al 1997) and AA and LA bind to PPARα in the range of 25-30 μM in ligand-induced complex formation assays (Forman et al 1997). 8-HETE, an 8-lipoxygenase product produced in skin, and a product of CYPs, also activates PPARα in transactivation assays (Yu et al 1995, Kliewer et al 1997). 5,6-EET, 8,9-EET, 11,12-EET, 14,15-EET and 20-HETE have been shown to displace *cis*-parinaric acid in ligand-receptor binding assays of PPARα (Cowart et al 2002). OEA also activates PPARα in transactivation assays with a half-maximal concentration (EC_{50}) of 120 ± 1 nM compared to the synthetic PPARα agonists of Wy-14643 and GW7647 which activated PPARα with EC_{50} values of 1.4 ± 0.1 μM and 150 ± 20 nM, respectively (Fu et al 2003). The half-maximal inhibitory concentration (IC_{50}) of OEA in binding

competition experiments was 120 ± 10.7 nM and saturation binding studies showed that [^{3}H]OEA associated with the ligand binding domain (LBD) of human and murine PPARα with dissociation constants (K_d) of 43.3 ± 1.6 nM and 37.4 ± 0.1 nM, respectively (Fu et al 2003). AEA has been shown to displace *cis*-parinaric acid in ligand-receptor binding assays for PPARα to give an IC_{50} between 10-30 μM, which is as potent as OEA (IC_{50} of 30 μM) for ligand occupancy, but gave a bigger reporter gene (agonist) response (Sun et al 2007). PEA has also been shown in transactivation assays to activate PPARα with an IC_{50} of 3.1 ± 0.4 μM. Once again Wy-14643 and GW7647 were used as positive controls to give IC_{50} values of 187 ± 42 nM and 1.4 ± 0.1 μM, respectively (LoVerme et al 2005). Palmitic acid, a product of PEA hydrolysis was found not to activate PPARα (LoVerme et al 2005). There are however, other inflammatory mediators which may also target this receptor. The HETEs (hydroxyeicosatetraenoic acids) and EETs (mentioned earlier) are biologically active arachidonic acid derivatives produced through the action of lipoxygenases, epoxygenases and CYPs. Some HETEs, such as 8-HETE activates PPARα *in vitro*, but binding to PPARα has yet to be described (Yu et al 1995). The potential role (s) of these novel PPARα ligands *in vivo* remains to be characterised.

3.1.2 Principles of TR-FRET

The principles of TR-FRET or time-resolved Forster resonance energy transfer is a phenomenon first described by Morrison (Morrison 1988). It is a recognised method for screening compounds and for overcoming interference from compound autofluorescence from precipitated compounds (Hemmila and Webb 1997). The principles of a TR-FRET assay are similar to that of a standard FRET assay where a suitable pair of fluorophores once brought within close proximity of one another will result in excitation of the first fluorophore (donor) and subsequent energy transfer to the second fluorophore (acceptor). An increase in the fluorescence emission of the acceptor and decreased emission of the donor is detected as a transfer in energy (Morrison 1988, Hemmila and Webb 1997).

In the Lanthascreen TR-FRET assays, a long-lifetime lanthanide chelate is used as the donor species, whereas in standard FRET assays this is not the case. The most common lanthanides used are terbium and europium (Hemmila and Webb 1997). Terbium is used in this particular assay and it offers several advantages over europium. Terbium-based TR-FRET assays can use fluorescein, a common fluorophore, as the acceptor. It is straightforward to label a molecule such as a peptide with fluorescein and it is not expensive. Directly labelled molecules may also be used in terbium-based assays which reduces cost, improves kinetics and avoids steric interactions when using large allophycocyanin (APC) conjugates; the acceptor needed if using europium. APC requires the use of biotinylated molecules that must be indirectly labelled via a streptavidin-mediated recruitment of APC and is more complicated (Blomberg et al 1999, Hemmila and Webb 1997). The excited-state lifetime (the average time that the molecule spends in the excited state after accepting a photon) of lanthanide chelates is a millisecond or longer. Other common fluorophores have a lifetime typically within the nanosecond range. Interference or scattered light from autofluorescent compounds are also within the nanosecond range, so this can be problematic and can negatively impact the assay. This can be overcome by measuring FRET after a suitable delay (Hemmila and Webb 1997).

The terbium-labelled anti-glutathione-S-transferase (anti-GST) antibody binds to the GST tag of the PPARα receptor, a nuclear receptor labelled NR (Figure 1) and is used to indirectly label this receptor. A fluorescent ligand or tracer in this case, the fluormone Pan-PPAR Green once bound to the receptor, leads to an energy transfer from the antibody to the tracer resulting in a high TR-FRET ratio. Competitive ligand binding is reflected in the ability of the test compound to displace the tracer from the receptor and results in a loss of TR-FRET signal.

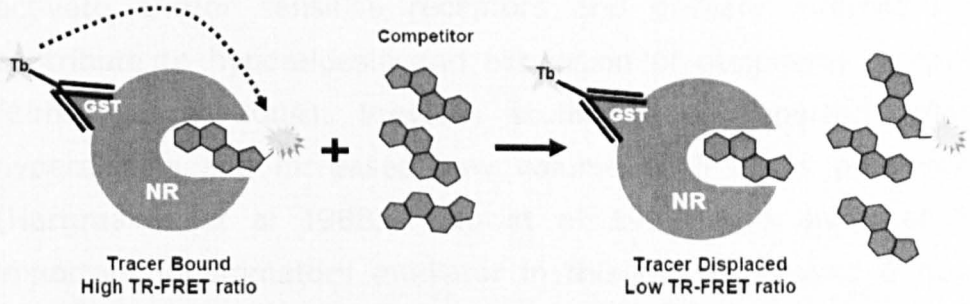

Figure 1. Principle of the this Lanthascreen competitive binding assay.

Image from Invitrogen Lanthascreen® Terbium Instrument and protocol booklet

3.1.3 Carrageenan model of inflammatory pain

The carrageenan model of inflammatory pain uses λ-carrageenan, a complex polysaccharide extract of the red algae, *Chrondus crispus*, first described by Winter et al 1962. It does not gel strongly at room temperature and produces a local inflammatory response on injection (Winter et al 1962, Di Rosa 1972). Classic signs of inflammation can be observed with this model, including oedema, hyperalgesia and erythema, and the inflammation induced is acute and a non-immune response (Hargreaves et al 1988). The level of inflammation is usually quantified by change in paw size and is maximal five hours post-injection (Morris 2003). During the inflammatory process, in response to the tissue damage, inflammatory mediators are generated *in situ* at the site of injury or by infiltrating cells such as neutrophils and mast cells (Morris 2003). These include prostaglandins, bradykinin, 5-hydroxytryptamine (5-HT) (Di Rosa et al 1971), histamine (Al-Haboubi and Zeitlin 1983), nerve growth factor (NGF) (Leon et al 1994), reactive oxygen and nitrogen species (Salvemini et al 1996) and pro-inflammatory cytokines (Loram et al 2007, Morris 2003) that all contribute to the inflammatory process. In addition to this, carrageenan-induced mechanical hyperalgesia is apparent, which can be assessed through changes in weight bearing and paw pressure sensitivity (Hargreaves et al 1988). This induction in pain behaviour is linked to the dependent release of histamine, 5-HT (Di Rosa et al 1971, Al-Haboubi and Zeitlin 1983) and NGF (Leon et al 1994) from infiltrating mast cells. These mediators can

activate and/or sensitise receptors and primary afferent fibres and contribute to hyperalgesia and expansion of peripheral receptive fields (Elmes et al 2004). Previous studies have reported inflammatory hyperalgesia and increased paw volume at 3 hours post-carrageenan (Hargreaves et al 1988, Hedo et al 1999) and levels of PGE_2, an important inflammatory mediator in this model, peaked 6 hours post-carrageenan (Guay et al 2004).

3.1.4 Effects of PPARα ligands in inflammation

PPARα regulates systemic inflammation by inducing the expression of anti-inflammatory proteins such as I kappa B alpha (IκB-α), reducing the expression of pro-inflammatory proteins such as tumour necrosis factor-alpha (TNF-α) and limiting immune cells recruitment to inflammation sites and cytokine production (See General Introduction, Delerive et al 2002, Delerive et al 2000). These effects are mediated through changes in gene expression by induction of responsive target genes and inhibition of transcription factor activities (Delerive et al 2002, Delerive et al 2000). Importantly, PPARα stimulates the catabolism of pro-inflammatory eicosanoids such as LTB_4 by inducing gene transcription (Devchand et al 1996). Activation of PPARα has also been shown to modulate inflammatory responses. PPARα ligands demonstrated inhibition of interleukin (IL) -1β-induced IL-6 secretion and 6-keto-prostaglandin $F_{1\alpha}$ production, and decreased gene expression of vascular cell adhesion molecule-1 (VCAM-1) and tissue factor in endothelial cells and monocytes (Marx et al 1999, Neve et al 2001). Studies focussing on the molecular mechanisms of PPARα showed that activation of this receptor also negatively interferes with the inflammatory response by antagonising nuclear factor-κB (NF-κB) signalling (Delerive et al 1999, Marx et al 1999). A number of endogenous ligands shown to activate PPARα in transactivation assays have also been shown to modulate inflammatory responses *in vivo* (See General Introduction). Oleoyl ethanolamide (OEA) and palmitoyl ethanolamide (PEA) reduced O-tetradecanoylphorbol-13-acetate induced oedema in mice, as effect absent in PPARα knockout mice (Lo Verme et al 2005). PEA prevented IκB-α degradation and NF-κB

nuclear translocation in the spinal cord, and also attenuated the development of carrageenan-induced hindpaw oedema (D'Agostino et al 2007).

3.1.5 Aims and Objectives

- To investigate the interaction of putative ligands with PPARα and to compare the affinity of putative PPARα ligands in a PPARα ligand binding assay
- To determine the levels of PPARα ligands in biological tissue.
- To determine whether the levels of PPARα ligands are altered in the carrageenan model of inflammatory pain

3.2 Materials and Methods

3.2.1 Chemicals

Dimethyl sulfoxide (DMSO) and ethanol were purchased from Sigma Aldrich (Gillingham, UK) and GW7647, a PPARα agonist used as a positive control was purchased from Tocris Bioscience (Bristol, UK). 9-hydroxyeicosatetraenoic acid (9-HETE), 11-hydroxyeicosatetraenoic acid (11-HETE), 12-hydroxyeicosatetraenoic acid (12-HETE), 15-hydroxyeicosatetraenoic acid (15-HETE), 16-hydroxyeicosatetraenoic acid (16-HETE), 20-hydroxyeicosatetraenoic acid (20-HETE), arachidonic acid (AA), linoleic acid (LA), palmitic acid (PA), oleic acid (OA), 2-linoleoyl glycerol (2-LG), 2-arachidonoyl glycerol (2-AG), N-arachidonoyl ethanolamide (AEA), N-palmitoyl ethanolamide (PEA) and N-oleoyl ethanolamide (OEA) were purchased from Cambridge Bioscience (Cambridge, UK). 5-hydroxyeicosatetraenoic acid (5-HETE), 8-hydroxyeicosatetraenoic acid (8-HETE), 5,6-epoxyeicosatrienoic acid (5,6-EET), 8,9-epoxyeicosatrienoic acid (8,9-EET), 11,12-epoxyeicosatrienoic acid (11,12-EET), 14,15-epoxyeicosatrienoic acid (14,15-EET), 12-hydroperoxyeicosatetraenoic acid (12-HPETE) and 15-hydroxyeicosatetraenoic acid-d8 (15-HETE-d8) were all purchased from Biomol International (Exeter, UK). The Lanthascreen TR-FRET peroxisome

proliferator receptor alpha competitive binding assay kit was purchased from Invitrogen Ltd (Paisley, UK) and contains the items in Table 1.

Table 1.

Component	Composition	Amount	Storage Temperature
Fluormone Pan-PPAR Green	2 µM in 95% ethanol/water	200 µL	-80 °C
PPARα-LBD (GST)	Human PPARα ligand-binding domain in buffer (ph 8.0) contains protein stabilising agents and glycerol. Concentration differs between kit.	10 µg	-80 °C
Lanthascreen Tb-anti-GST antibody	Terbium labelled anti-GST antibody in HEPES buffered saline (137 mM NaCl, 2.7 mM KCl, 10mM HEPES pH 7.5)	25 µg	-20 °C
TR-FRET PPAR assay buffer	Proprietary buffer (pH 7.5)	25 mL	4 °C
DTT (dithiothreitol), 1 M	In water	1 mL	-20 °C or -80 °C

Table 1. Kit contents of the Lanthascreen TR-FRET peroxisome proliferator receptor alpha competitive binding assay.

3.2.2 Materials

An Envision 2102 fluorescence multilabel plate reader from PerkinElmer (Cambridge, UK) was used for detection of fluorescent emission signals of terbium at 495 nm and fluorescein at 520nm. This was coupled with a Wallac Envision manager software program, version 1.12 to scan the plates and record the data. Black 384-well round-bottom, non-binding assay plates were purchased from Greiner Bio One (Stonehouse, UK). Multi-channel pipettes were used throughout the experiment.

3.2.3 TR-FRET PPARα assay

The TR-FRET assay was conducted according to the manufacturer's protocol (Invitrogen Ltd; Paisley, UK).

In summary, concentrations of test compounds and the control competitor (GW 7647) were made up according to the concentration range of interest, along with the Fluormone Pan-PPAR Green and the PPARα/Tb-Anti-GST Ab mixture. 20µL of test compound, control competitor, or test compound solvent (DMSO) were pipeted into a 384-well non-binding assay plate. 10 µL of Fluormone Pan-PPAR Green was then added to each well, followed by 10 µL of the PPARα/Tb-Anti-GST Ab mixture. The assay plate was then placed on an orbital plate shaker for 30 seconds to ensure an even mix of all the components and left to incubate at room temperature. After 3 hours, the plate was read at 520nm and 495nm using an Envision multi-label plate reader, which measured the fluorescent emission signal of each well at both these wavelengths. The settings of the Envision instrument and filters were set to specific bandwidths to minimise interference. Finally, the 520 nm/495 nm TR-FRET ratio for each well was calculated in Microsoft Excel and these ratios were plotted against concentration using Graphpad Prism 5.0 to create a one-site competition sigmoidal dose-response curve to calculate the IC_{50} (concentration of the ligand that displaces the binding of the Fluormone Pan-PPAR Green by 50%) of the test compound.

3.2.4 Animals

Experiments were performed on male Sprague Dawley rats (180-200g Charles River, UK) in accordance with the UK Scientific Procedures Act (1986). All animals were group housed and maintained on a 12 hour light/dark cycle with access to food and water *ad libitum*.

3.2.5 Experimental overview

Rats received an intraplantar injection of 2% carrageenan in saline (100µL), or saline (n=6 rats per group) and were killed 5 hours post-injection. Paw volume was measured before injection and prior to tissue collection to determine the level of oedema. This was carried out using a plethysmometer (Figure 2), which requires calibration using 1g and 2g probes.

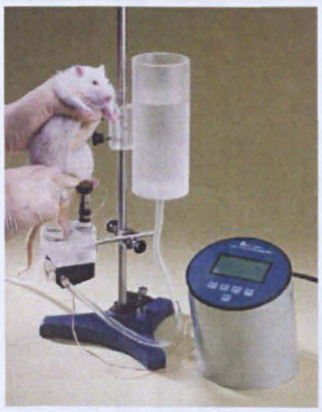

Figure 2. An image of a plethysmometer used for measuring paw volume (cm^3) and determining the level of oedema in the hind paw.

Plethysmetry fluid is made up by dissolving 0.5 g of sodium chloride and 3 mL of wetting compound (Ornano, IMBIBENTE, BBC7) in 1 L of distilled water. The rat was anaesthetised using isoflurane and a mixture of oxygen and nitric oxide (1:2). Laying the animal on its front and measuring from the tip of the toe upwards, a 4cm line is marked with permanent black pen. This line is used to ensure all paw volume measurements are consistent between readings and different animals. The rat hind paw is inserted into the fluid up to the marked line of the first tube and the paw volume is measured by the plethysmometer. This measures the fluid displaced by the paw, a volume change that is precisely mirrored by a second smaller tube containing a transducer. Three readings were recorded for both the ipsilateral and contralateral hind paws at each timepoint, including baseline values and immediately prior to tissue collection.

Five hours post-carrageenan injection, the rats were killed by stunning and decapitation by Professor David Kendall. Hindpaw, spinal cord, brain regions (frontal cortex, hippocampus, midbrain, rest of cortex and rest of brain) were rapidly dissected with help from Professor David Kendall (brain regions) and Professor Vicky Chapman (spinal cord) and frozen immediately with liquid nitrogen as described in Chapter 2. All samples were stored at -80 ^{o}C until needed.

3.2.6 LC-MS/MS analysis of lipids

The samples were extracted and analysed using the LC-MS/MS method detailed in Chapter 2 to quantify levels of PPARα ligands in the spinal cord, brain and hindpaw. However, when this study was conducted only 18 analytes were measured using this same method. These included 5-, 8-, 9-, 11-, 12-, 15-, 16-, 20-HETE, 5,6-, 8,9-, 11,12-, 14,15-EET, 12-HPETE, 2-AG, AEA, OEA, PEA and NADA, with 15-HETE-d8 as the internal standard. In summary, extraction of lipids was with ethyl acetate/hexane (9:1 v/v), followed by slow vortexing and centrifugation before the supernatants were collected and pooled. These were then evaporated under nitrogen and reconstituted with acetonitrile: water (50:50 v/v) and analysed immediately.Simultaneous measurement of bioactive lipids was performed using liquid chromatography tandem mass spectrometry (LC-MS/MS) using the methodology described in Chapter 2. Quantification was performed using Analyst 1.4.1 and imported into Microsoft Excel and Graphpad Prism.

3.2.7 Data Analysis

For the studies measuring hindpaw volume differences these were presented as mean ± SEM, statistical analysis was performed using one-way ANOVA and a Bonferonni *post hoc* test. LC-MS/MS data were expressed as mean ± SEM, statistical analysis was performed with a Mann Whitney test.

3.3 Results

3.3.1 TR-FRET PPAR alpha competitive binding assays

Previous studies using transactivation assays for PPARα have shown that some of the endocannabinoids and eicosanoids are also PPARα ligands. Transactivation studies confirm that the compound activates PPARα, however this does not demonstrate direct binding of the ligand to the receptor. Indeed, the effects of some ligands on PPARα activation may be indirect due to actions on other ligands. To address this question the TR-FRET PPAR alpha competitive binding assay was used, which is a sensitive and robust method for screening of potential PPARα ligands. This assay was used to investigate the interaction of different test compounds with the LBD of PPARα in TR-FRET-based competitive ligand binding assay. In this Lanthascreen assay (See Introduction for details), the Terbium-labelled PPARα LBD interacts with the Fluormone Pan-PPAR Green (acts as a PPAR ligand), which produces FRET. The fluorescent Fluormone Pan-PPAR Green can then be displaced by unlabelled ligands resulting in a quantifiable attenuation of FRET. GW 7647 was chosen as the positive control because it was identified as having the highest activity and being the most selective for PPARα, with 200-fold selectivity over PPARγ and PPARδ (Brown et al 2001). The negative control used was DMSO as this was the test compound solvent.

A number of test compounds were investigated, which were chosen based on evidence in the literature. These included the fatty acids arachidonic acid, linoleic acid, palmitic acid, oleic acid, the endocannabinoids 2-AG and AEA and the endocannabinoid-like 'entourage' compounds OEA, PEA and 2-LG. A selective number of HETEs were also chosen including 5-, 8-, 12-, 15-, 16-, 19- and 20-HETE and the four EETs. The positive control, GW 7647 showed detectable competition and displacement of the Fluormone Pan-PPAR Green, with an IC_{50} of 0.3 nM (Table 2, Figure 3). The fatty acids that were shown to competitively displace Fluormone Pan-PPAR Green were arachidonic acid and linoleic acid, with an IC_{50} of 0.4 μM and 0.1 μM respectively (Table 2,

Figure 3) and bind to the PPARα LBD. Oleic acid and palmitic acid however were not found to be PPARα ligands (Figure 4).

Table 2.

	GW 7647	AA	LA	8-HETE	5,6-EET	11,12-EET	14,15-EET	AEA	OEA	PEA
IC_{50}	0.3 nM	0.4 μM	0.1 μM	30 nM	2 μM	0.5 μM	13 nM	30 μM	8 μM	>30 μM

Table 2. IC_{50} values of endogenous ligands shown to bind to PPARα in the *in vitro* TR-FRET binding assay

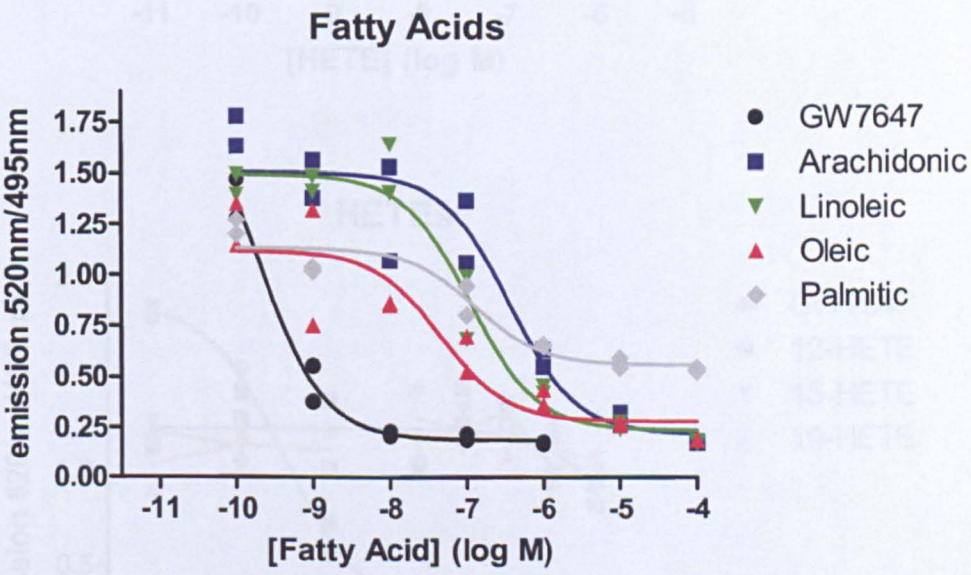

Figure 3. The curves were generated using a sigmoidal dose response (variable slope) equation in GraphPad™ Prism 5.01. GW 7647 (IC_{50} of 0.3 nM) was used as a positive control. Arachidonic acid (IC_{50} of 0.4 μM) and linoleic acid (IC_{50} of 0.1 μM) were shown to be PPAR alpha ligands in this TR-FRET assay. There were 2 repeats of each fatty acid and positive control for each assay and these were plotted as individual replicates. The TR-FRET assay was repeated twice to ensure reproducibility of the data.

8-HETE was found to competitively displace Fluormone Pan-PPAR Green with an IC_{50} of 30nM (Table 2, Figure 4a) and bind to the PPARα LBD. However, displacement of the Fluormone Pan-PPAR Green was undetectable for 5-, 12-, 15-, 16-, 19- and 20-HETE, which were not found to be PPARα ligands (Figure 4a and 4b).

a)

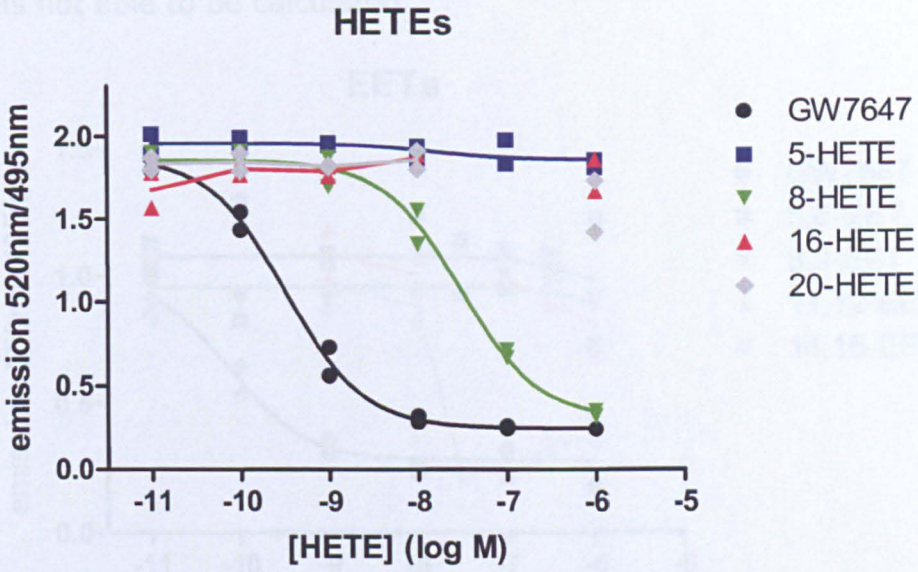

b)

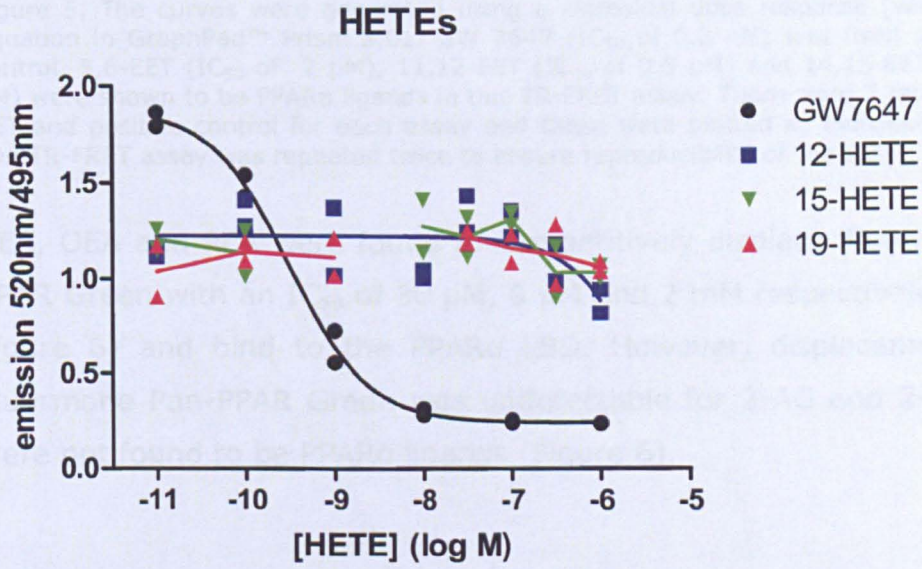

Figure 4. The curves were generated using a sigmoidal dose response (variable slope) equation in GraphPad™ Prism 5.01. GW 7647 (IC_{50} of 0.3 nM) was used as a positive control. Figure 5a. 8-HETE (IC_{50} of 30 nM) was shown to be a PPARα ligand in this TR-FRET assay. Figure 5a and 5b. However, 5-, 12-, 15-, 16-, 19- and 20-HETE were not found to be PPARα ligands. There were 2 repeats of each HETE and positive control for each assay and these were plotted as individual replicates. The TR-FRET assay was repeated twice to ensure reproducibility of the data.

5,6-, 11,12- and 14,15-EET were found to competitively displace Fluormone Pan-PPAR Green with an IC_{50} of 2 μM, 0.5 μM and 13 nM respectively (Table 2, Figure 5) and bind to the PPARα LBD. Unfortunately

in both assays, the data points for 8,9-EET were interrupted and an IC_{50} was not able to be calculated.

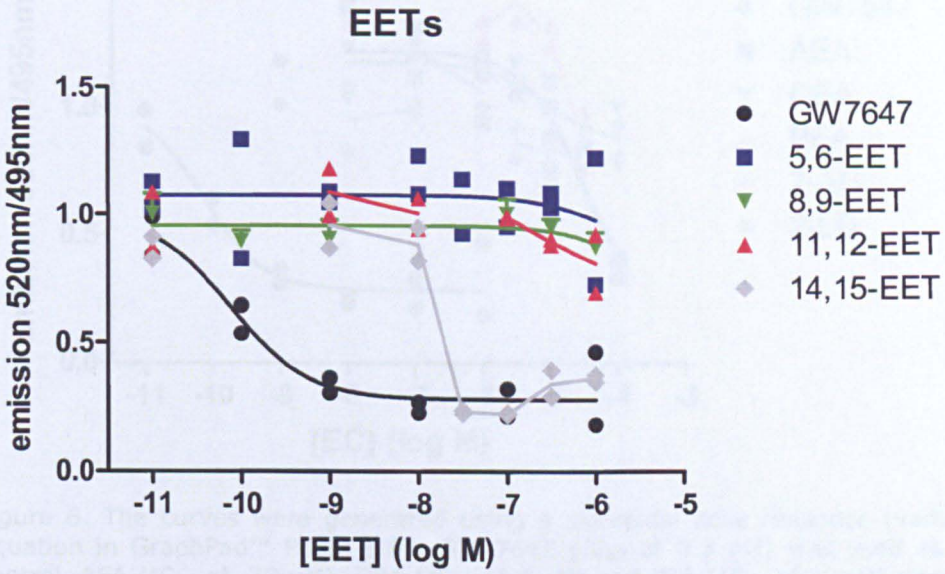

Figure 5. The curves were generated using a sigmoidal dose response (variable slope) equation in GraphPad™ Prism 5.01. GW 7647 (IC_{50} of 0.3 nM) was used as a positive control. 5,6-EET (IC_{50} of 2 μM), 11,12-EET (IC_{50} of 0.5 μM) and 14,15-EET (IC_{50} of 13 nM) were shown to be PPARα ligands in this TR-FRET assay. There were 2 repeats of each EET and positive control for each assay and these were plotted as individual replicates. The TR-FRET assay was repeated twice to ensure reproducibility of the data.

AEA, OEA and PEA were found to competitively displace Fluormone Pan-PPAR Green with an IC_{50} of 30 μM, 8 μM and 2 mM respectively (Table 2, Figure 6) and bind to the PPARα LBD. However, displacement of the Fluormone Pan-PPAR Green was undetectable for 2-AG and 2-LG, which were not found to be PPARα ligands (Figure 6).

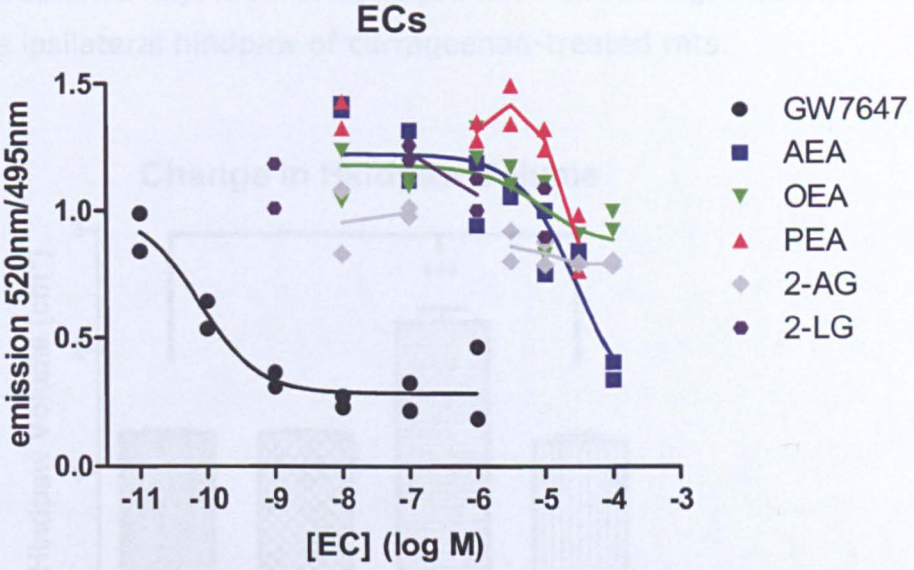

Figure 6. The curves were generated using a sigmoidal dose response (variable slope) equation in GraphPad™ Prism 5.01. GW 7647 (IC_{50} of 0.3 nM) was used as a positive control. AEA (IC_{50} of 30 μM), OEA (IC_{50} of 8 μM) and PEA (IC_{50} of 2 mM) were shown to be PPARα ligands in this TR-FRET assay. There were 2 repeats of each EC and positive control for each assay and these were plotted as individual replicates. The TR-FRET assay was repeated twice to ensure reproducibility of the data.

Using the TR-FRET PPARα competitive binding assay I have shown that arachidonic acid, linoleic acid, 8-HETE, 5,6-, 11,12-, 14,15-EET, AEA, OEA and PEA all bind to PPARα (Table 2). 8-HETE and 14,15-EET were high affinity PPARα ligands compared to endogenous ligands such as arachidonic acid and AEA (Table 2).

3.3.2 Investigating the effects of saline and carrageenan on inflammation and levels of PPARα ligands

3.3.2.1 Effects of saline or carrageenan injection on hindpaw inflammation

Hindpaw volume was measured to check for the presence of hindpaw inflammation and to confirm that carrageenan-induced inflammation was present in the carrageenan-treated rats. Intraplantar injection of saline did not significantly alter hindpaw volume at 5 hours post-injection in the ipsilateral hindpaw (Figure 7). Intraplantar injection of carrageenan produced a unilateral and significant ($P<0.001$) increase in hindpaw volume 5 hours post-injection in the ipsilateral hindpaw (Figure 7).

Intraplantar injection of carrageenan induced significant inflammation in the ipsilateral hindpaw of carrageenan-treated rats.

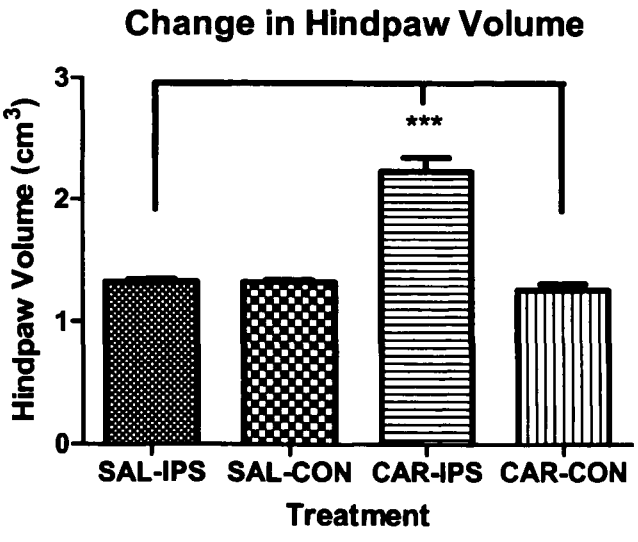

Figure 7. Intraplantar injection of 2% carrageenan significantly increased ipsilateral hindpaw volume five hours post-injection in carrageenan-treated rats compared to control (saline). Data were analysed using a one-way Anova with Bonferoni *post hoc* test, ***P<0.001. Data are expressed as mean ± SEM of ipsilateral (IPS) and contralateral (CON) hindpaws (n=6).

Hindpaw volume remained unchanged at 5 hours post-injection in the contralateral hindpaws in both saline and carrageenan-treated rats (Figure 7).

3.3.2.2 Effect of saline or carrageenan injection on levels of PPARα ligands in the hindpaw, spinal cord and brain regions

LC-MS/MS analysis was conducted to first determine the PPARα ligands present in different tissues *in vivo* under non-stimulated control conditions (injection of saline), and then to determine whether these levels were altered in a model of acute inflammatory pain.

3.3.2.3 Effect of non-stimulated conditions (saline injection) on the levels of PPARα ligands in the different tissues

Under non-stimulated conditions (saline-treated rats), 5- and 12-HETE were measured in the hindpaw, spinal cord and all brain regions of the rat, as were AEA, PEA, OEA and 2-AG. 8-HETE was measured in the hindpaw and all brain regions. 9-HETE was measured in the frontal cortex, rest of cortex and rest of brain. 11- and 15-HETE were measured in the spinal cord and all brain regions. 12-HPETE, 5,6-, 8,9-, 11,12- and 14,15-EET were measured in all brain regions (Table 3). Intraplantar injection of saline did not significantly alter lipid levels between ipsilateral and contralateral hindpaws and spinal cords (data not shown)

Under non-stimulated conditions, the majority of the total amount of lipid measured consisted of 2-AG: hindpaw (90%); spinal cord (90%); brain (98-99%) (Table 3). Therefore this lipid was excluded from the dataset to allow further analysis of the data.

	Hindpaw (Ips)		Spinal Cord (Ips)		Brain Regions									
					Frontal Cortex		Midbrain		Hippocampus		Rest of Cortex		Rest of Brain	
	Saline	Carrageenan	Saline	Carrageenan	Saline	Carrageenan	Saline	Carrageenan	Saline	Carrageenan	Saline	Carrageenan	Saline	Carrageenan
AEA	11 ± 2	3 ± 1	6 ± 1	8 ± 1	12 ± 2	12 ± 3	11 ± 2	16 ± 4	16 ± 2	14 ± 2	7 ± 1	7 ± 0.5	5 ± 1	7 ± 1
2-AG	4 ± 2	0.6 ± 0.4	38 ± 4	33 ± 4	27 ± 9	34 ± 14	85 ± 23	84 ± 25	61 ± 12	51 ± 15	16 ± 4	20 ± 7	30 ± 15	17 ± 4
OEA	63 ± 12	27 ± 5	117 ± 31	151 ± 46	25 ± 4	24 ± 3	30 ± 11	50 ± 24	11 ± 4	13 ± 5	9 ± 2	8 ± 2	9 ± 3	14 ± 7
PEA	205 ± 31	85 ± 17	789 ± 322	1191 ± 615	71 ± 35	90 ± 42	72 ± 22	118 ± 49	50 ± 19	55 ± 27	23 ± 10	12 ± 5	48 ± 31	21 ± 8
5-HETE	20 ± 6	16 ± 4	9 ± 3	7 ± 2	8 ± 5	7 ± 3	5 ± 1	6 ± 2	5 ± 2	7 ± 4	2 ± 1	2 ± 1	3 ± 2	2 ± 1
8-HETE	4 ± 1	2 ± 1	BLOQ	2 ± 1	4 ± 1	5 ± 1	5 ± 1	6 ± 1	4 ± 1	4 ± 1	2 ± 0.4	2 ± 0.2	3 ± 1	3 ± 1
9-HETE	BLOQ	BLOQ	BLOQ	BLOQ	3 ± 1	BLOQ	BLOQ	5 ± 2	BLOQ	BLOQ	1 ± 0.4	1 ± 0.4	1 ± 0.5	2 ± 1
11-HETE	BLOQ	7 ± 3	7 ± 2	12 ± 3	18 ± 2	19 ± 2	6 ± 1	10 ± 2	9 ± 1	9 ± 1	10 ± 1	9 ± 1	7 ± 2	7 ± 1
12-HETE	60 ± 24	17 ± 2	73 ± 23	49 ± 15	19 ± 3	31 ± 11	38 ± 15	93 ± 40	26 ± 5	25 ± 8	26 ± 7	23 ± 6	47 ± 14	72 ± 20
15-HETE	BLOQ	3 ±2	12 ± 4	31 ± 8	18 ± 2	16 ± 3	15 ± 4	20 ± 4	12 ± 1	15 ± 3	12 ± 2	11 ± 3	13 ± 4	11 ± 2
12-HPETE	BLOQ	BLOQ	BLOQ	BLOQ	6 ± 2	11 ± 4	1 ± 0.4	1 ± 0.4	10 ± 1	11 ± 4	4 ± 1	3 ± 1	2 ± 1	2 ± 1
5,6-EET	BLOQ	BLOQ	BLOQ	BLOQ	69 ± 30	35 ± 10	81 ± 40	133 ± 66	49 ± 9	48 ± 18	12 ± 4	11 ± 4	21 ± 13	12 ± 6
8,9-EET	BLOQ	BLOQ	BLOQ	BLOQ	29 ± 16	11 ± 4	20 ± 4	65 ± 34	16 ± 9	18 ± 11	3 ± 2	6 ± 2	12 ± 7	7 ± 3
11,12-EET	BLOQ	BLOQ	BLOQ	BLOQ	185 ± 135	179 ± 88	238 ± 102	185 ± 100	149 ± 48	130 ± 58	30 ± 20	19 ± 11	6 ± 4	4 ± 2
14,15-EET	BLOQ	BLOQ	BLOQ	BLOQ	27 ± 11	11 ± 5	36 ± 12	47 ± 24	17 ± 5	12 ± 6	3 ± 2	3 ± 2	8 ± 5	5 ± 2

Table 1. Levels of lipids measured per g wet tissue weight (n=6) in hindpaw, spinal cord and brain regions; frontal cortex, midbrain, hippocampus, rest of cortex, rest of brain of the rat. Values are expressed as mean ± SEM in pmol/g for all tissues except 2-AG, which is expressed in nmol/g. Some lipids were below the limit of quantification (BLOQ).

Under non-stimulated conditions, there were clear differences in lipid composition between the hindpaw, spinal cord and brain (Figure 8). Looking at the individual analytes (Figure 8a), a large proportion of the hindpaw consisted of PEA, along with OEA. 12-HETE was also a prominent lipid in this tissue. Likewise, in the spinal cord, these 3 lipids were also key features, with PEA the most prominent lipid in this tissue. In the brain, a large proportion of the total lipid measured consisted of the EETs, which were below the limit of quantification in the hindpaw and spinal cord, with 11,12-EET the most prominent lipid. There were also a larger number of HETEs measured in this tissue, whereas in the hindpaw and spinal cord a few of these lipids were below the limit of quantification (Table 3). 12-HPETE was also a lipid that was only detectable in the brain. Levels of the endocannabinoid-like compounds OEA and PEA were much lower in the brain compared to the hindpaw and spinal cord. Levels of the endocannabinoid 2-AG were similar in the brain and spinal cord, but much lower in the hindpaw (Table 3), whereas levels of AEA were similar in all tissues.

a)

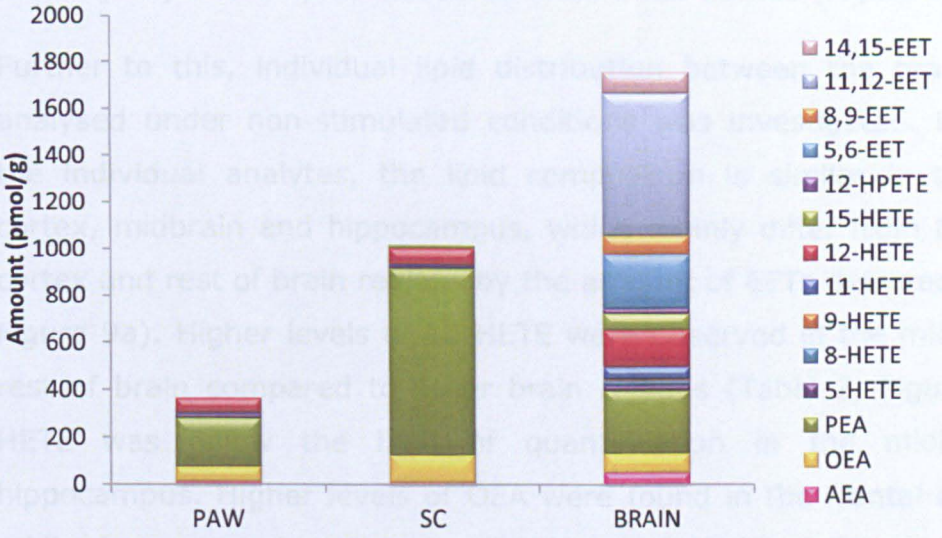

b)

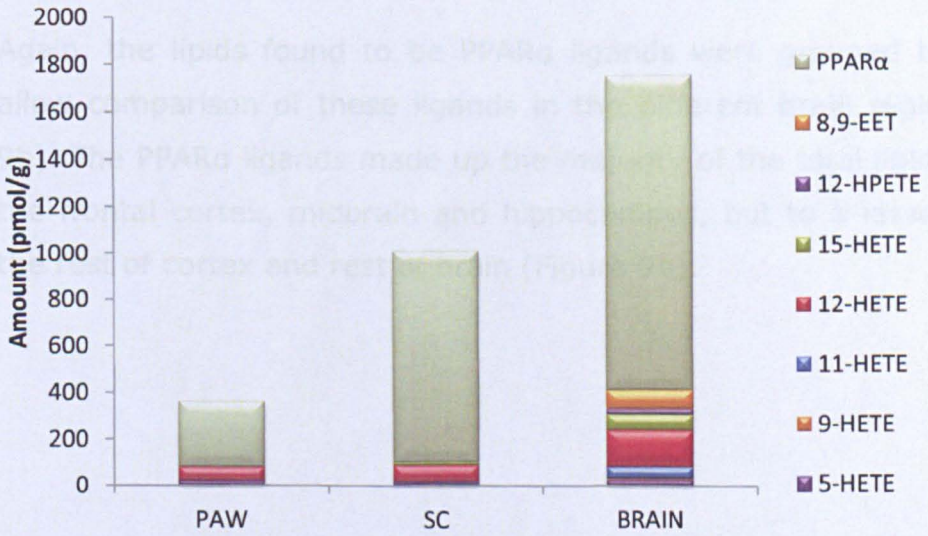

Figure 8. a) Lipid distribution of the analytes per g wet tissue weight (n=6) measured in hindpaw (PAW), spinal cord (SC) and brain of saline-treated rats, measured in pmol/g. 2-AG has been excluded to give a better distribution of remaining analytes, b) Lipid distribution of all PPARα ligands found in the TR-FRET assay, grouped to show the distribution of these in each tissue compared to other analytes measured.

Based on the results of the TR-FRET binding assay, the lipids found to be PPARα ligands were grouped together, to allow comparison of these ligands in the different tissues (Figure 8b). Half the number of lipids

measured were PPARα ligands and interestingly, these ligands made up the majority of the lipids measured in all three tissues (Figure 8b).

Further to this, individual lipid distribution between the brain regions analysed under non-stimulated conditions was investigated. Looking at the individual analytes, the lipid composition is similar in the frontal cortex, midbrain and hippocampus, which mainly differ from the rest of cortex and rest of brain regions by the amount of EETs detected (Table 3, Figure 9a). Higher levels of 12-HETE were observed in the midbrain and rest of brain compared to other brain regions (Table 3, Figure 9a). 9-HETE was below the limit of quantification in the midbrain and hippocampus. Higher levels of OEA were found in the frontal cortex and midbrain compared to the other brain regions (Table 3, Figure 9a). Lower levels of PEA and 2-AG were found in the rest of cortex compared to all other brain regions (Table 3).

Again, the lipids found to be PPARα ligands were grouped together, to allow comparison of these ligands in the different brain regions (Figure 9b). The PPARα ligands made up the majority of the total lipid amount in the frontal cortex, midbrain and hippocampus, but to a lesser extent in the rest of cortex and rest of brain (Figure 9b).

a)

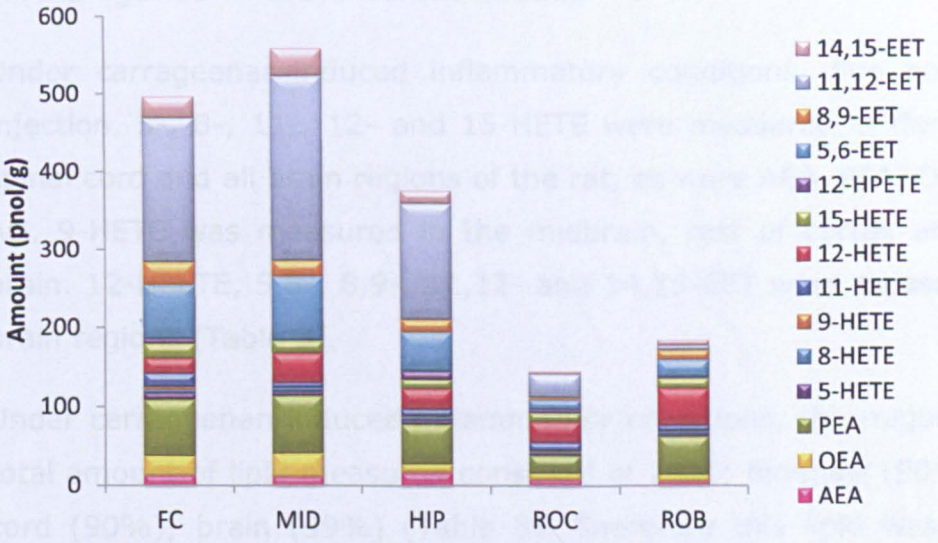

b)

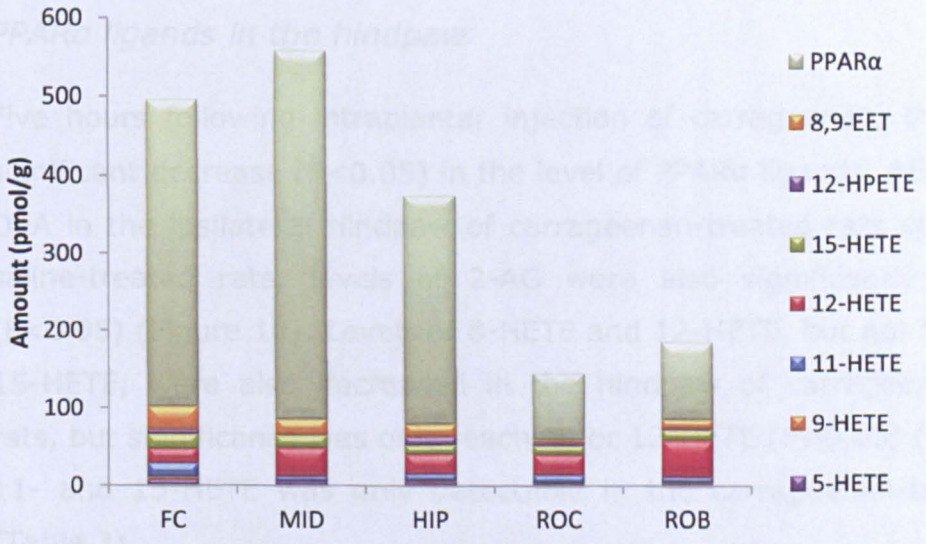

Figure 9. a) Lipid distribution of the analytes measured per g wet tissue weight (n=6) in frontal cortex (FC), midbrain (MID), hippocampus (HIP), rest of cortex (ROC) and rest of brain (ROB) of saline-treated rats, measured in pmol/g. 2-AG has been excluded to give a better distribution of remaining analytes, b) Lipid distribution of all PPARα ligands found in the TR-FRET assay, grouped to show the distribution of these in each brain region compared to other analytes measured.

3.3.2.4 Effect of carrageenan-induced inflammation on the levels of PPARα ligands in the different tissues

Under carrageenan-induced inflammatory conditions, five hours post-injection, 5-, 8-, 11-, 12- and 15-HETE were measured in the hindpaw, spinal cord and all brain regions of the rat, as were AEA, PEA, OEA and 2-AG. 9-HETE was measured in the midbrain, rest of cortex and rest of brain. 12-HPETE, 5,6-, 8,9-, 11,12- and 14,15-EET were measured in all brain regions (Table 3).

Under carrageenan-induced inflammatory conditions, the majority of the total amount of lipid measured consisted of 2-AG: hindpaw (90%); spinal cord (90%); brain (99%) (Table 3). Therefore this lipid was excluded from the dataset to allow further analysis of the data.

3.3.2.5 Effect of carrageenan-induced inflammation on the levels of PPARα ligands in the hindpaw

Five hours following intraplantar injection of carrageenan, there was a significant decrease ($P<0.05$) in the level of PPARα ligands, AEA, PEA and OEA in the ipsilateral hindpaw of carrageenan-treated rats compared to saline-treated rats, levels of 2-AG were also significantly decreased ($P<0.05$) (Figure 10). Levels of 8-HETE and 12-HETE, but not 5-, 11- and 15-HETE, were also decreased in the hindpaw of carrageenan-treated rats, but significance was only reached for 12-HETE ($P<0.05$) (Figure 10). 11- and 15-HETE was only detectable in the carrageenan-treated rats (Table 3).

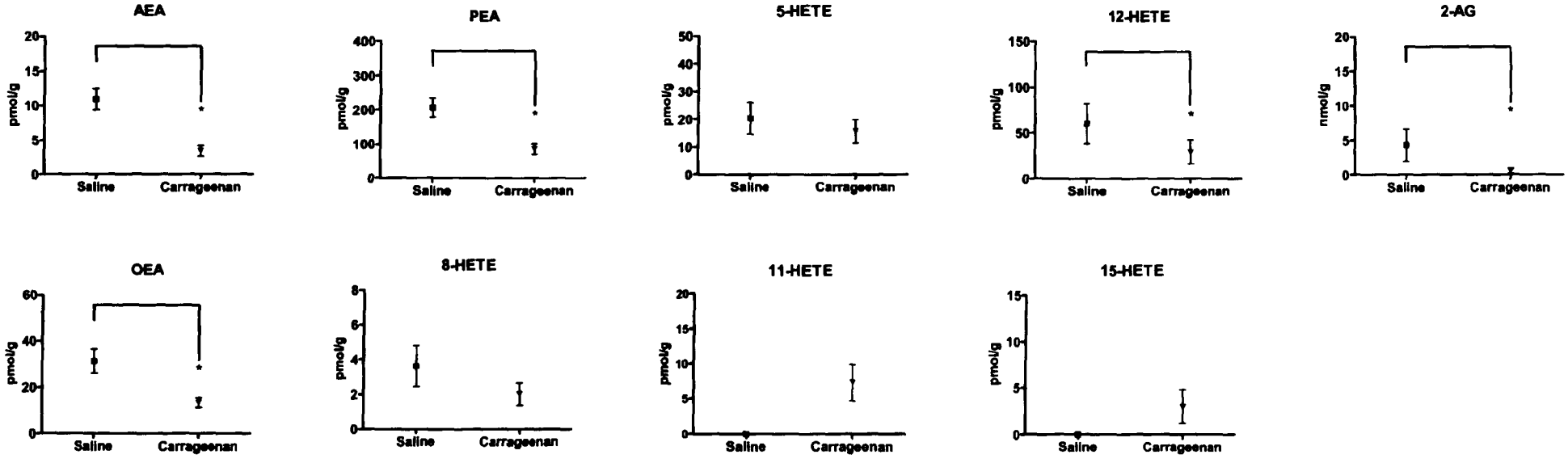

Figure 10. Levels of the PPARα ligands AEA, PEA, OEA, 8-HETE and levels of 5-, 11-, 12-, 15-HETE and 2-AG in the ipsilateral hindpaw (assessed per g wet tissue weight) following intraplantar injection of saline or carrageenan (n=6). Levels of PPARα ligands AEA, OEA, PEA decreased significantly, 8-HETE levels also tended to decrease but was no significant. Levels of 12-HETE and 2-AG also decreased significantly, whereas 5-, 11- and 15-HETE remained unchanged. Statistical analysis was conducted using a Mann-Whitney test, *$P<0.05$.

3.3.2.6 Effect of carrageenan-induced inflammation on the levels of PPARα ligands in the spinal cord

Five hours following intraplantar injection of carrageenan, there were no significant changes in PPARα ligand lipid levels between saline-treated and carrageenan-treated rats in the ipsilateral spinal cord (Table 3). However, 15-HETE was found to increase ($P<0.05$) significantly in the ipsilateral spinal cord of carrageenan-treated rats compared to saline-treated rats (Figure 11).

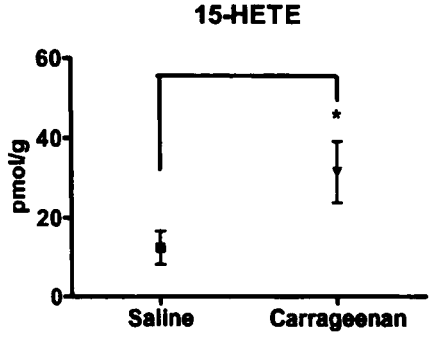

Figure 11. Levels of 15-HETE per g wet tissue weight increased significantly in the ipsilateral spinal cord of carrageenan-treated rats compared to saline-treated rats (n=6). Statistical analysis was conducted using a Mann-Whitney test, *$P<0.05$.

3.3.2.7 Effect of carrageenan-induced inflammation on the levels of PPARα ligands in the brain

Five hours following intraplantar injection of carrageenan, levels of PPARα ligand 5,6-EET and levels of 8,9-EET were significantly decreased in the frontal cortex in the carrageenan-treated rats, compared to saline-treated rats (Figure 12). There were no significant changes observed with other PPARα ligands or other lipids measured in the brain regions (Table 3).

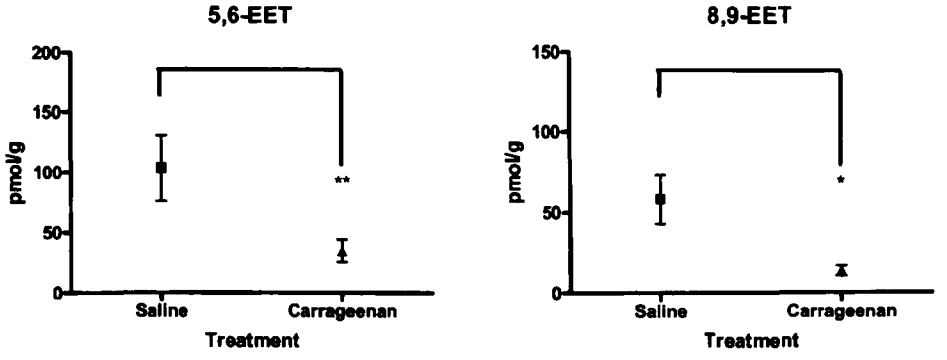

Figure 12. Levels of 5,6-EET and 8,9-EET per g wet weight tissue were shown to decrease significantly in the frontal cortex following intraplantar injection of saline or carrageenan (n=6). Other lipids detected in the frontal cortex and other brain regions were not shown to alter in carrageenan-treated rats compared to saline-treated rats. Statistical analysis was conducted using a Mann-Whitney test, *$P<0.05$.

3.3.3 Summary of findings

Experiments using the TR-FRET PPARα competitive binding assay showed that arachidonic acid, linoleic acid, 8-HETE, 5,6-, 11,12-, 14,15-EET, AEA, OEA and PEA all bind to PPARα. 8-HETE and 14,15-EET were high affinity PPARα ligands compared to endogenous ligands such as arachidonic acid and AEA. In the *in vivo* study, intraplantar injection of carrageenan induced significant ($P<0.001$) inflammation in the ipsilateral hindpaw of carrageenan-treated rats. Levels of PPARα ligands AEA, OEA and PEA were significantly decreased ($P<0.05$) in the ipsilateral hindpaw of carrageenan-treated rats. Along with significant ($P<0.05$) decreases in 2-AG and 12-HETE. Levels of 15-HETE were increased ($P<0.05$) significantly in the ipsilateral spinal cord of carrageenan-treated rats. Levels of 5,6-EET and 8,9-EET were decreased ($P<0.01$ and $P<0.05$ respectively) significantly in the frontal cortex of carrageenan-treated rats.

3.4 Discussion

3.4.1 TR-FRET competitive binding assays

TR-FRET PPARα competitive binding assays demonstrated significant binding of AEA, OEA, PEA, 8-HETE, 5,6-, 11,12-, 14,15-EET, arachidonic acid and linoleic acid to PPARα. Previous work has shown that 8-HETE, PEA and 5,6-, 11,12-, 14,15-EET activate the PPARα receptor (Yu et al 1995, Kliewer et al 1997, Cowart et al 2002, Fu et al 2003), results presented in this chapter show that these ligands bind directly to the receptor. Also, previous work has focussed on individual or, at best, a small number of compounds, but investigation of all these ligands together allows a useful comparison of the potencies of these endogenous PPARα ligands. 14,15-EET (IC_{50} 13 nM) was found to have the highest affinity for PPARα, followed by 8-HETE (IC_{50} 30 nM), compared to the positive control GW7647 (IC_{50} 0.3 nM). The order of affinity was found to be 14,15-EET > 8-HETE > LA > AA > 11,12-EET > 5,6-EET > OEA > AEA > PEA. In previous studies, 5,6-EET, 8,9-EET, 11,12-EET, 14,15-EET and 20-HETE have been shown to displace *cis*-parinaric acid in ligand-receptor binding assays of PPARα (Cowart et al 2002). Therefore, 20-HETE was investigated using the TR-FRET competitive binding assay in the 1 μM to 100 nM range. There was no occupancy at concentrations less than 1 μM; however, higher concentrations could not be investigated due to limitations of commercial stock solutions. Previous work looking at *cis*-parinaric acid displacement used a concentration range of 20 μM to 1 nM to be able to calculate a value for 20-HETE (Cowart et al 2002). The order of potency for the EETs for *cis*-parinaric acid displacement was found to be 8,9-EET > 14,15-EET > 5,6-EET > 11,12-EET, although in this assay these were found to be more potent than Wy-14643 (Cowart et al 2002). 8,9-EET was also investigated using the TR-FRET competitive binding assay; however, an IC_{50} value could not be calculated for this ligand due to interruption of data points in both assays. Arachidonic acid (IC_{50} 0.4 μM) and linoleic acid (IC_{50} 0.1 μM) also bound to PPARα in this assay with a higher affinity than previously reported at 25-30 μM (Forman et al 1997), although the

latter values were calculated using ligand-induced complex formation assays. The EETs are cytochrome P450 (CYP450) metabolites of arachidonic acid, and the identification of both the precursor and metabolites as PPARα ligands is important. PPARα is a nuclear receptor that induces transcription of a number of gene products that are involved in the metabolism of fatty acids such as arachidonic acid, including enzymes involved in the metabolism of arachidonic acid to the EETs. PPARα also regulates processes such as modulating the rate of fatty acid uptake and oxidation (Michalik and Wahlie 1999). Arachidonic acid and linoleic acid binding to PPARα provides evidence for metabolic intermediate involvement in the regulation of transcription, modulating feedback control and promoting allosteric changes in enzyme activity (Forman et al 1997). AEA (IC_{50} 30 μM), OEA (IC_{50} 8 μM) and PEA (IC_{50} 2 mM) have also been shown to bind to PPARα, whereas, previously, PEA has only been shown to activate this receptor (Lo Verme et al 2005). AEA, however, has previously been shown to have a higher affinity for PPARα than OEA (Sun et al 2007). Overall, the affinity of these endocannabinoids were not shown to be as high as the eicosanoids, and are known to have other receptor targets (Alexander and Kendall 2007).

3.4.2 Identification and quantification of PPARα ligands

Following identification of putative PPARα ligands, these were measured *in vivo* to determine their levels in biological tissue and whether these were altered in a model of inflammatory pain. The analytical method described in Chapter 2 was used to measure all the 18 lipids detected.

The results showed that intraplantar injection of 2% carrageenan produced erythema and oedema, measured using a plethysmometer. At 5 hours post-carrageenan injection, this gave an almost 2-fold significant increase in ipsilateral hindpaw volume that was not observed in saline-treated rats. This was a good indication that the carrageenan injection produced an inflammatory response.

Levels of PPARα ligands AEA, OEA and PEA were significantly decreased in the inflamed hindpaw, 8-HETE also decreased although this was not

significant. Levels of 2-AG and 12-HETE were also significantly decreased in the inflamed hindpaw. By contrast, levels of 5-, 11- and 15-HETE were not significantly altered, suggesting that these changes were due to specific modulation of eicosanoid metabolism in this model of inflammatory pain. Interestingly, 11- and 15-HETE were also only detected in carrageenan-treated rats. 11-HETE has been shown to be potent neutrophil chemoattractant in vitro and in experimental models (Goetzl et al 1980a, Goetzl et al 1980b). 15-HETE has been shown to be a pro-inflammatory mediator, involved in the stimulation of chemotaxis and chemokinesis of neutrophils and eosinophils (Vanderhoek et al 1982). Previous work in our group also reported decreased levels of AEA and PEA in the hindpaw, using this experimental paradigm (Jhaveri et al 2008), although, in those experiments, the tissue was collected 3 hours post-carrageenan injection. OEA levels were shown to decrease significantly 5 hours post-carrageenan injection, but not at 3 hours (Jhaveri et al 2008), which may indicate that this particular lipid is involved much later in the inflammatory process. It has been suggested that decreased levels of these PPARα ligands is due to increased metabolism in the presence of inflammation (Jhaveri et al 2008). Cyclooxygenase-2 (COX-2) enzyme expression has been shown to increase in the carrageenan-inflamed hindpaw (Guay et al 2004), as does monoacyl glycerol lipase (MAGL), the enzyme responsible for 2-AG metabolism (Jhaveri et al 2008), which may explain the significantly reduced levels of 2-AG observed. However, the reverse also applies where intracerebroventricular administration of PEA significantly reduced the expression of pro-inflammatory enzymes in COX-2 and inducible nitric oxide synthase (iNOS), as well as reduced oedema formation in the mouse carrageenan model (D'Agostino et al 2007), implying a possible feedback mechanism in inflammation.

Levels of the PPARα ligands AEA, OEA and PEA measured in the spinal cord were not significantly altered in the carrageenan-treated animals. Levels of the other lipids 5-, 11-, 12-HETE and 2-AG were also unaltered, except for 15-HETE, which was significantly increased in the ipsilateral

spinal cord. As mentioned earlier, 15-HETE is a pro-inflammatory mediator, important in chemotaxis and contributing to the inflammatory process. Increased levels of this pro-inflammatory mediator under inflamed conditions can be expected. Levels of HETEs and EETs have previously been measured in the rat spinal cord (Buczynski et al 2010). Levels of the PPARα ligands AEA, OEA, PEA and 8-HETE were also unaltered in the brain. In addition to these lipids, 5,6-EET, 8,9-EET, 11,12-EET, 14,-15-EET and 12-HPETE were also measured, with 5,6-, 11,12- and 14,15-EET shown to be PPARα ligands. 5,6-EET and 8,9-EET were shown to decrease significantly in the frontal cortex of carrageenan-treated rats compared to saline-treated rats. As mentioned, 5,6-EET has been shown to be a PPARα ligand in this study, however 8,9-EET has been shown previously to bind to PPARα (Cowart et al 2002). This links in with the decreased levels of other PPARα ligands observed in the hindpaw. HETEs and EETs have previously been measured in the rat cortex (Yue et al 2007) and mouse brain (Amruthesh et al 1992, Roman 2002), and EETs are considered to be neuroprotective due to their anti-inflammatory effects (Roman 2002, Larsen et al 2006).

3.4.3 Distribution of PPARα ligands in rat tissue

Expression of PPARα has been characterised in mouse brain and spinal cord, and has been shown to increase following inflammation (Gofflot et al 2007, Benani et al 2003a, Benani et al 2003b). Expression of PPARα is highest in the brain stem and cerebral cortex, although it is also found in many regions of the brain including the hippocampus (Gofflot et al 2007). This may explain the reason for the higher levels of PPARα ligands observed in the frontal cortex, midbrain and hippocampus compared to the rest of the brain. The expression of PPARα is, however, only present in distinct parts of the spinal cord. PPARα expression was found to be lower in the spinal gray matter compared to the spinal white matter and high expression of PPARα was found in the astrocytes (Benani et al 2003a). These findings suggest an importance of PPARα in cerebral inflammation through modulation of cytokine production, as astrocytes act as immune effector cells in cerebral inflammation and immune

reactivity (Benani et al 2003a). The fact that the majority of lipid levels measured in the spinal cord and brain remained unchanged in the carrageenan-treated animals may be due to the time points at which the tissues were collected (5-hours post-carrageenan injection) not being appropriate to enable the detection of change. It is widely accepted that lipid turnover is rapid; metabolism *in vivo* occurs at such a fast rate that it is often difficult to capture these moments. Also, the fact that whole spinal cord was analysed, rather than the areas where PPARα expression is prominent may be a confounding factor.

The distribution of the lipids measured in the spinal cord comprise mainly 2-AG (90%), followed by PEA, whereas the brain is made up of predominantly 2-AG (98-99%), followed by a much more even distribution of the other lipids. However, when the PPARα ligands are grouped together, we see a similar distribution of these in the spinal cord and brain. It is believed that the CYP4A subfamily is involved in the metabolism of arachidonic acid to physiologically important metabolites that are active in the brain (Simpson 1997). These CYP enzymes work alongside PPARα to modulate fatty acid metabolism in the body and the presence of these CYP metabolites (EETs), which are also PPARα ligands may act as a method of regulating these processes (Simpson 1997).

Finally, changes in the levels of PPARα ligands observed in the inflamed hindpaw but not in the spinal cord and brain may suggest that modulation through PPARα is via a peripheral rather than a central site. This has previously been suggested since intraplantar administration of PPARα agonists strongly suppresses nociceptive behaviour without them entering the central nervous system (LoVerme et al 2006). Therefore, by modulating changes in the levels of PPARα ligands peripherally and altering the metabolism of these ligands, we may be able to target PPARα in inflammation.

3.5 Conclusions

A number of PPARα ligands have been shown, some for the first time, to bind directly to the receptor using TR-FRET competitive binding assays.

The data also showed that levels of PPARα ligands were altered in the inflamed hindpaw, suggesting that changes in eicosanoid and endocannabinoid metabolism may influence the role of PPARα in inflammatory pain states.

Chapter 4.

Investigating the role of 15-lipoxygenase in the generation of endogenous ligands that activate transient receptor potential vanilloid-1 channels

4.1 Introduction

4.1.1 TRPV1 channels

The transient receptor potential vanilloid 1 (TRPV1) receptor is a part of a large family of chemically-gated, non-selective cation channels (See General Introduction). TRPV1 are activated by different stimuli such as heat (>43 °C, Caterina et al 1997), capsaicin (Hwang et al 2000), AEA (Smart et al 2000) and low pH (Tominaga et al 1998). TRPV1 is mainly found in small- to medium-diameter neurons of primary sensory ganglia (dorsal root ganglia, trigeminal ganglia and sympathetic ganglia) (Vay et al 2012). TRPV1 has also been shown to be expressed on the terminals of primary afferent sensory nerve fibres A and C (See General Introduction), in addition to being present in the brain, including areas involved in nociceptive transmission (Mezey et al 2000, Toth et al 2005). Nociceptors also have an efferent function and release pro-inflammatory and pro-nociceptive mediators in the periphery in addition to transmitting nociceptive information to the spinal cord (See references in Szallasi and Blumberg 1999). The ability of TRPV1 to sensitise following exposure to painful stimuli has led to the hypothesis that TRPV1 is a prime factor in hyperalgesia (See references in Holzer 2008). Sensitisation of the TRPV1 channel depends on several mechanisms among which phosphorylation of the ion channel by protein kinase A, C and other kinases are important (Zhang and McNaughton 2006, Bhave et al 2003, Vellani et al 2001). Increased TRPV1 activity by bradykinin and nerve growth factor via phospholipase C-mediated hydrolysis of phosphatidylinositol-4,5-bisphosphate is another mechanism of TRPV1 upregulation (Prescott and Julius 2003). Additionally, rapid recruitment of an intracellular pool of TRPV1 to the cell membrane also sensitises the ion channel, a process most importantly involving phosphoinositide 3-kinase and Src kinase (Stein et al 2006, Zhang et al 2005). Interestingly, TRPV1 appear to be up-regulated in inflammatory conditions in which expression of TRPV1 is found on primary sensory neurons that do not normally express the channel (Ji et al 2002, Cortright and Szallasi 2004). As mentioned, TRPV1 is thought to be a prime factor in hyperalgesia, thus this evidence

suggests a link between TRPV1 and the development of inflammatory hyperalgesia (Cortright and Szallasi 2004).

4.1.2 Role of TRPV1 in inflammatory pain

There is substantial evidence for TRPV1 involvement in inflammatory hyperalgesia. Expression of TRPV1 is altered under inflammatory conditions; TRPV1 mRNA and protein levels are increased in the skin, sciatic nerve and dorsal root ganglia (DRGs) following complete Freund's adjuvant (CFA) (Kanai et al 2007) or carrageenan (Tohda et al 2001) administration. Carrageenan-induced acute inflammation produced a decrease, and increase, in TRPV1 mRNA in the DRG and lumbar cord respectively (Tohda et al 2001). Intrathecal colchicine-pretreatment (axonal transport inhibitor) prevented carrageenan-induced changes in the level of TRPV1 mRNA in the DRG and the dorsal part of the lumbar cord (Tohda et al 2001). This finding suggests that the inflammation may increase the transcription of TRPV1 in the lumbar cord and that this up-regulation involves axonal transport of TRPV1 mRNA in primary afferent terminals during inflammation (Tohda et al 2001). The results of these pharmacological studies further confirm the up-regulation of TRPV1 receptors during inflammation.

Knockout studies provided clear evidence for TRPV1 involvement in inflammatory heat hyperalgesia and TRPV1 antagonists have been shown to be effective in reducing inflammatory mechanical hyperalgesia in pharmacological studies (See references in Vay et al 2012). TRPV1 knockout mice largely failed to develop thermal hyperalgesia in response to CFA or carrageenan, showing that TRPV1 is a key element in the generation of thermal hyperalgesia (Caterina et al 2000, Davis et al 2000).

Blockade of TRPV1 receptors attenuates hyperalgesia. For example, TRPV1 antagonists BCTC and SB-366791 administered intraplantarly inhibited CFA-induced thermal hyperalgesia but not mechanical hyperalgesia. However, intrathecal administration of BCTC and SB-366791 inhibited both CFA-induced thermal and mechanical hyperalgesia

(Kanai et al 2007). These findings suggest peripheral TRPV1 involvement in thermal hyperalgesia and central TRPV1 involvement in thermal and mechanical hyperalgesia (Kanai et al 2007). The wide distribution of TRPV1 in the CNS raises the possibility that this ion channel can be involved in many brain functions (Steenland et al 2006), including participation of pain processing within the brain (Palazzo et al 2008, Cui et al 2006, Steenland et al 2006). TRPV1 stimulation in the periaqueductal grey by anandamide or capsaicin produces analgesia, via glutamate release and stimulation of descending antinociceptive pathways (Palazzo et al 2008). Other sites where TRPV1 may modify nociception in the brain include the ventral tegmental area (Marinelli et al 2005) and the anterior cingulate cortex (Steenland et al 2006). Central involvement of TRPV1 under inflammatory conditions has also been shown. Electrophysiological studies showed that spinal neuronal responses were attenuated by treatment with TRPV1 antagonists under inflammatory conditions, although this was found to be equally true in the absence of inflammation (Kelly and Chapman 2002, Jhaveri et al 2005).

Based on a number of findings, TRPV1 antagonists have therefore been shown to be a potential treatment for hyperalgesia (Roberts and Connor 2006). However, TRPV1 antagonism has been shown to affect core body temperature and reduced sensitivity to painful or damaging heat stimuli and has therefore lost promise in clinical applications (Vay et al 2012, Krarup et al 2011, Round et al 2011).

4.1.3 Endogenous agonists of TRPV1

Many endogenous TRPV1 agonists have been identified, including anandamide (AEA) (Smart et al 2000), *N*-arachidonoyldopamine (NADA) (Huang et al 2002), 12(S)-hydroperoxyeicosatetraenoic acid (12(S)-HPETE), 15(S)-hydroperoxyeicosatetraenoic acid (15(S)-HPETE) (Flores et al 2010, Hwang et al 2000). Recently, there has been interest in a family of linoleate-derived lipids, shown to selectively activate TRPV1 in native and expression systems (Patwardhan et al 2009).

Hydroxyoctadecadienoic acids (HODEs) are metabolites generated from linoleic acid (LA) by 15-lipoxygenase (15-LOX, Vangaveti et al 2010). They are stable oxidation products of this essential fatty acid, which are increased during oxidation stress. (Vangaveti et al 2010, Banni et al 2002). LA is only available from the diet, including sources such as beef, lamb and dairy products, and it is stored in the cell membranes until needed (Belury 2002). There are a number of physiological properties associated with LA, it is thought to be antiadipogenic (Sisk et al 2001), antidiabetogenic (Houseknecht et al 1998), anticarcinogenic (Ip et al 2001, Hubbard et al 2000), and antiatherosclerotic (Wilson et al 2000). It is also thought to be involved in bone formation, gene expression and the immune system, along with fatty acid and lipid metabolism (See references in Belury 2002).

Recent *in vitro* and *in vivo* studies have investigated the mechanisms by which TPRV1 mediates heat-induced hyperalgesia and thermoregulation (Patwardhan et al 2009, Patwardhan et al 2010). *In vitro,* dissected rat spinal cords were superfused in modified Hanks buffer followed by exposure to high potassium Hanks buffer (50 mM potassium chloride) for 30 minutes at 37 °C (Patwardhan et al 2009). This resulted in depolarisation of the spinal cord and consequent release of an LA metabolite, identified as 9-HODE, shown to activate TRPV1 in transfected CHO cells and potently activated spinal TRPV1 (Patwardhan et al 2009). In mice, skin biopsies were exposed to basal (37 °C, control) and noxious (48 °C, heated) temperatures, but intracellular calcium levels only increased in the WT cultured trigeminal ganglia (TG) neurons and not in the TRPV1 knockout neurons (Patwardhan et al 2010). These results indicate that the heated skin released compound(s) that activate TRPV1, which were then identified by LC-MS/MS as 9- and 13-HODE (Patwardhan et al 2010). In the same publication, the application of synthetic 9-HODE to cultured rat TG neurons triggered the release of immunoreactive CGRP, which was significantly ($P<0.001$) blocked by I-RTX (TRPV1 antagonist) pre-treatment. The metabolites of the respective HODEs, 9- and 13-oxoODE, shown to activate TRPV1 in transfected CHO cells also

elevated intracellular calcium levels in cultured TG neurons from WT mice (Patwardhan et al 2010). Furthermore, a combination of anti-9- and anti-13-HODE antibodies (0.06 and 0.012 μg, respectively) significantly ($P<0.01$) decreased cultured TG neuron responsiveness to noxious heat (Patwardhan et al 2010). These findings *in vitro* suggest TRPV1 involvement in sensory neuron responsiveness to noxious heat and that this receptor system is essential in its function.

In vivo, studies showed that the 15-LOX metabolites of LA, 9-, 13-HODE, 9- and 13-oxoODE, produced behavioural pain responses following peripheral and spinal administration. Intraplantar injection of 9-HODE in rats produced a dose-related increase in spontaneous nocifensive behaviour that significantly ($P<0.001$) increased following co-administration with 13-HODE, 9- and 13-oxoODE (Patwardhan et al 2010). Intraplantar injection of 9-HODE induced thermal hyperalgesia which was detected in wild-type (WT), but not TRPV1 knockout, mice (Patwardhan et al 2010). Intraplantar co-administration of anti-9- and anti-13-HODE antibodies significantly ($P<0.001$) attenuated CFA-induced mechanical allodynia in the inflamed hindpaw without affecting mechanical thresholds in the contralateral hindpaw (Patwardhan et al 2009). These findings suggest significant attenuation of TRPV1-mediated peripheral nociception through a localised site of action of these 15-LOX metabolites. However, these TRPV1 ligands were not identified or measured. Intrathecal administration of the oxidised metabolites of LA, 9-, 13-HODE, 9-, 13-oxoODE rapidly evoked mechanical allodynia, which was blocked by AMG9810 (TRPV1 antagonist) co-injection, demonstrating a TRPV1 specific effect (Patwardhan et al 2009).

Overall there is mounting evidence that increased TRPV1 function contributes to inflammatory hyperalgesia, particularly thermal hyperalgesia, however the ligands which mediate this sensitisation of TRPV1 are yet to be identified. Recent studies have shown that 9- and 13-HODE can activate TRPV1 *in vitro,* and can contribute to nociceptive responses *in vivo*, via TRPV1. On this basis, I hypothesised that 9- and 13-HODE may also mediate the sensitisation of TRPV1 associated with

inflammatory hyperalgesia. To test this hypothesis LC-MS/MS was used to measure levels of 9- and 13-HODE in the paw in the presence and absence of inflammation, and then investigated the effects of blocking the generation of 9- and 13-HODE (with a 15-LOX inhibitor) on carrageenan-induced inflammatory pain responses and levels of 9- and 13-HODE in the paw. To further substantiate this hypothesis, the effects of anti-9- and anti-13-HODE antibodies on inflammatory hyperalgesia and levels of 9- and 13-HODE were determined.

4.1.4 Aims and Objectives

- To investigate the effects of linoleic acid exposure and 15-LOX inhibition on levels of LA, 15-LOX metabolites and other inflammatory mediators in the dorsal root ganglia.
- To measure the levels of LA, 15-LOX metabolites and other inflammatory mediators in a model of inflammatory pain.
- To determine the effect of inhibiting 15-lipoxygenase (15-LOX) on levels of LA, 15-LOX metabolites and other inflammatory mediators in a model of inflammatory pain.
- To investigate the contribution of 9- and 13-HODE to inflammatory pain responses.

4.2 Methods

4.2.1 Animals

Experiments were performed using male Sprague Dawley rats (180-200g Charles River, UK) in accordance with the UK Scientific Procedures Act (1986). All procedures were approved by the University of Nottingham Ethical Review Committee and IASP guidelines. All rats were group-housed in a temperature-controlled environment (22°C ± 1°C) and maintained on a 12 hour light/dark cycle with access to food and water *ad libitum*.

4.2.2 Weight Bearing

Weight distribution (change in weight bearing) between the ipsilateral (left) and contralateral (right) hindpaws was measured using an Incapacitance Tester (Linton Instrumentation, UK) with help from Dr Mohammad Alsalem. The Incapacitance Tester consists of two sensitive strain gauge transducers; the rats' hindpaws were placed on the separate sensors, which measure the force exerted by each limb (in grams) on the transducer plate over a given time period. In the present study, the weight distribution was calculated over a period of 3 seconds, with measurements taken three times at each time point and averaged. Studies have shown that less weight is applied on the inflamed paw, and that the difference in weight bearing is a measure of the hypersensitivity to the inflammatory pain (Clayton et al 2002). The experimenter was blind to all treatments.

4.2.3 Paw volume and paw circumference

Changes in the paw volume (oedema formation) were measured using a plethysmometer (Chapter 3, Methods) and increases in paw circumference were also recorded with a loop of cotton thread and ruler as described in Chapter 3. Weight bearing and paw volume were assessed in the same rats in all behavioural studies.

4.2.4 Overview of *in vivo* studies

4.2.4.1 Pilot studies

Pilot studies were performed to determine the dose of PD 146176 for peripheral administration, previously only given systemically (Jeon et al 2009) or orally (Bocan et al 1998) and also the timing of the injections of 9- and 13-HODE antibodies. These were carried out with help from Dr Mohammad Alsalem.

In the first pilot study, the dose of PD 146176 was investigated along with optimum timepoint for the measurement of changes in weight bearing. Intraplantar doses of 1, 50 and 100 μg of PD 146176 in 50 μL of

vehicle (3% Tween 80 in saline) were given to rats (n=2), 30 minutes prior to 100 µL of 2% carrageenan to determine a suitable dose for the main study. Weight bearing was monitored for four hours post-carrageenan and paw volume and paw circumference were also monitored prior to both injections and after the last weight bearing measurement (See Methods). 50 µg of PD 146176 in 50 µL of vehicle (3% Tween 80 in saline) inhibited pain behaviour and was considered a suitable dose. To assess this against control groups, we repeated the pilot study with rats (n=2), given either 50 µL of vehicle (3% Tween 80 in saline) or 50 µg in 50 µL of PD 146176, followed by 100 µL of 2% carrageenan. Another group were given 50 µg in 50 µl of PD 146176 followed by 100 µL of saline.

In the second pilot study, we investigated the timing of administration of the 9- and 13-HODE antibodies. Rats were given intraplantar injections of 50 µL of 9- and 13-HODE (25 µg of each) antibodies of 50 µL of vehicle (PBS), followed 30 minutes later by intraplantar injection of 100 µL of 2% carrageenan (2 rats per group). Inhibition of pain behaviour was observed on the first repeat but not a second repeat of the study. After discussion of these data, the timing of the injection of antibodies was changed so that it was given 1 minute after carrageenan. The rationale for this was due to concerns about the stability of the antibodies *in vivo*, since they are degradable peptides. Injection of the antibodies 1 minute post-carrageenan would eliminate the possibility of the antibodies degrading prior to the carrageenan injection and subsequent effects from this.

4.2.4.2 Main study

These experiments were carried out with help from Dr Mohammad Alsalem. Weight bearing measurements were recorded 30 minutes prior to the first injection. Rats were anaesthetised with isoflurane / N_2O / O_2 (1.5-2% in 66% N_2O and 33% O_2), and received an intraplantar injection of either 50 µl of a 50 µg/50 µL solution of PD 146176 made up in vehicle (3% Tween 80 in saline) or 50 µL of vehicle in the left hindpaw

(ipsilateral), followed 30 minutes later by an intraplantar injection of either 100 µL of a 2% carrageenan injection or 100 µL of saline in the same hindpaw. A naïve group (no injections, but anaesthetised) was also used as an additional control. This gave a total of five groups of 6 rats. For the study investigating the effects of 9- and 13-HODE antibodies, rats received an intraplantar injection of either 100 µL of a 2% carrageenan injection or 100 µL of saline in the left hindpaw (ipsilateral), followed 1 minute later by either 50 µL of a mixture of the antibodies (25 µg each) or 50 µL of vehicle (PBS) in the same hindpaw. This study also consisted of five groups, with a naïve group as a control (n=6 per group).

All solutions were made up fresh on the day of the experiment apart from 2% carrageenan, which was prepared several days beforehand. Effects of intraplantar injection of 2% carrageenan (100 µL) were measured at 1, 2, 3 and 4 hours post-injection using weight bearing to monitor pain behaviour. Paw volume and paw circumference were measured prior to the rats receiving the injections and immediately before tissue collection.

4.2.5 *In vitro* DRG experiment

This experiment was designed to investigate the effects of DRG stimulation with linoleic acid and whether the levels of the HODEs generated were altered after treatment with PD 146176. Rats (n=2) were killed using CO_2 overdose, the spinal columns removed and the dorsal root ganglia (DRGs) were collected by a method previously described (Lindsay 1988). Cell culture and preparation methods were similar to those described previously (Millns et al 2001) and were conducted by Dr Mohammad Alsalem, along with help in this *in vitro* experiment. The DRGs (20-40 in number), were washed in calcium imaging buffer and separated into left thoracic, right thoracic, left lumbar and right lumbar regions. PD 146176 (PD) was prepared by diluting 11.9 µL of stock (10 mg/mL or 42.1 mM) in 50 mL of calcium buffer to give a final concentration of 10 µM. Linoleic acid (LA) was prepared by mixing 20 µL of stock (3.2 M) with 36 µL of ethanol, then 43.6 µL of the mixture was diluted in 50 mL of calcium buffer to give a final concentration of 1 mM.

Vehicle 1 (veh 1) was 0.024% of 100% ethanol and vehicle 2 (veh 2) was 0.057% ethanol, both prepared in calcium buffer. Petri dishes were labelled as groups A-H and filled with solution according to the groupings shown in Table 1, which were designed to investigate the effects of linoleic acid and PD 146176 at 15 or 30 minute post-administration.

Table 1. Different groups of treatment to investigate the timing and effects of LA and PD

GROUP	A	B	C	D	E	F	G	H
DISH 1	Veh 1 15 mins	Veh 1 15 mins	Veh 1 15 mins	Veh 1 15 mins	PD 15 mins	PD 15 mins	PD 30 mins	Veh 1 30 mins
DISH 2	Veh 2 15 mins	LA 15 mins	Veh 2 30 mins	LA 30 mins	LA 15 mins	LA 30 mins	LA 30 mins	LA 30 mins

Individual DRGs were cut in the Petri dishes containing the solutions for particular groupings, which were arranged to incorporate the different timings allocated. Each group (n=6) contained 2 right thoracic, 2 left thoracic, 1 right lumbar and 1 left lumbar DRG. Following the allocated time intervals in the different solutions, individual DRGs were placed in labelled cryovials and snap frozen on dry ice. These samples were kept at -80°C until LC-MS/MS analysis.

4.2.6 LC/MS-MS analysis

Following the final set of weight bearing measurements, animals were killed by stunning and decapitation by Paul Millns. Hindpaw tissue was rapidly collected from all rats used in the weight bearing and paw diameter and paw volume experiments and frozen immediately with liquid nitrogen. These hindpaw samples were then extracted and analysed following the methods detailed in Chapter 2. DRG samples collected from the *in vitro* experiment were also extracted and analysed following the same method. Simultaneous measurement of bioactive lipids was performed using the LC-MS/MS methodology described in Chapter 2. Quantification was performed using Analyst 1.4.1 and imported into Microsoft Excel and Graphpad Prism.

4.2.7 Data Analysis

For the studies measuring hindpaw volume differences these were presented as mean ± SEM, statistical analysis was performed using one-way ANOVA and a Bonferonni post hoc test. LC-MS/MS data were expressed as mean ± SEM, statistical analysis was performed with a Mann Whitney test, an unpaired t test with f-test and paired t test.

4.3 Results

4.3.1 Investigating the influence of linoleic acid exposure and PD 146176 on levels of lipids in rat dorsal root ganglia

Calcium imaging experiments were performed by Dr Mohammad Alsalem (Appendices: Figure 1&2, Table 1). Linoleic acid produced a slow, but robust, increase in intracellular calcium in adult rat dorsal root ganglion (DRGs) neurones, an effect which was blocked by the TRPV1 antagonist capsazepine, demonstrating that these effects were mediated, at least in part, by TRPV1. The onset time of the response to linoleic acid, the ability of lipoxygenase inhibition to reduce the number of cells responding to linoleic acid, and the magnitude of their responses to linoleic acid support the proposal that linoleic acid is metabolised to an active TRPV1 ligand. Data collected from the calcium imaging experiments involving 9- and 13-HODE, PD 146176 and anti-9- and anti-13-HODE antibodies also supported the notion that the 15-LOX metabolites of linoleic acid, 9 and 13-HODE, activate TRPV1 in sensory neurones.

Based on these results, the levels of these 15-LOX metabolites, along with other lipids were measured in the DRGs (See Methods). A range of treatment groups designed to investigate linoleic acid (1 mM) exposure time and the effect of PD 146176 (10 μM) at 15 and 30 minutes were used, with control groups for the different time intervals included (Table 1).

For each treatment group (n = 6), individual DRGs were exposed to either vehicle 1 or PD 146176 for 15 or 30 minutes, followed by vehicle 2 or linoleic acid for 15 or 30 minutes. DRG exposure to vehicle 1 or PD 146176 and vehicle 2 or linoleic acid for 30 minutes did not alter levels of the lipids measured (data not shown).

Exposure of the DRGs to linoleic acid for either 15 or 30 minutes did not alter the levels of linoleic acid measured in the DRGs using LC-MS/MS, compared to levels following exposure to vehicle (Figure 1). By contrast, pre-exposure to PD 146176 significantly increased the levels of linoleic

acid present in the DRGs following exposure to linoleic acid for 15 minutes, but not 30 minutes (Figure 1).

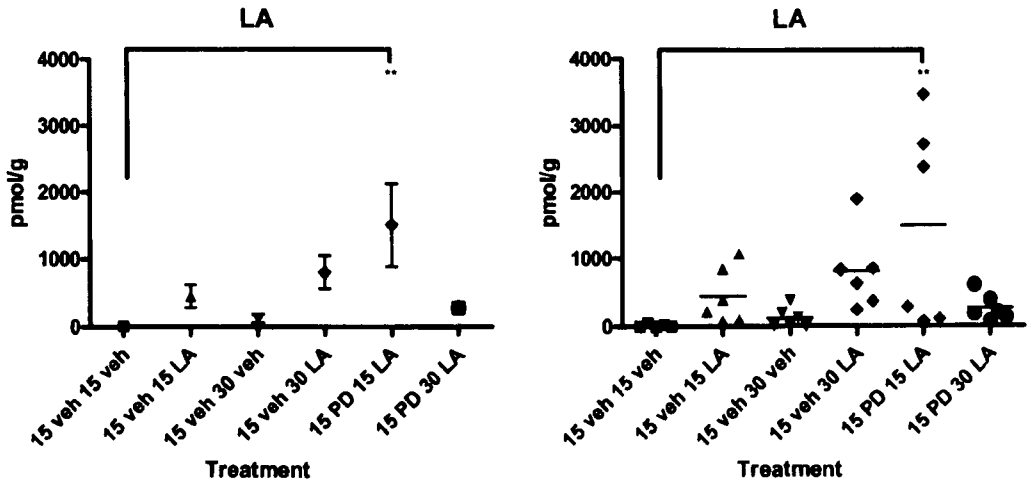

Figure 1. Levels of the LA detected in wet weight tissue of dorsal root ganglia (DRGs) following treatment of vehicle (veh) or PD 146176 (PD) followed by vehicle (veh) or linoleic acid (LA) exposure for 15 or 30 minutes, represented as mean±SEM and a scatter plot (n=6). The two different styles for presenting the information is to allow for difference in interpretation and also to clearly show the distribution of data points. Statistical analysis was conducted using a one-way Anova with Bonferroni *post hoc* test, *P<0.05, **P<0.01. All outlier values greater than 2 standard deviations from the mean were excluded, maximum of one per tissue group for each lipid measured.

LC-MS/MS analysis could not detect either 9- or 13-HODE in adult DRGs under un-stimulated conditions (Figure 2), the limit of quantification (LOQ) in this method was 0.1 pmol/g respectively for both 9- and 13-HODE (LOQ for 9- and 13-oxoODE = 0.05 pmol/g, LOQ for AA = 2.5 pmol/g, LOQ for LA = 0.1 pmol/g). By contrast, following exposure to linoleic acid, 9- and 13-HODE were detected in the DRGs (Figure 2). Pre-exposure to PD 146176 did not significantly alter the absolute levels of 9- and 13-HODE in the DRGs. Similar trends for the effects of treatments were observed for 13-oxoODE and 9-oxoODE with the exception that levels of 9-oxoODE were decreased in the PD-treated group (15 minutes) followed by 15 minute linoleic acid, which was opposite to that observed with 9-, 13-HODE and 13-oxoODE (Figure 2).

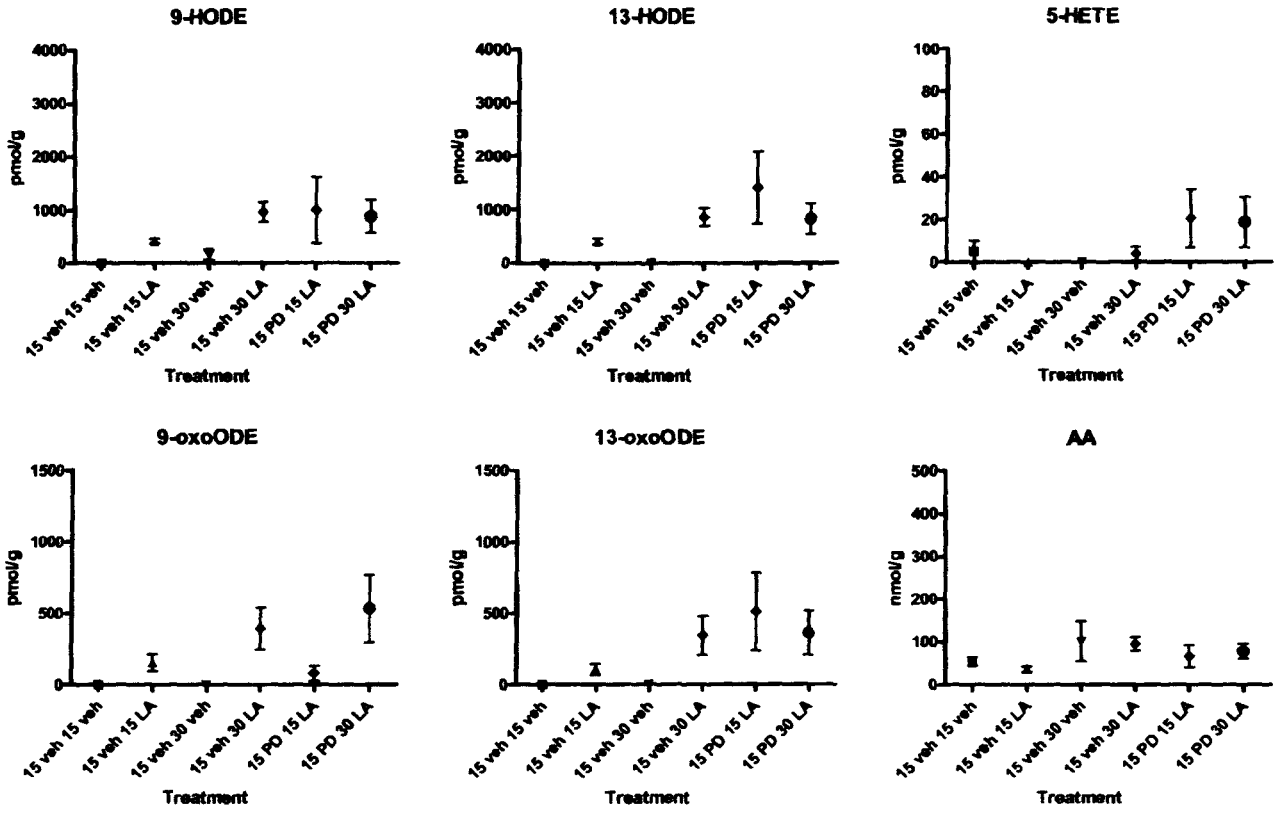

Figure 2. Levels of the lipids detected per g wet tissue weight in the dorsal root ganglia (DRGs) following treatment of vehicle (veh) or PD 146176 (PD) followed by vehicle (veh) or linoleic acid (LA) exposure for 15 or 30 minutes (n=6). Statistical analysis was conducted using a one-way Anova with Bonferroni *post hoc* test, *P<0.05, **P<0.01. All outlier values greater than 2 standard deviations from the mean were excluded, maximum of one per tissue group for each lipid measured.

Given the importance of considering the flux through enzymatic pathways and the amount of substrate available, levels of 9- and 13-HODE were re-analysed as ratios of absolute levels of linoleic acid in the individual DRG preparations to take into account for any variance in linoleic acid uptake by the DRGs. Interestingly, when expressed in this manner the levels of 9- and 13-HODE (expressed as a ratio of the levels of linoleic acid) were significantly decreased following pre-exposure to PD 146176 for 15 minutes, but not 30 minutes (Figure 3).

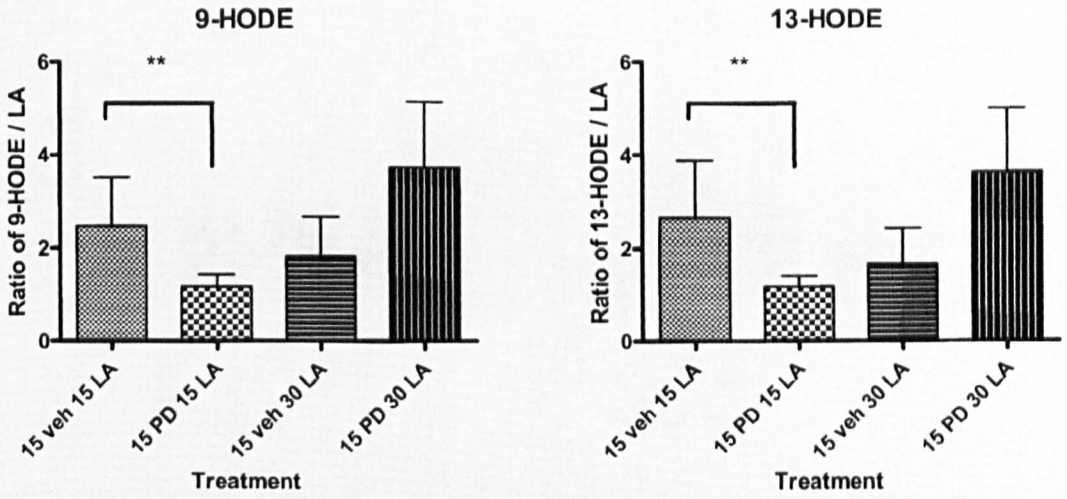

Figure 3. Levels of the 9- and 13-HODE detected per g wet tissue weight in dorsal root ganglia (DRGs) following pre-exposure to vehicle (veh) or PD 146176 (PD) followed by vehicle (veh) or linoleic acid (LA) for 15 or 30 minutes (n=6). Data were expressed as a ratio of linoleic acid in the individual DRG preparation. Statistical analysis was conducting using an unpaired t test with f-test to compare variances, where **P<0.01.

TXB_2 and PGD_2/PGE_2 were not measured in these DRG samples and arachidonic acid remained unaltered for all treatment groups (Figure 2). 5-HETE (TRPV1 agonist) was the only HETE detected in these DRG samples, although its levels were unchanged by linoleic acid exposure (Figure 2). Levels of the endocannabinoids, AEA and 2-AG increased significantly ($P<0.01$, Figure 4) following exposure to linoleic acid for 15 minutes, but not 30 minutes, following pre-treatment with PD 146176 (Figure 4). PEA and OEA also followed the same trend (Figure 4), although these were not shown to be significant.

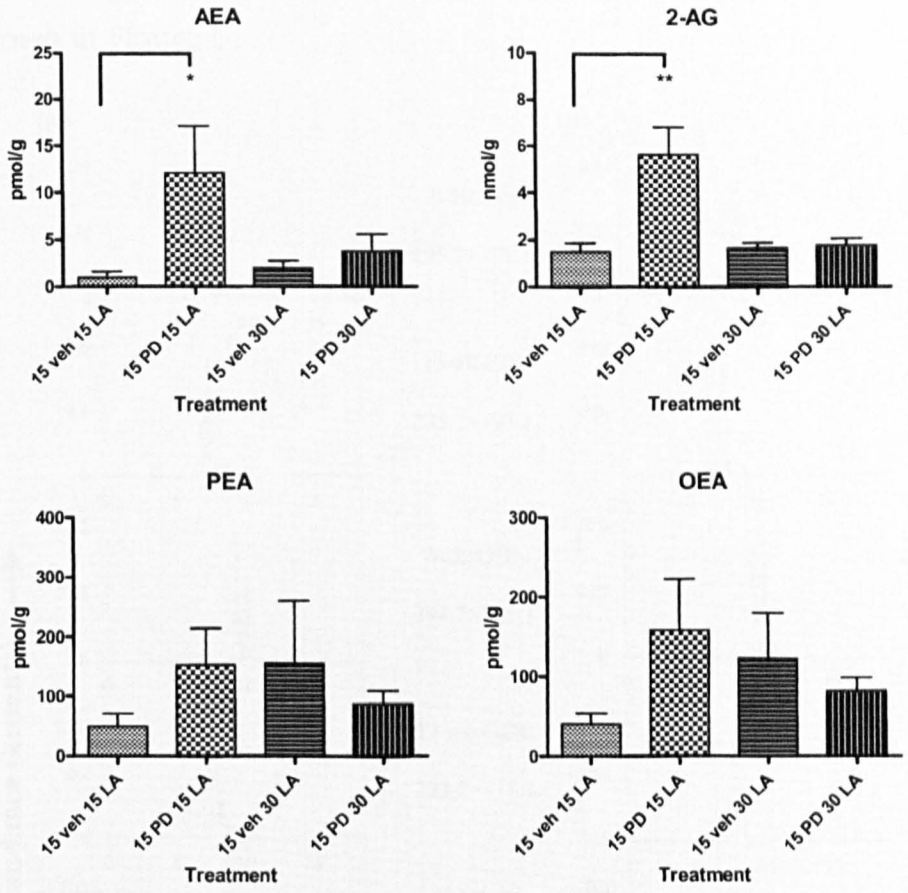

Figure 4. Levels of the AEA, 2-AG, PEA and OEA detected per g wet tissue weight in dorsal root ganglia (DRGs) following treatment of vehicle (veh) or PD 146176 (PD) followed by vehicle (veh) or linoleic acid (LA) exposure for 15 or 30 minutes (n=6). Statistical analysis was conducted using a one-way Anova with Bonferroni *post hoc* test, *P<0.05, **P<0.01. All outlier values greater than 2 standard deviations from the mean were excluded, maximum of one per tissue group for each lipid measured.

4.3.2 Investigating the effects of saline and carrageenan on lipid levels and inflammatory hyperalgesia in the hindpaw

Hindpaw tissue was collected 1 hour and 4 hours post-saline or -carrageenan and the samples were analysed by LC-MS/MS (See methods). LC-MS/MS analysis was used to measure levels of 15-LOX metabolites and other inflammatory mediators to investigate the effects of saline and carrageenan on these lipid levels. The same lipids were detected at the one hour time-point as for the four hour time-point, apart from 15-HETE, which was only detectable at the four hour timepoint. The

chromatograms of several of these lipids measured in hindpaw tissue are shown in Figure 5.

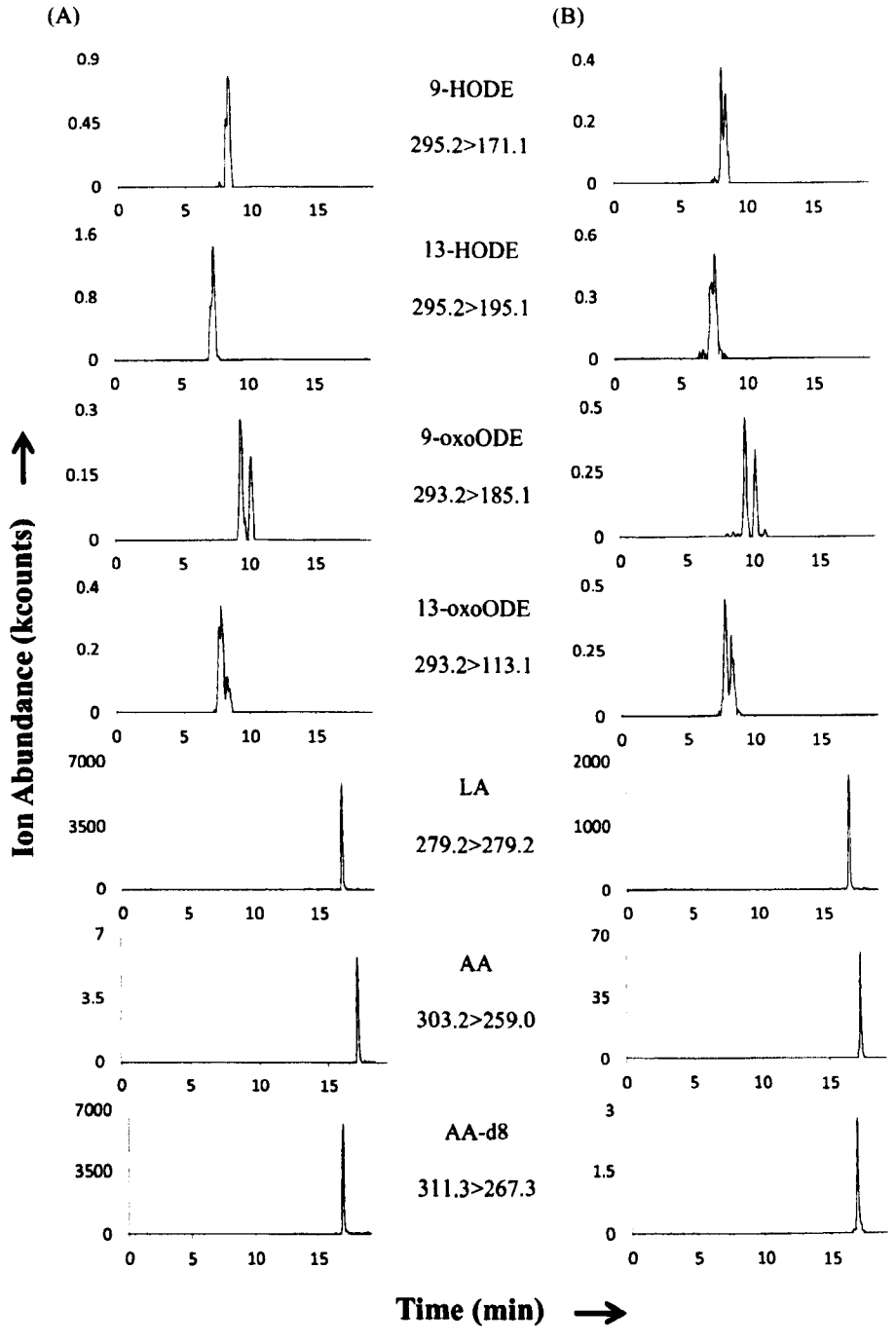

Figure 5. Representative selective ion chromatograms. (A) Analyte standards. (B) Metabolites extracted from samples. Each chromatogram is individually normalized. Samples were analysed on a 150, 2.0 mm C18 column using a gradient of methanol:acetonitrile (20:80 v/v) and aqueous formic acid with ammonium hydroxide. The mass spectrometer was operated in MRM mode.

4.3.2.1 The effects of saline or carrageenan on lipid levels in the hindpaw at one hour post-injection

One hour following intraplantar injection of carrageenan there was a significant decrease in the levels of TRPV1 agonists 12-HETE ($P<0.05$), 9-HODE ($P<0.05$) and 13-HODE ($P<0.05$) in the carrageenan-treated hindpaw at one hour post injection, compared to the vehicle saline-treated group (Figure 6). There were, however, no significant changes in the levels of the other lipids measured at this timepoint (Figure 7), including TRPV1 agonists 5-HETE, 9-oxoODE and 13-oxoODE (Figure 6). 8-HETE (PPARα agonist) and 15-HETE (TRPV1 agonist) were both below the limit of quantification (BLOQ), 0.1 pmol/g and 0.5 pmol/g respectively.

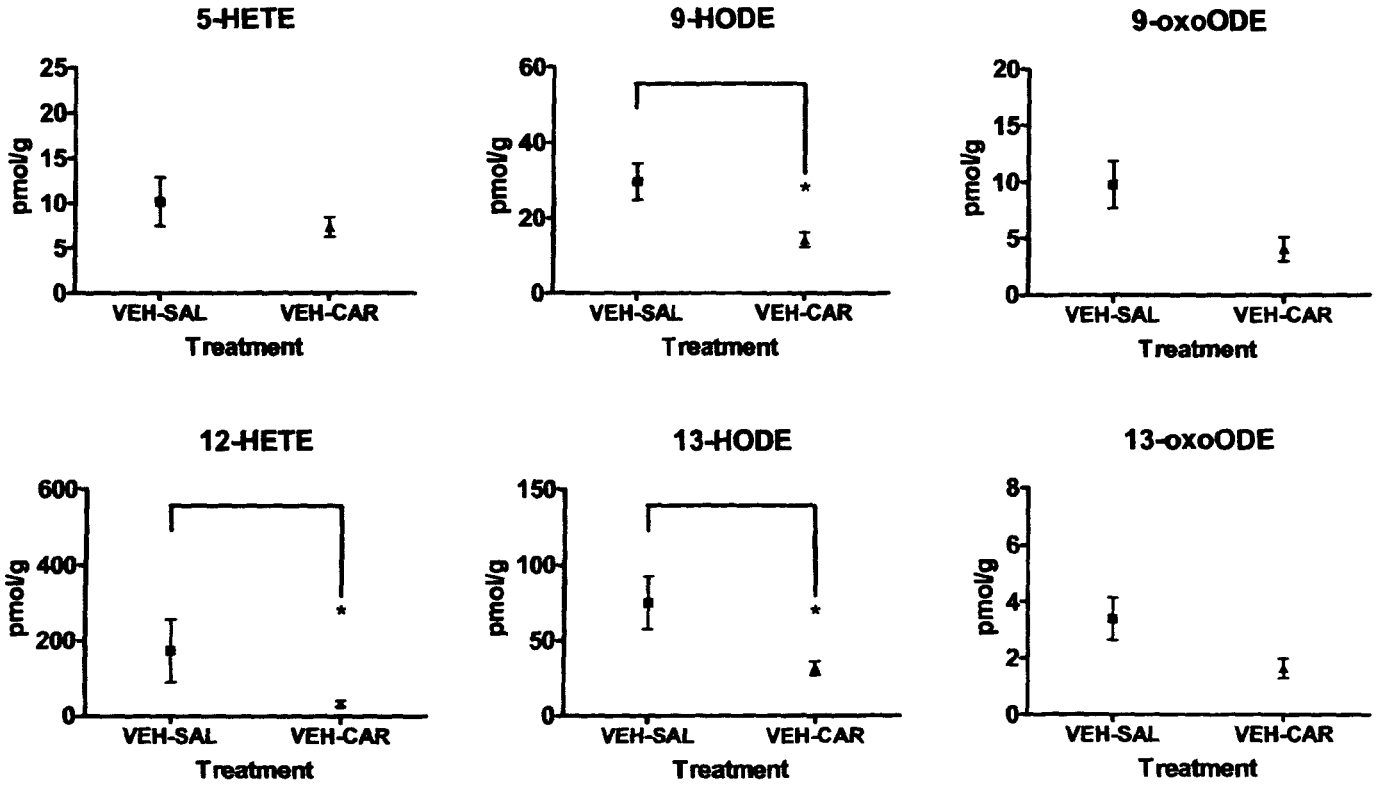

Figure 6. Levels of the 15-LOX metabolites and other TRPV1 agonists detected in the ipsilateral hindpaw per g wet tissue weight following intraplantar injection of vehicle (VEH) followed by saline (SAL) or carrageenan (CAR) one hour post-carrageenan (n=6). Statistical analysis was conducted using a Mann Whitney test, *P<0.05. All outlier values greater than 2 standard deviations from the mean were excluded, maximum of one per tissue group for each lipid measured.

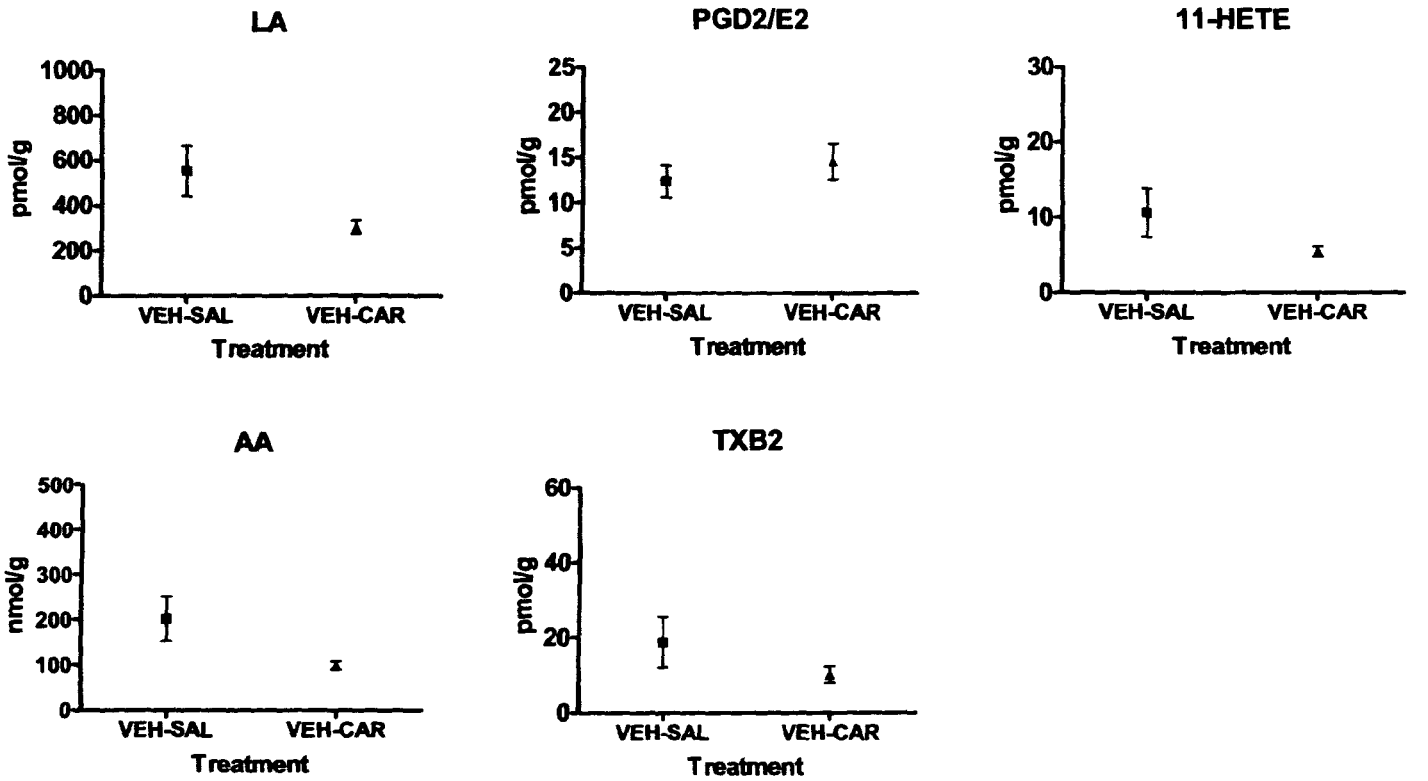

Figure 7. Levels of the lipid mediators detected per g wet tissue weight in the ipsilateral hindpaw following intraplantar injection of vehicle (VEH) followed by saline (SAL) or carrageenan (CAR) one hour post-carrageenan (n=6). Statistical analysis was conducted using a Mann Whitney test, *P<0.05. All outlier values greater than 2 standard deviations from the mean were excluded, maximum of one per tissue group for each lipid measured.

There was also a significant decrease in the levels of the endocannabinoid 2-AG ($P<0.05$), and the endocannabinoid like compounds PEA ($P<0.05$) and OEA ($P<0.05$), where OEA is also a known TRPV1 agonist (Figure 8). Levels of the endocannabinoid and TRPV1 agonist AEA, followed this trend, but did not alter significantly.

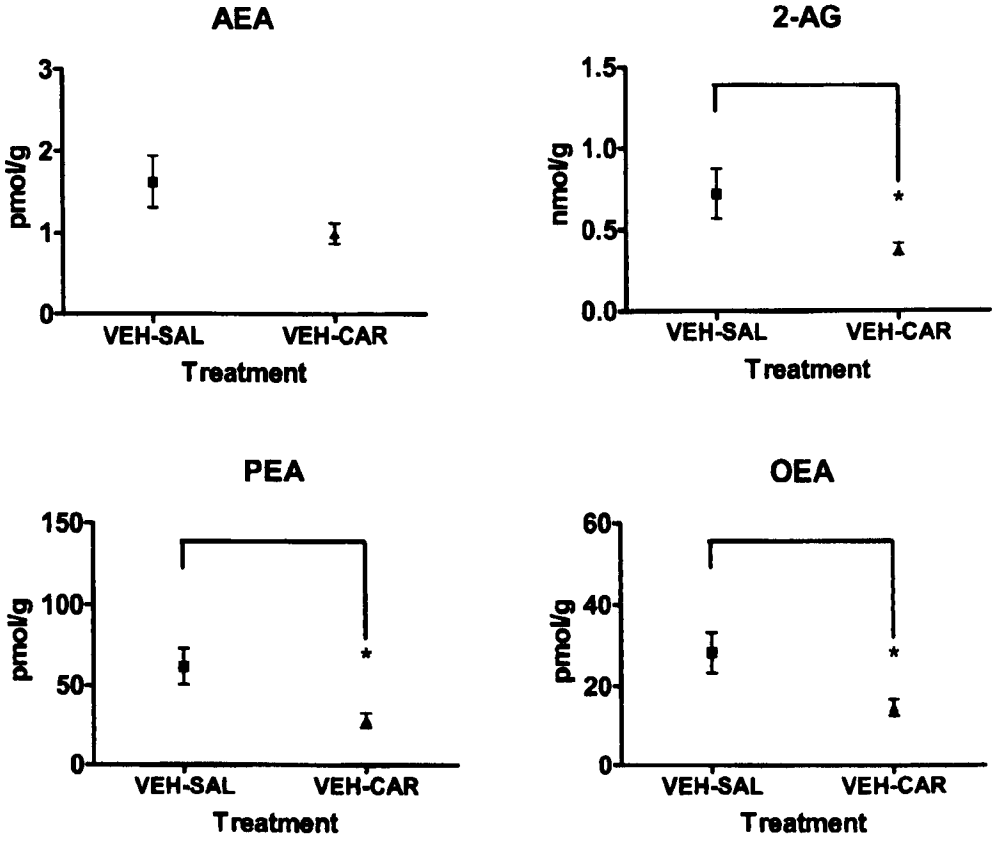

Figure 8. Levels of the endocannabinoids AEA and 2-AG, and the endocannabinoid-like compounds PEA and OEA detected per g wet tissue weight in the ipsilateral hindpaw following intraplantar injection of vehicle (VEH) followed by saline (SAL) or carrageenan (CAR) one hour post-carrageenan (n=6). Statistical analysis was conducted using a Mann Whitney test, *$P<0.05$. All outlier values greater than 2 standard deviations from the mean were excluded, maximum of one per tissue group for each lipid measured.

4.3.2.2 The effects of saline or carrageenan on lipid levels in the hindpaw at four hours post-injection

Four hours post-carrageenan injection, levels of the 15-LOX metabolites, 9-HODE and 13-HODE, both TRPV1 agonists, were significantly decreased ($P<0.01$) in the hindpaw, compared to saline-treated rats (Figure 9).

There was a similar trend for 9-oxoODE ($P<0.05$) and 13-oxoODE (Figure 9), although significance was not reached for 13-oxoODE. Levels of linoleic acid and TXB_2 were significantly increased ($P<0.05$) in the carrageenan-treated hindpaw, compared to saline-treated hindpaw at the four hour timepoint (Figure 10). Levels of linoleic acid increased by nearly 2-fold, whereas levels of TXB_2 increased by nearly 12-fold, compared to saline-treated rats, where this lipid was below the limit of detection. By contrast, levels of arachidonic acid and PGD_2/PGE_2 were not altered in the carrageenan-treated hindpaw, compared to saline-treated rats at this four hour timepoint (Figure 10). A number of HETEs were also detected, these included TRPV1 agonists 5-HETE, 12-HETE and 15-HETE (Figure 9), and also levels of 11-HETE (Figure 10), which were all not altered in the carrageenan-treated rats, compared to saline-treated rats at this timepoint. These data support a specific modulation of the LA / HODE / oxoODE pathway during carrageenan inflammation.

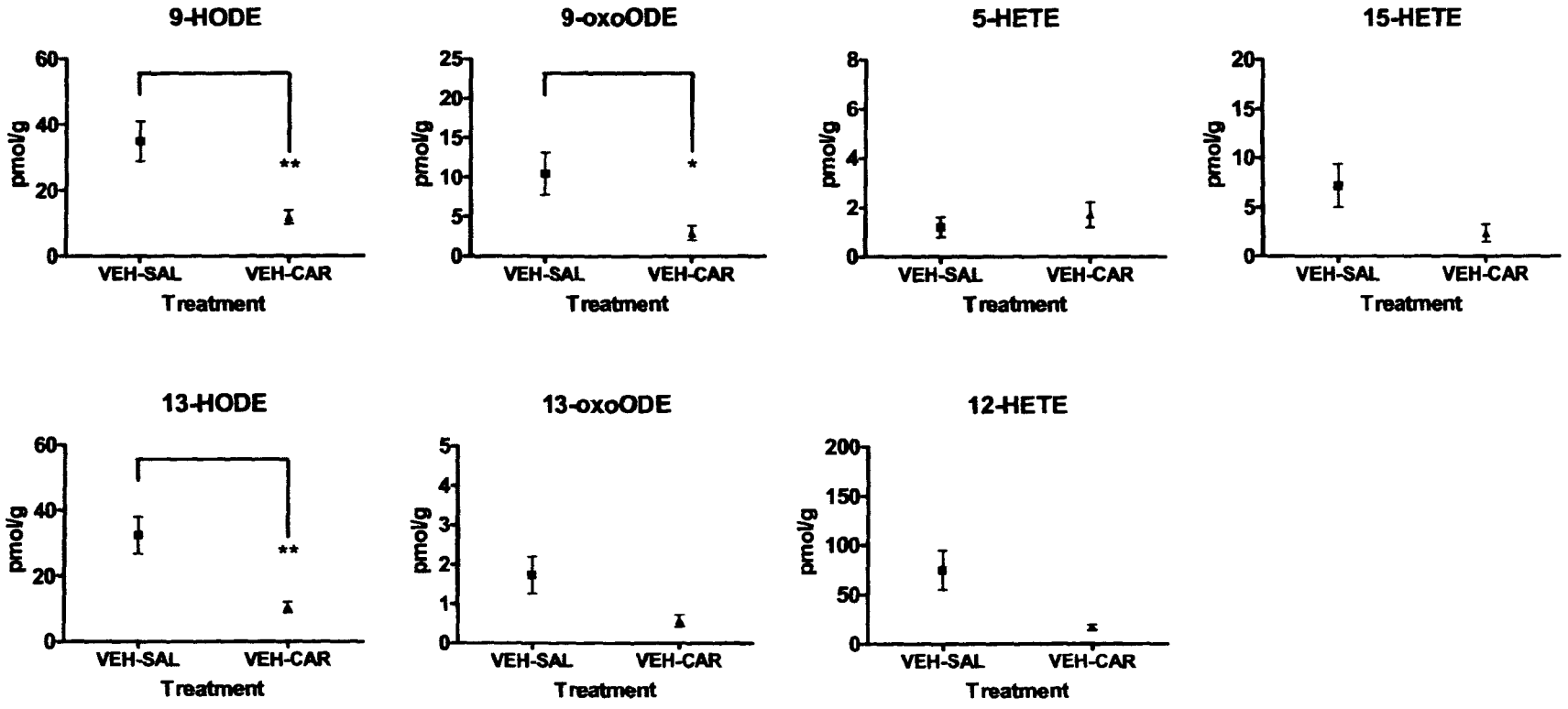

Figure 9. Levels of the 15-LOX metabolites and other TRPV1 agonists detected per g wet tissue weight in the ipsilateral hindpaw following intraplantar injection of vehicle (VEH) followed by saline (SAL) or carrageenan (CAR) four hours post-carrageenan (n=6). Statistical analysis was conducted using a Mann Whitney test, *P<0.05. All outlier values greater than 2 standard deviations from the mean were excluded, maximum of one per tissue group for each lipid measured.

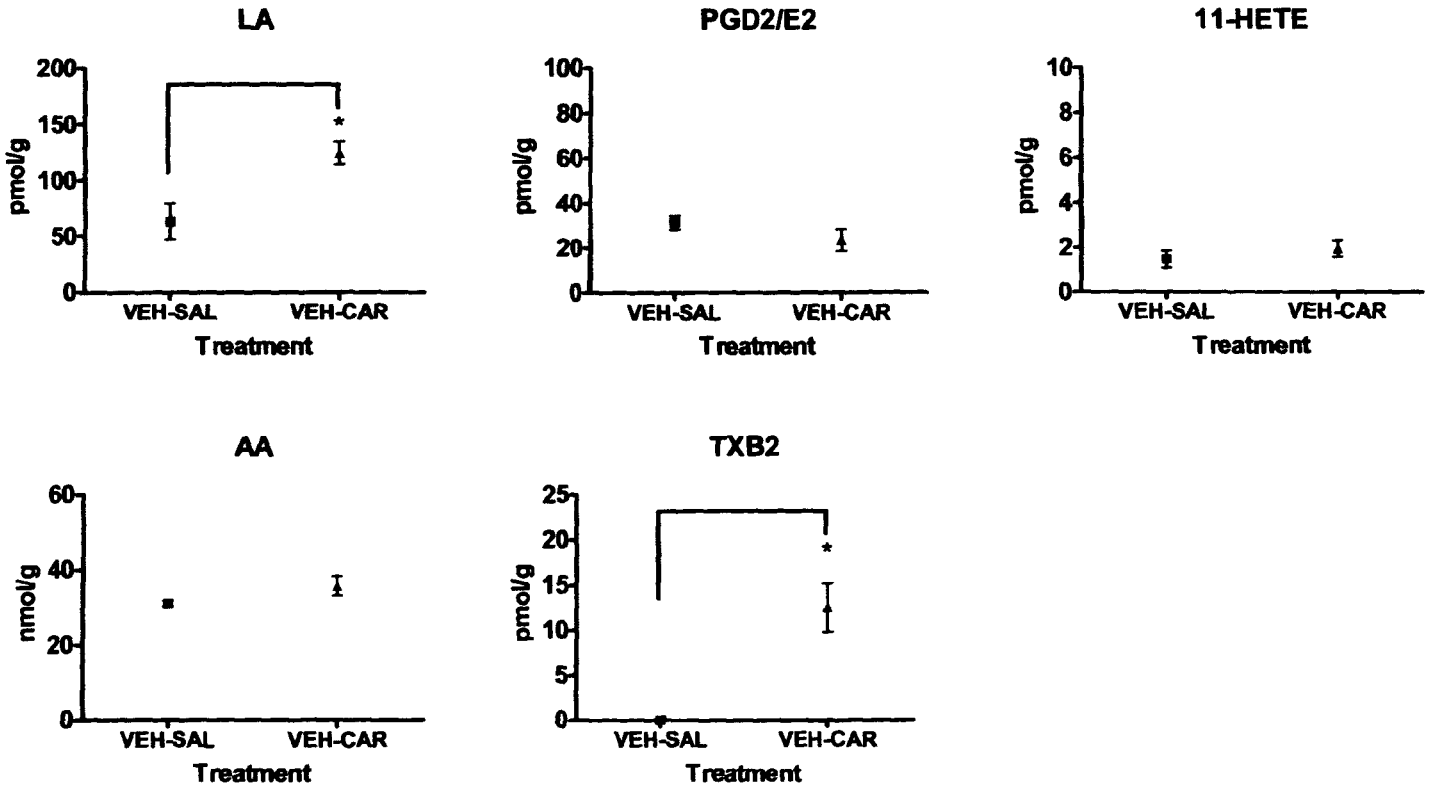

Figure 10. Levels of the lipid mediators detected per g wet tissue weight in the ipsilateral hindpaw following intraplantar injection of vehicle (VEH) followed by saline (SAL) or carrageenan (CAR) four hours post-carrageenan (n=6). Statistical analysis was conducted using a Mann Whitney test, *P<0.05. All outlier values greater than 2 standard deviations from the mean were excluded, maximum of one per tissue group for each lipid measured.

Levels of the endocannabinoids AEA and 2-AG in the hindpaw were not altered at four hours in carrageenan-treated rats, compared to saline-treated. However, levels of the endocannabinoid-like lipids PEA and OEA, were significantly decreased ($P<0.01$ and $P<0.05$ respectively) in the carrageenan-treated rats at this four hour timepoint (Figure 11).

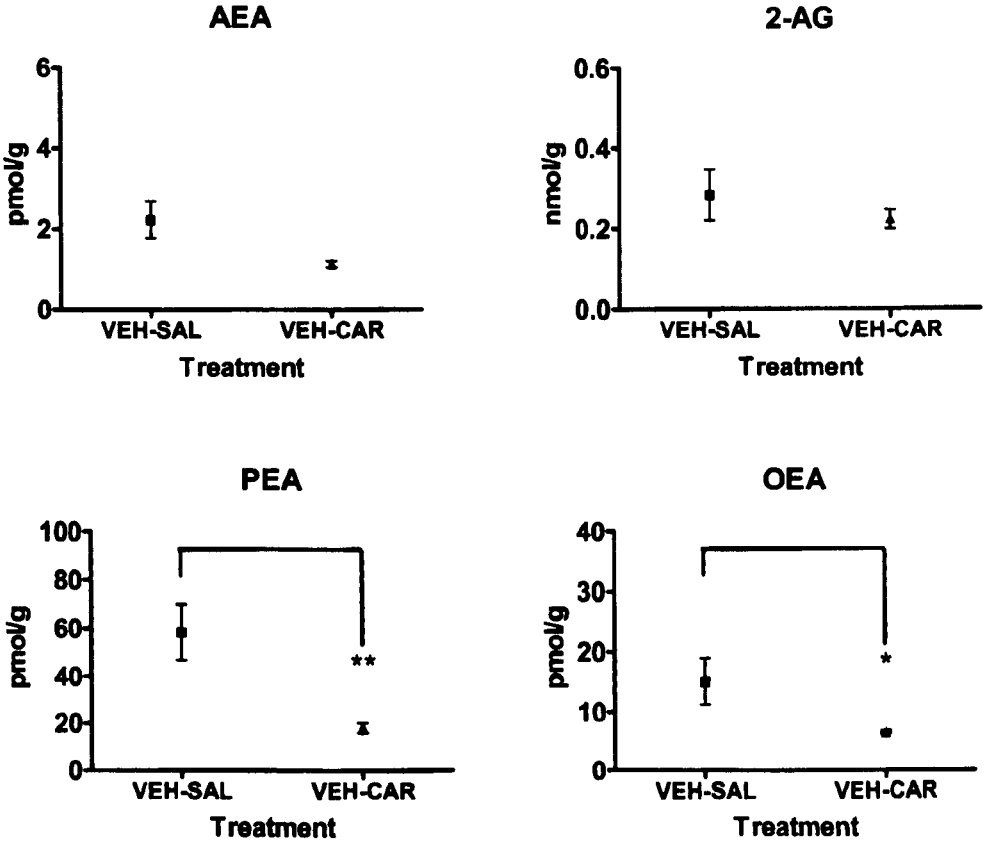

Figure 11. Levels of the endocannabinoids AEA and 2-AG, and the endocannabinoid-like compounds PEA and OEA detected per g wet tissue weight in the ipsilateral hindpaw following intraplantar injection of vehicle (VEH) followed by saline (SAL) or carrageenan (CAR) four hours post-carrageenan (n=6). Statistical analysis was conducted using a Mann Whitney test, *$P<0.05$. All outlier values greater than 2 standard deviations from the mean were excluded, maximum of one per tissue group for each lipid measured.

4.3.2.3 The effects of saline and carrageenan on hindpaw inflammation at one and four hours

Hindpaw volume and circumference were measured several times over the course of the experiment. For collection of baseline values they were measured before injection of drug treatment or vehicle (See methods)

and measured immediately before tissue collection, one hour post-carrageenan in one study and four hours post-carrageenan in another to investigate the effects on hindpaw inflammation at both these time points.

Intraplantar injection of saline did not significantly alter paw volume or paw circumference at 1 and 4 hours post-injection in the ipsilateral hindpaw. Intraplantar injection of carrageenan significantly altered hindpaw volume and circumference one hour and four hour post-injection (Figure 12).

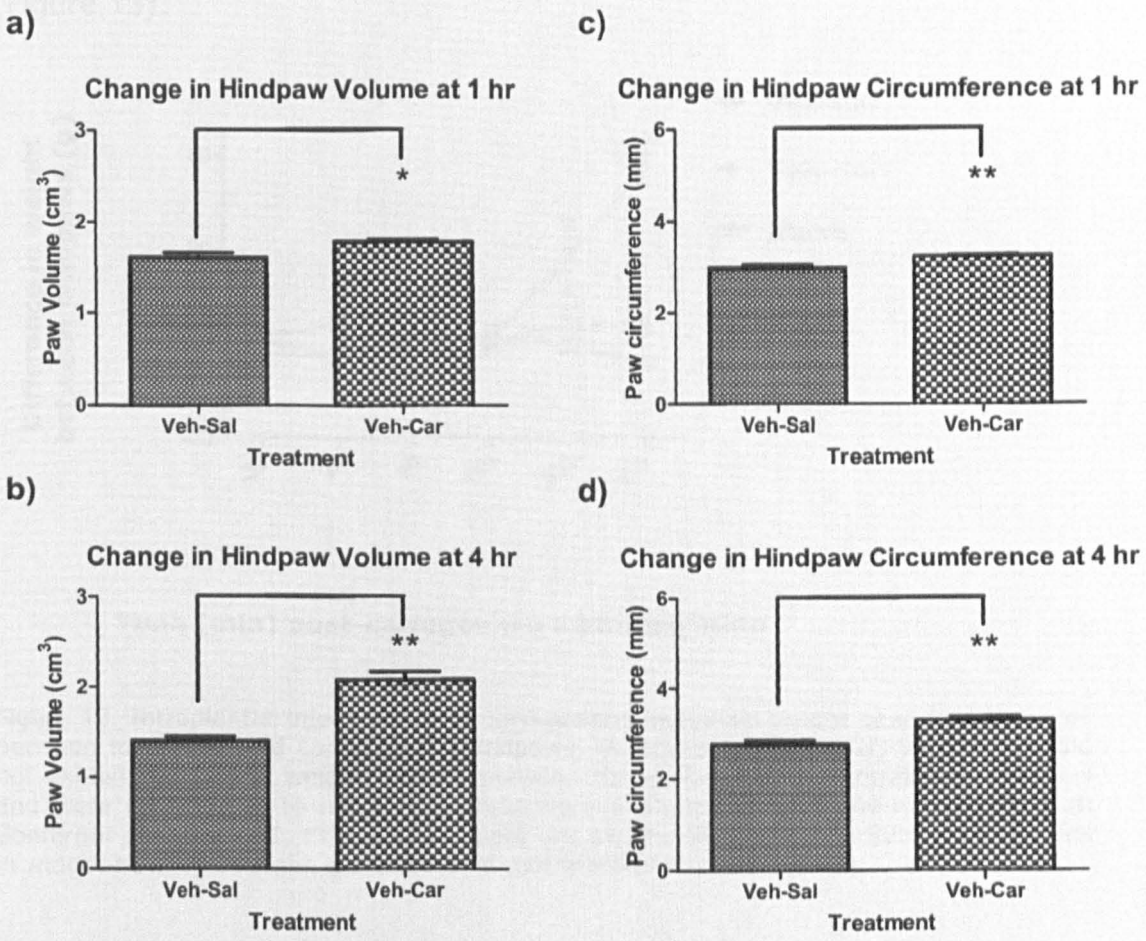

Figure 12. Intraplantar injection of 2% carrageenan significantly increased the hindpaw volume at (Figure 12a and b) and hindpaw circumference (Figure 12c and d) in ipsilateral hindpaws compared to control (Veh-Sal) at one hour and four hours post-injection. Data were analysed using a Mann Whitney test, **P<0.01 and *P<0.05. Data are expressed as mean ± SEM of ipsilateral hindpaws (n=6).

Hindpaw volume and hindpaw circumference remained unchanged in the contralateral hindpaws at both timepoints (data not shown). The effects of saline and carrageenan on pain behaviour was also investigated, but only at the four hour timepoint.

4.3.2.4 The effects of saline and carrageenan on pain behaviour

Intraplantar injection of saline in vehicle pre-treated rats did not significantly alter weight bearing between ipsilateral and contralateral hindpaws throughout the four hours (Figure 13) and weight-bearing was comparable to pre-injection baseline values and also to the naïve group (Figure 13).

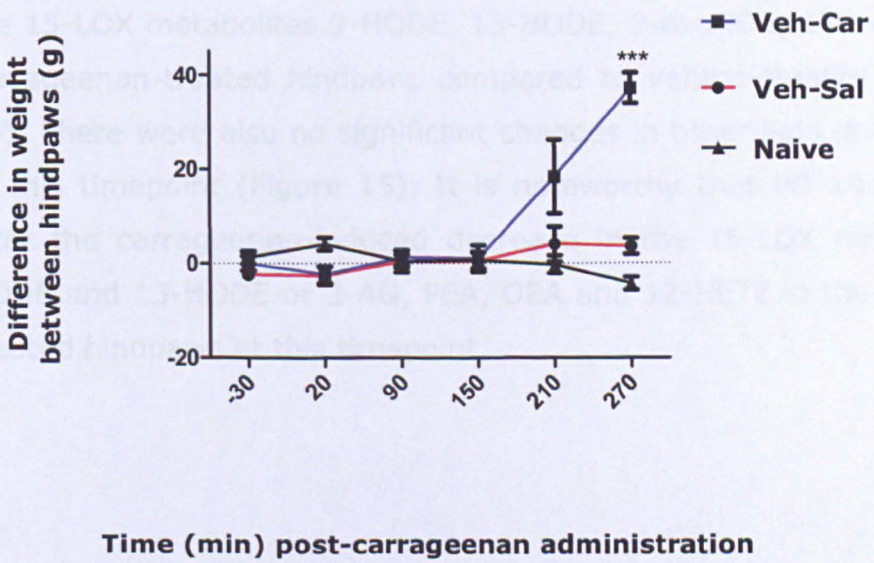

Figure 13. Intraplantar injection of 2% carrageenan increased weight bearing differences between ipsilateral and contralateral hindpaws. Vehicle-saline (veh-sal)-treated rats did not exhibit changes in weight bearing between the ipsilateral and contralateral hindpaw and were comparable to naïve rats. Data were analysed using a one-way Anova with Bonferoni *post hoc* test, ***P<0.001. Data are expressed as mean ± SEM of differences in weight bearing between ipsilateral and contralateral hindpaws (n=6).

Intraplantar injection of 2% carrageenan significantly (P<0.001) altered the difference in weight bearing between ipsilateral and contralateral hindpaws (Figure 13). These carrageenan-induced changes in weight bearing were accompanied by significant changes in hindpaw inflammation.

4.3.3 Investigating the effects of 15-LOX inhibition on lipid levels and inflammatory hyperalgesia in the hindpaw at one and four hours-post carrageenan

4.3.3.1 The effects of 15-LOX inhibition on lipid levels in the hindpaw at one hour post-carrageenan

LC-MS/MS analysis was used to measure levels of 15-LOX metabolites and other inflammatory mediators to investigate whether inhibition of 15-LOX with PD 146176 altered the levels of these lipids in the carrageenan model of inflammatory pain.

At the one hour timepoint, PD 146176 did not significantly alter levels of the 15-LOX metabolites 9-HODE, 13-HODE, 9-oxoODE, 13-oxoODE in the carrageenan-treated hindpaw, compared to vehicle-treated rats (Figure 14). There were also no significant changes in other lipid levels observed at this timepoint (Figure 15). It is noteworthy that PD 146176 did not alter the carrageenan-induced decrease in the 15-LOX metabolites, 9-HODE and 13-HODE or 2-AG, PEA, OEA and 12-HETE in the carrageenan treated hindpaws at this timepoint.

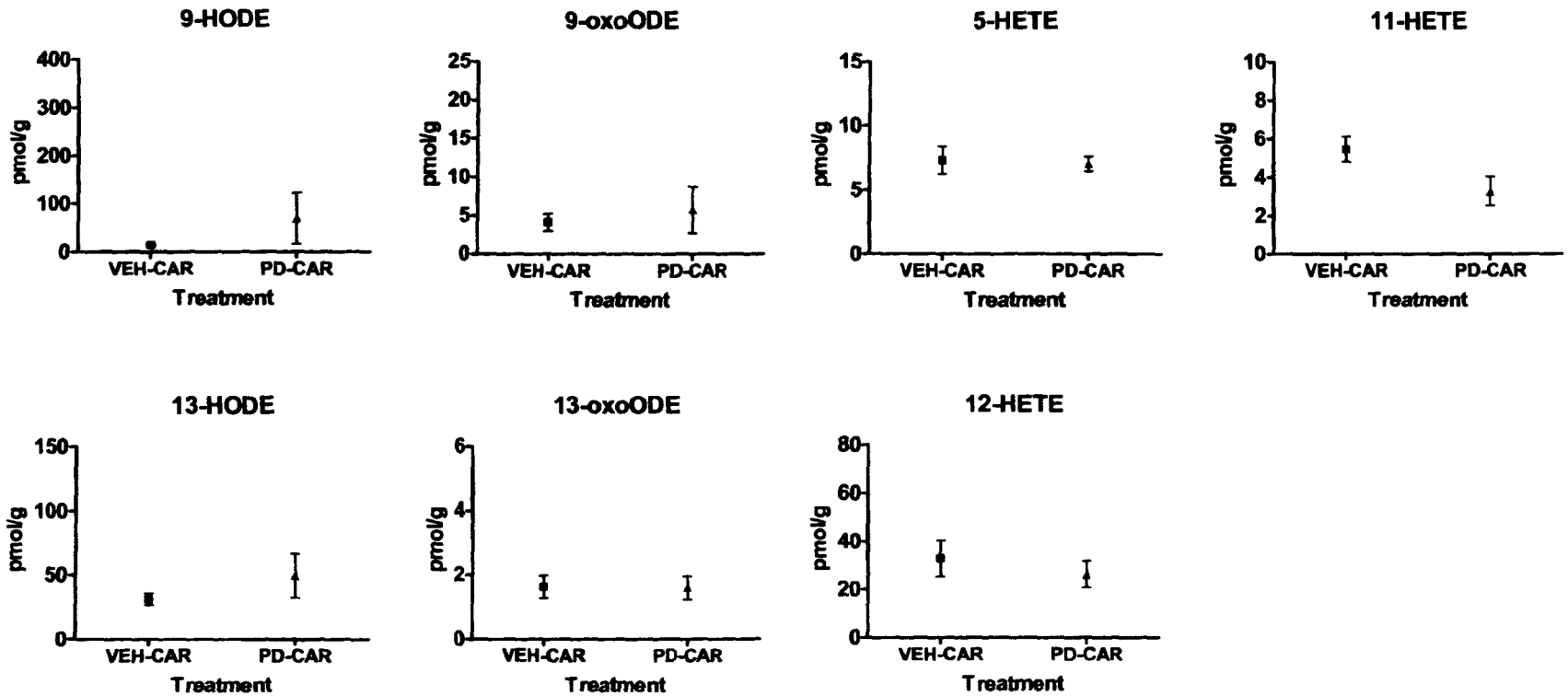

Figure 14. Levels of the 15-LOX metabolites and other TRPV1 agonists detected per g wet tissue weight in the ipsilateral hindpaw following intraplantar injection of vehicle (VEH) or PD 146176 (PD) followed by carrageenan (CAR) one hour post-carrageenan (n=6). Statistical analysis was conducted using a Mann Whitney test, *P<0.05. All outlier values greater than 2 standard deviations from the mean were excluded , maximum of one per tissue group for each lipid measured.

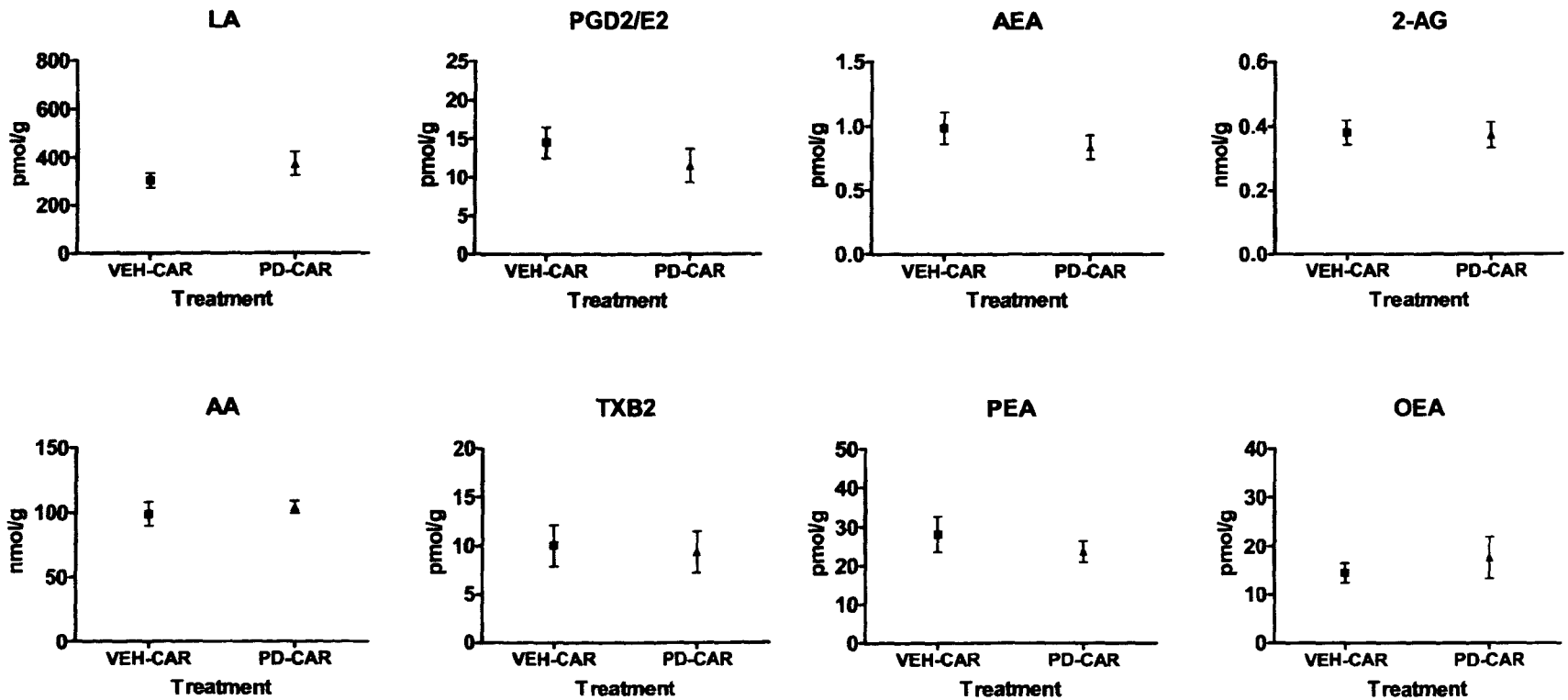

Figure 15. Levels of the lipid mediators detected per g wet tissue weight in the ipsilateral hindpaw following intraplantar injection of vehicle (VEH) or PD 146176 (PD) followed by carrageenan (CAR) one hour post-carrageenan (n=6). Statistical analysis was conducted using a Mann Whitney test, *P<0.05. All outlier values greater than 2 standard deviations from the mean were excluded, maximum of one per tissue group for each lipid measured.

Four hours following treatment with PD 146176 and carrageenan, there were also no significant differences in the levels of lipids in the hindpaw of PD 146176 carrageenan-treated rats compared to vehicle carrageenan treated rats (Figures 16 and 17). It is noteworthy that PD 146176 did not alter the carrageenan-induced decrease in the 15-LOX metabolites, 9-HODE, 13-HODE and 9-oxoODE or PEA and OEA in the carrageenan treated hindpaws at this timepoint. In addition, PD 146176 did not alter the carrageenan-induced increase in levels of linoleic acid and TXB_2.

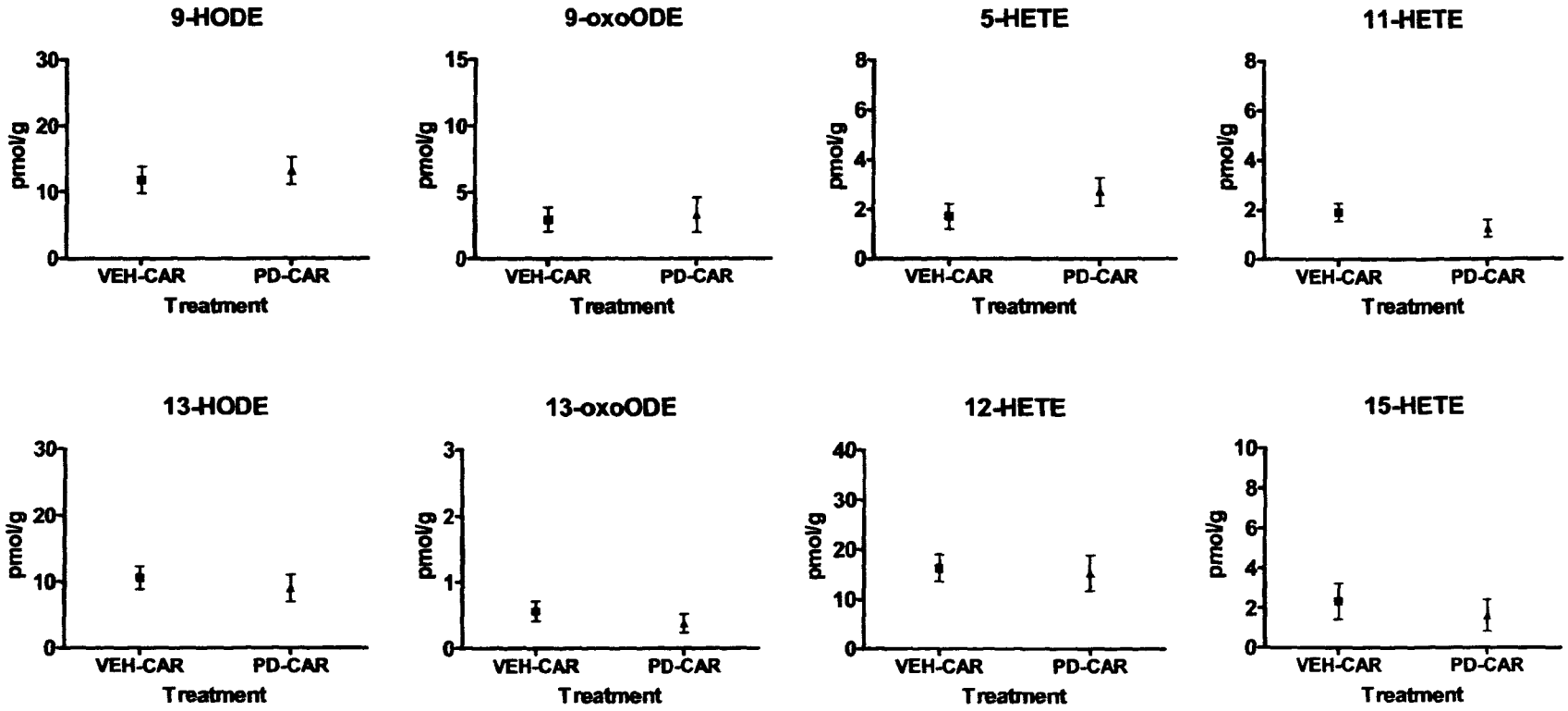

Figure 16. Levels of the 15-LOX metabolites and other TRPV1 agonists detected per g wet tissue weight in the ipsilateral hindpaw following intraplantar injection of vehicle (VEH) or PD 146176 (PD) followed by carrageenan (CAR) four hours post-carrageenan (n=6). Statistical analysis was conducted using a Mann Whitney test, *P<0.05. All outlier values greater than 2 standard deviations from the mean were excluded, maximum of one per tissue group for each lipid measured.

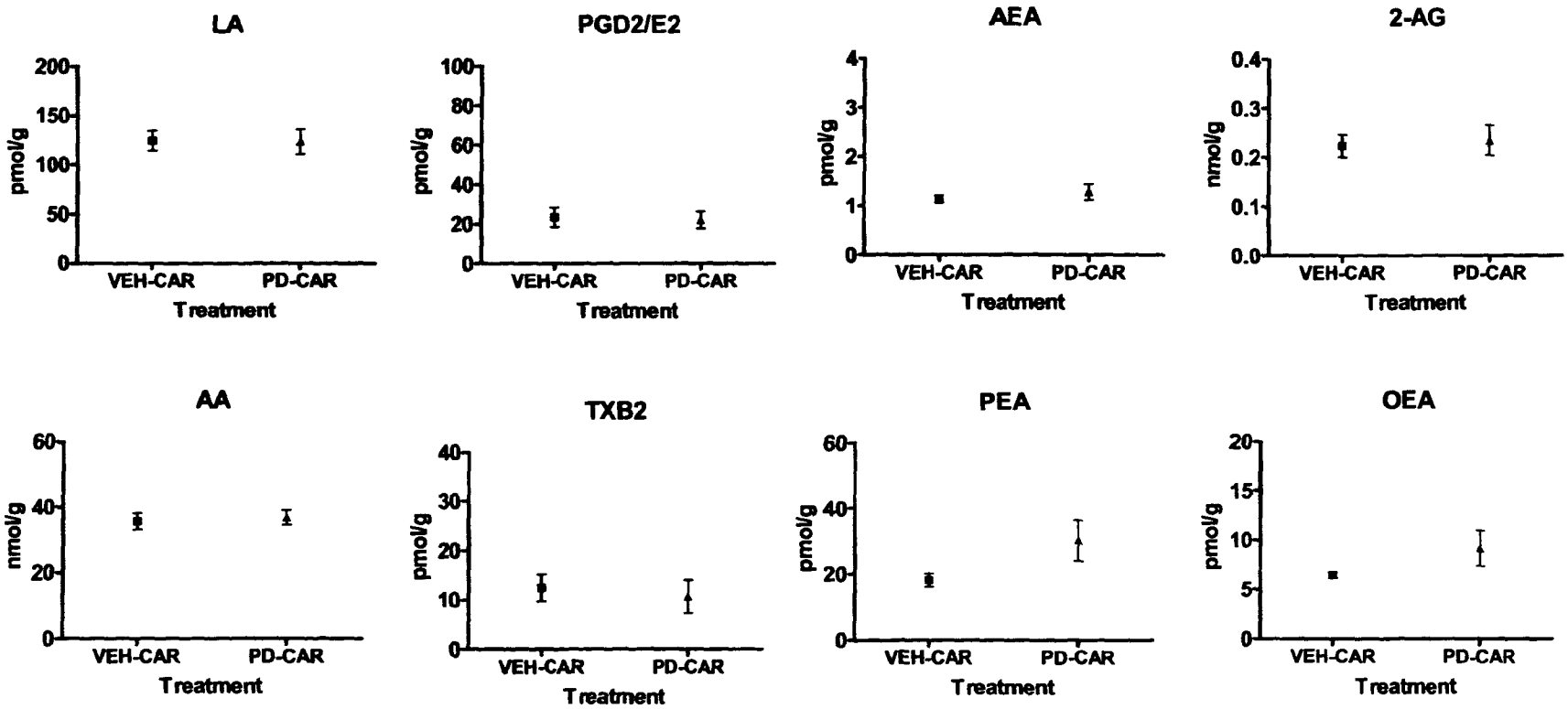

Figure 17. Levels of the lipid mediators detected per g wet tissue weight in the ipsilateral hindpaw following intraplantar injection of vehicle (VEH) or PD 146176 (PD) followed by carrageenan (CAR) four hours post-carrageenan (n=6). Statistical analysis was conducted using a Mann Whitney test, *P<0.05. All outlier values greater than 2 standard deviations from the mean were excluded, maximum of one per tissue group for each lipid measured.

4.3.3.2 The effects of 15-LOX inhibition on carrageenan-induced inflammatory hyperalgesia in the hindpaw

PD 146176 pre-treatment did not significantly alter the carrageenan-induced increase in the hindpaw volume and hindpaw circumference at one hour and four hours (Figure 18). However, the change in hindpaw volume and hindpaw circumference were still significant in the PD 146176-carrageenan treatment group four hours post-injection compared to control (Appendices: Table 2).

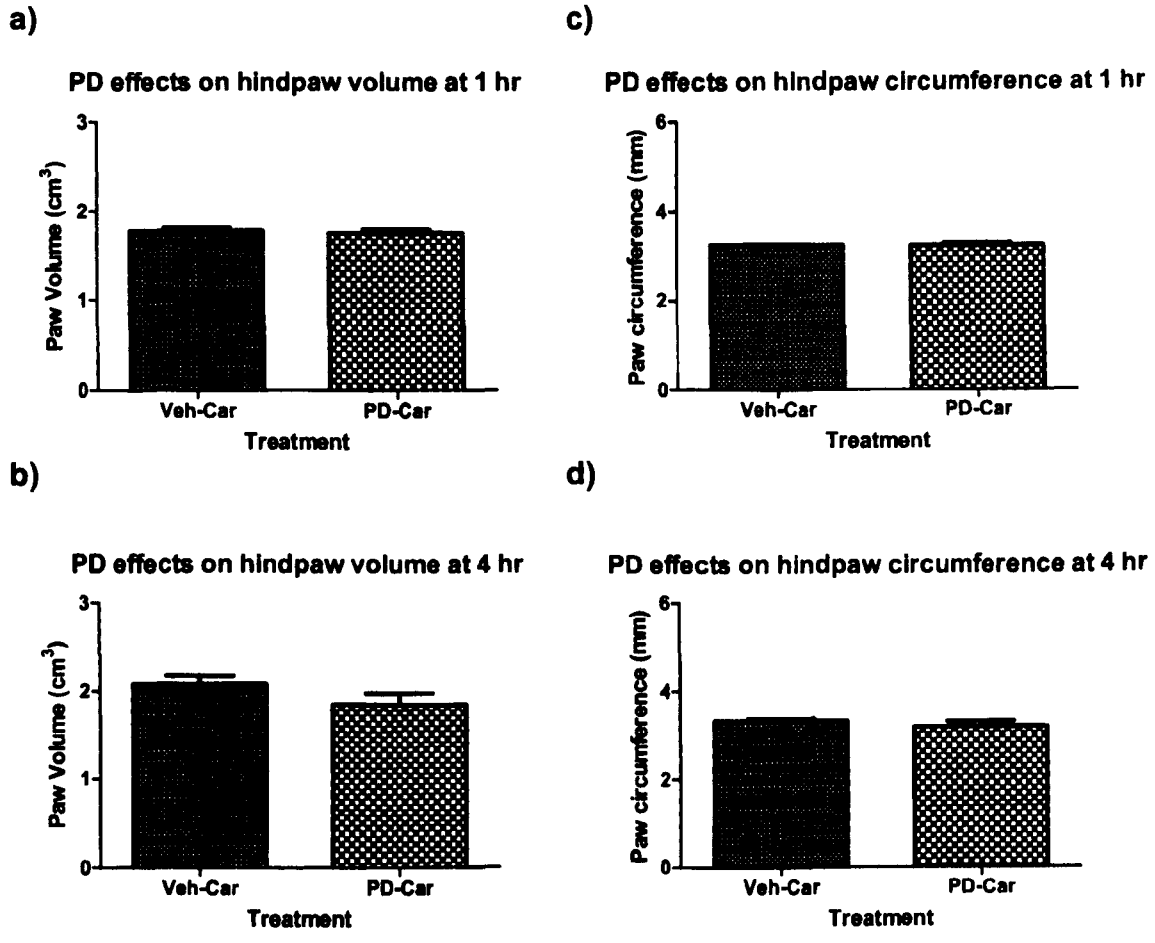

Figure 18. PD 146176 pre-treatment did not significantly alter the carrageenan-induced increase in the hindpaw volume (Figure 18a and b) and hindpaw circumference (Figure 18 c and d) at one hour and four hours. Data were analysed using a Mann Whitney test, **P<0.01 and *P<0.05. Data are expressed as mean ± SEM of ipsilateral hindpaws (n=6).

Hindpaw volume and hindpaw circumference remained unchanged in the contralateral hindpaws in all measurements (data not shown).

At 4 hours post-carrageenan injection, there was a significant increase in weight bearing difference between the carrageenan-treated rats compared to saline-treated rats (Figure 13). To investigate whether 15-LOX inhibition alters pain behaviour, we explored the effects of intraplantar injection of the 15-LOX inhibitor PD 146176 (50 µg/50 µL) on carrageenan-induced differences in weight bearing. Intraplantar administration of PD 146176 30 minutes prior to 2% carrageenan significantly ($P<0.01$) reduced the carrageenan-induced weight bearing difference at 4 hours post-injection compared to vehicle pre-treated rats (Figure 19). Rats treated with PD 146176 followed by saline did not show any changes in weight bearing, which was comparable to the naïve and vehicle-saline treated groups (Appendices: Figure 3).

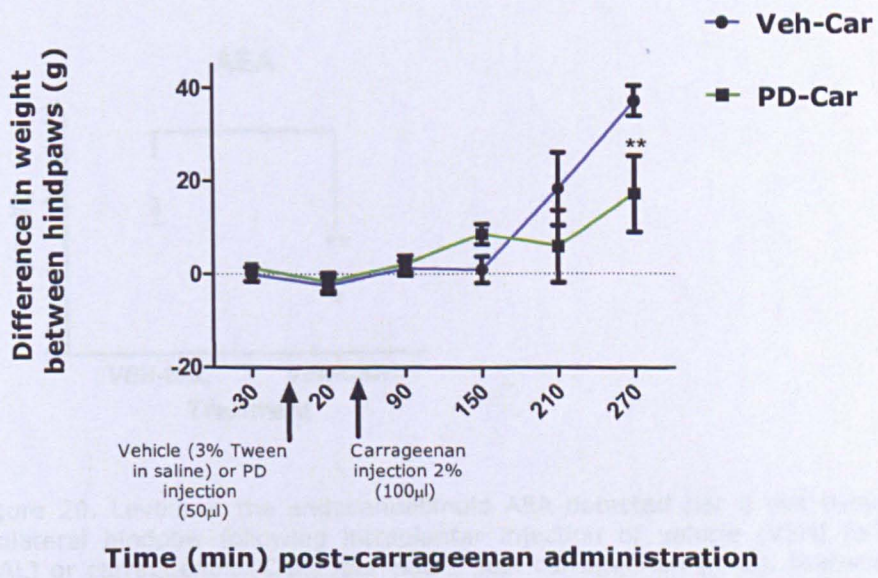

Figure 19. Pre-administration of PD 146176 significantly reduced the effect of carrageenan on differences in weight bearing four hours post-carrageenan in the ipsilateral hindpaw. Data were analysed using a one-way Anova with Bonferoni *post hoc* test, **P<0.01. Data are expressed as mean ± SEM of differences in weight bearing between ipsilateral and contralateral hindpaws (n=6).

4.3.4 Investigating the effects of 9- and 13-HODE neutralisation on lipid levels and inflammatory hyperalgesia in the hindpaw four hours-post carrageenan

4.3.4.1 The effects of 9- and 13-HODE neutralisation on lipid levels in the hindpaw four hours post-carrageenan

LC-MS/MS analysis was used to measure levels of 15-LOX metabolites and other inflammatory mediators to investigate whether 9- and 13-HODE neutralisation with selective antibodies altered the levels of lipids *in vivo*. This experiment was conducted to complement the 15-LOX investigation. Overall the effects of intraplantar injection of carrageenan on levels of lipids in the hindpaw were consistent with the earlier PD 146176 4-hour study (data not shown). There was however, a significant decrease in AEA ($P<0.01$) in the carrageenan-treated rats compared to saline-treated, which did not reach significance in the earlier study (Figure 20).

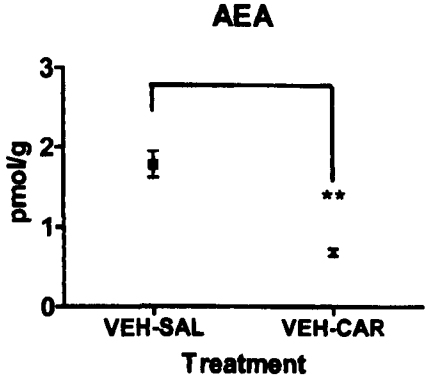

Figure 20. Levels of the endocannabinoid AEA detected per g wet tissue weight in the ipsilateral hindpaw following intraplantar injection of vehicle (VEH) followed by saline (SAL) or carrageenan (CAR) four hours post-carrageenan (n=6). Statistical analysis was conducted using a Mann Whitney test, *P<0.05. All outlier values greater than 2 standard deviations from the mean were excluded, maximum of one per tissue group for each lipid measured.

Four hours following treatment with 9- and 13-HODE antibodies and carrageenan, there were no significant differences in the levels of lipids in the hindpaw of 9- and 13-HODE antibodies-carrageenan-treated rats

compared to vehicle-carrageenan-treated rats (Figures 21 and 22). It is noteworthy that 9- and 13-HODE antibodies did not alter the carrageenan-induced decrease in the 15-LOX metabolites, 9-HODE, 13-HODE and 9-oxoODE or AEA, PEA and OEA in the carrageenan treated hindpaws. In addition, 9- and 13-HODE antibodies did not alter the carrageenan-induced increase in levels of linoleic acid and TXB_2.

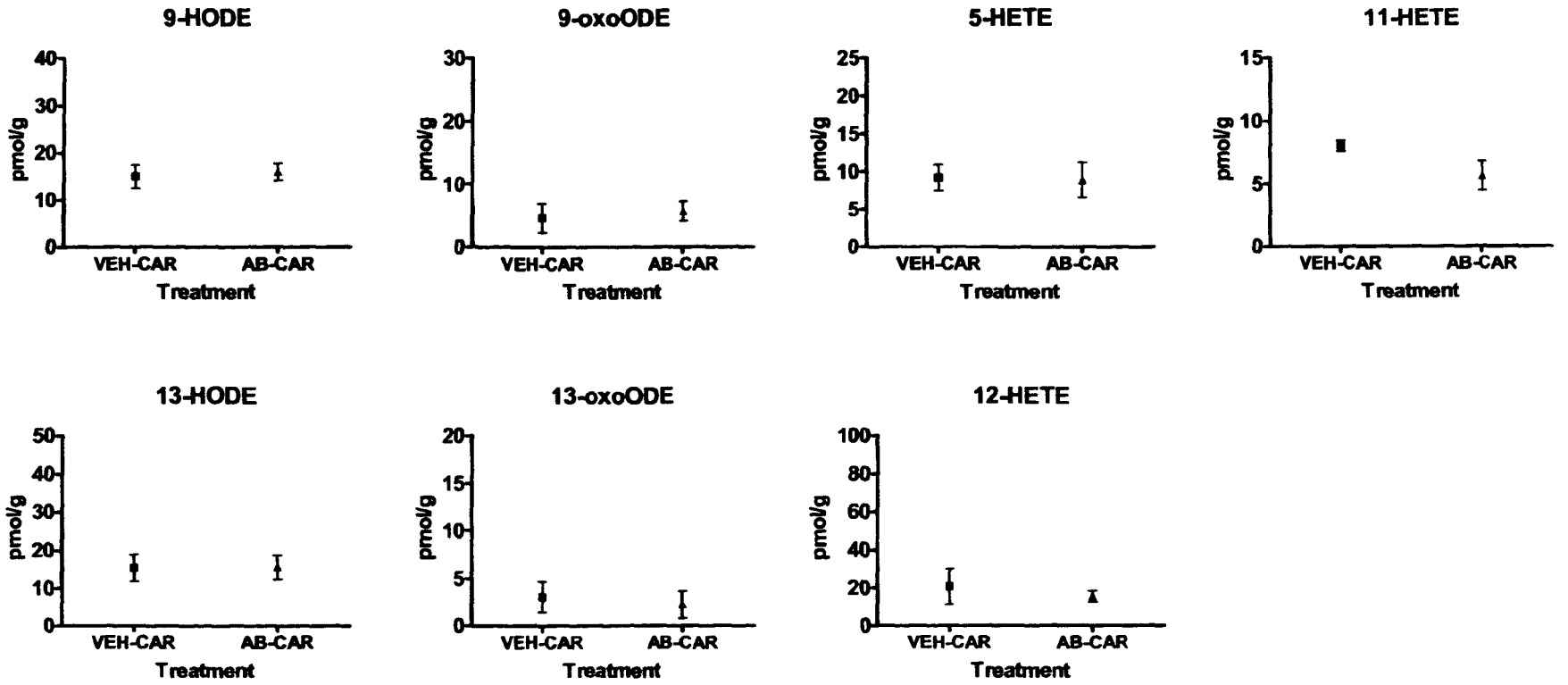

Figure 21. Levels of the 15-LOX metabolites and other TRPV1 agonists detected per g wet tissue weight in the ipsilateral hindpaw following intraplantar injection of vehicle (VEH) or 9- and 13-HODE antibodies (AB) co-administered with carrageenan (CAR) four hours post-injection (n=6). Statistical analysis was conducted using a Mann Whitney test, *P<0.05. All outlier values greater than 2 standard deviations from the mean were excluded, maximum of one per tissue group for each lipid measured.

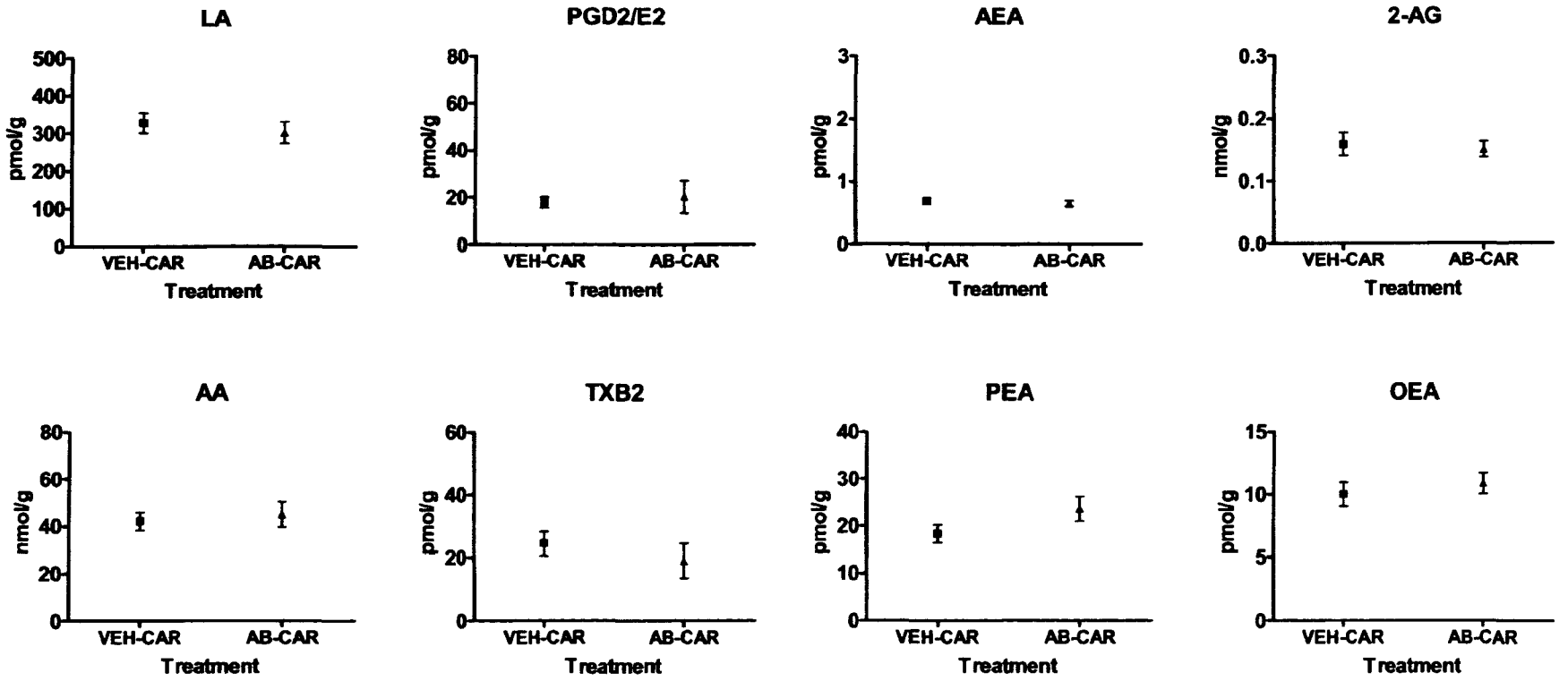

Figure 22. Levels of the lipid mediators detected per g wet tissue weight in the ipsilateral hindpaw following intraplantar injection of vehicle (VEH) or 9- and 13-HODE antibodies (AB) co-administered with carrageenan (CAR) four hours post-injection (n=6). Statistical analysis was conducted using a Mann Whitney test, *P<0.05. All outlier values greater than 2 standard deviations from the mean were excluded, maximum of one per tissue group for each lipid measured.

4.3.4.2 The effects of 9- and 13-HODE neutralisation on carrageenan-induced inflammatory hyperalgesia in the hindpaw

Co-administration of 9- and 13-HODE antibodies did not significantly alter the carrageenan-induced increase in the hindpaw volume and hindpaw circumference at four hours (Figure 23). However, the change in hindpaw volume and hindpaw circumference were still significant in the 9- and 13-HODE antibodies -carrageenan treatment group four hours post-injection compared to control (Appendices: Table 3). Hindpaw volume and hindpaw circumference remained unchanged in the contralateral hindpaws in all measurements (data not shown).

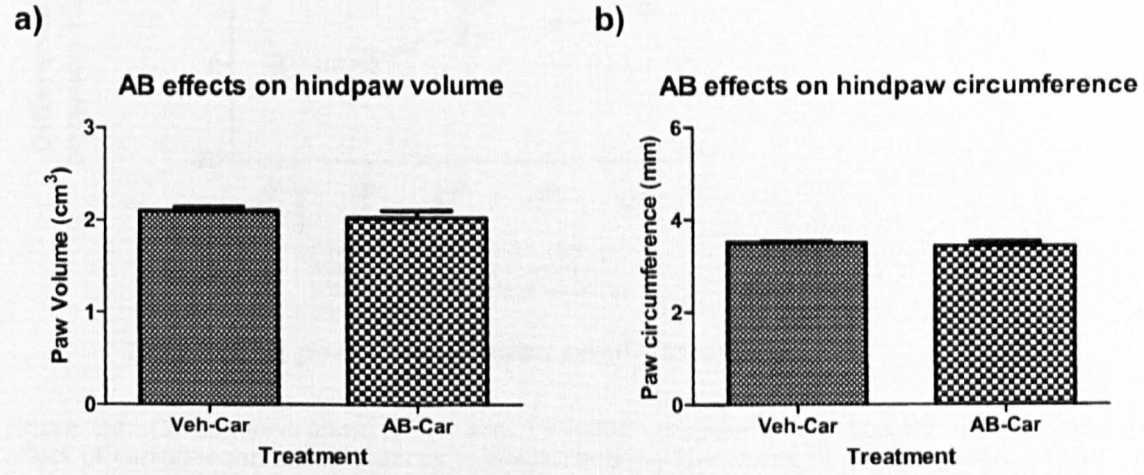

Figure 23. Co-administration of 9- and 13-HODE antibodies did not significantly alter the carrageenan-induced increase in the hindpaw volume (Figure 23a) and hindpaw circumference (Figure 23b) at four hours. Data were analysed using a Mann Whitney test, **P<0.01 and *P<0.05. Data are expressed as mean ± SEM of ipsilateral hindpaws (n=6).

To complement the investigation of 15-LOX inhibition, we examined the role of 9- and 13-HODEs in inflammatory hyperalgesia using a combination of antibodies raised against 9- and 13-HODE (25 µg of each) and monitored changes in pain behaviour. The effect of intraplantar injection of these antibodies on carrageenan-induced difference in the weight bearing was examined. Intraplantar injection of saline to the vehicle-treated rats did not induce significant changes in weight bearing between ipsilateral and contralateral hindpaws throughout the four hours,

which were comparable to pre-injection baseline values and also to the naïve group (Appendices: Figure 4). Intraplantar injection of the antibodies significantly reduced the carrageenan-induced weight bearing difference at 4 hours post-injection (Figure 24). Rats treated with antibodies followed by saline did not exhibit any weight bearing differences between hindpaws which was comparable to the naïve and vehicle-saline treatment groups (Appendices: Figure 4).

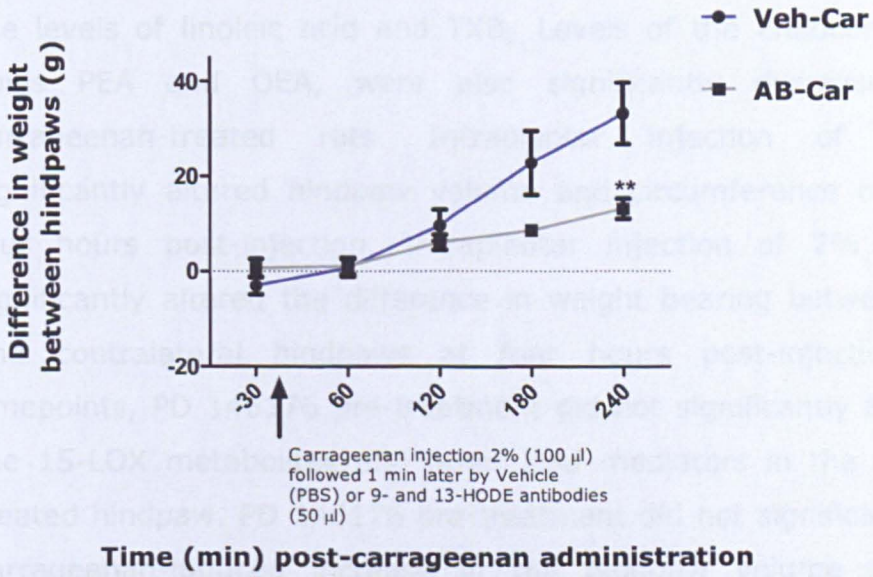

Figure 24. Co-administration of 9- and 13-HODE antibodies significantly reduced the effect of carrageenan on differences in weight bearing four hours post-carrageenan in the ipsilateral hindpaw. Data were analysed using a one-way Anova with Bonferoni *post hoc* test, **P<0.01. Data are expressed as mean ± SEM of differences in weight bearing between ipsilateral and contralateral hindpaws (n=6).

4.3.5 Summary of findings

In vitro, PD 146176 significantly increased linoleic acid levels in the DRGs following exposure to linoleic acid for 15 minutes, but not 30 minutes. Levels of 9- and 13-HODE, expressed as a ratio of the levels of linoleic acid, were significantly decreased following pre-exposure to PD 146176 for 15 minutes, but not 30 minutes. Levels of the endocannabinoids, AEA and 2-AG increased significantly following exposure to linoleic acid for 15 minutes, but not 30 minutes, following pre-treatment with PD 146176.

In vivo, one hour following intraplantar injection of carrageenan there was a significant decrease in the levels of TRPV1 agonists 12-HETE, 9-HODE and 13-HODE in the carrageenan-treated hindpaw. Levels of the endocannabinoid 2-AG, and the endocannabinoid like compounds PEA and OEA also significantly decreased in the carrageenan-treated hindpaw. Four hours post-carrageenan injection, levels of the 15-LOX metabolites, 9-HODE and 13-HODE in the hindpaw were significantly decreased, compared to saline-treated hindpaw, along with significant increases in the levels of linoleic acid and TXB_2. Levels of the endocannabinoid-like lipids PEA and OEA, were also significantly decreased in the carrageenan-treated rats. Intraplantar injection of carrageenan significantly altered hindpaw volume and circumference one hour and four hours post-injection. Intraplantar injection of 2% carrageenan significantly altered the difference in weight bearing between ipsilateral and contralateral hindpaws at four hours post-injection. At both timepoints, PD 146176 pre-treatment did not significantly alter levels of the 15-LOX metabolites and other lipid mediators in the carrageenan-treated hindpaw. PD 146176 pre-treatment did not significantly alter the carrageenan-induced increase in the hindpaw volume and hindpaw circumference at both timepoints. However, PD 146176 pre-treatment significantly reduced the carrageenan-induced weight bearing difference at 4 hours post-injection. Four hours following co-administration of 9- and 13-HODE antibodies and carrageenan, there were no differences in the levels of lipids in the hindpaw of 9- and 13-HODE antibodies-carrageenan-treated rats. Co-administration of 9- and 13-HODE antibodies did not significantly alter the carrageenan-induced increase in the hindpaw volume and hindpaw circumference. However, co-administration of 9- and 13-HODE antibodies significantly reduced the carrageenan-induced weight bearing difference at 4 hours post-injection.

4.4 Discussion

4.4.1 Effects of linoleic acid exposure and PD 146176 on lipid levels in rat dorsal root ganglia

Linoleic acid was found to produce slow but robust increases in intracellular calcium in adult rat dorsal root ganglia (DRGs) neurones, which were blocked by capsazepine, a TRPV1 antagonist and these effects are, therefore, likely to be mediated, at least in part, by TRPV1. The onset time of the response to linoleic acid, the ability of 15-lipoxygenase inhibition to reduce the number of responding cells, and the magnitude of their responses to linoleic acid support the proposal that linoleic acid is metabolised to an active TRPV1 ligand. Data collected from the calcium imaging experiments involving 9- and 13-HODE, PD 146176 and anti-9- and anti-13-HODE antibodies also show that the 15-LOX metabolites of linoleic acid, 9 and 13-HODE, directly activate TRPV1 in sensory neurones. These data also showed that PD 146176 reduced the linoleic acid-mediated calcium responses in DRG neurones and the number of neurones responding to linoleic acid (Appendices: Figure 1&2, Table 1). Overall, this suggests that the HODEs could be mediators of the linoleic acid response and this was investigated.

Levels of linoleic acid, HODEs and oxoODEs in DRG neurones were measured by LC-MS/MS to investigate whether 15-LOX metabolism of linoleic acid to the HODEs might contribute to the TRPV1-mediated response produced by linoleic acid. Previous studies have shown that 9 and 13-HODE are the major 15-LOX metabolites of linoleic acid (Baer et al 1991, Daret et al 1989).The effects of LA in the absence and presence of PD 146176 (10μM), a selective 15-LOX inhibitor, which lacks antioxidant activity (Sendobry et al 1997) were also determined. Exposure of the DRG cells to linoleic acid resulted in a time-dependent accumulation of linoleic acid. Pre-treatment of PD 146176 altered linoleic acid levels in the DRGs, however, this was also dependent of linoleic acid exposure time. PD 146176 alone did not affect lipid levels; however, pre-exposure to PD 146176 tended to reduce the levels of 9- and 13-HODE

15 minutes after linoleic acid suprafusion, although this was not significant. Pre-exposure to PD 146176 also reduced the levels of the oxidised metabolites 9- and 13-oxoODE, 15 minutes after treatment with linoleic acid. 30 minutes after suprafusion with linoleic acid, levels of 9- and 13-HODE had returned to control values. These results suggest that the PD 146176 might be blocking the production of the HODEs and oxoODEs at 15 minutes and that this is time-dependent because these effects were not seen at 30 minutes.

Linoleic acid can be metabolised via sequential Δ-6- and Δ-5-desaturase activity to arachidonic acid in many tissues (Sampath et al 2011, Horrobin 1993), linoleic acid exposure did not alter the levels of arachidonic acid or its lipoxygenase metabolite 5-HETE in the DRGs, which shows that any changes observed are due to linoleic acid metabolism only. Levels of AEA and 2-AG increased significantly ($P<0.01$) after 15 minutes of PD 146176 treatment suprafused with linoleic acid for 15 minutes, compared to control. PEA and OEA also followed the same trend, although these were not shown to be significant. Increased levels of the endocannabinoids can either be due to increased synthesis or the levels to be influenced by decreased metabolism. Increased synthesis could involve NAPE-phospholipase D (NAPE-PLD), which generates AEA, OEA and PEA from their precursors, N-arachidonoyl phosphatidylethanolamine (NArPE), N-oleoyl phosphatidylethanolamine or N-palmitoyl phosphatidylethanolamine respectively, or through alternative synthetic pathways (Sagar et al 2009). However, this cannot be confirmed as none of these precursors mentioned are measured with this LC-MS/MS analytical method. We also know that 15-LOX can metabolise AEA and 2-AG to 15-hydroperoxyeicosatetraenoic acid-ethanolamide (15-HPETE-EA) and 15-hydroperoxyeicosatetraenoic acid-glycerol (15-HPETE-G) respectively. 15-LOX oxidation of AEA has been shown to produce 15-HPETE-EA *in vitro* and *in vivo* (Khairy and Houssen 2010). By blocking this metabolic pathway with PD 146176, we may potentially increase the levels of AEA and 2-AG.

4.4.2 Effects of 2% carrageenan on lipid levels, inflammation and hyperalgesia

4.4.2.1 Effects of 2% carrageenan on lipid levels at one hour and four hours

The effects of 2% carrageenan on lipids levels was investigated on the basis that changes in lipid levels may occur at an earlier timepoint. Levels of the LOX metabolites 9-, 13-HODE, 9- and 13-oxoODE were all decreased in the one hour carrageenan-treated hindpaw tissue compared with saline-treated controls; 12-HETE, linoleic acid and TXB_2 were also found decreased, while arachidonic acid and PGD_2/PGE_2 remained unchanged. 5- and 11-HETE both did not alter significantly at one hour. The endocannabinoids 2-AG, PEA and OEA decreased significantly, AEA also followed this trend, but was not significant at this one hour time-point.

Levels of the 15-LOX metabolites 9- and 13-HODE were found to decrease significantly in the ipsilateral hindpaw following carrageenan administration at four hours; which was not as prominent at one hour. These data are consistent with earlier reports that levels of 13-HODE are reduced in synovial fluid in carrageenan-induced knee arthritis (Herlin et al 1988). This trend was also observed with the oxidation products of the HODEs, 9- and 13-oxoODE in the ipsilateral hindpaw, which was significant for 9-oxoODE at the four hour timepoint. All four 15-LOX metabolites have been shown to activate TPRV1 receptors (Patwardhan et al 2010). This decrease in 15-LOX metabolites was accompanied by an increase in linoleic acid levels in the ipsilateral hindpaw. Linoleic acid increased by nearly 2-fold, in the carrageenan-treated rats compared to saline. Since linoleic acid is an essential fatty acid that is only available from the diet, reduced metabolism could explain the increase in linoleic acid observed at four hours. If indeed metabolism in the hindpaw at this time-point is decreased, we would expect to see a decrease in the levels of linoleic acid metabolites, which is confirmed by the significant reduction of 9- and 13-HODE and decreased 9- and 13-oxoODE levels.

TXB_2 also increased significantly in the carrageenan-treated rats compared to saline while arachidonic acid and PGD_2/PGE_2, along with 5-, 11- and 12-HETE levels remained unchanged at four hours. The elevation in TXB_2 observed at four hours is consistent with previous reports that this is due to increased expression of COX-2 in peripheral inflammation. COX-2 mRNA was measured using real time quantitative PCR and was found to be elevated in inflamed hindpaws. Western blot analysis also measured an increase in COX-2 protein at 3 hours post-carrageenan injection (Guay et al 2004). Levels of PGD_2/PGE_2 remained unchanged at this four hour time-point. Previous reports have shown that levels of PGE_2 monitored for 24 hours post-carrageenan remained unchanged between 1 to 6 hours post-carrageenan with a significant increase observed between 6 and 24 hours. This was noticeably different to the transient effects on TXB_2 whose levels returned to baseline after 12 hours (Guay et al 2004). Levels of arachidonic acid also remained unchanged along with other metabolites of this pathway i,e. 5- and 11-HETE at four hours. An increase in the COX-2 metabolite of arachidonic acid, TXB_2, might be expected to be associated with a decrease in arachidonic acid levels. However, the levels remain unchanged suggesting increased synthesis of arachidonic acid from other pathways may compensate for these changes.

As mentioned, 2-AG, OEA and PEA were found to decrease significantly in the carrageenan-treated ipsilateral hindpaws at one hour compared to control, whereas AEA also followed the same trend, but did not reach significance. However, at four hours post-injection, AEA, OEA and PEA decreased significantly in the carrageenan-treated ipsilateral hindpaws. 2-AG levels also followed the same trend but were not significant. 2-AG has previously been shown to decrease significantly in the ipsilateral hindpaw at three hours, which was accompanied by a reduction in levels of AEA, PEA and OEA (Jhaveri et al 2008). These changes suggest either increased metabolism of these lipids or decreased synthesis. AEA is an ethanolamide derivative of arachidonic acid; the level of which does not alter, suggesting alternate pathways of metabolism of AEA. The activities

of FAAH (fatty acid amide hydrolase) and MAGL (monoacyl glycerol lipase) enzymes responsible for the metabolism of AEA and 2-AG respectively, were not shown to differ significantly between carrageenan- and saline-treated rats (Jhaveri et al 2008). However, COX-2, CYP and 15-LOX have all been shown to metabolise AEA and 2-AG which may suggest that increased metabolism of these lipids may occur through these alternative pathways. Interestingly, AEA is also a TRPV1 agonist (Huang et al 2002) and there have been many established papers on the interaction of AEA with TRPV1 in pain pathways (Di Marzo et al 2002, Iverson and Chapman 2002, Rice et al 2002). Along with other TRPV1 agonists, 9- and 13-HODE, which were also shown to decrease significantly in the carrageenan-treated rats, these data suggests involvement of TRPV1 in this model of inflammatory pain.

4.4.2.2 Effects of 2% carrageenan on lipid levels, inflammation and hyperalgesia

The significant changes in a number of lipids measured using LC-MS/MS was also accompanied by inflammation and hyperalgesia observed in the carrageenan-treated rats at four hours. Intraplantar injection of carrageenan resulted in significant hindpaw oedema and hyperalgesia, four hours post-injection. This is consistent with previous studies which have also shown that carrageenan administration into the hindpaw results in increased hindpaw volume, oedema and hyperalgesia at four hours (Thorpe et al 2011, Pabreja et al 2010). This significant change in hindpaw volume and hindpaw diameter was also observed in the rats one hour post-carrageenan injection. Pro-inflammatory agents are generated *in situ* at the site of injury or by infiltrating cells. These include bradykinin, tachykinins, histamine, reactive oxygen and nitrogen species and complements (Morris 2003). Recently, it has been suggested that histamine release sensitises acid-induced responses through TRPV1 activation via the coupling of the histamine-1 receptor to the phospholipase C / protein kinase C pathway (Kajihara et al 2010). During inflammation, the extracellular pH decreases and this tissue acidosis is at least partially responsible for the hyperalgesia observed. TPRV1 receptors

which are activated by protons are highly expressed in sensory neurons and are important in nociception and pain perception. Mice lacking TRPV1 receptors show signs of impaired nociception and several TRPV1 antagonists are shown to attenuate hyperalgesia *in vivo* (Kajihara et al 2010, Caterina et al 2000). Reactive oxygen species (ROS) such as hydrogen peroxide are also produced during inflammation at the affected site and increased levels of this were found to be significantly raised in the carrageenan-induced inflamed hindpaw (Keeble et al 2009). This evidence along with significant changes in lipid levels of TRPV1 agonists, may suggest involvement of TRPV1 in this model of inflammatory pain.

4.4.3 Effects of selective 15-lipoxygenase inhibition on lipid levels, inflammation and hyperalgesia

Selective 15-LOX inhibition with PD 146176 pre-treatment (50µg /50µl) was shown to significantly attenuate hyperalgesia at four hours post-carrageenan administration; however PD 146176 did not have any effect on inflammation, which was reflected by the lack of change in hindpaw volume and hindpaw circumference between PD 146176-treated and vehicle-treated rats. The precursor of the 15-LOX metabolites, linoleic acid, is largely distributed in membrane phospholipids (Banni et al 2001), whereas 15-LOX is present in the cytosol (Spanbroek et al 2001). Importantly, in sensory nerve processing of noxious inputs, increases in intracellular Ca^{2+} produces a translocation of 15-LOX to the plasma membrane (Andersson et al 2006), increasing substrate availability and possibly favouring the generation of 15-LOX metabolites. Thus, if this Ca^{2+}-mobilising stimuli in sensory nerves may lead to HODE and oxoODE generation, then activation of TRPV1 channels may occur, followed by further influx of intracellular calcium. In this context, conversion of linoleic acid to HODEs and oxoODEs may act as an amplifying mechanism to enhance nociceptive stimuli, in a similar manner as proposed for the endocannabinoid anandamide (van der Stelt et al 2005). However, PD 146176 was not shown to have any effect on the carrageenan-induced changes in lipid levels at both timepoints measured and may therefore add value to the hypothesis that the levels of HODEs and oxoODEs are

affected by physiological processes such as oxidative stress as these changes are observed *in vitro* but not *in vivo*.

We hypothesised that a decrease in 15-LOX metabolites such as 9-, 13-HODE, 9-, 13-oxoODE would be found in the PD 146176-treated rats, yet this was not the case. A decrease in HODE and oxoODE levels through 15-LOX inhibition was not observed at this four hour time-point, suggesting the analgesia seen in these rats is not due to a change in 15-LOX metabolite levels. However, there may be a number of factors that may explain the reason for these observations. First, the change in these metabolites may be transient and one of the main limitations of LC-MS/MS is to be able to find the exact time-point for tissue collection and to capture this "snapshot moment " to show these changes occur, which can be extremely difficult. Second, all the lipids present in the whole section of hindpaw tissue collected are extracted so we are unable to differentiate as to whether these lipids are intracellular or extracellular or the cells involved in the production of these lipids. Measurements in the inflamed hindpaw may reflect the most abundant cells, in this case the epidermis rather than the sensory nerves and activated immune cells. Therefore subtle changes in levels of the bioactive lipids that may explain the attenuation of pain behaviour through 15-LOX inhibition by PD 146176 may not be detectable. Finally, HODEs are the stable oxidation products of linoleic acid, the generation of which is increased in oxidative stress, such as atherosclerosis and other inflammatory conditions (Vangeveti et al 2010, Banni et al 2002). At the four hour time-point, there was a significant amount of oedema and therefore pronounced inflammation, which would possibly increase the production of the HODEs, which can also be generated through non-enzymatic oxidation of linoleic acid (Vangaveti et al 2010). Although we have, in this study, inhibited 15-LOX with PD 146176, the production of these lipids can also be generated via alterative pathways. We know 9- and 13-HODE can be generated enzymatically by 15-LOX and this occurs in some tissues (Baer et al 1991, Daret et al 1989) or they can be formed spontaneously via

free radical generation (Yoshida et al 2006), which may explain these observations.

4.4.4 Effects of 9- and 13-HODE neutralisation on lipid levels, inflammation and hyperalgesia

Intraplantar administration of the antibodies of 9- and 13-HODE significantly reduced the carrageenan-induced difference in weight bearing, attenuating hyperalgesia but had no effect on hindpaw oedema and inflammation at the four hour time-point. The effects observed with the antibodies mimicked those seen with selective 15-LOX inhibition. These data provide the first evidence that 9- and 13-HODE may have an endogenous role in the peripheral mechanisms of inflammatory hyperalgesia and that 15-LOX may contribute to their generation, although, 15-LOX involvement was shown only *in vitro*. These data are also consistent with the demonstration that local hindpaw neutralisation of 9- and 13-HODE with anti-9- and 13-HODE antibodies attenuates thermal nociception (Patwardhan et al 2009) and that spinal administration of anti 9- and 13-HODE antibodies attenuates CFA evoked mechanical allodynia (Patwardhan et al 2010). However, co-administration of the 9- and 13-HODE antibodies failed to prevent any of the carrageenan-induced changes in lipid levels in the hindpaw tissue at the four hour time point, again, mimicking the majority of the trends observed following 15-LOX inhibition. This included similar trends observed for the 15-LOX metabolites; HODEs and oxoODES, linoleic acid and the endocannabinoids. These data also adds further value to the hypothesis that the levels of HODEs and oxoODEs are affected by physiological processes *in vivo*, and that changes, if any, in these lipid levels may be transient and would require further investigation.

4.5 Conclusions

Two independent studies investigating effects of 15-LOX enzyme inhibition and neutralisation of the HODEs, both showed significant attenuation of hyperalgesia in the carrageenan inflammatory model, which was not coupled to changes in inflammation or lipid levels

measured. This physiological effect was observed in both cases, but we could not relate this to a change in the 15-LOX metabolites measured. Investigation at an earlier time-point also did not show any modulating effects of PD 146176 on linoleic acid and its 15-LOX metabolites *in vivo*. A significant reduction in the 15-LOX metabolites 9- and 13-HODE was observed *in vitro* in DRG neurons, which was shown to be time-dependent. Thus 15-LOX inhibition has been shown to be analgesic, but not anti-inflammatory, which may be due to transient blockade of pro-inflammatory mediators such as the HODEs acting via TRPV1 pro-nociceptive channels. Further work may be required to determine whether these lipids alter *in vivo* under other inflammatory conditions and to further establish the therapeutic potential of 15-LOX as a target for inflammatory pain responses.

Chapter 5.

Investigating the pain behaviour and the lipid profile of different tissues in a rat model of osteoarthritis

5.1 Introduction

5.1.1 Osteoarthritis

Osteoarthritis is a condition that affects the synovial joints and is characterised pathologically by damage in focal areas to articular cartilage involving the load-bearing areas. It is also associated with new bone formation at the joint margins (osteophytosis), variable degrees of mild synovitis, changes in the subchondral bone and thickening of the joint capsule (See references in Dieppe and Lohmander 2005). These biomechanical and biochemical joint changes and the failure of the repair process of damaged cartilage are characteristics of OA (Bijlsma et al 2011). Cartilage is non-vascularised and the supply of nutrients and oxygen to the chondrocytes (cells responsible for maintenance of a large extracellular matrix) is restricted (Bijlsma et al 2011). Initially, clusters of chondrocytes form in the damaged areas of the joint in an attempt to repair and increases the concentration of growth factors in the matrix (Aurich et al 2005). Increased synthesis of tissue-destructive proteinases such as matrix metalloproteinases (MMPs, Baragi et al 2009), coupled with inadequate matrix component synthesis, lead to a matrix incapable of withstanding normal mechanical stresses (Bijlsma et al 2011). A vicious cycle of synthesis and degradation of chondrocyte clusters ends in an inbalance which ultimately leads to degradation of the extracellular matrix (Bijlsma et al 2011).

The pathology of osteoarthritis has long been thought to be cartilage-driven; however, recent evidence shows the involvement of bone and synovial tissue (See references in Bijlsma et al 2011). Synovial macrophages produce catabolic and pro-inflammatory mediators during the inflammatory process, which negatively impacts on the balance of degradation and repair of the extracellular matrix. This amplifies synovial inflammation, which is linked to joint swelling and inflammatory hyperalgesia (See references in Bijlsma et al 2011). In synovitis, overproduction of cytokines and growth factors, in particular, tumour necrosis factor alpha (TNF-α) and interleukin-1 (IL-1, Bondeson et al

2006) may contribute to the pathophysiology of OA. Both are thought to be key cytokines in synovial inflammation and activation of chondrocytes (Fernandes et al 2002), driving their own production and inducing synovial cell and chondrocyte production of IL-6, IL-8, leukocyte inhibitory factor, proteases and prostaglandins (Bondeson et al 2006). These mediators, released from the synovium, bone and other tissues induce sensitisation of articular nociceptors, which are not confined to the periphery. Pain perception at the site of injury is enhanced, along with the development of pain and tenderness in normal tissues adjacent to and distant from the primary site. In OA patients, spinal nociceptive processing is under the influence of descending inhibitory controls and inputs from other somatic structures (Kidd et al 2007).

5.1.2 Molecular pathways in OA pain

Chronic pain is often associated with osteoarthritis and the mechanisms underlying this are known to be complex; however, recent developments have led to improved understanding of molecular pathways in OA pain (Sofat et al 2011). Ongoing joint destruction is known to occur in OA (Dieppe and Lohmander 2005) including osteophyte and subchondral cyst formation and bone sclerosis, which may impair joint motility and induce pain (Sofat et al 2011). Physiological mechanisms of pain operate at different levels; locally in the joint, in the dorsal root ganglia (DRG) and in higher brain processing centres. As stated earlier, pro-inflammatory mediators released into the OA joint can cause localised damage to tissues such as the synovium and activate peripheral nociceptors (Sofat et al 2011, Kidd et al 2007). During chronic activation, the nociceptive system becomes sensitised, leading to hyperalgesia (heightened sensitivity to noxious stimuli), and allodynia (pain in response to non-noxious stimuli; Bolay and Moskowitz 2002). Nociceptor activation is transmitted via the DRG, up through the spinothalamic tract to higher cortical centres where signals are processed and perceived as pain (Woolf 2004). Mediators of pain at the DRG level in OA include calcitonin gene-related peptide (CGRP), nerve growth factor (NGF) and transient receptor potential cation channel subfamily V member 1 (TRPV1; Schuelert et al

2010). In the brain, chemical mediators of pain include substance P, glutamate and serotonin (Niissalo et al 2002). Additionally, ion channel-linked receptors on sensory afferent neurons are activated by primary sensory neurons stimulated by prostaglandins, bradykinin and CGRP, including heat-sensitive TRPV1 (Sofat et al 2011). Changes in joint temperature during chronic inflammation may also activate this particular receptor (Sofat et al 2011).

Another phenomenon, central sensitisation, has also been shown to be a component of OA pain with evidence relating to models of musculoskeletal pain suggesting that OA is associated with enhanced nociceptive transmission at the dorsal horn and secondary hyperalgesia (Pinto et al 2007, Naeini et al 2005). Central sensitisation consists of several components; increased response to input from an injured or inflamed region, increased response from regions adjacent to or remote from the injured/inflamed region and expansion of the receptive field of the spinal cord neuron (Schaible et al 2006). It is also widely appreciated that the descending pain pathways directly modulate nociceptive processing in the dorsal horn (Tracey and Mantyh 2007). In chronic pain states, in which central sensitisation is a component, descending facilitation is thought to play a pivotal role in its maintenance (Suzuki and Dickenson 2005, Gebhart 2004). Recently, evidence has emerged that central sensitisation occurs in humans (Gwilym et al 2009, Lee et al 2008). Functional magnetic resonance imaging (fMRI) and quantitative sensory testing (QST) methods were used to identify areas of increased brain activity and analyse psychophysical and behavioural aspects in OA patients. Increased activity was found in the periaqueductal grey and this was associated with stimulation of the skin in referred pain areas of the OA patients (Gwilym et al 2009).

5.1.3 Current treatment for osteoarthritis

In the early stages of osteoarthritis, pain and stiffness of the joints are the most prominent symptoms and treatment is focussed around the reduction of these and maintaining function (Bijilsma et al 2011).

Paracetamol is the recommended analgesic of choice for mild to moderate pain in OA and is generally well tolerated for up to 12 months. Non-steroidal anti-inflammatory drugs (NSAIDs), such as ibuprofen, diclofenac and naproxen have been shown to be highly effective in treating acute pain, (Bijilsma et al 2011). However, over time, the need for stronger analgesics, such as opioids, may be required due to decreased effectiveness and the appearance of side effects associated with the long-term use of NSAIDs (Scott et al 2000). Adverse effects include gastrointestinal bleeding and ulceration, with long-term use leading to gastrointestinal damage and renal irritation (Koeberle and Werz 2009, Scott et al 2000). Currently there are no treatments that delay the onset of OA or repair joint damage and, for this reason coupled with inadequate analgesic medication, novel targets are under investigation.

5.1.4 Models of OA pain

Studies using models of knee joint pathology are important tools for understanding the mechanisms underlying osteoarthritis and also to investigate new potential targets of treatment. Biochemical, cell or organ culture models can only provide information on short-term biological events within cartilage, bone, synovium or selective cells investigated. *In vitro* models are not able to simulate the structural and biochemical processes that occur within these joint tissues over time. Animal models of OA are, therefore, required to study complex changes in the joint tissues that evolve over time and other factors such as the environment which may have an effect (Pritzker 1994). There are two classes of animal models of OA in use; spontaneous or naturally occurring disease models and experimentally-induced models. Relevance, availability and appropriateness are considered when deciding on the choice of animal model. This includes how comparable the animal model is to the human form of the disease and depending on the objectives of the study, the simplicity and reproducibility of the model. Practical factors such as animal supply, maintenance of controlled environments, cost and ease of handling are also considered (Neugebauer 2007, Pritzker 1994).

5.1.4.1 Spontaneous disease models

Spontaneous OA occurs in a number of different animals such as guinea pigs, non-human primates, Syrian hamsters and mice. The OA model in Duncan-Hartley guinea pigs is well characterised; damage occurs in the medial joint compartment of male and female guinea pigs, although pathological alterations are more consistent in males (Little and Smith 2008, Bendele 2001). Spontaneous OA in the knee joints has also been described in non-human primates; however, variability in the severity of lesions, availability of adequate animal numbers and ethical issues are disadvantages of employing these animals (Bendele 2001). Syrian hamsters (Silberberg et al 1952) and mice are also used as spontaneous OA models, although the cartilage layers are less substantial compared to larger species and are more difficult to analyse for cartilage degeneration (Bendele 2001).

5.1.4.2 Experimentally-induced models

Models of OA can be experimentally-induced either surgically or chemically. A unilateral medial meniscal tear in 300-400g rats, where the meniscus is cut at the narrowest point, results in chondrocyte and proteoglycan loss, osteophyte formation and chondrocyte cloning. Progressive cartilage degeneration occurs where the lesions are morphologically similar to the human disease, but occurs much more rapidly (Bendele 2001). This surgical procedure can also be performed in guinea pigs and, since spontaneous OA occurs in this species, the non-operated joint can also be used to evaluate the model (Little and Smith 2008, Bendele 2001). Rabbits and dogs have also been used; both species, especially rabbits attempt to regenerate the transected meniscus with fibrous tissue after the procedure (Bendele 2001). The main disadvantage of this technique is that the onset and severity of the disease caused by transection is usually much higher than that observed in humans (Little and Smith 2008). Transection of the anterior cruciate ligament can result in a lesion which mimics naturally occuring OA in dogs or in humans following traumatic injury. However, this model of OA

progression requires extended periods of time and is more suitable for investigating OA of slow progression and representative of the condition in humans (Bendele 2001). Subcutaneous administration of naladixic acid 350mg/kg (quinolone antibiotic) in guinea pigs causes a characteristic blister-like lesion in the mid-zone cartilage, in which degenerative changes are observed 24 hours post-administration (Bendele 2001). Pathological changes can also be induced via intra-articular injection of enzymes (papain, collagenase, trypsin, hyaluronidase) cytokines (interleukin-1, transforming growth factor-β) and chemicals (monosodium iodoacetate). Many of these agents induce significant acute local inflammation at the site of injection and may not replicate the naturally occurring disease process of OA observed in humans (Little and Smith 2008, Bendele 2001).

The monosodium iodoacetate (MIA) model has emerged as a particularly useful model of OA pain as it is reproducible and mimics the histopathological changes and pain observed in human OA (Barve et al 2007). Intra-articular injection of MIA inhibits glycolysis and causes chondrocyte necrosis, resulting in decreased articular cartilage thickness and fibrillation of the cartilage surface (Little and Smith 2008). This separates the necrotic cartilage from the underlying bone, exposing the subchondral bone, resulting in osteolysis and swelling of the joint (Little and Smith 2008, Neugebauer 2007). Advantages of using rats are the rapid speed of onset of the disease, easy management, low cost and ease of performing surgical procedures (Little and Smith 2008). Rats are also a species with virtually no spontaneous knee OA, so the lesions observed are usually due to the procedure performed (Bendele 2001).

5.1.5 MIA model of OA and measurement of lipids

The majority of OA animal model experiments have investigated the pathophysiology and progression of joint damage and have incorporated characterisation of pain behaviour (Orita et al 2011, Schuelert et al 2011, Takeshita et al 2011, Chu et al 2011, Ferland et al 2011, Im et al 2010, Yoshimi et al 2010, Puttfarcken et al 2010, Baragi et al 2009, Chandran

et al 2009, Clements et al 2009, Prochazkova et al 2009, Pulichino et al 2006). The MIA model of OA, in particular, is commonly used because the pathological changes induced by the monosodium iodoacetate injection share many similarities with human OA (Guzman et al 2003). The injection also leads to chronic degeneration of the joint associated with chronic pain behaviour and alteration in hind limb weight bearing (Pomonis et al 2005, Guzman et al 2003). The severity of the disease can also be easily manipulated by varying the concentration of monoiodoacetate injected, and the rapid induction of disease (28 day model) in the rats allows evaluation of pain modifying compounds (Pomonis et al 2005). At post-operative (PO) day 7 as a result of intra-articular injection of MIA, mild synovial membrane hyperplasia and sub-synovial fibroplasia are known to occur (Clements et al 2009). To a lesser extent, patellar cartilage necrosis, chondroplasia and bone necrosis have also been shown to occur at this timepoint (Clements et al 2009). The extent of cartilage damage at this time-point is characterised by loss of chondrocytes, with thinning and complete collapse of the cartilaginous matrix. Bone lesions consistent with bone resorption also begin to develop within 7 days of MIA injection (Guzman et al 2003). In addition to further progression of the histological and pathological changes seen at PO day 7 and 14, sub-synovial fibroplasia and fibrosis, patellar chondral fragmentation and disintegration of necrotic subchondral bone are observed at PO day 21, with further progression at PO day 28 (Clements et al 2009).

Progressive tactile allodynia and elevated cytokine concentrations have been observed in MIA-treated Sprague-Dawley rats (Orita et al 2011, Im et al 2010). Allodynia was detectable in all MIA-treated rats 7 days post-injection, and was also accompanied by a change in hind limb weight distribution, with the greatest effects observed between day 14 and 42 post-injection (Combe et al 2004).

Several pain-modifying compounds have been tested in the MIA model due to links with the cannabinoid and TRPV1 pathways (Sagar et al 2010, Schuelert et al 2008). Systemic administration of the FAAH inhibitor

URB597 significantly reduced hind limb incapacitance in MIA-treated animals, which was abolished by co-administration of a CB_1 antagonist AM251 (Schuelert et al 2011). Grip force deficit was also shown to improve following systemic administration of the selective TRPV1 receptor antagonist A-889425 (Chu et al 2011). Another area of research involves studies that identify target molecules involved in OA onset and progression, and these have focussed on genomic and proteomic profiling of synovial fluids (Gobezie et al 2007) and cartilage (Iliopoulos et al 2008, Ijiri et al 2008). However, to date, there has been little focus on the bioactive lipids involved in OA, which has a strong inflammatory and pain component. *In vitro* genomic and proteomic profiling of tissues was able to show certain classes of molecules to be differentially expressed in OA, but the scope was limited (Goldring et al 2011). Also, the mechanisms underlying the development of OA and pain are still poorly understood and current drug treatments are not targeted to a specific mechanism. It is clear that the changes in sensory input in the joint are critical in driving the disease and many bioactive lipids have either pro- or anti-inflammatory actions. The ability to monitor and measure the changes in these bioactive lipids may lead to identification of potential targets for OA pain and highlight key enzymatic pathways.

5.1.6 Aims and Objectives

- To investigate the effects of intra-articular injection of monosodium iodoacetate (MIA) on pain behaviour in rats
- To identify and measure pro- and anti-inflammatory mediators in different tissues in the MIA rat model
- To determine whether any effects on pain behaviour observed are associated with changes in the levels of measured lipids in the spinal cord, dorsal root ganglia (DRGs), knee joint, plasma and brain regions

5.2 Methods

5.2.1 Animals

Experiments were performed on male Sprague Dawley rats (130-150g Charles River, UK) in accordance with the UK Scientific Procedures Act (1986). All procedures were approved by the University of Nottingham Ethical Review Committee and IASP guidelines. All animals were group-housed in a temperature-controlled environment (22°C ± 1°C) and maintained on a 12 hour light/dark cycle with access to food and water *ad libitum*.

5.2.2 Intra-articular injections

This procedure was carried out by Dr Devi Rani Sagar.

Rats were anaesthetised with isoflurane / N_2O / O_2 (1.5-2% in 66% N_2O and 33% O_2) before receiving an intra-articular injection of either monosodium iodoacetate (MIA, 1mg / 50 µL) in saline or 50 µL of saline (control) through the infra-patellar ligament of the left knee. The dose of MIA received by the rats was based on previous work within the group and on the published literature (Pomonis et al 2005, Bove et al 2003, Kobayashi et al 2003). The rats were then weighed, placed in individual cages and allowed to recover in a suitable environment (correct temperature, lighting and minimal noise). The animals were then monitored throughout the following 28-day period.

5.2.3 Pain behaviour testing

The following procedures were carried out by Dr Bright Okine.

After receiving the intra-articular injections, rats were kept under the same conditions as described earlier (see Animals). The animals were carefully monitored following recovery from the first post-operative (PO) day, when they were weighed following the measurement of pain behaviour. The general behaviour of all the rats was also monitored throughout the period of the study. Baseline values for weight-bearing

and von Frey behavioural testing were taken prior to the intra-articular injection (PO day 0). Pain behaviour testing was then conducted 3 days post-injection (PO day 3), 7 days post-injection (PO day 7), 14 days post-injection (PO day 14), 21 days post-injection (PO day 21) and 28 days post injection (PO day 28).

5.2.3.1 Weight Bearing

Weight bearing measurements using an Incapacitance Tester (Linton Instrumentation, UK) were performed to examine the effects of the MIA injection on weight distribution between the left (ipsilateral) and the right (contralateral) knee. Measurements were taken on PO day 0, PO day 3, PO day 7, PO day 14, PO day 21 and PO day 28, following the intra-articular injection, using the methods previously described in Chapter 4.

5.2.3.2 Von Frey testing

Pain behaviour was also tested using von Frey monofilaments (Semmes-Weinstein monofilaments, applied bending forces used 0.6, 1.0, 1.4, 2.0, 4.0, 6.0, 6.0, 10.0 and 15.0 g). This test measured the withdrawal threshold to a mechanical stimulus (von Frey monofilaments); a decrease in withdrawal threshold is indicative of mechanical allodynia. The development of mechanical allodynia over the time course measured was also monitored. Measurements were taken PO day 0, PO day 3, PO day 7, PO day 14, PO day 21 and PO day 28, following the intra-articular injection. Rats were placed in plastic transparent cubicles containing a mesh floor and allowed to acclimatise to the environment before testing commenced. Application of von Frey microfilaments in ascending order of bending force to the plantar surface of the left and right hindpaws of each rat tested lasted for a period of three seconds per microfilament, until a withdrawal reflex was observed. The hindpaw was then re-tested with the von Frey microfilament at a lower force (the next lowest microfilament) to check that no response occurs. The lowest force required to produce a withdrawal reflex was recorded for both the left and the right hindpaw, this is known as the paw withdrawal threshold.

5.2.4 LC-MS/MS Analysis of lipids

On PO day 28, following the last set of pain behaviour tests, the animals were killed by stunning and decapitation by Professor David Kendall. Dissection of the spinal cord (ipsilateral and contralateral) by Dr James Burston, dorsal root ganglia (DRGs, ipsilateral and contralateral) by Paul Millns, knee joint (ipsilateral and contralateral) and brain regions (frontal cortex, hippocampus, midbrain, rest of cortex and rest of brain) by Professor David Kendall and were frozen immediately in liquid nitrogen. Blood was also collected from these rats, centrifuged and the plasma frozen immediately in liquid nitrogen. All samples were stored at -80°C until needed. The samples were then extracted and analysed following the methods detailed in Chapter 2.

5.2.5 Data Analysis

For the studies measuring weight-bearing, differences are presented as means ± SEM; statistical analysis was performed using one-way ANOVA and a Bonferonni *post hoc* test. LC-MS/MS data are expressed as mean ± SEM, statistical analysis was performed with a Mann Whitney test.

Principal component analysis (PCA) was used for further data processing (See Chapter 2 for details). PCA was performed by importing the levels of each individual lipid measured from different tissue types from Microsoft Excel into the SIMCA-P software package (Version 11, Umetrics AB, Umea, Sweden). Data were reduced to two latent variables (or principle components) that will describe the maximum variation within the data (Law et al 2008) to create a two-component model expressed as scores and loadings plots. The principle components obtained from the scores highlighted clusters, trends and outliers within the dataset.

5.3 Results

5.3.1 Effect of saline injection on pain behaviour in rats

Differences in weight distribution between ipsilateral and contralateral hindpaws and hindpaw withdrawal threshold in rats were monitored for 28 days (see methods), during which baseline values were recorded pre-saline or MIA intra-articular injection (Figure 1). Intra-articular injection of saline did not alter weight distribution (Figure 1a) or hindpaw withdrawal thresholds in the ipsilateral hind limb (Figure 1b) and contralateral hind limb (data not shown).

5.3.2 Effect of MIA injection on pain behaviour in rats

Intra-articular injection of 1 mg MIA significantly decreased weight bearing on the ipsilateral hind limb ($P<0.01$ for day 7 and 14; $P<0.001$ for day 21 and 28) compared to saline-treated rats (Figure 1a). Intra-articular injection of MIA also significantly decreased hindpaw withdrawal thresholds to mechanical punctuate stimulation at day 21 and 28 ($P<0.01$) compared to saline-treated rats (Figure 1b). Intra-articular injection of MIA did not alter contralateral hindpaw withdrawal thresholds (data not shown).

a)

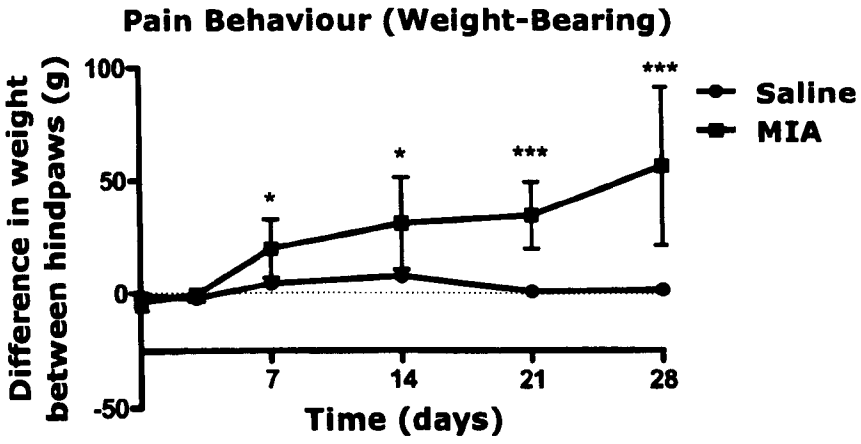

b)

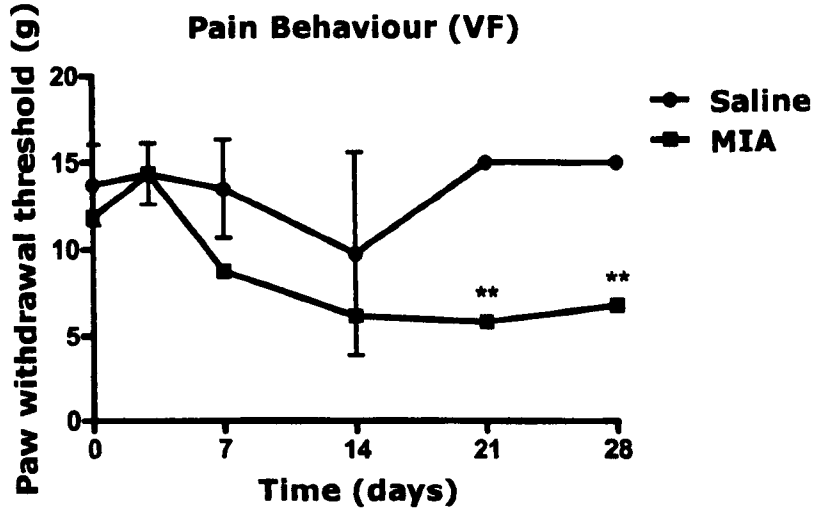

Figure 1. Changes observed in MIA- or saline-treated rats over the 28 day time course in; a) weight distribution between ipsilateral and contralateral hindpaws and b) hindpaw withdrawal threshold to mechanical punctuate stimulation. Statistical analysis comparing weight distribution between ipsilateral and contralateral hindpaws was calculated using an unpaired t test for comparison of saline and MIA, *P<0.05, **P<0.01, ***P<0.001. Statistical analysis comparing hindpaw withdrawal was calculated using a paired t test for comparison of saline and MIA, **P<0.01. Data is expressed as mean ± SEM of differences in weight bearing between ipsilateral and contralateral hindpaws (n=8).

5.3.3 Effects of MIA and saline injection on lipid levels in knee joint, plasma, spinal cord, DRGs and brain regions of rats

Knee joint, plasma, spinal cord, dorsal root ganglia (DRGs; L3-L5) and 5 brain regions: frontal cortex, midbrain, hippocampus, rest of cortex and rest of brain were collected following saline or MIA intra-articular

injection at PO day 28. These samples were analysed using the validated LC-MS/MS method described in Chapter 2, the levels of individual analytes measured are shown in Table 1. The lipids were grouped according to their associated enzyme pathways to enable differences between these groups of lipids to be easily visible. These included the LOX (lipoxygenase) group comprised of 9-, 13-HODE, 9-, 13-oxoODE, 12- and 15-HETE; COX (cyclooxygenase) group of PGD_2/PGE_2 and TXB_2, CYP (cytochrome P450) group of 5-, 8- and 11-HETE, EC group of AEA, OEA, PEA, 2-AG and AraGly and the FA (fatty acid) group of AA and LA.

5.3.3.1 Effects of saline injection on lipid levels in knee joint, plasma, spinal cord, DRGs and brain regions of rats

In saline-treated rats, 5-, 11-, 12-, 15-HETE, AEA, PEA, OEA, 2-AG, PGD_2/PGE_2, TXB_2, AA, LA and 13-HODE were all detected in the knee joint, plasma, DRGs, spinal cord and brain regions. 9-HODE was measured in the knee joint, plasma, DRGs, spinal cord, frontal cortex, rest of cortex and rest of brain. 9- and 13-oxoODE were measured in the knee joint and plasma. 8-HETE was measured in the knee joint, plasma and brain regions (Table 1). Intra-articular injection of saline did not alter lipid levels between ipsilateral and contralateral knee joints, DRGs and spinal cords (Appendices: Table 4). In saline-treated rats, the majority of the total lipid measured consisted of AA: knee joint (97%); plasma (98%); DRGs (98%); spinal cord (87%); brain (97-99%) (Table 1). In saline-treated rats, levels of 2-AG also comprised a large proportion of the total lipid, particularly in the spinal cord (13%, Table 1). Therefore, both lipids were excluded from the graphs, to show a clearer distribution of the other lipids in the tissues.

Table 1.

		Knee Joint		DRGs (L3-L5)		Spinal Cord		Frontal Cortex		Midbrain		Hippocampus		Rest of Cortex		Rest of Brain		Plasma	
		Saline	MIA	Saline	MIA	Saline	MIA	Saline	MIA	Saline	MIA	Saline	MIA	Saline	MIA	Saline	MIA	Saline	MIA
COX	PGD2/ PGE2	39 ± 5	43 ± 3	270 ± 100	187 ± 42	30 ± 6	33 ± 9	27 ± 5	30 ± 6	19 ± 5	18 ± 2	14 ± 1	13 ± 2	32 ± 4	28 ± 1	13 ± 1	15 ± 2	2 ± 1	3 ± 0.5
	TXB2	8 ± 1	9 ± 1	190 ± 68	218 ± 45	53 ± 5	61 ± 18	7 ± 2	9 ± 3	7 ± 1	7 ± 1	5 ± 2	3 ± 1	7 ± 1	6 ± 1	9 ± 1	11 ± 2	5 ± 2	7 ± 3
LOX	13-HODE	49 ± 7	61 ± 7	86 ± 29	95 ± 36	4 ± 1	2.5 ± 1.6	0.6 ± 0.1	1 ± 0.3	1 ± 0.3	0.6 ± 0.1	0.7 ± 0.1	1 ± 0.2	1 ± 0.6	2 ± 0.5	2 ± 0.3	2 ± 0.3	6 ± 0.7	8 ± 1
	9-HODE	19 ± 4	22 ± 4	86 ± 34	79 ± 21	4 ± 1	2.7 ± 2.6	0.5 ± 0.2	1 ± 0.3	BLOQ	0.4 ± 0.2	BLOQ	0.5 ± 0.2	1 ± 0.3	1 ± 0.1	1 ± 0.1	1 ± 0.1	3 ± 0.4	3 ± 0.5
	13-oxoODE	0.4 ± 0.1	0.5 ± 0.1	ND	37 ± 16	ND	ND	ND	ND	ND	ND	ND	ND	ND	ND	ND	ND	0.3 ± 0.1	0.4 ± 0.1
	9-oxoODE	0.5 ± 0.1	0.5 ± 0.1	ND	ND	ND	ND	ND	ND	ND	ND	ND	ND	ND	ND	ND	ND	0.5 ± 0.1	0.5 ± 0.1
	15-HETE	6 ± 1	11 ± 2	5 ± 2	31 ± 12	4 ± 2	BLOQ	1 ± 0.2	2 ± 0.3	1 ± 0.1	0.6 ± 0.1	1 ± 0.2	1 ± 0.3	1 ± 0.1	1 ± 0.1	1 ± 0.1	1 ± 0.1	0.6 ± 0.1	1 ± 0.3
	12-HETE	10 ± 1	23 ± 5	262 ± 67	428 ± 144	16 ± 2	17 ± 4	3 ± 1	4 ± 1	5 ± 1	6 ± 2	3 ± 1	4 ± 1	3 ± 0.5	4 ± 1	7 ± 1	8 ± 2	8 ± 3	25 ± 8
CYP	11-HETE	4 ± 0.5	4 ± 0.4	40 ± 20	39 ± 11	14 ± 1	18 ± 4	2 ± 0.3	5 ± 2	1 ± 0.1	1 ± 0.1	1 ± 0.6	1 ± 0.1	2 ± 1	1 ± 0.2	1 ± 0.4	1 ± 0.5	2 ± 0.4	2 ± 0.7
	8-HETE	1 ± 0.2	1 ± 0.3	BLOQ	BLOQ	BLOQ	BLOQ	0.3 ± 0.1	0.5 ± 0.2	0.2 ± 0.1	0.3 ± 0.1	0.2 ± 0.1	0.3 ± 0.1	0.3 ± 0.1	0.2 ± 0.1	0.2 ± 0.1	0.3 ± 0.1	0.1 ± 0.03	0.1 ± 0.03
	5-HETE	1 ± 0.2	1 ± 0.1	10 ± 5	18 ± 6	2 ± 1	2 ± 1	1 ± 0.1	1 ± 0.2	1 ± 0.1	1 ± 0.1	0.6 ± 0.1	0.6 ± 0.1	0.5 ± 0.1	0.5 ± 0.1	0.5 ± 0.1	0.6 ± 0.1	0.3 ± 0.02	0.4 ± 0.1
EC	AraGly	0.1 ± 0.02	0.1 ± 0.02	BLOQ	BLOQ	13 ± 3	18 ± 8	0.5 ± 0.1	0.5 ± 0.1	0.6 ± 0.1	0.7 ± 0.1	0.7 ± 0.3	0.7 ± 0.2	0.8 ± 0.1	0.8 ± 0.1	0.6 ± 0.1	0.7 ± 0.1	0.02 ± 0.002	0.03 ± 0.003
	AEA	2 ± 0.4	2 ± 0.3	14 ± 6	13 ± 4	9 ± 1	21 ± 11	6 ± 1	5 ± 0.3	6 ± 1	5 ± 0.5	6 ± 1	5 ± 0.5	5 ± 0.5	4 ± 0.3	4 ± 1	4 ± 0.5	0.7 ± 0.1	0.7 ± 0.1
	2-AG	1 ± 0.2	1 ± 0.1	4 ± 1	3 ± 1	24 ± 3	24 ± 3	4 ± 0.3	4 ± 1	11 ± 1	10 ± 1	9 ± 1	7 ± 0.5	5 ± 0.5	4 ± 0.3	5 ± 0.5	6 ± 0.6	31 ± 0.3	43 ± 8
	PEA	6 ± 0.5	6 ± 1	323 ± 93	163 ± 49	176 ± 22	299 ± 65	46 ± 7	40 ± 9	47 ± 9	55 ± 5	33 ± 5	32 ± 4	16 ± 2	17 ± 2	18 ± 3	19 ± 2	3 ± 0.3	3 ± 0.4
	OEA	4 ± 0.4	4 ± 0.5	122 ± 35	79 ± 24	128 ± 14	184 ± 39	35 ± 5	31 ± 5	41 ± 9	44 ± 3	26 ± 4	21 ± 2	15 ± 2	15 ± 2	19 ± 2	19 ± 2	5 ± 0.5	5 ± 0.3
FA	LA	480 ± 61	471 ± 36	230 ± 82	303 ± 95	154 ± 14	135 ± 19	63 ± 11	49 ± 6	60 ± 15	55 ± 9	41 ± 9	39 ± 9	59 ± 3	51 ± 4	55 ± 5	58 ± 4	332 ± 23	352 ± 32
	AA	44 ± 4	46 ± 3	376 ± 126	261 ± 74	156 ± 28	162 ± 21	328 ± 29	338 ± 18	354 ± 84	318 ± 38	355 ± 35	301 ± 31	285 ± 17	239 ± 20	212 ± 16	233 ± 22	25 ± 1	26 ± 2

Table 1. Levels of lipids measured per g wet tissue weight in the spinal cord, DRGs, knee joint, brain regions; frontal cortex, midbrain, hippocampus, rest of cortex, rest of brain and plasma (n=8). Values are expressed as mean ± SEM in pmol/g for all tissues except AA, which is expressed in nmol/g. Values for plasma are expressed in pmol/mL except AA, which is expressed as nmol/mL. Lipids have also been grouped according to enzymatic pathways and common groups; COX=cycloxygenase, LOX=lipoxygenase, CYP=cytochrome-p450, EC=endocannabinoids and FA=fatty acids.

5.3.3.2 Effects of MIA injection on lipid levels in knee joint, plasma, spinal cord, DRGs and brain regions of rats

In MIA-treated rats, 5-, 11-, 12-HETE, AEA, PEA, OEA, 2-AG, PGD_2/PGE_2, TXB_2, AA, LA, 9- and 13-HODE were all detected in the knee joint, plasma, DRGs, spinal cord and brain regions. 9-oxoODE was measured in the knee joint and plasma. 13-oxoODE was measured in the knee joint, plasma and DRGs. 8-HETE was measured in the knee joint, plasma and brain regions. 15-HETE was measured in the knee joint, plasma, DRGs and brain regions (Table 1).

In MIA-treated rats, the majority of the total amount of lipid measured consisted of AA and 2-AG (Table 1), comparable to saline-treated rats and both lipids were excluded from the graphs, to show a clearer distribution of the other lipids in the tissues.

Principle component analysis (PCA) was used to investigate differences between saline- and MIA-injected rats and for identification of trends and outliers. Each individual sample represented a value from either the MIA- or saline-treated group (variable 1) from a tissue type (variable 2) of the lipid measured (variable 3). As described in Chapter 2, individual points were then mapped in the space spanned by principal components 1 and 2 and colour coded for tissue type (Figure 2). Any variance, or connection between individual points, is clearly mapped into distinct areas of the plot.

In Figure 2.A the scores plot illustrates visible groupings of samples into each distinct tissue type, with separation apparent between knee joint, plasma, DRGs, spinal cord and brain. Individual brain samples measured for the five brain regions; frontal cortex, midbrain, hippocampus, rest of cortex and rest of brain are also clearly grouped together in this plot. The groupings between the different tissue types are consistent with previous work discussed in Chapter 2. The lipids that contribute to the mapping of these samples in the scores plot are shown in the loadings plot (Figure 2.B), which is also consistent with previous work discussed in Chapter 2.

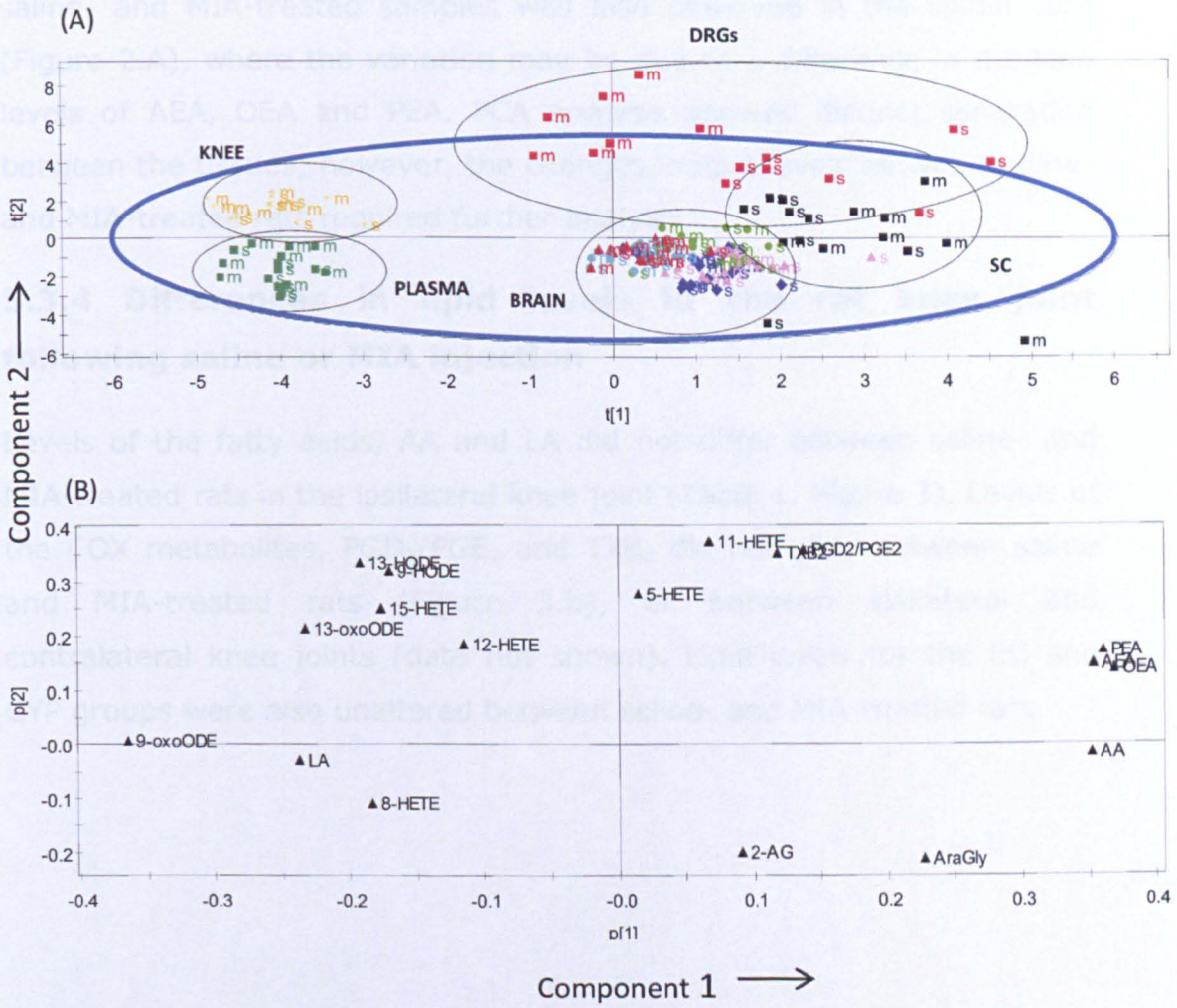

Figure 2. Individual samples were independently analysed using Principle Component Analysis (PCA) to look at variation between samples represented by (A) scores plot of a two-component PCA model of the dataset and (B) loadings plot of the same model dataset. Each sample was colour coded according to tissue type: yellow=knee joint, green=plasma, red=DRGs, black=spinal cord, lime=frontal cortex, blue=hippocampus, purple=midbrain, maroon=rest of cortex and turquoise=rest of brain. These tissue groups have been circled in black for better visualisation. Samples that fit within the 95% confidence interval are included within the blue circle. Each sample was also labelled m=MIA and s=Saline to look at differences between these two treatment groups.

Minimal variation was observed between saline- and MIA-treated samples in the knee joint, plasma and brain regions. There was, however, an obvious disconnection between the saline- and MIA-treated samples in the DRGs (Figure 2.A). This variation may be due to differences in 12- and 15-HETE lipid levels between MIA- and saline-treated groups, and, to

a lesser extent, 5-HETE (Figure 2.B and Table 1). Variation between saline- and MIA-treated samples was also observed in the spinal cord (Figure 2.A), where the variation may be due to a difference in the lipid levels of AEA, OEA and PEA. PCA analysis showed distinct separation between the tissues; however, the changes in lipid levels between saline- and MIA-treated rats required further analysis.

5.3.4 Differences in lipid levels in the rat knee joint following saline or MIA injection

Levels of the fatty acids, AA and LA did not differ between saline- and MIA-treated rats in the ipsilateral knee joint (Table 1, Figure 3). Levels of the COX metabolites, PGD_2/PGE_2 and TXB_2 did not alter between saline and MIA-treated rats (Figure 3.b), or between ipsilateral and contralateral knee joints (data not shown). Lipid levels for the EC and CYP groups were also unaltered between saline- and MIA-treated rats.

a)

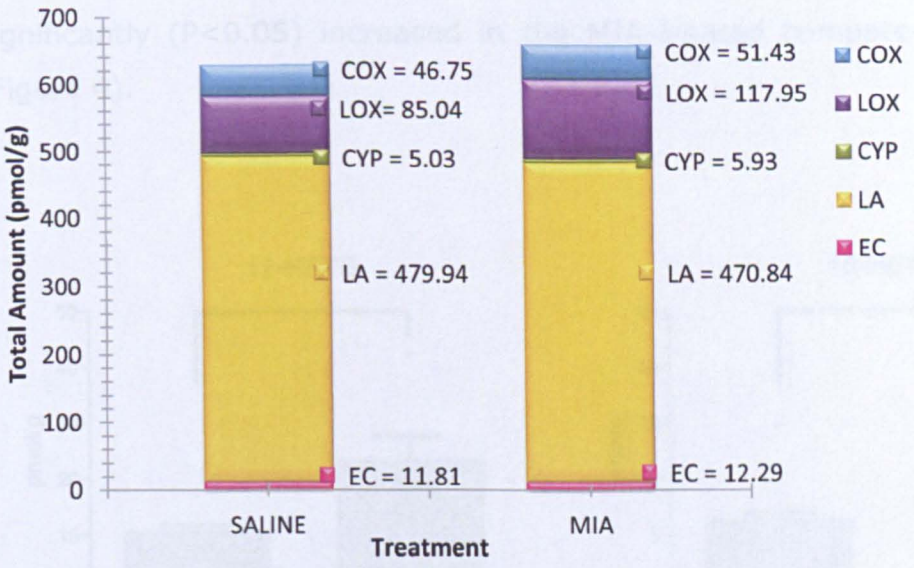

b)

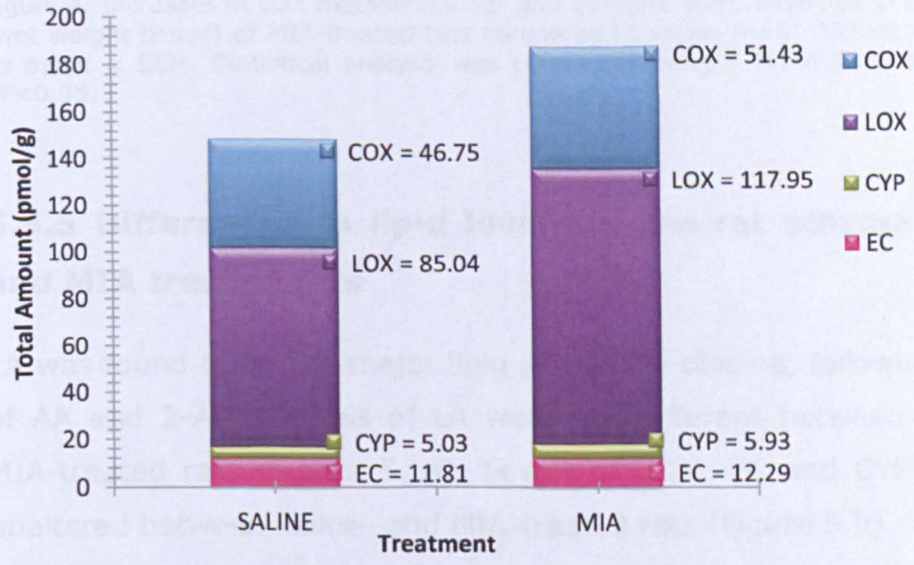

Figure 3. a) Lipid distribution per g wet tissue weight of the metabolites of COX, LOX, CYP450 (CYP) and the endocannabinoids (EC) in knee joint in saline and MIA rats, excluding 2-AG and AA (n=8), b) Lipid distribution per g wet tissue weight of the metabolites of COX, LOX, CYP450 (CYP) and the endocannabinoids (EC) in knee joint in saline and MIA rats, excluding LA, 2-AG and AA (n=8).

There was, however, a clear difference for the LOX group of lipids between saline and MIA-treated rats. Levels of 12- and 15-HETE were significantly ($P<0.05$) increased in the MIA-treated compared to saline (Figure 4).

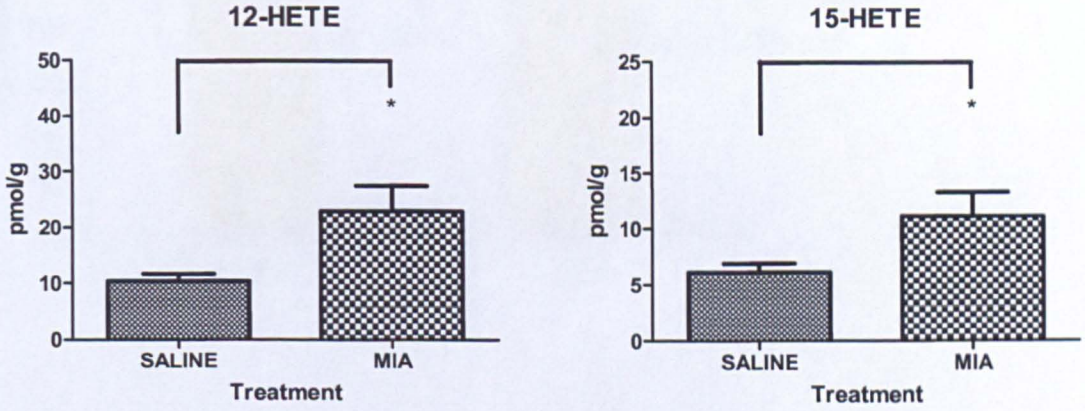

Figure 4. Increases in LOX metabolites 12- and 15-HETE were observed in the knee joints (wet weight tissue) of MIA-treated rats compared to saline (n=8). Values are expressed as mean ± SEM. Statistical analysis was conducted using a Mann Whitney test, where *$P<0.05$.

5.3.5 Differences in lipid levels in the rat plasma in saline and MIA treated rats

LA was found to be the major lipid present in plasma, following exclusion of AA and 2-AG. Levels of LA were not different between saline- and MIA-treated rats (Figure 5. a). Levels of COX, EC and CYP lipids were unaltered between saline- and MIA-treated rats (Figure 5.b).

a)

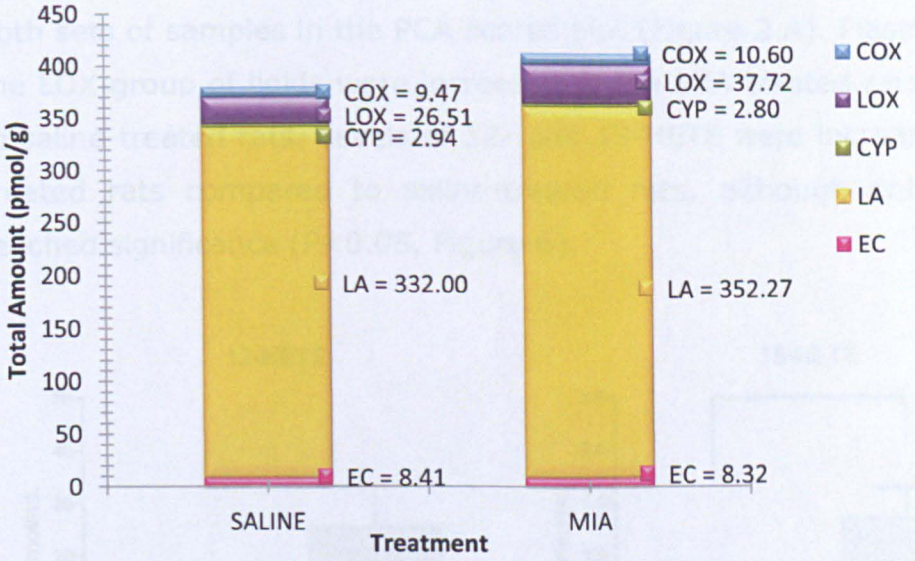

b)

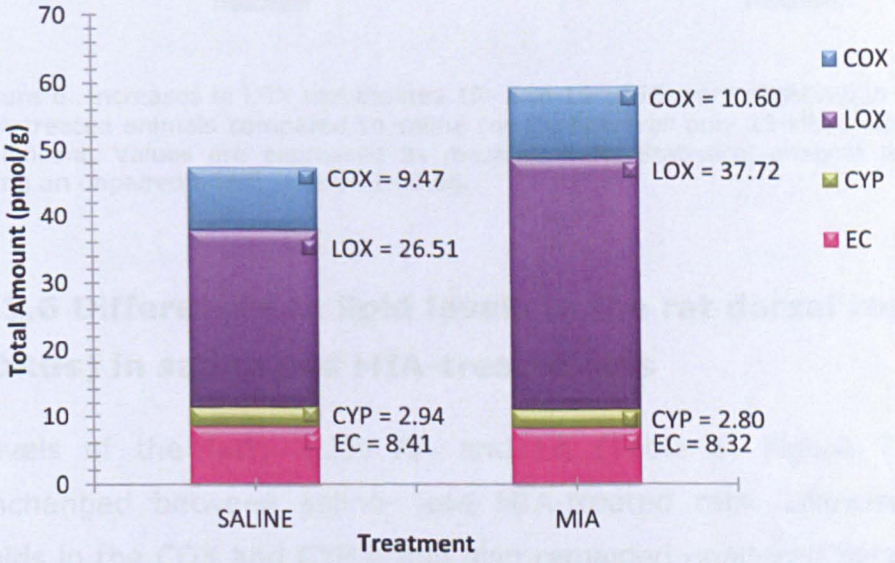

Figure 5. a) Lipid distribution per g wet tissue weight of the metabolites of COX, LOX, CYP450 (CYP) and the endocannabinoids (EC) in plasma in saline and MIA rats, excluding 2-AG and AA (n=8), b) Lipid distribution per g wet tissue weight of the metabolites of COX, LOX, CYP450 (CYP) and the endocannabinoids (EC) in plasma in saline and MIA rats, excluding LA, 2-AG and AA (n=8).

The distribution of the remaining lipids measured in plasma was similar to the knee joint and this is reflected in the close proximity positioning of both sets of samples in the PCA scores plot (Figure 2.A). Plasma levels of the LOX group of lipids were increased in the MIA-treated rats compared to saline-treated rats. Levels of 12- and 15-HETE were increased in MIA-treated rats compared to saline-treated rats, although only 15-HETE reached significance ($P<0.05$, Figure 6).

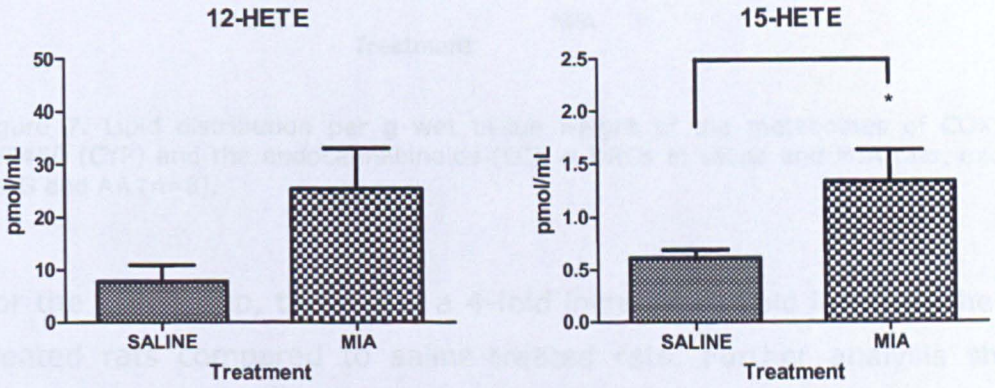

Figure 6. Increases in LOX metabolites 12- and 15-HETE were observed in the plasma of MIA-treated animals compared to saline (n=8), however only 15-HETE was found to be significant. Values are expressed as mean ± SEM. Statistical analysis was conducted using an unpaired t-test, where *P<0.05.

5.3.6 Differences in lipid levels in the rat dorsal root ganglia (DRGs) in saline and MIA-treated rats

Levels of the fatty acids AA and LA (Table 1, Figure 7) remained unchanged between saline- and MIA-treated rats. Likewise, levels of lipids in the COX and CYP group also remained unaltered between saline- and MIA-treated rats (Figure 7).

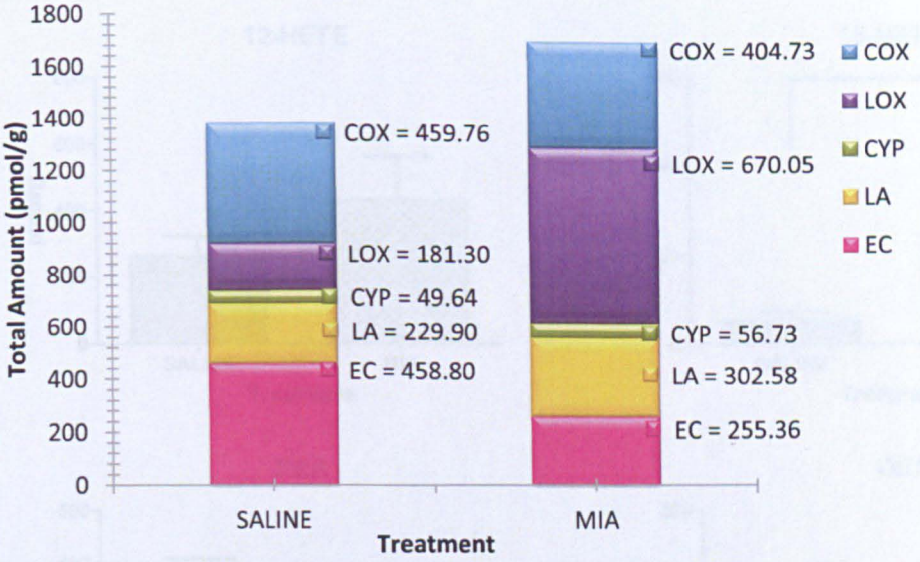

Figure 7. Lipid distribution per g wet tissue weight of the metabolites of COX, LOX, CYP450 (CYP) and the endocannabinoids (EC) in DRGs in saline and MIA rats, excluding 2-AG and AA (n=8).

For the LOX group, there was a 4-fold increase in lipid levels in the MIA-treated rats compared to saline-treated rats. Further analysis showed that the increases in total LOX metabolites were due to increased levels of 12- and 15-HETE ($P<0.05$, Figure 8) and, also, 13-oxoODE in the MIA-treated rats, as this lipid was not detectable in saline-treated rats (Table 1). In the DRGs, lipid levels in the EC group decreased in the MIA-treated rats compared to saline, mainly due to changes in levels of PEA and OEA; however, these changes were not significant (Figure 8).

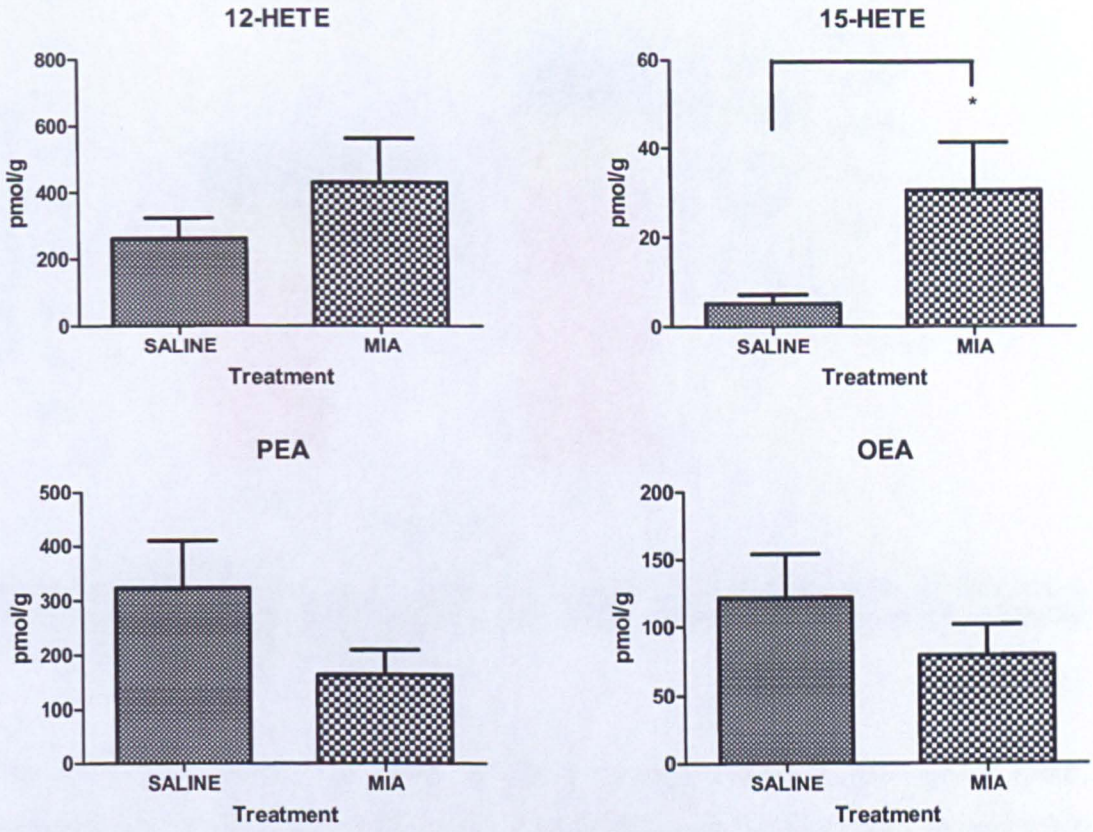

Figure 8. Increases in 12- and 15-HETE, along with decreases in PEA and OEA were observed in the DRGs (g wet weight tissue) of MIA-treated rats compared to saline (n=8). Values are expressed as mean ± SEM. Statistical analysis was conducted using a Mann Whitney test, where *P<0.05.

5.3.7 Differences in lipid levels in the rat spinal cord in saline- and MIA-treated rats

Levels of the fatty acids AA and LA (Table 1, Figure 9) in the spinal cord remained unchanged between saline and MIA-treated rats. Likewise, levels of LOX- and CYP-associated lipids in the spinal cord were unaltered between saline- and MIA-treated rats (Figure 9).

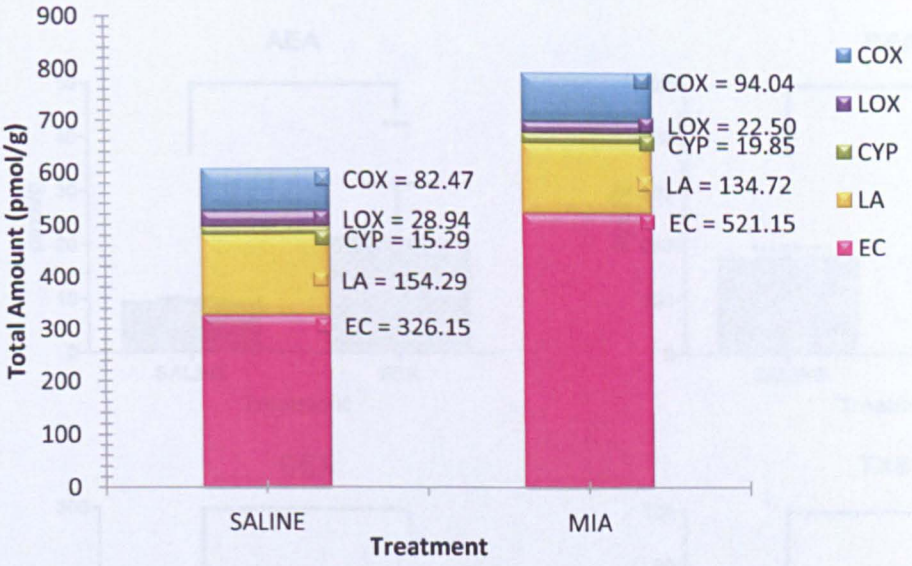

Figure 9. Lipid distribution per g wet tissue weight of the metabolites of COX, LOX, CYP450 (CYP) and the endocannabinoids (EC) in the spinal cord in saline and MIA-treated rats, excluding 2-AG and AA (n=8).

The EC group were the main group of lipids found in the spinal cord, comprising 2-AG, AEA, OEA, PEA and AraGly. Increased lipid levels were observed mainly in the EC group but also in the COX group in the MIA-treated rats compared to saline-treated rats (Figure 9); increased levels of AEA ($P<0.001$), PEA ($P<0.05$), OEA ($P<0.05$) and TXB_2 ($P<0.01$) in the spinal cord of MIA-treated rats were significant (Figure 10).

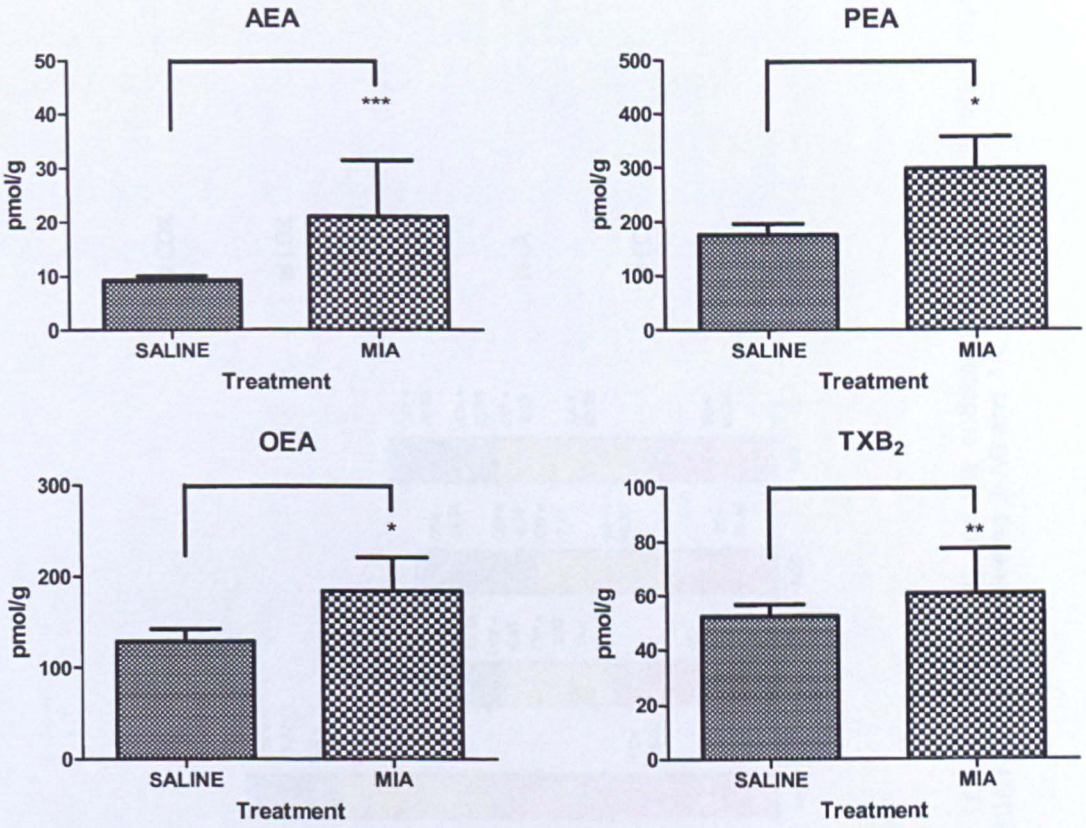

Figure10. Increases in AEA, PEA, OEA and TXB_2 were observed in the spinal cord (wet weight tissue) of MIA-treated animals compared to saline (n=8). Values are expressed as mean ± SEM. Statistical analysis was conducted using an f-test to compare variances, where *P<0.05, **P<0.01 and **P<0.001.

5.3.8 Differences in lipid levels in the rat brains regions (frontal cortex, hippocampus, midbrain, rest of cortex, rest of brain) in saline and MIA-treated rats

Levels of the fatty acids AA and LA (Table 1, Figure 11) in all five brain regions were no different between saline- and MIA-treated rats. Likewise, COX- and CYP-associated lipid levels in all five brain regions were unaltered between saline and MIA-treated rats (Figure 11).

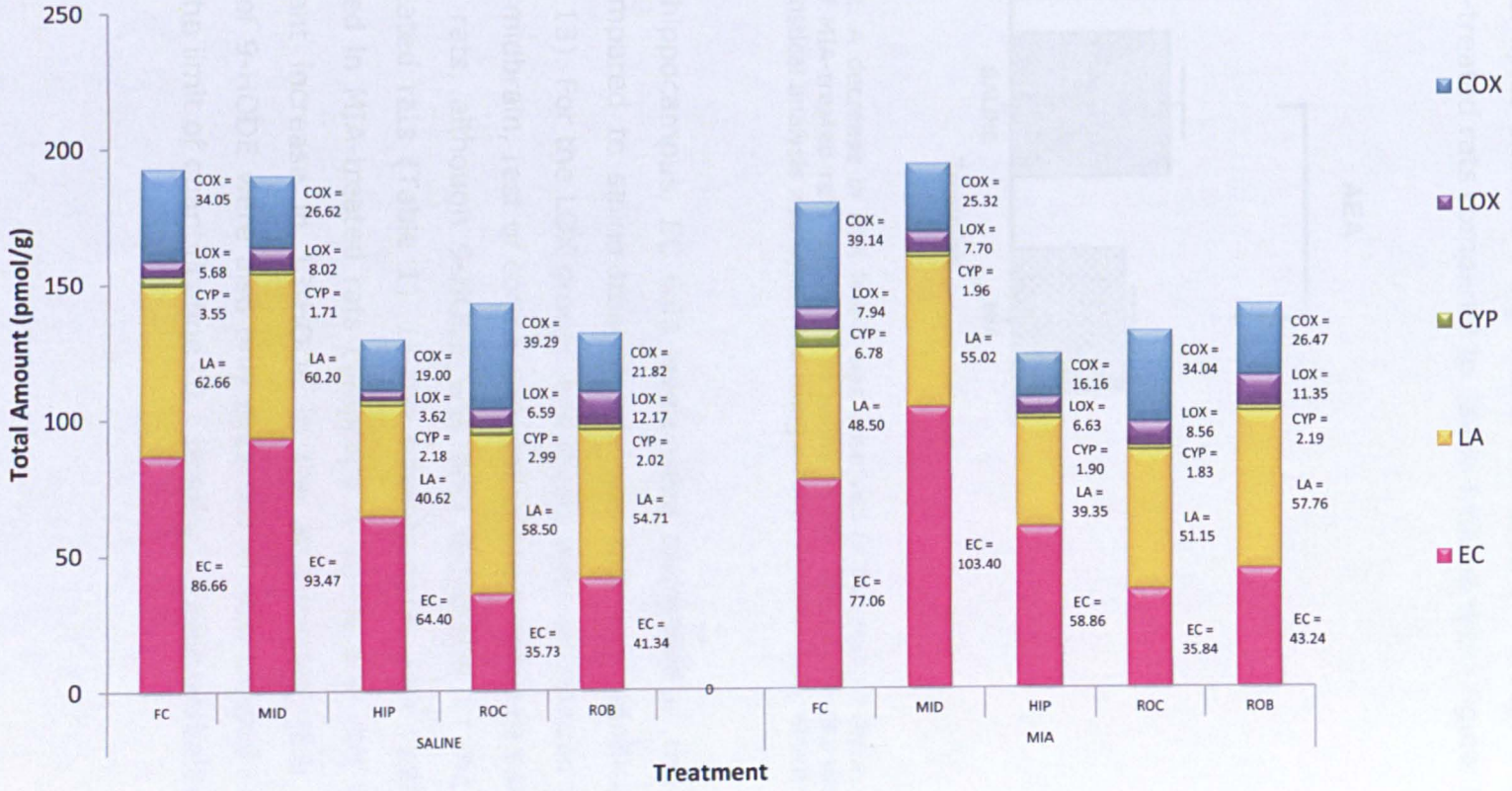

Figure 11. Lipid distribution per g wet tissue weight of the metabolites of COX, LOX, CYP450 (CYP) and the endocannabinoids (EC) in brain regions (frontal cortex, hippocampus, midbrain, rest of cortex, rest of brain) in saline and MIA rats (n=8), excluding 2-AG and AA.

For the EC group, levels in the frontal cortex, midbrain and rest of brain were no different between saline- and MIA-treated rats (Table 1). For the rest of cortex brain region, there were no obvious changes in levels of EC lipids between saline and MIA-treated rats; however, further analysis of individual lipids showed a significant decrease ($P<0.05$) in AEA levels in the MIA-treated rats compared to saline-treated rats (Figure 12).

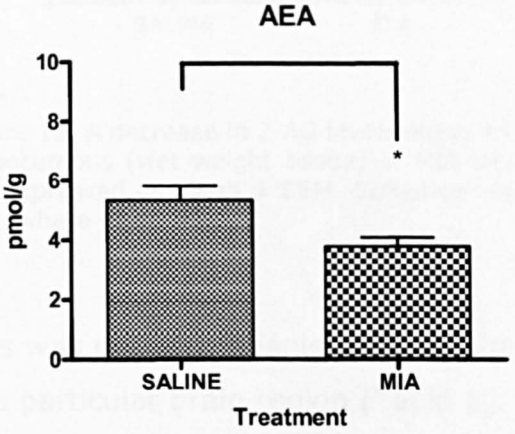

Figure 12. A decrease in AEA levels was observed in the rest of cortex (g wet weight tissue) of MIA-treated rats compared to saline (n=8). Values are expressed as mean ± SEM. Statistical analysis was conducted using a Mann Whitney test, where *$P<0.05$.

In the hippocampus, EC lipid levels were decreased in the MIA-treated rats compared to saline-treated rats and this was significant for 2-AG (Figure 13). For the LOX group, lipid levels were unchanged in the frontal cortex, midbrain, rest of cortex and rest of brain between saline and MIA-treated rats, although 9-HODE was only detectable in the midbrain of MIA-treated rats (Table 1). In the hippocampus, LOX lipid levels were increased in MIA-treated rats compared to saline and this was due to a significant increase in 13-HODE in the MIA-treated rats (Figure 13). Levels of 9-HODE were also only detected in MIA-treated rats and were below the limit of quantification (0.1 pmol/g) in saline-treated rats.

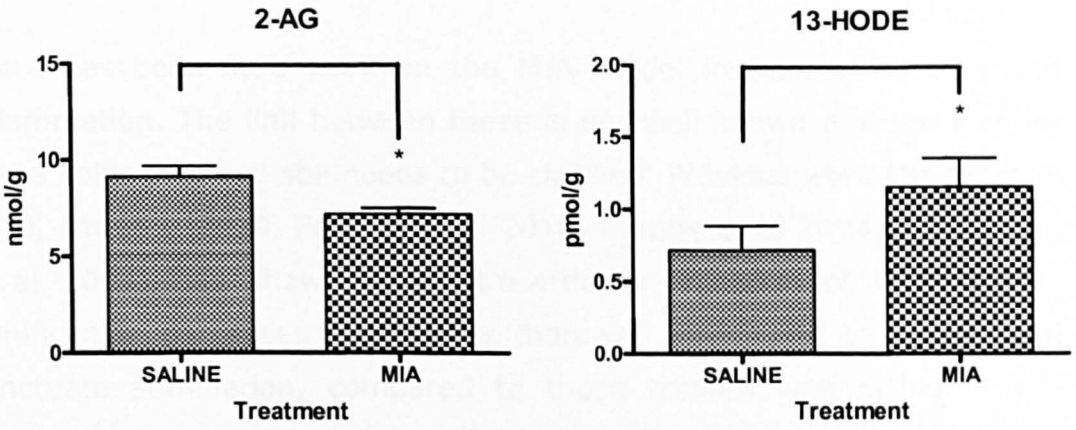

Figure 13. A decrease in 2-AG levels along with increase in 13-HODE were observed in the hippocampus (wet weight tissue) of MIA-treated rats compared to saline (n=8). Values are expressed as mean ± SEM. Statistical analysis was conducted using a Mann Whitney test, where *P<0.05.

This was not accompanied by any significant changes in the other lipids in this particular brain region (Table 1).

5.3.9 Summary of findings

The MIA model of OA pain was associated with changes in some bioactive lipids in the different rat tissues analysed. In the knee joint, 12- and 15-HETE levels were increased (P<0.05) in the MIA-treated rats compared to saline-treated rats. Both 12- and 15-HETE levels were increased in the plasma and the DRGs, of MIA-treated rats, however only 15-HETE reached significant (P<0.05). Levels of AEA, OEA, PEA and TXB_2 increased in the spinal cord of MIA-treated rats compared to saline-treated rats (P<0.001, P<0.05, P<0.05 and P<0.01 respectively). In the hippocampus, 2-AG levels were decreased (P<0.05) and levels of 13-HODE were increased (P<0.05) in the MIA-treated rats, compared to saline-treated rats. AEA levels also decreased (P<0.05) in the rest of cortex in the MIA-treated group.

5.4 Discussion

There has been little work on the MIA model in relation to pain and inflammation. The link between these is not well known and the identity of the lipids involved still needs to be clarified. Previous work (Sagar et al 2010, Im et al 2010, Ferland et al 2010, Combe et al 2004, Fernihough et al 2004) has shown that intra-articular injection of MIA in rats significantly decreases hindpaw withdrawal thresholds to mechanical punctuate stimulation, compared to those treated with saline. These observations were also accompanied by significant increases in 2-AG, PEA and OEA levels in the spinal cord at PO day 14 and 28. In the present study, the pain and inflammation experiments were repeated to show that the model exhibits pain behaviour consistent with the previous studies, and different tissues were collected to investigate, using LC-MS/MS, possible changes in a larger number of lipids.

5.4.1 Effects of intra-articular injection of MIA on weight bearing

Consistent with previous work (Sagar et al 2010), intra-articular injection of MIA produced a time-dependent increase in weight bearing difference, which was significant throughout the 28 day time course of measurements and a time-dependent decrease in paw withdrawal threshold, significant at PO day 21 and 28, both on the ipsilateral side. A significant increase in weight bearing difference was evident from PO day 7. Since subchondral bone is richly innervated and articular cartilage is not, it is thought that the initiation and progression of these bone lesions is related to the onset of joint pain and may account for the significant changes in weight bearing observed here (Guzman et al 2003). The effects observed at PO day 7 are also not likely to be caused by any inflammatory changes as these have been shown to be largely resolved by PO day 7 (Pulichino et al 2006, Combe et al 2004). Increases in weight bearing difference were also observed at PO day 14, at which time the histological features mentioned at PO day 7 remain but to a greater

extent, and pathological changes in patellar bone and cartilage are shown to be more extensive in distribution and severity (Clements et al 2009).

5.4.2 Effects of intra-articular injection of MIA on hindpaw withdrawal thresholds

Consistent with previous work (Sagar et al 2010), decreases in hindpaw withdrawal thresholds were not shown to be significant until PO day 21 of the study as peripheral sensitisation and allodynia developed at a later stage following intra-articular injection of MIA. This change in hindpaw withdrawal threshold was also accompanied by a sharp increase in weight bearing difference at PO day 21. Peripheral sensitisation as a result of increased nociceptor activity (Im et al 2010), elevates cytokine release (Im et al 2010, Combe et al 2004) and contributes to hyperalgesia and allodynia at this stage (Im et al 2010, Schuelert and McDougall 2009, Combe et al 2004), which extends further to PO day 28. This is shown by the significant changes seen in weight-bearing and paw-withdrawal thresholds at PO day 28.

5.4.3 Changes in lipid levels in different rat tissues

Quantification and profiling of lipids in different tissues in the MIA model of OA pain has not previously been explored. The work presented in this thesis demonstrates that, when individual lipid levels of each analyte measured is analysed using principle component analysis (PCA), tissue types are evident, based on the composition and amount of lipid measured in that particular tissue. It is apparent that, for each tissue type, there are distinct differences in the lipids measured, which can be clearly shown with the PCA scores plot. Plasma and knee joints are very similar in lipid composition but quite different to neural tissue. Likewise, all neural tissue studied (DRGs, spinal cord and brain) are similar in their lipid composition. Further analysis showed that the differences between the tissues were due to specific lipids, which is shown with the PCA loadings plot. Plasma and the knee joints were shown to exhibit a similar distribution of lipids and are, therefore, in close proximity to each other on the PCA score plot. The LOX metabolites 9-, 13-HODE, 9- and 13-

oxoODE, which are known TRPV1 agonists (Patwardhan et al 2009, Patwardhan et al 2010) are shown on the PCA loadings plot to be the lipids that distinguish the knee joint from the other tissues. In plasma, the main lipids that distinguish this tissue from the others investigated included high levels of LA, and also 8- and 12-HETE, which can be produced via the lipoxygenase or the cytochrome p450 pathways (Yue et al 2007). According to the loadings plot, AEA, OEA, PEA, TXB_2, PGD_2/PGE_2 were quantified in the spinal cord and the DRGs, and the levels of these lipids separated the spinal cord and the DRGs from the other tissues. In the brain, high levels of 2-AG and AA were detected and the levels of these two lipids were much higher in this particular tissue compared to the other tissues analysed.

5.4.3.1 Changes in lipid levels in the rat knee joint

Analysis of the individual tissues revealed significant changes in certain lipids when comparing MIA- to saline-treated rats, in which most levels were found to be increased and these changes occurred at a time when there was pronounced hyperalgesia and allodynia present. In the knee joint, there was a greater proportion of LOX metabolites found in the MIA-treated rats compared to saline-treated rats. These included the LOX metabolites of LA; 9-, 13-HODE, 9-, 13-oxoODE and the LOX metabolites of AA; 12- and 15-HETE, of which the AA metabolites were both found to increase significantly. As described previously, the majority of research investigating expression of LOX in bone has been conducted in mouse models, where increased expression is shown to be detrimental to skeletal development (Almeida et al 2009, Klein et al 2004). It is known that, at PO day 28, the pathological changes in the knee joint in MIA-treated rats include focal compression and fragmentation of subchondral bone with replacement of bone and marrow by dense fibrous tissue (Guzman et al 2003). These pathological changes in the knee joint may be linked to increased LOX expression and the increased levels of LOX metabolites of LA and AA present in the joint. Both 12-HETE and 15-HETE are known to be TRPV1 receptor agonists (Shin et al 2002, Caterina and Julius 2001, Hwang et al 2000) and there is a strong link between TRPV1

and hyperalgesia as discussed in Chapter 4. TRPV1 is highly expressed on the terminals of primary afferent Aδ- and C-fibres, as well as being present in the brain, including areas involved in nociceptive transmission (Patwardhan et al 2009, Toth et al 2005). In the knee joint, where the subchondral bone is richly innervated, the resulting hyperalgesia may be caused by increased TRPV1 activation in the MIA-treated animals due to increased 12- and 15-HETE ligand production. TRPV1 expression has been found in articular chondrocytes and synovial fibroblasts of human OA patients (Chu et al 2010) and TRPV1 expression is elevated in MIA-induced rats on the primary afferent neurons of the knee (Fernihough et al 2005). Expression of TRPV1 receptors has been shown in the mouse DRGs and that these TRPV1-positive fibres also innervate the knee joints of these animals (Cho and Valtschanoff 2008).

5.4.3.2 Changes in lipid levels in rat plasma

In plasma there was also a higher proportion of LOX metabolites in samples from MIA-treated rats, compared to saline-treated rats. As stated previously, lipooxgenases are highly expressed in blood and immune cells (Hampson and Grimaldi 2002), which may account for the high levels of LOX products in plasma. The TRPV1 ligands 12- and 15-HETE were also increased, with changes in the levels of 15-HETE being significant, complimenting the data observed in the knee joint.

5.4.3.3 Changes in lipid levels in the DRGs

The DRGs had a higher proportion of the LOX metabolites, similar to the knee joint and plasma, and a lower proportion of the endocannabinoids compared to the spinal cord. Further analysis of the LOX metabolites found that levels of the TRPV1 ligands 12- and 15-HETE were significantly increased in the DRGs from MIA-treated rats compared to saline-treated rats, whereas the apparent decreases in PEA and OEA were not significant. In the MIA model, enhanced spontaneous firing of spinal wide dynamic range neurons is reduced by systemic administration of a TRPV1 antagonist A-889425, an effect absent in sham-operated control rats, indicating an enhanced role of TRPV1 in this form of chronic injury (Chu

et al 2010). Furthermore, antibody staining of DRGs showed co-localisation of TRPV1 and cannabinoid CB_2 receptor expression in the small and medium diameter neurons in both sham-operated and MIA-treated animals (Schuelert et al 2010). It may be possible, therefore, that the TRPV1 and CB_2 receptor systems work synergistically in the DRGs. An increase was observed in the pro-nociceptive TRPV1 ligands, 12- and 15-HETE, along with an increase in LOX metabolites as a whole, most of which are also TRPV1 ligands, coupled with a decrease in the endocannabinoids, some of which mediate anti-nociceptive effects via an action at CB_2 receptors.

5.4.3.4 Changes in lipid levels in the spinal cord

In the rat spinal cord, there were significant increases in AEA, OEA and PEA in MIA-treated rats, which is consistent with previous work (Sagar et al 2010). In addition, there was also a significant increase in TXB_2 in MIA-treated rats. The increases in AEA, OEA and PEA may be due to increased expression or activity of N-acyl phosphatidylethanolamine phospholipase D (NAPE-PLD), the enzyme responsible for the synthesis of these lipids, which has been shown to be increased in the spinal cord of MIA-treated rats, compared to saline-treated rats (Sagar et al 2010). In the MIA model, it is well known that joint nociceptors are sensitised leading to the generation of joint pain. One of the main mechanisms responsible for this is activation of nociceptors located on Aδ and C primary afferent nerve fibres, which show increased activity in this particular OA model (Schuelert and McDougall 2009). It is a possibility that this increased neuronal activity may be responsible for the increased synthesis of these lipids. In the spinal cord, a significant increase was observed in TXB_2, a COX-2 metabolite of AA, whose levels are found to increase under inflammatory conditions (Guay et al 2004). Increased levels of TXB_2 in the spinal cord are seen when spinal cord injury is present (Mitsuhashi et al 1994).

5.4.3.5 Changes in lipid levels in the rat brain

In the brain, a larger proportion of the COX metabolites TXB_2, PGD_2/PGE_2 were present, compared to the knee joint and plasma. PGE_2 is the main product of the COX pathway, in which COX-1 and COX-2 convert arachidonic acid to prostaglandin H_2 which is further metabolised by prostaglandin E_2 synthases into PGE_2 (See references in Alix et al 2008). In the brain, COX-2 is constitutively expressed in several neuronal cell populations, especially in hippocampal and cortical glutamatergic neurons. COX-2 is involved in brain maturation and the regulation of synaptic activity and plasticity (Alix et al 2008). Comparison of the different regions in the brain, revealed no significant changes in lipid levels in the frontal cortex, midbrain and rest of brain when comparing MIA-treated and saline-treated rats. However in the hippocampus, there was a significantly higher level of 13-HODE, a LOX metabolite of LA and a known TRPV1 agonist, in MIA-treated rats, compared to saline-treated rats. Another LOX metabolite of LA, the TRPV1 agonist 9-HODE, was also only detected in MIA-treated rats and not saline-treated rats. There is evidence for the existence of TRPV1 receptors in the brain including the hippocampus, although its function is still unclear (Gibson et al 2008, Steenland et al 2006). Intracerebroventricular administration of A-784168 (a TRPV1 antagonist) significantly attenuated MIA-induced differences in weight bearing, which suggests that TRPV1 receptors in the CNS play a role in OA pain (Cui et al 2006). There is also evidence for TRPV1 receptors in the CNS having a role in pain mediated by central sensitisation (Cui et al 2006). TRPV1 receptors expressed by hippocampal neurons can be activated in several ways, one of which includes lipoxygenase derivatives that are synthesized as a result of glutamate receptor activation (Gibson et al 2008). There is also evidence linking TRPV1 to long-term synaptic depression or LTD in hippocampal neurons, although these excitatory synapses were not blocked by AM251 (a CB1 receptor antagonist), suggesting that CB1 involvement was not required for this form of LTD (Gibson et al 2008). This may be a possible reason for the significant decrease in 2-AG in the hippocampus in the MIA-

treated animals. 2-AG is a crucial retrograde messenger mediating on-demand forms of LTD via CB1 activation (Ludanyi et al 2011); however, in this case, if CB1 involvement is not required for this form of LTD, it may explain the change in 2-AG levels in the hippocampus. Finally, in the rest of the cortex, there was a significant decrease in levels of AEA in MIA-treated rats, compared to saline-treated rats. The cortex is involved in pain processing, in the formation of pain-associated memory and the descending modulation of nociception (Steenland et al 2006). At PO day 28, hyperalgesia and allodynia were evident in the MIA-treated rats and there were significant changes in levels of lipids involved in pain processing, which may suggest CNS modulation of pain processing in different regions of the brain.

5.5 Conclusions

This study illustrates that the MIA model of OA pain produces robust pain behaviour, with rats exhibiting signs of hyperalgesia and allodynia at day 28 following model induction. It demonstrates an increase in the levels of endogenous ligands for TRPV1 at multiple levels in this model of OA pain, which is consistent with the previous reports that blockade of TRPV1 with various antagonists blocks the associated pain behaviour. The data supports the proposal that blockade of TRPV1 may provide a novel pharmacological target for the reduction of OA pain.

Chapter 6.

General Discussion

6. General Discussion

Bioactive lipids or lipids that activate specific signalling pathways are involved in the regulation and maintenance of normal bodily functions. Furthermore, bioactive lipid targets have been implicated in a number of conditions such as cancer, asthma and arthritis, all of which contain an inflammatory element (Evans and Hutchinson 2010). It is widely recognised that the regulation of inflammation is a highly complex biological process that involves many receptors, cells and molecules. The presence of bioactive lipids contributes to the biological response to tissue injury or insult and governs distinct mechanisms such as vasodilatation, increased capillary permeability and infiltration of immune cells (Chopade and Mulla 2010). Macrophages, neutrophils and dendritic cells are the main producers of eicosanoids typically in sub-nanomolar concentrations, which target local receptors (Harizi et al 2008, Mbvundula et al 2004). The synthetic, metabolic and signalling pathways of these bioactive lipids are activated in response to the multicellular signalling status of the environment (Evans and Hutchinson 2010).

The measurement of levels of bioactive lipids in these biological systems is essentail for understanding their role in cell function and pathological events. In this thesis, a validated LC-MS/MS that allows the simultaneous identification and measurement of 42 bioactive lipids is described. This analytical method is capable of measuring known lipid mediators of the inflammatory response, including COX metabolites; PGD/PGE, TXB, LOX metabolites; 5-, 12-, 15-HETE, HODEs, oxoODEs, CYP metabolites; 8- and 11-HETE, EETs and the endocannabinoids; AEA and 2-AG and endocannabinoid-like compounds PEA and OEA.

The sites of action of bioactive lipids include various different receptors, including G-protein coupled receptors such as the cannabinoid receptors, the nuclear PPAR receptors, and the cation channel TRPV1. Experiments in this thesis using the TR-FRET PPARα competitive binding assay showed that 8-HETE and PEA bind to PPARα, along with other lipids such as fatty acids and EETs. However, previous work have only demonstrated

activation of the PPARα receptor by 8-HETE and PEA (Yu et al 1995, Fu et al 2003). Furthermore, 8-HETE was shown to be a high affinity PPARα ligand compared to endogenous ligands such as arachidonic acid and AEA.

In this thesis, the carrageenan model of inflammation and pain was used to investigate how levels of bioactive lipids altered at different stages of the inflammatory process. In view of this, the changes in lipid levels can be compared at 1, 3, 4 and 5 hours post-carrageenan for selective lipids measured (Table 1).

Table 1.

Time (post-carrageenan) (hr)	AEA	2-AG	PEA	OEA	12-HETE	9-HODE	13-HODE	9-oxoODE	LA	TXB_2
1	↔	↓	↓	↓	↓	↓	↓	↔	↔	↔
3	↓	↓	↓	↓	unknown	unknown	unknown	unknown	unknown	unknown
4	↓	↔	↓	↓	↔	↓	↓	↓	↑	↑
5	↓	↓	↓	↓	↓	unknown	unknown	unknown	unknown	unknown

Table 1. Summary of the significant effects of intraplantar injection of 2% carrageenan on bioactive lipid levels in the hindpaw at different timepoints, 1, 3, 4 and 5 hour post-carrageenan. The changes of some of these lipids were unknown, because they were not measured at that particular timepoint. Data from the 1, 4 and 5 hour timepoints are presented in this thesis in Chapter 3 and Chapter 4. Data at the 3 hour timepoint is from previous work conducted in our group (Jhaveri et al 2008).

Previous work investigated the changes in prostanoid levels at 0, 1, 3, 5, 6, 12 and 24 hours post-carrageenan compared to saline in rat hindpaw (Guay et al 2004). Levels of TXB_2 were significantly increased at 3 hours, but by 5 hours, had returned to baseline (Guay et al 2004). This thesis reports that levels of TXB_2 remained unchanged at 1 hr, which is consistent with previous work (Guay et al 2004) and are significantly elevated at 4 hours. Levels of PGE_2 were previously reported to be significantly raised in hindpaw tissue from 1 hour post-carrageenan, which was maintained to 6 hours, before increasing sharply at 12 hours, and again at 24 hours (Guay et al 2004). In my experiments, levels of PGD_2/PGE_2 were unaltered at 1 or 4 hours post-carrageenan. However, limitations in the analytical methodology presented in this thesis meant that measurements of this prostanoid are expressed as a sum of PGD_2 and PGE_2. Therefore, any subtle changes in PGE_2 may not have been detectable. Levels of PGE_2 and TXB_2 have also been analysed previously by GC-MS and shown to peak at 3 hours post-carrageenan in pleural exudate of rats (Harada et al 1982) and PGD_2 was undetectable in these samples.

In the carrageenan model of inflammation, significant reductions in lipid levels were observed for AEA, 2-AG, PEA, OEA, 12-HETE, 9-HODE, 13-HODE and 9-oxoODE, which were also time-dependent. The N-acyl ethanolamines (NAEs) AEA, PEA and OEA have been measured previously over a time course of 24 hours and changes in lipid levels were also time-dependent, following inhibition of AEA hydrolysis (Fegley et al 2005). This data is consistent with earlier reports that levels of 13-HODE are reduced in synovial fluid in carrageenan-induced knee arthritis (Herlin et al 1988). However, to date, the levels of bioactive lipids in the carrageenan model have not been profiled using LC-MS/MS until now. Additionally, HODEs and oxoODEs have not previously been measured in the carrageenan model. Therefore, it is difficult to draw comparisons with my data and previous studies. However, it does provide confidence that the changes in these LOX metabolites mirror those seen with the endocannabinoids, changes of which have been

shown previously (Jhaveri et al 2008). Data in this thesis also found significant carrageenan-induced hyperalgesia at 4 hours. This is consistent with previous studies which have also shown that carrageenan administration into the hindpaw results in increased hindpaw volume, oedema and hyperalgesia at 4 hours (Thorpe et al 2011, Pabreja et al 2010) and 3 hours (Jhaveri et al 2008). Increased metabolism and/or decreased synthesis during inflammation may explain these time-dependent reductions in lipid levels. The metabolism of bioactive lipids are achieved either by COX, LOX or CYP enzymes and the endocannabinoids AEA and 2-AG are also metabolised by fatty acid amide hydrolase (FAAH) and monoacyl glycerol lipase (MAGL) respectively. However, elevated activity of FAAH and MAGL was not observed in carrageenan-treated rats compared to saline-treated, suggesting that these metabolic pathways were not responsible for reduced levels of AEA and 2-AG (Jhaveri et al 2008, Holt et al 2005). It is established from in vitro studies that COX-2 can metabolise AEA and 2-AG (Yu et al 1997, Kozak et al 2004) and under conditions of peripheral inflammation, hindpaw injection of the COX-2 inhibitor rofecoxib enhances the inhibitory effects of AEA on pain behaviour. Also, levels of AEA, PEA and OEA were elevated in the hindpaw, indicating a role of peripheral COX-2 in the modulation of endocannabinoid function under these conditions (Guindon et al 2006). However, previous work in our group did not find overt increases in AEA and OEA, but found significant decreases in these lipids following COX-2 inhibition with nimesulide, suggesting involvement of other metabolic pathways. Indeed, metabolism of AEA and 2-AG via the LOX enzymes (Hampson et al 1995, Ueda et al 1995) and CYP enzymes (Snider et al 2007, Snider et al 2009, Awumey et al 2008, Stark et al 2008) has been reported. Involvement of LOX and metabolites of this enzyme in behavioural pain responses has recently been presented *in vitro* and *in vivo*. 9-HODE has been shown to activate TRPV1 in transfected CHO cells and produces behavioural pain responses following spinal administration, released following depolarisation of the spinal cord *in vitro* (Patwardhan et al 2009). Noxious thermal stimulation also increases levels of 9- and 13-

HODE in the skin and HODE-evoked TRPV1 responses of neurones are absent in cells from TRPV1 knockout mice (Patwardhan et al 2010), further supporting a potential role of these lipids in LOX-mediated nociception. Data in this thesis showed that inhibition of 15-LOX with PD 146176 and co-administration of 9- and 13-HODE antibodies, significantly reduced the carrageenan-induced weight bearing difference at 4 hours post-injection, suggesting 15-LOX mediated nociception. However, PD 146176 pre-treatment did not significantly alter the carrageenan-induced increase in the hindpaw volume and hindpaw circumference, suggesting that PD 146176 alters nociceptive pathways, rather than inflammatory pathways. *In vitro*, levels of 9- and 13-HODE, expressed as a ratio of the levels of linoleic acid, were significantly decreased following pre-exposure to PD 146176 for 15 minutes, but not 30 minutes, suggesting that PD 146176 may block the production of the HODEs. Levels of the endocannabinoids, AEA and 2-AG increased significantly following pre-treatment with PD 146176, suggesting reduced metabolism of these endocannabinoids via 15-LOX. *In vivo*, however, PD 146176 pre-treatment did not significantly alter levels of the 15-LOX metabolites and other lipid mediators in the carrageenan-treated hindpaw. Therefore, these results may add value to the hypothesis that the levels of bioactive lipids are affected by physiological processes such as oxidative stress and/or other routes of metabolism, as these changes are observed *in vitro* but not *in vivo*. It also draw attentions to the limitations of the analytical methodology and measurement of lipid levels that are a 'snapshot' in time of these physiological processes. A reason for this, may be that the changes *in vivo* occur at a different timepoint to those investigated in these studies. Therefore, future work may need to repeat these experiments at different timepoints or utilise alternative methodology to measure lipid changes over a period of time, to be able to provide further clarification of the 15-LOX mediated nociceptive effects.

Bioactive lipid targets have been implicated in a number of conditions such as cancer, asthma and arthritis, all of which contain an

inflammatory element. The MIA rat model of OA pain, is a robust model of osteoarthritis and this was used to investigate the potential changes in bioactive lipids under chronic inflammatory conditions in arthritis. It is important to note that, to date, profiling of bioactive lipids in different tissues of the MIA rat model has yet to be investigated until now. Eicosanoid profiling in the synovial joints of horses has been reported (De Grauw et al 2011), along with measurement of the endocannabinoids in synovial tissue and fluid (Richardson et al 2008). Intra-articular injection of MIA produced a time-dependent increase in weight bearing difference and a time-dependent decrease in paw withdrawal threshold in the ipsilateral hind paw, consistent with early studies (Sagar et al 2010). In the knee joint, levels of the known endogenous TRPV1 agonists, 12- and 15-HETE levels were significantly increased in MIA-treated rats compared to saline-treated rats. This elevation in levels of 12- and 15-HETE was also observed in plasma and in the DRGs of MIA-treated rats. Expression of TRPV1 receptors has been shown in the mouse DRGs and that these TRPV1-positive fibres also innervate the knee joints of these animals (Cho and Valtschanoff 2008). In addition, TRPV1 expression has been found in articular chondrocytes and synovial fibroblasts of human OA patients (Chu et al 2010) and TRPV1 expression is elevated in MIA-induced rats on the primary afferent neurons of the knee (Fernihough et al 2005). Recently, TRPV1 activity was reported to be increased in the rat knee joint in the MIA model of OA (Puttfarcken et al 2010). In the hippocampus, levels of 13-HODE, another known TRPV1 ligand, was increased in MIA-treated rats, compared to saline-treated rats. These data demonstrate an increase in the levels of endogenous ligands for TRPV1 at multiple levels, in this model of OA pain and proposes that blockade of TRPV1 may provide a novel pharmacological target for the reduction of OA pain. Previous reports demonstrate that blockade of TRPV1 with various antagonists blocks the associated pain behaviour peripherally and centrally (For review see: Roberts and Connor 2006, Chu et al 2010, Puttfarcken et al 2010). However, TRPV1 antagonism has been shown to alter core body temperature and reduced sensitivity to painful or

damaging heat stimuli and has therefore lost promise in clinical applications (Vay et al 2012, Krarup et al 2011, Round et al 2011). Therefore, the TRPV1 ligands themselves may prove to be potential targets for MIA-mediated pain behaviour, although future investigations are required to confirm this.

Levels of AEA, OEA, PEA and TXB_2 were increased in the spinal cord of MIA-treated rats compared to saline-treated rats. Increases in OEA and PEA in the spinal cord have previously been reported in our group in MIA-treated rats compared to saline-treated (Sagar et al 2010). Protein levels of NAPE-PLD and diacylglycerol lipase alpha (DAGLα), the major synthetic enzymes for the NAEs and 2-AG, respectively, were increased in the spinal cords of MIA-treated rats compared with saline-treated rats (Sagar et al 2010). Therefore, the increased spinal cord levels of AEA, PEA and OEA in MIA-treated rats are most likely as the result of increased synthesis via NAPE-PLD. Future work investigating the levels of precursors of the NAEs via the NAPE-PLD pathway, including N-acyl phosphatidyl ethanolamine, would need to be conducted to be able to confirm this hypothesis *in vivo*.

In conclusion, the development of a novel LC-MS/MS analytical method capable of measuring a large number of bioactive lipids *in vitro* and *in vivo*, have provided novel findings to support the involvement of these lipids in inflammation and pain. Furthermore, these data provide evidence for the involvement of PPARα and TRPV1 receptors in acute inflammatory pain and TRPV1 in chronic inflammatory pain. Reductions in levels of 9-HODE, 13-HODE, 9-oxoODE, AEA and 12-HETE, all known TRPV1 ligands were detected in the carrageenan model of acute inflammatory pain. Interestingly, opposing effects were observed in the MIA model of chronic inflammatory pain, where elevation of lipid levels of TRPV1 ligands 12-, 15-HETE and 13-HODE were detected. Overall, the evidence provides support for the proposal of TRPV1 receptors and also, TRPV1 ligands, as potential novel pharmacological targets for the reduction of acute and chronic pain.

Future Work

Further work that could be conducted following the results of this thesis include repeating the experiment involving intraplantar administration of PD 146176, 15-LOX inhibitor, carried out in exactly the same way, but with the addition of a TRPV1 antagonist, either BCTC or SB-366791 also administered intraplantarly. If attenuation of pain behaviour is blocked through the use of a TRPV1 antagonist, it would further confirm the involvement of TRPV1. Furthermore, collection of hindpaw tissue could also be repeated at closer time intervals. In this thesis, results for the analysis of lipid levels were shown at 1 hour and 4 hour, post-carrageenan injection. It may clarify the time course of lipid changes if a larger number of rats were used to include 2 and 3 hour timepoints. A rapid rise in pro-inflammatory agents may be expected earlier than the rise in anti-inflammatory or 'resolution-associated' agents. It may also clarify whether changes in HODE and oxoODE levels are occurring before the 4 hour timepoint measured.

In terms of the results observed in the MIA-model, it would be interesting to draw comparisons with human data. Since the knee joint dissected in the experiments conducted in this thesis contains mainly synovial fluid, collection of this particular biological sample from patients of OA would provide an interesting comparison between human OA and the rat MIA model of the disease. Profiling of human synovial fluid would then allow comparison of this to the lipid profile observed in the MIA-treated rat knee joints.

Reviewing the data in a more global sense, PD 146176 may be irritant to the mucous membranes and upper respiratory tract, and could potentially be harmful through inhalation, ingestion and skin absorption, which do not provide confidence for human use and performance in clinical trials. However, 15-LOX inhibition is a potential target for analgesia, but a drug that has a better toxicology profile would be necessary.

Chapter 7.

References

References

Aharoni A, De Vos CHR, Verhoeven HA, Maliepaard CA, Kruppa G, Bino R, *et al.* (2002). Nontargeted metabolome analysis by use of fourier transform ion cyclotron mass spectrometry. *OMICS A Journal of Integrative Biology* **6**(3): 217-234.

Ahluwalia J, Urban L, Bevan S, Nagy I (2003). Anandamide regulates neuropeptide release from capsaicin-sensitive primary sensory neurons by activating both the cannabinoid 1 receptor and the vanilloid receptor 1 in vitro. *European Journal of Neuroscience* **17**(12): 2611-2618.

Ahluwalia J, Urban L, Capogna M, Bevan S, Nagy I (2000). Cannabinoid 1 receptors are expressed in nociceptive primary sensory neurons. *Neuroscience***100**(4): 685-688.

Ahmadi S, Lippross S, Neuhuber WL, Zeilhofer HU (2002). PGE(2) selectively blocks inhibitory glycinergic neurotransmission onto rat superficial dorsal horn neurons. *Nature Neuroscience* **5**(1): 34-40.

Alexander SPH, Kendall DA (2007). The complications of promiscuity: endocannabinoid action and metabolism. *British Journal of Pharmacology* **152**(5): 602-623.

Alhaboubi HA, Zeitlin IJ (1983). REAPPRAISAL OF THE ROLE OF HISTAMINE IN CARRAGEENAN-INDUCED PAW EDEMA. *European Journal of Pharmacology* **88**(2-3): 169-176.

Alix E, Schmitt C, Strazielle N, Ghersi-Egea J-F (2008). Prostaglandin E2 metabolism in rat brain: Role of the blood-brain interfaces. *Cerebrospinal Fluid Res* **5**:5.

Almeida M, Ambrogini E, Han L, Manolagas SC, Jilka RL (2009). Increased Lipid Oxidation Causes Oxidative Stress, Increased Peroxisome Proliferator-activated Receptor-gamma Expression, and Diminished Pro-osteogenic Wnt Signaling in the Skeleton. *Journal of Biological Chemistry* **284**(40): 27438-27448.

Alstergren P, Kopp S (2000). Prostaglandin E-2 in temporomandibular joint synovial fluid and its relation to pain and inflammatory disorders. *Journal of Oral and Maxillofacial Surgery* **58**(2): 180-186.

Amruthesh SC, Falck JR, Ellis EF (1992). Brain synthesis and cerebrovascular action of epoxygenase metabolites of arachidonic acid. *Journal of Neurochemistry* **58**(2): 503-510.

Andersson E, Schain F, Svedling M, Claesson H-E, Forsell PKA (2006). Interaction of human 15-lipoxygenase-1 with phosphatidylinositol

bisphosphates results in increased enzyme activity. *Biochimica Et Biophysica Acta-Molecular and Cell Biology of Lipids* **1761**(12): 1498-1505.

Aronoff DM, Canetti C, Peters-Golden M (2004). Prostaglandin E-2 inhibits alveolar macrophage phagocytosis through an E-prostanoid 2 receptor-mediated increase in intracellular cyclic AMP. *Journal of Immunology* **173**(1): 559-565.

Aronoff DM, Carstens JK, Chen G-H, Toews GB, Peters-Golden M (2006). Differences between macrophages and dendritic cells in the cyclic AMP-dependent regulation of lipopolysaccharide-induced cytokine and chemokine synthesis. *Journal of Interferon and Cytokine Research* **26**(11): 827-833.

Artmann A, Petersen G, Hellgren LI, Boberg J, Skonberg C, Nellemann C, *et al.* (2008). Influence of dietary fatty acids on endocannabinoid and N-acylethanolamine levels in rat brain, liver and small intestine. *Biochimica Et Biophysica Acta-Molecular and Cell Biology of Lipids* **1781**(4): 200-212.

Ashton JC, Friberg D, Darlington CL, Smith PF (2006). Expression of the cannabinoid CB2 receptor in the rat cerebellum: An immunohistochemical study.*Neuroscience Letters* **396**(2): 113-116.

Auboeuf D, Rieusset J, Fajas L, Vallier P, Frering V, Riou JP, *et al.* (1997). Tissue distribution and quantification of the expression of mRNAs of peroxisome proliferator-activated receptors and liver X receptor-alpha in humans - No alteration in adipose tissue of obese and NIDDM patients. *Diabetes* **46**(8): 1319-1327.

Aurich M, Squires GR, Reiner A, Mollenhauer JA, Kuettner KE, Poole AR, *et al.* (2005). Differential matrix degradation and turnover in early cartilage lesions of human knee and ankle joints. *Arthritis and Rheumatism* **52**(1): 112-119.

Awumey EM, Hill SK, Diz DI, Bukoski RD (2008). Cytochrome P-450 metabolites of 2-arachidonoylglycerol play a role in Ca2+-induced relaxation of rat mesenteric arteries. *American Journal of Physiology-Heart and Circulatory Physiology* **294**(5): H2363-H2370.

Bacon KB, Camp RDR, Cunningham FM, Woollard PM (1988). Contrasting invitro lymphocyte chemotactic activity of the hydroxyl enantiomers of 12-hydroxy-5,8,10,14-eicosatetraenoic acid. *British Journal of Pharmacology* **95**(3): 966-974.

Baer AN, Costello PB, Green FA (1991). Invivo activation of a delta-6-oxygenase in human skin. *Biochemical and Biophysical Research Communications* **180**(1): 98-104.

Bai YJ, Gao XY, Lu JQ, Zhang HG (2010). A LC-MS-Based Method for Quantification of Biomarkers from Serum of Allergic Rats. *Molecules* **15**(5): 3356-3365.

Balvers MGJ, Verhoeckx KCM, Witkamp RF (2009). Development and validation of a quantitative method for the determination of 12 endocannabinoids and related compounds in human plasma using liquid chromatography-tandem mass spectrometry. *Journal of Chromatography B-Analytical Technologies in the Biomedical and Life Sciences* **877**(14-15): 1583-1590.

Bandell M, Macpherson LJ, Patapoutian A (2007). From chills to chilis: mechanisms for thermosensation and chemesthesis via thermoTRPs. *Current Opinion in Neurobiology* **17**(4): 490-497.

Banni S (2002). Conjugated linoleic acid metabolism. *Current Opinion in Lipidology* **13**(3): 261-266.

Baragi VM, Becher G, Bendele AM, Biesinger R, Bluhm H, Boer J, *et al.* (2009). A New Class of Potent Matrix Metalloproteinase 13 Inhibitors for Potential Treatment of Osteoarthritis Evidence of Histologic and Clinical Efficacy Without Musculoskeletal Toxicity in Rat Models. *Arthritis and Rheumatism* **60**(7): 2008-2018.

Barve RA, Minnerly JC, Weiss DJ, Meyer DM, Aguiar DJ, Sullivan PM, *et al.* (2007). Transcriptional profiling and pathway analysis of monosodium iodoacetate-induced experimental osteoarthritis in rats: relevance to human disease. *Osteoarthritis and Cartilage* **15**(10): 1190-1198.

Beck F, Plummer S, Senior PV, Byrne S, Green S, Brammar WJ (1992). The ontogeny of peroxisome-proliferator-activated receptor gene expression in the mouse and rat. *Proceedings of the Royal Society of London Series B-Biological Sciences* **247**(1319): 83-87.

Bednar MM, Gross CE, Balazy MK, Belosludtsev Y, Colella DT, Falck JR, *et al.* (2000). 16(R)-hydroxy-5,8,11,14-eicosatetraenoic acid, a new arachidonate metabolite in human polymorphonuclear leukocytes. *Biochemical Pharmacology* **60**(3): 447-455.

Behm DJ, Ogbonna A, Wu C, Burns-Kurtis CL, Douglas SA (2009). Epoxyeicosatrienoic Acids Function as Selective, Endogenous Antagonists of Native Thromboxane Receptors: Identification of a Novel Mechanism of Vasodilation. *Journal of Pharmacology and Experimental Therapeutics* **328**(1): 231-239.

Belury MA (2002). Dietary conjugated linoleic acid in health: Physiological effects and mechanisms of action. *Annual Review of Nutrition* **22**: 505-531.

Benani A, Kremarik-Bouillaud P, Bianchi A, Netter P, Minn A, Dauca M (2003a). Evidence for the presence of both peroxisome proliferator-activated receptors alpha and beta in the rat spinal cord. *Journal of Chemical Neuroanatomy* **25**(1): 29-38.

Benani A, Vol C, Heurtaux T, Asensio C, Dauca M, Lapicque F, *et al.* (2003b). Up-regulation of fatty acid metabolizing-enzymes mRNA in rat spinal cord during persistent peripheral local inflammation. *European Journal of Neuroscience* **18**(7): 1904-1914.

Bendele AM (2001). Animal models of osteoarthritis. *Journal of Musculoskeletal & Neuronal Interactions* **1**(4): 363-376.

Bequet F, Uzabiaga F, Desbazeille M, Ludwiczak P, Maftouh M, Picard C, *et al.* (2007). CB1 receptor-mediated control of the release of endocannabinoids (as assessed by microdialysis coupled with LC/MS) in the rat hypothalamus. *European Journal of Neuroscience* **26**(12): 3458-3464.

Bhave G, Hu HJ, Glauner KS, Zhu WG, Wang HB, Brasier DJ, *et al.* (2003). Protein kinase C phosphorylation sensitizes but does not activate the capsaicin receptor transient receptor potential vanilloid 1 (TRPV1). *Proceedings of the National Academy of Sciences of the United States of America* **100**(21): 12480-12485.

Bijlsma JWJ, Berenbaum F, Lafeber F (2011). Osteoarthritis: an update with relevance for clinical practice. *Lancet* **377**(9783): 2115-2126.

Bisgaard H, Kristensen JK (1985). Leukotriene-B4 produces hyperalgesia in humans. *Prostaglandins* **30**(5): 791-797.

Bisogno T, Melck D, Bobrov MY, Gretskaya NM, Bezuglov VV, De Petrocellis L, *et al.* (2000). N-acyl-dopamines: novel synthetic CB1 cannabinoid-receptor ligands and inhibitors of anandamide inactivation with cannabimimetic activity in vitro and in vivo. *Biochemical Journal* **351**: 817-824.

Bjork J, Hedqvist P, Arfors KE (1982). Increase in vascular permeability induced by leukotriene B4 and the role of polymorphonuclear leukocytes. *Inflammation* **6**(2): 189-200.

Blaho VA, Buczynski MW, Brown CR, Dennis EA (2009). Lipidomic Analysis of Dynamic Eicosanoid Responses during the Induction and Resolution of Lyme Arthritis. *Journal of Biological Chemistry* **284**(32): 21599-21612.

Blewett AJ, Varma D, Gilles T, Libonati JR, Jansen SA (2008). Development and validation of a high-performance liquid chromatography-electrospray mass spectrometry method for the

simultaneous determination of 23 eicosanoids. *Journal of Pharmaceutical and Biomedical Analysis* **46**(4): 653-662.

Blomberg K, Hurskainen P, Hemmila I (1999). Terbium and rhodamine as labels in a homogeneous time-resolved fluorometric energy transfer assay of the beta subunit of human chorionic gonadotropin in serum. *Clinical Chemistry* **45**(6): 855-861.

Bocan TMA, Rosebury WS, Mueller SB, Kuchera S, Welch K, Daugherty A, *et al.* (1998). A specific 15-lipoxygenase inhibitor limits the progression and monocyte-macrophage enrichment of hypercholesterolemia-induced atherosclerosis in the rabbit. *Atherosclerosis* **136**(2): 203-216.

Bolay H, Moskowitz MA (2002). Mechanisms of pain modulation in chronic syndromes. *Neurology* **59**(5): S2-S7.

Bondeson J, Wainwright SD, Lauder S, Amos N, Hughes CE (2006). The role of synovial macrophages and macrophage-produced cytokines in driving aggrecanases, matrix metalloproteinases, and other destructive and inflammatory responses in osteoarthritis. *Arthritis Research & Therapy* **8**(6): 12.

Borel V, Gallot D, Marceau G, Sapin V, Blanchon L (2008). Placental Implications of Peroxisome Proliferator-Activated Receptors in Gestation and Parturition.*Ppar Research*: 9.

Borgeat P, Naccache PH (1990). Biosynthesis and biological activity of leukotriene B4. *Clinical Biochemistry* **23**(5): 459-468.

Bouaboula M, Rinaldi M, Carayon P, Carillon C, Delpech B, Shire D, *et al.* (1993). Cannabinoid-receptor expression in human leukocytes. *European Journal of Biochemistry* **214**(1): 173-180.

Bove SE, Calcaterra SL, Brooker RM, Huber CM, Guzman RE, Juneau PL, *et al.* (2003). Weight bearing as a measure of disease progression and efficacy of anti-inflammatory compounds in a model of monosodium iodoacetate-induced osteoarthritis. *Osteoarthritis and Cartilage* **11**(11): 821-830.

Braissant O, Foufelle F, Scotto C, Dauca M, Wahli W (1996). Differential expression of peroxisome proliferator-activated receptors (PPARs): Tissue distribution of PPAR-alpha, -beta, and -gamma in the adult rat. *Endocrinology* **137**(1): 354-366.

Braissant O, Wahli W (1998). Differential expression of peroxisome proliferator-activated receptor-alpha, -beta, and -gamma during rat embryonic development. *Endocrinology* **139**(6): 2748-2754.

Brierley SM, Carter R, Jones W, Xu LJ, Robinson DR, Hicks GA, *et al.* (2005). Differential chemosensory function and receptor expression of splanchnic and pelvic colonic afferents in mice. *Journal of Physiology-London* **567**(1): 267-281.

Brophy JM (2005). Celecoxib and cardiovascular risks. *Expert opinion on drug safety* **4**(6): 1005-1015.

Brose SA, Thuen BT, Golovko MY (2011). LC/MS/MS method for analysis of E-2 series prostaglandins and isoprostanes. *Journal of Lipid Research* **52**(4): 850-859.

Buczynski MW, Dumlao DS, Dennis EA (2009). An integrated omics analysis of eicosanoid biology. *Journal of Lipid Research* **50**(6): 1015-1038.

Buczynski MW, Svensson CI, Dumlao DS, Fitzsimmons BL, Shim JH, Scherbart TJ, *et al.* (2010). Inflammatory hyperalgesia induces essential bioactive lipid production in the spinal cord. *Journal of Neurochemistry* **114**(4): 981-993.

Bunger M, van den Bosch HM, van der Meijde J, Kersten S, Hooiveld GJEJ, Muller M (2007). Genome-wide analysis of PPAR alpha activation in murine small intestine. *Physiological Genomics* **30**(2): 192-204.

Burnier M (2005). The safety of rofecoxib. *Expert opinion on drug safety* **4**(3): 491-499.

Capdevila JH, Falck JR, Dishman E, Karara A (1990). Cytochrome P450 arachidonate oxygenase. *Methods in Enzymology* **187**: 385-394.

Caraceni P, Viola A, Piscitelli F, Giannone F, Berzigotti A, Cescon M, *et al.* (2010). Circulating and hepatic endocannabinoids and endocannabinoid-related molecules in patients with cirrhosis. *Liver International* **30**(6): 816-825.

Caterina MJ, Julius D (2001). The vanilloid receptor: A molecular gateway to the pain pathway. *Annual Review of Neuroscience* **24**: 487-517.

Caterina MJ, Leffler A, Malmberg AB, Martin WJ, Trafton J, Petersen-Zeitz KR, *et al.* (2000). Impaired nociception and pain sensation in mice lacking the capsaicin receptor. *Science* **288**(5464): 306-313.

Caterina MJ, Schumacher MA, Tominaga M, Rosen TA, Levine JD, Julius D (1997). The capsaicin receptor: a heat-activated ion channel in the pain pathway.*Nature* **389**(6653): 816-824.

Chan CC, Boyce S, Brideau C, Fordhutchinson AW, Gordon R, Guay D, *et al.* (1995). Pharmacology of a selective cyclooxygenase-2 inhibitor,

L-745,337-a novel non-steroidal anti-inflammatory agent with an ulcerogenic sparing effect in rat and non-human primate stomach. *Journal of Pharmacology and Experimental Therapeutics* **274**(3): 1531-1537.

Chandran P, Pai M, Blomme EA, Hsieh GC, Decker MW, Honore P (2009). Pharmacological modulation of movement-evoked pain in a rat model of osteoarthritis. *European Journal of Pharmacology* **613**(1-3): 39-45.

Chapman CR, Casey KL, Dubner R, Foley KM, Gracely RH, Reading AE (1985). Pain measurement - an overview. *Pain* **22**(1): 1-31.

Chen J, Paudel KS, Derbenev AV, Smith BN, Stinchcomb AL (2009a). Simultaneous Quantification of Anandamide and Other Endocannabinoids in Dorsal Vagal Complex of Rat Brainstem by LC-MS. *Chromatographia* **69**(1-2): 1-7.

Chen J, Wang WZ, Lv S, Yin PY, Zhao XJ, Lu X, *et al.* (2009b). Metabonomics study of liver cancer based on ultra performance liquid chromatography coupled to mass spectrometry with HILIC and RPLC separations. *Analytica Chimica Acta* **650**(1): 3-9.

Chen JK, Chen JC, Imig JD, Wei S, Hachey DL, Guthi JS, *et al.* (2008). Identification of novel endogenous cytochrome P450 arachidonate metabolites with high affinity for cannabinoid receptors. *Journal of Biological Chemistry* **283**(36): 24496-24506.

Cho WG, Valtschanoff JG (2008). Vanilloid receptor TRPV1-positive sensory afferents in the mouse ankle and knee joints. *Brain Research* **1219**: 59-65.

Chopade AR, Mulla WA (2010). Novel strategies for the treatment of inflammatory hyperalgesia. *European Journal of Clinical Pharmacology* **66**(5): 429-444.

Christianson JA, McIlwrath SL, Koerber HR, Davis BM (2006). Transient receptor potential vanilloid 1-immunopositive neurons in the mouse are more prevalent within colon afferents compared to skin and muscle afferents. *Neuroscience* **140**(1): 247-257.

Chu KL, Chandran P, Joshi SK, Jarvis MF, Kym PR, McGaraughty S (2011). TRPV1-related modulation of spinal neuronal activity and behavior in a rat model of osteoarthritic pain. *Brain Research* **1369**: 158-166.

Clapham DE (2003). TRP channels as cellular sensors. *Nature* **426**(6966): 517-524.

Clayton N, Marshall FH, Bountra C, O'Shaughnessy CT (2002). CB1 and CB2 cannabinoid receptors are implicated in inflammatory pain. *Pain* **96**(3): 253-260.

Clements KM, Ball AD, Jones HB, Brinckmann S, Read SJ, Murray F (2009). Cellular and histopathological changes in the infrapatellar fat pad in the monoiodoacetate model of osteoarthritis pain. *Osteoarthritis and Cartilage* **17**(6): 805-812.

Combe R, Bramwell S, Field MJ (2004). The monosodium iodoacetate model of osteoarthritis: a model of chronic nociceptive pain in rats? *Neuroscience Letters***370**(2-3): 236-240.

Cortright DN, Szallasi A (2004). Biochemical pharmacology of the vanilloid receptor TRPV1 - An update. *European Journal of Biochemistry* **271**(10): 1814-1819.

Costa B, Comelli F, Bettoni I, Colleoni M, Giagnoni G (2008). The endogenous fatty acid amide, palmitoylethanolamide, has anti-allodynic and anti-hyperalgesic effects in a murine model of neuropathic pain: involvement of CB1, TRPV1 and PPAR gamma receptors and neurotrophic factors. *Pain* **139**(3):541-550.

Cowart LA, Wei SZ, Hsu MH, Johnson EF, Krishna MU, Falck JR, *et al.* (2002). The CYP4A Isoforms hydroxylate epoxyeicosatrienoic acids to form high affinity peroxisome proliferator-activated receptor ligands. *Journal of Biological Chemistry* **277**(38): 35105-35112.

Cui M, Honore P, Zhong C, Gauvin D, Mikusa J, Hernandez G, *et al.* (2006). TRPV1 receptors in the CNS play a key role in broad-spectrum analgesia of TRPV1 antagonists. *Journal of Neuroscience* **26**(37): 9385-9393.

Cullingford TE, Bhakoo K, Peuchen S, Dolphin CT, Patel R, Clark JB (1998). Distribution of mRNAs encoding the peroxisome proliferator-activated receptor alpha, beta and gamma and the retinoid X receptor alpha, beta and gamma rat central nervous system. *Journal of Neurochemistry* **70**(4): 1366-1375.

Cuzzocrea S, Mazzon E, Di Paola R, Peli A, Bonato A, Britti D, *et al.* (2006). The role of the peroxisome proliferator-activated receptor-alpha (PPAR-alpha) in the regulation of acute inflammation. *Journal of Leukocyte Biology* **79**(5): 999-1010.

D'Agostino G, La Rana G, Russo R, Sasso O, Iacono A, Esposito E, *et al.* (2009). Central administration of palmitoylethanolamide reduces hyperalgesia in mice via inhibition of NF-kappa B nuclear signalling in dorsal root ganglia. *European Journal of Pharmacology* **613**(1-3): 54-59.

Daaka Y, Klein TW, Friedman H (1995). Expression of cannabinoid receptor mRNA in murine and human leukocytes. *Brain Immune Axis and Substance Abuse***373:** 91-96.

Daret D, Blin P, Larrue J (1989). Synthesis of hydroxy fatty acids from linoleic acid by human blood platelets. *Prostaglandins* **38**(2)**:** 203-214.

Davis JB, Gray J, Gunthorpe MJ, Hatcher JP, Davey PT, Overend P, *et al.* (2000). Vanilloid receptor-1 is essential for inflammatory thermal hyperalgesia. *Nature***405**(6783)**:** 183-187.

Daviss B (2005). Growing pains for metabolomics. *Scientist* **19**(8)**:** 25-28.

de Grauw JC, van de Lest CHA, van Weeren PR (2011). A targeted lipidomics approach to the study of eicosanoid release in synovial joints. *Arthritis Research & Therapy* **13**(4)**:** 12.

De Petrocellis L, Melck D, Bisogno T, Di Marzo V (2000). Endocannabinoids and fatty acid amides in cancer, inflammation and related disorders. *Chemistry and Physics of Lipids* **108**(1-2)**:** 191-209.

Delerive P, De Bosscher K, Besnard S, Vanden Berghe W, Peters JM, Gonzalez FJ, *et al.* (1999). Peroxisome proliferator-activated receptor alpha negatively regulates the vascular inflammatory gene response by negative cross-talk with transcription factors NF-kappa B and AP-1. *Journal of Biological Chemistry***274**(45)**:** 32048-32054.

Delerive P, De Bosscher K, Vanden Berghe W, Fruchart JC, Haegeman G, Staels B (2002). DNA binding-independent induction of I kappa B alpha gene transcription by PPAR alpha. *Molecular Endocrinology* **16**(5)**:** 1029-1039.

Delerive P, Furman C, Teissier E, Fruchart JC, Duriez P, Staels B (2000a). Oxidized phospholipids activate PPAR alpha in a phospholipase A2-dependent manner. *Febs Letters* **471**(1)**:** 34-38.

Delerive P, Gervois P, Fruchart JC, Staels B (2000b). Induction of I kappa B alpha expression as a mechanism contributing to the anti-inflammatory activities of peroxisome proliferator-activated receptor-alpha activators. *Journal of Biological Chemistry* **275**(47)**:** 36703-36707.

Desvergne B, Wahli W (1999). Peroxisome proliferator-activated receptors: Nuclear control of metabolism. *Endocrine Reviews* **20**(5)**:** 649-688.

Devchand PR, Keller H, Peters JM, Vazquez M, Gonzalez FJ, Wahli W (1996). The PPAR alpha-leukotriene B-4 pathway to inflammation control. *Nature* **384**(6604)**:** 39-43.

Dewitt DL, Smith WL (1983). Purification of prostacyclin synthase from bovine aorta by immunoaffinity chromatography - evidence that the enzyme is a hemoprotein. *Journal of Biological Chemistry* **258**(5): 3285-3293.

Dhaka A, Viswanath V, Patapoutian A (2006). TRP ion channels and temperature sensation. In: (ed)^(eds). *Annual Review of Neuroscience*, edn, Vol. 29. Palo Alto: Annual Reviews. p^pp 135-161.

Di Marzo V, Bifulco M, De Petrocellis L (2004). The endocannabinoid system and its therapeutic exploitation. *Nature Reviews Drug Discovery* **3**(9): 771-784.

Di Rosa M, Giroud JP, Willoughby DA (1971). Studies of the mediators of the acute inflammatory response induced in rats in different sites by carrageenan and turpentine. *Journal of Pathology* **104**(1): 15-29.

Dieppe PA, Lohmander LS (2005). Pathogenesis and management of pain in osteoarthritis. *Lancet* **365**(9463): 965-973.

Dirosa M (1972). Biological properties of carrageenan. *Journal of Pharmacy and Pharmacology* **24**(2): 89-&.

Dowd PM, Black AK, Woollard PM, Camp RDR, Greaves MW (1985). Cutaneous responses to 12-hydroxy-5,8,10,14,-eicosatetraenoic acid (12-HETE). *Journal of Investigative Dermatology* **84**(6): 537-541.

Dowell P, Ishmael JE, Avram D, Peterson VJ, Nevrivy DJ, Leid M (1999). Identification of nuclear receptor corepressor as a peroxisome proliferator-activated receptor alpha interacting protein. *Journal of Biological Chemistry* **274**(22): 15901-15907.

Doyle DA, Lee A, Lewis J, Kim E, Sheng M, MacKinnon R (1996). Crystal structures of a complexed and peptide-free membrane protein-binding domain: Molecular basis of peptide recognition by PDZ. *Cell* **85**(7): 1067-1076.

Dubois RN, Abramson SB, Crofford L, Gupta RA, Simon LS, Van De Putte LBA, *et al.* (1998). Cyclooxygenase in biology and disease. *Faseb Journal* **12**(12):1063-1073.

Eckenfel.A, Vane JR (1972). Prostaglandins, oxygen-tension and smooth muscle tone. *British Journal of Pharmacology* **45**(3): 451-&.

Elmes SJR, Jhaveri MD, Smart D, Kendall DA, Chapman V (2004). Cannabinoid CB2 receptor activation inhibits mechanically evoked responses of wide dynamic range dorsal horn neurons in naive rats and in rat models of inflammatory and neuropathic pain. *European Journal of Neuroscience* **20**(9): 2311-2320.

Escher P, Wahli W (2000). Peroxisome proliferator-activated receptors: insight into multiple cellular functions. *Mutation Research-Fundamental and Molecular Mechanisms of Mutagenesis* **448**(2): 121-138.

Evans JF, Hutchinson JH (2010). Seeing the future of bioactive lipid drug targets. *Nature Chemical Biology* **6**(7): 476-479.

Farias SE, Basselin M, Chang L, Heidenreich KA, Rapoport SI, Murphy RC (2008). Formation of eicosanoids, E-2/D-2 isoprostanes, and docosanoids following decapitation-induced ischemia, measured in high-energy-microwaved rat brain. *Journal of Lipid Research* **49**(9): 1990-2000.

Farooqui AA, Horrocks LA, Farooqui T (2007). Modulation of inflammation in brain: a matter of fat. *Journal of Neurochemistry* **101**(3): 577-599.

Fegley D, Gaetani S, Duranti A, Tontini A, Mor M, Tarzia G, *et al.* (2005). Characterization of the fatty acid amide hydrolase inhibitor cyclohexyl carbamic acid 3 '-carbamoyl-biphenyl-3-yl ester (URB597): Effects on anandamide and oleoylethanolamide deactivation. *Journal of Pharmacology and Experimental Therapeutics* **313**(1): 352-358.

Feldberg W, Gupta KP (1973). Pyrogen fever and prostaglandin-like activity in cerebrospinal fluid. *Journal of Physiology-London* **228**(1): 41-53.

Feldberg W, Saxena PN (1971). Fever produced by prostaglandin-E1. *Journal of Physiology-London* **217**(3): 547-&.

Felder CC, Joyce KE, Briley EM, Mansouri J, Mackie K, Blond O, *et al.* (1995). Comparison of the pharmacology and signal-transduction of the human cannabinoid CB1 and CB2 receptors. *Molecular Pharmacology* **48**(3): 443-450.

Ferland CE, Laverty S, Beaudry F, Vachon P (2011). Gait analysis and pain response of two rodent models of osteoarthritis. *Pharmacology Biochemistry and Behavior* **97**(3): 603-610.

Fernandes JC, Martel-Pelletier J, Pelletier JP (2002). The role of cytokines in osteoarthritis pathophysiology. *Biorheology* **39**(1-2): 237-246.

Fernihough J, Gentry C, Malcangio M, Fox A, Rediske J, Pellas T, *et al.* (2004). Pain related behaviour in two models of osteoarthritis in the rat knee. *Pain***112**(1-2): 83-93.

Ferreira SH, Nakamura M, Castro M (1978). Hyperalgesic effects of prostacyclin and prostaglandin-E2. *Prostaglandins* **16**(1): 31-37.

Ferreira SH, Vane JR, Herman A (1972). Prostaglandin generation maintains smooth muscle tone of rabbit isolated jejunum. *British Journal of Pharmacology* **44**(2): P328-&.

Ferreiro-Vera C, Mata-Granados JM, Priego-Capote F, Quesada-Gomez JM, de Castro MDL (2011). Automated targeting analysis of eicosanoid inflammation biomarkers in human serum and in the exometabolome of stem cells by SPE-LC-MS/MS. *Analytical and Bioanalytical Chemistry* **399**(3): 1093-1103.

Fiehn O (2002). Metabolomics - the link between genotypes and phenotypes. *Plant Molecular Biology* **48**(1-2): 155-171.

Fiehn O, Kopka J, Dormann P, Altmann T, Trethewey RN, Willmitzer L (2000). Metabolite profiling for plant functional genomics. *Nature Biotechnology* **18**(11):1157-1161.

Fields HL, Heinricher MM (1985). Anatomy and physiology of a nociceptive modulatory system. *Philosophical Transactions of the Royal Society of London Series B-Biological Sciences* **308**(1136): 361-374.

Finn DP, Chapman V (2004). Cannabinoids as analgesic agents: Evidence from in vivo studies. *Current Neuropharmacology* **2**(1): 75-89.

Fleming I (2007). DiscrEET regulators of homeostasis: epoxyeicosatrienoic acids, cytochrome P450 epoxygenases and vascular inflammation. *Trends in Pharmacological Sciences* **28**(9): 448-452.

Flores CM, Vasko MR (2010). The Deorphanization of TRPV1 and the Emergence of Octadecadienoids as a New Class of Lipid Transmitters. *Molecular Interventions* **10**(3): 137-140.

Fonseca BM, Correia-da-Silva G, Taylor AH, Lam PMW, Marczylo TH, Konje JC, *et al.* (2010). N-Acylethanolamine Levels and Expression of Their Metabolizing Enzymes during Pregnancy. *Endocrinology* **151**(8): 3965-3974.

Forman BM, Chen J, Evans RM (1997). Hypolipidemic drugs, polyunsaturated fatty acids, and eicosanoids are ligands for peroxisome proliferator-activated receptors alpha and delta. *Proceedings of the National Academy of Sciences of the United States of America* **94**(9): 4312-4317.

Fosslien E (2000). Biochemistry of cyclooxygenase (COX)-2 inhibitors and molecular pathology of COX-2 in neoplasia. *Critical Reviews in Clinical Laboratory Sciences* **37**(5): 431-502.

Fowler CJ (2007). The contribution of cyclooxygenase-2 to endocannabinoid metabolism and action. *British Journal of Pharmacology* **152**(5): 594-601.

Fox A, Bevan S (2005). Therapeutic potential of cannabinoid receptor agonists as analgesic agents. *Expert Opinion on Investigational Drugs* **14**(6): 695-703.

Freund TF, Katona I, Piomelli D (2003). Role of endogenous cannabinoids in synaptic signaling. *Physiological Reviews* **83**(3): 1017-1066.

Fu J, Gaetani S, Oveisi F, Lo Verme J, Serrano A, de Fonseca FR, *et al.* (2003). Oleylethanolamide regulates feeding and body weight through activation of the nuclear receptor PPAR-alpha. *Nature* **425**(6953): 90-93.

Funk CD (2001). Prostaglandins and leukotrienes: Advances in eicosanoid biology. *Science* **294**(5548): 1871-1875.

Furst S (1999). Transmitters involved in antinociception in the spinal cord. *Brain Research Bulletin* **48**(2): 129-141.

Gabay C, Kushner I (1999). Mechanisms of disease: Acute-phase proteins and other systemic responses to inflammation. *New England Journal of Medicine***340**(6): 448-454.

Galiegue S, Mary S, Marchand J, Dussossoy D, Carriere D, Carayon P, *et al.* (1995). Expression of central and peripheral cannabinoid receptors in human immune tissues and leukocyte subpopulations. *European Journal of Biochemistry* **232**(1): 54-61.

Garscha U, Nilsson T, Oliw EH (2008). Enantiomeric separation and analysis of unsaturated hydroperoxy fatty acids by chiral column chromatography-mass spectrometry. *Journal of Chromatography B-Analytical Technologies in the Biomedical and Life Sciences* **872**(1-2): 90-98.

Gebhart GF (2004). Descending modulation of pain. *Neuroscience and Biobehavioral Reviews* **27**(8): 729-737.

Gibson HE, Edwards JG, Page RS, Van Hook MJ, Kauer JA (2008). TRPV1 channels mediate long-term depression at synapses on hippocampal interneurons.*Neuron* **57**(5): 746-759.

Giuffrida A, de Fonseca FR, Piomelli D (2000). Quantification of bioactive acylethanolamides in rat plasma by electrospray mass spectrometry. *Analytical Biochemistry* **280**(1): 87-93.

Gobezie R, Kho A, Krastins B, Sarracino DA, Thornhill TS, Chase M, *et al.* (2007). High abundance synovial fluid proteome: distinct profiles in health and osteoarthritis. *Arthritis Research & Therapy* **9**(2): 15.

Goetzl EJ, Brash AR, Tauber AI, Oates JA, Hubbard WC (1980a). Modulation of human neutrophil function by monohydroxy-eicosatetraenoic acids. *Immunology* **39**(4): 491-501.

Goetzl EJ, Goldman DW, Naccache PH, Shaafi RI, Pickett WC (1982). Mediation of leukocyte components of inflammatory reactions by lipoxygenase-products of arachidonic acid. *Advances in Prostaglandin Thromboxane and Leukotriene Research* **9**: 273-282.

Goetzl EJ, Pickett WC (1980b). The human-PMN leukocyte chemotactic activity of complex hydroxyl-eicosatetraenoic acids (HETEs). *Journal of Immunology* **125**(4): 1789-1791.

Gofflot F, Chartoire N, Vasseur L, Heikkinen S, Dembele D, Le Merrer J, *et al.* (2007). Systematic gene expression mapping clusters nuclear receptors according to their function in the brain. *Cell* **131**(2): 405-418.

Gold EW, Anderson LB, Schwartz ER, Miller CW (1976). Effect of salicylate on prostaglandin levels in rabbit knees following inducement of osteoarthritic changes. *Prostaglandins* **12**(5): 837-842.

Goldring MB, Otero M (2011). Inflammation in osteoarthritis. *Current Opinion in Rheumatology* **23**(5): 471-478.

Gong JP, Onaivi ES, Ishiguro H, Liu QR, Tagliaferro PA, Brusco A, *et al.* (2006). Cannabinoid CB2 receptors: Immunohistochemical localization in rat brain.*Brain Research* **1071**(1): 10-23.

Granneman J, Skoff R, Yang XY (1998). Member of the peroxisome proliferator-activated receptor family of transcription factors is differentially expressed by oligodendrocytes. *Journal of Neuroscience Research* **51**(5): 563-573.

Grotenhermen F (2005). Cannabinoids. *Current Drug Targets - CNS and Neurological Disorders* **4**(5): 507-530.

Gschwendt M, Furstenberger G, Kittstein W, Besemfelder E, Hull WE, Hagedorn H, *et al.* (1986). Generation of the arachidonic acid metabolites 8-HETE by extracts of mouse skin treated with phorbol ester in vivo-identification by H-1 NMR and GC-MS spectroscopy. *Carcinogenesis***7**(3): 449-455.

Gu SH, Jiye A, Wang GJ, Zha WB, Yan B, Zhang Y, *et al.* (2010). Metabonomic profiling of liver metabolites by gas chromatography-

mass spectrometry and its application to characterizing hyperlipidemia. *Biomedical Chromatography* **24**(3): 245-252.

Guay J, Bateman K, Gordon R, Mancini J, Riendeau D (2004). Carrageenan-induced paw edema in rat elicits a predominant prostaglandin E-2 (PGE(2)) response in the central nervous system associated with the induction of microsomal PGE(2) synthase-1. *Journal of Biological Chemistry* **279**(23): 24866-24872.

Guindon J, Guijarro A, Piomelli D, Hohmann AG (2011). Peripheral antinociceptive effects of inhibitors of monoacylglycerol lipase in a rat model of inflammatory pain. *British Journal of Pharmacology* **163**(7): 1464-1478.

Guzman RE, Evans MG, Bove S, Morenko B, Kilgore K (2003). Mono-iodoacetate-induced histologic changes in subchondral bone and articular cartilage of rat femorotibial joints: An animal model of osteoarthritis. *Toxicologic Pathology* **31**(6): 619-624.

Gwilym SE, Keltner JR, Warnaby CE, Carr AJ, Chizh B, Chessell I, *et al.* (2009). Psychophysical and Functional Imaging Evidence Supporting the Presence of Central Sensitization in a Cohort of Osteoarthritis Patients. *Arthritis & Rheumatism-Arthritis Care & Research* **61**(9): 1226-1234.

Hamberg M, Samuelss.B (1973). Detection and isolation of an endoperoxide intermediate in prostaglandin biosynthesis. *Proceedings of the National Academy of Sciences of the United States of America* **70**(3): 899-903.

Hammarstrom S, Orning L, Bernstrom K (1985). Metabolism of leukotrienes. *Molecular and Cellular Biochemistry* **69**(1): 7-16.

Hampson AJ, Grimaldi M (2002). 12-Hydroxyeicosatetrenoate (12-HETE) attenuates AMPA receptor-mediated neurotoxicity: Evidence for a G-protein-coupled HETE receptor. *Journal of Neuroscience* **22**(1): 257-264.

Hampson AJ, Hill WAG, Zanphillips M, Makriyannis A, Leung E, Eglen RM, *et al.* (1995). Anandamide hydroxylation by brain lipoxygenase - metabolite structures and potencies at the cannabinoid receptor. *Biochimica Et Biophysica Acta-Lipids and Lipid Metabolism* **1259**(2): 173-179.

Han XL, Gross RW (2005). Shotgun lipidomics: Electrospray ionization mass spectrometric analysis and quantitation of cellular lipidomes directly from crude extracts of biological samples. *Mass Spectrometry Reviews* **24**(3): 367-412.

Harada Y, Tanaka K, Uchida Y, Ueno A, Ohishi S, Yamashita K, *et al.* (1982). Changes in the levels of prostaglandins and thromboxane and their roles in the accumulation of exudate in rat carrageenan-induced pleurisy - a profile analysis using gas chromatography mass spectrometry. *Prostaglandins* **23**(6): 881-895.

Hardison S, Weintraub ST, Giuffrida A (2006). Quantification of endocannabinoids in rat biological samples by GC/MS: Technical and theoretical considerations.*Prostaglandins & Other Lipid Mediators* **81**(3-4): 106-112.

Hargreaves K, Dubner R, Brown F, Flores C, Joris J (1988). A new and sensitive method for measuring thermal nociception in cutaneous hyperalgesia. *Pain* **32**(1): 77-88.

Harizi H, Corcuff JB, Gualde N (2008). Arachidonic-acid-derived eicosanoids: roles in biology and immunopathology. *Trends in Molecular Medicine* **14**(10): 461-469.

Harizi H, Juzan M, Pitard V, Moreau JF, Gualde N (2002). Cyclooxygenase-2-issued prostaglandin E-2 enhances the production of endogenous IL-10, which down-regulates dendritic cell functions. *Journal of Immunology* **168**(5): 2255-2263.

Hata AN, Breyer RM (2004). Pharmacology and signaling of prostaglandin receptors: Multiple roles in inflammation and immune modulation. *Pharmacology & Therapeutics* **103**(2): 147-166.

Havrilla CM, Hachey DL, Porter NA (2000). Coordination (Ag+) ion spray-mass spectrometry of peroxidation products of cholesterol linoleate and cholesterol arachidonate: High-performance liquid chromatography-mass spectrometry analysis of peroxide products from polyunsaturated lipid autoxidation. *Journal of the American Chemical Society* **122**(33): 8042-8055.

Hayashi H, Fujii Y, Watanabe K, Urade Y, Hayaishi O (1989). Enzymatic conversion of prostaglandin-H2 to prostaglandin-F2-alpha by aldehyde reductase from human liver - comparison to the prostaglandin-F-synthetase from bovine lung. *Journal of Biological Chemistry* **264**(2): 1036-1040.

Hedo G, Laird JMA, Lopez-Garcia JA (1999). Time-course of spinal sensitization following carrageenan-induced inflammation in the young rat: A comparative electrophysiological and behavioural study in vitro and in vivo. *Neuroscience* **92**(1): 309-318.

Hemmila I, Webb S (1997). Time-resolved fluorometry: an overview of the labels and core technologies for drug screening applications. *Drug Discovery Today***2**(9): 373-381.

Herkenham M, Lynn AB, Johnson MR, Melvin LS, Decosta BR, Rice KC (1991). Characterisation and localisation of cannabinoid receptors in rat brain - a quantitative in vitro autoradiographic study. *Journal of Neuroscience* **11**(2): 563-583.

Herlin T, Fogh K, Ewald H, Hansen ES, Knudsen VE, Holm I, *et al.* (1988). Changes in lipoxygenase products from synovial fluid in carrageenan-induced arthritis in dogs. *Apmis* **96**(7): 601-604.

Hermann H, De Petrocellis L, Bisogno T, Moriello AS, Lutz B, Di Marzo V (2003). Dual effect of cannabinoid CB1 receptor stimulation on a vanilloid VR1 receptor-mediated response. *Cellular and Molecular Life Sciences* **60**(3): 607-616.

Higgs EA, Moncada S, Vane JR (1978). Inflammatory effects of prostacyclin (PGI2) and 6-oxo-PGF1-alpha in rat paw. *Prostaglandins* **16**(2): 153-162.

Hinson RM, Williams JA, Shacter E (1996). Elevated interleukin 6 is induced by prostaglandin E(2) in a murine model of inflammation: Possible role of cyclooxygenase-2. *Proceedings of the National Academy of Sciences of the United States of America* **93**(10): 4885-4890.

Hirai H, Tanaka K, Yoshie O, Ogawa K, Kenmotsu K, Takamori Y, *et al.* (2001). Prostaglandin D2 selectively induces chemotaxis in T helper type 2 cells, eosinophils, and basophils via seven-transmembrane receptor CRTH2. *Journal of Experimental Medicine* **193**(2): 255-261.

Hohmann AG, Suplita RL (2006). Endocannabinoid mechanisms of pain modulation. *Aaps Journal* **8**(4): E693-E708.

Holt S, Comelli F, Costa B, Fowler CJ (2005). Inhibitors of fatty acid amide hydrolase reduce carrageenan-induced hind paw inflammation in pentobarbital-treated mice: comparison with indomethacin and possible involvement of cannabinoid receptors. *British Journal of Pharmacology* **146**(3): 467-476.

Holzer P (2008). The pharmacological challenge to tame the transient receptor potential vanilloid-1 (TRPV1) nocisensor. *British Journal of Pharmacology***155**(8): 1145-1162.

Horrobin DF (1993). Fatty acid metabolism in health and disease - the role of delta-6-desaturase. *American Journal of Clinical Nutrition* **57**(5):S732-S737.

Houseknecht KL, Vanden Heuvel JP, Moya-Camarena SY, Portocarrero CP, Peck LW, Nickel KP, *et al.* (1998). Dietary conjugated linoleic acid normalizes impaired glucose tolerance in the Zucker diabetic fatty fa/fa

rat. *Biochemical and Biophysical Research Communications* **244**(3): 678-682.

Huang SM, Bisogno T, Trevisani M, Al-Hayani A, De Petrocellis L, Fezza F, *et al.* (2002). An endogenous capsaicin-like substance with high potency at recombinant and native vanilloid VR1 receptors. *Proceedings of the National Academy of Sciences of the United States of America* **99**(12): 8400-8405.

Huang SM, Strangman NM, Walker JM (1999). Liquid chromatographic-mass spectrometric measurement of the endogenous cannabinoid 2-arachidonylgiycerol in the spinal cord and peripheral nervous system. *Acta Pharmacologica Sinica* **20**(12): 1098-1102.

Hubbard NE, Lim D, Summers L, Erickson KL (2000). Reduction of murine mammary tumor metastasis by conjugated linoleic acid. *Cancer Letters* **150**(1): 93-100.

Huin C, Corriveau L, Bianchi A, Keller JM, Collet P, Kremarik-Bouillaud P, *et al.* (2000). Differential expression of peroxisome proliferator-activated receptors (PPARs) in the developing human fetal digestive tract. *Journal of Histochemistry & Cytochemistry* **48**(5): 603-611.

Hunt SP, Mantyh PW (2001). The molecular dynamics of pain control. *Nature Reviews Neuroscience* **2**(2): 83-91.

Hwang SJ, Oh JM, Valtschanoff JG (2005). Expression of the vanilloid receptor TRPV1 in rat dorsal root ganglion neurons supports different roles of the receptor in visceral and cutaneous afferents. *Brain Research* **1047**(2): 261-266.

Hwang SW, Cho H, Kwak J, Lee SY, Kang CJ, Jung J, *et al.* (2000). Direct activation of capsaicin receptors by products of lipoxygenases: Endogenous capsaicin-like substances. *Proceedings of the National Academy of Sciences of the United States of America* **97**(11): 6155-6160.

Ijiri K, Zerbini LF, Peng H, Otu HH, Tsuchimochi K, Otero M, *et al.* (2008). Differential expression of GADD45 beta in normal and osteoarthritic cartilage - Potential role in homeostasis of articular chondrocytes. *Arthritis and Rheumatism* **58**(7): 2075-2087.

Ijpenberg A, Jeannin E, Wahli W, Desvergne B (1997). Polarity and specific sequence requirements of peroxisome proliferator-activated receptor (PPAR) retinoid X receptor heterodimer binding to DNA - A functional analysis of the malic enzyme gene PPAR response element. *Journal of Biological Chemistry***272**(32): 20108-20117.

Iliff JJ, Fairbanks SL, Balkowiec A, Alkayed NJ (2010). Epoxyeicosatrienoic acids are endogenous regulators of vasoactive

neuropeptide release from trigeminal ganglion neurons. *Journal of Neurochemistry* **115**(6): 1530-1542.

Iliopoulos D, Malizos KN, Oikonomou P, Tsezou A (2008). Integrative MicroRNA and Proteomic Approaches Identify Novel Osteoarthritis Genes and Their Collaborative Metabolic and Inflammatory Networks. *Plos One* **3**(11): 10.

Im HJ, Kim JS, Li X, Kotwal N, Sumner DR, van Wijnen AJ, *et al.* (2010). Alteration of Sensory Neurons and Spinal Response to an Experimental Osteoarthritis Pain Model. *Arthritis and Rheumatism* **62**(10): 2995-3005.

Imhof BA, Aurrand-Lions M (2004). Adhesion mechanisms regulating the migration of monocytes. *Nature Reviews Immunology* **4**(6): 432-444.

Inceoglu B, Jinks SL, Ulu A, Hegedus CM, Georgi K, Schmelzer KR, *et al.* (2008). Soluble epoxide hydrolase and epoxyeicosatrienoic acids modulate two distinct analgesic pathways. *Proceedings of the National Academy of Sciences of the United States of America* **105**(48): 18901-18906.

Inceoglu B, Schmelzer K, Jinks S, Waite T, Hammock B (2006). Soluble epoxide hydrolase inhibitors and/or epoxyeicosatrianoic acids attenuate hyperalgesia and allodynia in a rat model. *Faseb Journal* **20**(4): A687-A687.

Inceoglu B, Schmelzer KR, Morisseau C, Jinks SL, Hammock BD (2007). Soluble epoxide hydrolase inhibition reveals novel biological functions of epoxyeicosatrienoic acids (EETs). *Prostaglandins & Other Lipid Mediators* **82**(1-4): 42-49.

Ip C, Dong Y, Thompson HJ, Bauman DE, Ip MM (2001). Control of rat mammary epithelium proliferation by conjugated linoleic acid. *Nutrition and Cancer-an International Journal* **39**(2): 233-238.

Jean-Gilles L, Feng S, Tench CR, Chapman V, Kendall DA, Barrett DA, *et al.* (2009). Plasma endocannabinoid levels in multiple sclerosis. *Journal of the Neurological Sciences* **287**(1-2): 212-215.

Jemal M (2000). High-throughput quantitative bioanalysis by LC/MS/MS. *Biomedical Chromatography* **14**(6): 422-429.

Jeon SG, Moon HG, Kim YS, Choi JP, Shin TS, Hong SW, *et al.* (2009). 15-lipoxygenase metabolites play an important role in the development of a T-helper type 1 allergic inflammation induced by double-stranded RNA. *Clinical and Experimental Allergy* **39**(6): 908-917.

Jhaveri MD, Elmes SJR, Kendall DA, Chapman V (2005). Inhibition of peripheral vanilloid TRPV1 receptors reduces noxious heat-evoked responses of dorsal horn neurons in naive, carrageenan-inflamed and neuropathic rats. *European Journal of Neuroscience* **22**(2): 361-370.

Jhaveri MD, Elmes SJR, Richardson D, Barrett DA, Kendall DA, Mason R, *et al.* (2008a). Evidence for a novel functional role of cannabinoid CB2 receptors in the thalamus of neuropathic rats. *European Journal of Neuroscience* **27**(7): 1722-1730.

Jhaveri MD, Richardson D, Kendall DA, Barrett DA, Chapman V (2006). Analgesic effects of fatty acid amide hydrolase inhibition in a rat model of neuropathic pain. *Journal of Neuroscience* **26**(51): 13318-13327.

Jhaveri MD, Richardson D, Robinson I, Garle MJ, Patel A, Sun Y, *et al.* (2008b). Inhibition of fatty acid amide hydrolase and cyclooxygenase-2 increases levels of endocannabinoid related molecules and produces analgesia via peroxisome proliferator-activated receptor-alpha in a model of inflammatory pain.*Neuropharmacology* **55**(1): 85-93.

Ji RR, Kohno T, Moore KA, Woolf CJ (2003). Central sensitization and LTP: do pain and memory share similar mechanisms? *Trends in Neurosciences* **26**(12):696-705.

Ji RR, Samad TA, Jin SX, Schmoll R, Woolf CJ (2002). p38 MAPK activation by NGF in primary sensory neurons after inflammation increases TRPV1 levels and maintains heat hyperalgesia. *Neuron* **36**(1): 57-68.

Jiang HL, McGiff JC, Quilley J, Sacerdoti D, Reddy LM, Falck JR, *et al.* (2004). Identification of 5,6-trans-epoxyeicosatrienoic acid in the phospholipids of red blood cells. *Journal of Biological Chemistry* **279**(35): 36412-36418.

Johnson HG, McNee ML, Sun FF (1985). 15-Hydroxyeicosatetraenoic acid is a potent inflammatory mediator and agonist of canine tracheal mucus secretion. *American Review of Respiratory Disease* **131**(6): 917-922.

Jonsson KO, Holt S, Fowler CJ (2006). The endocannabinoid system: Current pharmacological research and therapeutic possibilities. *Basic & Clinical Pharmacology & Toxicology* **98**(2): 124-134.

Julius D, Basbaum AI (2001). Molecular mechanisms of nociception. *Nature* **413**(6852): 203-210.

Kajihara Y, Murakami M, Imagawa T, Otsuguro K, Ito S, Ohta T (2010). Histamine potentiates acid-induced responses mediating

transient receptor potential V1 in mouse primary sensory neurons. *Neuroscience* **166**(1): 292-304.

Kaley G, Hintze TH, Panzenbeck M, Messina EJ (1985). Role of prostaglandins in microcirculatory function. *Serneri, G. G. N. Et Al. (Ed.). Advances in Prostaglandin Thromboxane and Leukotriene Research, Vol. 13. Platelets, Prostaglandins, and the Cardiovascular System; Meeting, Florence, Italy, Feb., 1984. Xxviii+393p. Raven Press: New York, N.Y., USA. Illus*: 27-36.

Kanai Y, Hara T, Imai A, Sakakibara A (2007). Differential involvement of TRPV1 receptors at the central and peripheral nerves in CFA-induced mechanical and thermal hyperalgesia. *Journal of Pharmacy and Pharmacology* **59**(5): 733-738.

Kanani H, Chrysanthopoulos PK, Klapa MI (2008). Standardizing GC-MS metabolomics. *Journal of Chromatography B-Analytical Technologies in the Biomedical and Life Sciences* **871**(2): 191-201.

Kanicky JR, Shah DO (2002). Effect of degree, type, and position of unsaturation on the pK(a) of long-chain fatty acids. *Journal of Colloid and Interface Science* **256**(1): 201-207.

Kaplan K, Dwivedi P, Davidson S, Yang Q, Tso P, Siems W, *et al.* (2009). Monitoring Dynamic Changes in Lymph Metabolome of Fasting and Fed Rats by Electrospray Ionization-Ion Mobility Mass Spectrometry (ESI-IMMS). *Analytical Chemistry* **81**(19): 7944-7953.

Kaufmann WE, Andreasson KL, Isakson PC, Worley PF (1997). Cyclooxygenases and the central nervous system. *Prostaglandins & Other Lipid Mediators* **54**(3):601-624.

Keeble JE, Bodkin JV, Liang LH, Wodarski R, Davies M, Fernandes ES, *et al.* (2009). Hydrogen peroxide is a novel mediator of inflammatory hyperalgesia, acting via transient receptor potential vanilloid 1-dependent and independent mechanisms. *Pain* **141**(1-2): 135-142.

Kelly S, Chapman V (2002). Spinal administration of capsazepine inhibits noxious evoked responses of dorsal horn neurons in non-inflamed and carrageenan inflamed rats. *Brain Research* **935**(1-2): 103-108.

Khanapure SP, Garvey DS, Janero DR, Letts LG (2007). Eicosanoids in inflammation: Biosynthesis, pharmacology, and therapeutic frontiers. *Current Topics in Medicinal Chemistry* **7**(3): 311-340.

Kidd BL, Langford RM, Wodehouse T (2007). Arthritis and pain - Current approaches in the treatment of arthritic pain. *Arthritis Research & Therapy* **9**(3): 7.

Kidd BL, Urban LA (2001). Mechanisms of inflammatory pain. *British Journal of Anaesthesia* **87**(1): 3-11.

Kihara Y, Matsushita T, Kita Y, Uematsu S, Akira S, Kira J, *et al.* (2009). Targeted lipidomics reveals mPGES-1-PGE2 as a therapeutic target for multiple sclerosis. *Proceedings of the National Academy of Sciences of the United States of America* **106**(51): 21807-21812.

Kikuchi K, Itoh Y, Tateoka R, Ezawa A, Murakami K, Niwa T (2010). Metabolomic analysis of uremic toxins by liquid chromatography/electrospray ionization-tandem mass spectrometry. *Journal of Chromatography B-Analytical Technologies in the Biomedical and Life Sciences* **878**(20): 1662-1668.

Kilaru A, Isaac G, Tamura P, Baxter D, Duncan SR, Venables BJ, *et al.* (2010). Lipid Profiling Reveals Tissue-Specific Differences for Ethanolamide Lipids in Mice Lacking Fatty Acid Amide Hydrolase. *Lipids* **45**(9): 863-875.

Kim SR, Bok E, Chung YC, Chung ES, Jin BK (2008). Interactions between CB1 receptors and TRPV1 channels mediated by 12-HPETE are cytotoxic to mesencephalic dopaminergic neurons. *British Journal of Pharmacology* **155**(2): 253-264.

King R, Bonfiglio R, Fernandez-Metzler C, Miller-Stein C, Olah T (2000). Mechanistic investigation of ionization suppression in electrospray ionization. *Journal of the American Society for Mass Spectrometry* **11**(11): 942-950.

Kingsley PJ, Marnett LJ (2007). LC-MS-MS analysis of neutral eicosanoids. In: (ed)^(eds). *Lipidomics and Bioactive Lipids*, edn, Vol. 433. San Diego: Elsevier Academic Press Inc. p^pp 91-+.

Kitchen EA, Boot JR, Dawson W (1978). Chemotactic activity of thromboxane B2, prostaglandins and their metabolites for polymorphonuclear leukocytes. *Prostaglandins* **16**(2): 239-244.

Kittlaus S, Schimanke J, Kempe G, Speer K (2011). Assessment of sample cleanup and matrix effects in the pesticide residue analysis of foods using postcolumn infusion in liquid chromatography-tandem mass spectrometry. *Journal of Chromatography A* **1218**(46): 8399-8410.

Klein RF, Allard J, Avnur Z, Nikolcheva T, Rotstein D, Carlos AS, *et al.* (2004). Regulation of bone mass in mice by the lipoxygenase gene Alox15. *Science***303**(5655): 229-232.

Kliewer SA, Sundseth SS, Jones SA, Brown PJ, Wisely GB, Koble CS, *et al.* (1997). Fatty acids and eicosanoids regulate gene expression

through direct interactions with peroxisome proliferator-activated receptors alpha and gamma. *Proceedings of the National Academy of Sciences of the United States of America* **94**(9): 4318-4323.

Kobayashi K, Imaizumi R, Sumichika H, Tanaka H, Goda M, Fukunari A, *et al.* (2003). Sodium iodoacetate-induced experimental osteoarthritis and associated pain model in rats. *Journal of Veterinary Medical Science* **65**(11): 1195-1199.

Koeberle A, Werz O (2009). Inhibitors of the Microsomal Prostaglandin E(2) Synthase-1 as Alternative to Non Steroidal Anti-Inflammatory Drugs (NSAIDs) - A Critical Review. *Current Medicinal Chemistry* **16**(32): 4274-4296.

Koltzenburg M, Torebjork HE, Wahren LK (1994). Nociceptor modulated central sensitisation causes mechanical hyperalgesia in acute chemogenic and chronic neuropathic pain. *Brain* **117**: 579-591.

Komaba J, Matsuda D, Shibakawa K, Nakade S, Hashimoto Y, Miyata Y, *et al.* (2009). Development and validation of an on-line two-dimensional reversed-phase liquid chromatography-tandem mass spectrometry method for the simultaneous determination of prostaglandins E-2 and F-2 alpha and 13, 14-dihydro-15-keto prostaglandin F-2 alpha levels in human plasma. *Biomedical Chromatography* **23**(3): 315-323.

Komoriya K, Ohmori H, Azuma A, Kurozumi S, Hashimoto Y (1978). Prostaglandin-I2 as a potentiator of acute inflammation in rats. *Prostaglandins* **15**(4): 557-564.

Kortz L, Geyer R, Ludwig U, Planert M, Bruegel M, Leichtle A, *et al.* (2009). Simultaneous eicosanoid profiling and identification by liquid chromatography and hybrid triple quadrupole-linear ion trap mass spectrometry for metabolomic studies in human plasma. *Laboratoriumsmedizin-Journal of Laboratory Medicine***33**(6): 341-348.

Krarup AL, Ny L, Astrand M, Bajor A, Hvid-Jensen F, Hansen MB, *et al.* (2011). Randomised clinical trial: the efficacy of a transient receptor potential vanilloid 1 antagonist AZD1386 in human oesophageal pain. *Alimentary Pharmacology & Therapeutics* **33**(10): 1113-1122.

Krey G, Braissant O, Lhorset F, Kalkhoven E, Perroud M, Parker MG, *et al.* (1997). Fatty acids, eicosanoids, and hypolipidemic agents identified as ligands of peroxisome proliferator-activated receptors by coactivator-dependent receptor ligand assay. *Molecular Endocrinology* **11**(6): 779-791.

Kuhn H, O'Donnell VB (2006). Inflammation and immune regulation by 12/15-lipoxygenases. *Progress in Lipid Research* **45**(4): 334-356.

Kunkel SL, Spengler M, May MA, Spengler R, Larrick J, Remick D (1988). Prostaglandin-E2 regulates macrophage-derived tumour necrosis factor gene expression. *Journal of Biological Chemistry* **263**(11): 5380-5384.

Labianca R, Sarzi-Puttini P, Zuccaro SM, Cherubino P, Vellucci R, Fornasari D (2012). Adverse Effects Associated with Non-opioid and Opioid Treatment in Patients with Chronic Pain. *Clinical drug investigation* **32 Suppl 1:** 53-63.

Lam BK, Gagnon L, Austen KF, Soberman RJ (1990). The mechanism of leukotriene-B4 export from human polymorphonuclear leukocytes. *Journal of Biological Chemistry* **265**(23): 13438-13441.

Lam PMW, Marczylo TH, El-Talatini M, Finney M, Nallendran V, Taylor AH, *et al.* (2008). Ultra performance liquid chromatography tandem mass spectrometry method for the measurement of anandamide in human plasma. *Analytical Biochemistry* **380**(2): 195-201.

Larsen BT, Gutterman DD, Hatoum OA (2006). Emerging role of epoxyeicosatrienoic acids in coronary vascular function. *European Journal of Clinical Investigation* **36**(5): 293-300.

Larsen GL, Henson PM (1983). Mediators of inflammation. *Annual Review of Immunology* **1:** 335-359.

Law WS, Huang PY, Ong ES, Ong CN, Li SFY, Pasikanti KK, *et al.* (2008). Metabonomics investigation of human urine after ingestion of green tea with gas chromatography/mass spectrometry, liquid chromatography/mass spectrometry and H-1 NMR spectroscopy. *Rapid Communications in Mass Spectrometry***22**(16): 2436-2446.

Lawrence T (2002). Modulation of inflammation in vivo through induction of the heat shock response, effects on NF-kappa B activation. *Inflammation Research***51**(2): 108-109.

Lee MC, Zambreanu L, Menon DK, Tracey I (2008). Identifying Brain Activity Specifically Related to the Maintenance and Perceptual Consequence of Central Sensitization in Humans. *Journal of Neuroscience* **28**(45): 11642-11649.

Lehtonen M, Storvik M, Malinen H, Hyytia P, Lakso M, Auriola S, *et al.* (2011). Determination of endocannabinoids in nematodes and human brain tissue by liquid chromatography electrospray ionization tandem mass spectrometry. *Journal of Chromatography B-Analytical Technologies in the Biomedical and Life Sciences* **879**(11-12): 677-694.

Leier I, Jedlitschky G, Buchholz U, Keppler D (1994). Characterisation of the ATP-dependent leukotriene C4 export carrier in mastocytoma cells. *European Journal of Biochemistry* **220**(2): 599-606.

Lenz EM, Wilson ID (2007). Analytical strategies in metabonomics. *Journal of Proteome Research* **6**(2): 443-458.

Leon A, Buriani A, Daltoso R, Fabris M, Romanello S, Aloe L, *et al.* (1994). Mast cells synthesise, store and release nerve growth factor. *Proceedings of the National Academy of Sciences of the United States of America* **91**(9): 3739-3743.

Lewis AJ, Nelson DJ, Sugrue MF (1975). Ability of prostaglandin-E1 and arachidonic acid to modulate experimentally induced oedema in rat paw. *British Journal of Pharmacology* **55**(1): 51-56.

Lewis RA, Austen KF, Drazen JM, Clark DA, Marfat A, Corey EJ (1980). Slow reacting substances of anaphylaxis - identification of leukotrienes-C1 and leukotrienes-D from human and rat sources. *Proceedings of the National Academy of Sciences of the United States of America-Biological Sciences* **77**(6): 3710-3714.

Liminga M, Oliw E (2000). Qualitative and quantitative analysis of lipoxygenase products in bovine corneal epithelium by liquid chromatography-mass spectrometry with an ion trap. *Lipids* **35**(2): 225-232.

Lin C-R, Amaya F, Barrett L, Wang H, Takada J, Samad TA, *et al.* (2006). Prostaglandin E-2 receptor EP4 contributes to inflammatory pain hypersensitivity.*Journal of Pharmacology and Experimental Therapeutics* **319**(3): 1096-1103.

Lin QO, Ruuska SE, Shaw NS, Dong D, Noy N (1999). Ligand selectivity of the peroxisome proliferator-activated receptor alpha. *Biochemistry* **38**(1): 185-190.

Lin SY, Khanolkar AD, Fan PS, Goutopoulos A, Qin C, Papahadjis D, *et al.* (1998). Novel analogues of arachidonylethanolamide (anandamide): Affinities for the CB1 and CB2 cannabinoid receptors and metabolic stability. *Journal of Medicinal Chemistry* **41**(27): 5353-5361.

Lindon JC, Nicholson JK (2008). Analytical technologies for metabonomics and metabolomics, and multi-omic information recovery. *Trac-Trends in Analytical Chemistry* **27**(3): 194-204.

Lindsay RM (1988). Nerve growth factors (NGF, BDNF) enhance axonal regeneration but are not required for survival of adult sensory neurons. *Journal of Neuroscience* **8**(7): 2394-2405.

Lo Verme J, Fu J, Astarita G, La Rana G, Russo R, Calignano A, *et al.* (2005a). The nuclear receptor peroxisome proliferator-activated receptor-alpha mediates the anti-inflammatory actions of palmitoylethanolamide. *Molecular Pharmacology* **67**(1): 15-19.

Lo Verme J, Fu J, Astarita G, La Rana G, Russo R, Calignano A, *et al.* (2005b). The nuclear receptor peroxisome proliferator-activated receptor-alpha mediates the anti-inflammatory actions of palmitoylethanolamide. *Molecular Pharmacology* **67**(1): 15-19.

Loeser JD, Melzack R (1999). Pain: an overview. *Lancet* **353**(9164): 1607-1609.

Lopshire JC, Nicol GD (1998). The cAMP transduction cascade mediates the prostaglandin E-2 enhancement of the capsaicin-elicited current in rat sensory neurons: Whole-cell and single-channel studies. *Journal of Neuroscience* **18**(16): 6081-6092.

Loram LC, Fuller A, Fick LG, Cartmell T, Poole S, Mitchell D (2007). Cytokine profiles during carrageenan-induced inflammatory hyperalgesia in rat muscle and hind paw. *Journal of Pain* **8**(2): 127-136.

LoVerme J, Russo R, La Rana G, Fu J, Farthing J, Mattace-Raso G, *et al.* (2006). Rapid broad-spectrum analgesia through activation of peroxisome proliferator-activated receptor-alpha. *Journal of Pharmacology and Experimental Therapeutics* **319**(3): 1051-1061.

Ludanyi A, Hu SJ, Yamazaki M, Tanimura A, Piomelli D, Watanabe M, *et al.* (2011). Complementary synaptic distribution of enzymes responsible for synthesis and inactivation of the endocannabinoid 2-arachidonoyl glycerol in the human hippocampus. *Neuroscience* **174**: 50-63.

Lundstrom SL, D'Alexandri FL, Nithipatikom K, Haeggstrom JZ, Wheelock AM, Wheelock CE (2009). HPLC/MS/MS-Based Approaches for Detection and Quantification of Eicosanoids. In: Armstrong D (ed)^(eds). *Lipidomics: Vol 1: Methods and Protocols*, edn: Humana Press Inc. p^pp 161-187.

Luo M, Jones SM, Phare SM, Coffey MJ, Peters-Golden M, Brock TG (2004). Protein kinase A inhibits leukotriene synthesis by phosphorylation of 5-lipoxygenase on Serine 523. *Journal of Biological Chemistry* **279**(40): 41512-41520.

Lynch KR, O'Neill GP, Liu QY, Im DS, Sawyer N, Metters KM, *et al.* (1999). Characterization of the human cysteinyl leukotriene CysLT(1) receptor. *Nature***399**(6738): 789-793.

MacMillan DK, Murphy RC (1995). Analysis of lipid hydroperoxides and long-chain conjugated keto acids by negative ion electrospray mass spectrometry.*Journal of the American Society for Mass Spectrometry* **6**(12): 1190-1201.

Main IHM (1964). Inhibitory actions of prostaglandins on respiratory smooth muscle. *British Journal of Pharmacology and Chemotherapy* **22**(3):511-&.

Malinen H, Lehtonen M, Hyytia P (2009). Modulation of Brain Endocannabinoid Levels by Voluntary Alcohol Consumption in Alcohol-Preferring AA Rats.*Alcoholism-Clinical and Experimental Research* **33**(10): 1711-1720.

Malmberg AB, Brandon EP, Idzerda RL, Liu HT, McKnight GS, Basbaum AI (1997). Diminished inflammation and nociceptive pain with preservation of neuropathic pain in mice with a targeted mutation of the type I regulatory subunit of cAMP-dependent protein kinase. *Journal of Neuroscience* **17**(19): 7462-7470.

Marcheselli VL, Hong S, Lukiw WJ, Tian XH, Gronert K, Musto A, *et al.* (2003). Novel docosanoids inhibit brain ischemia-reperfusion-mediated leukocyte infiltration and pro-inflammatory gene expression. *Journal of Biological Chemistry* **278**(44): 43807-43817.

Margalit A, Duffin KL, Isakson PC (1996). Rapid quantitation of a large scope of eicosanoids in two models of inflammation: Development of an electrospray and tandem mass spectrometry method and application to biological studies. *Analytical Biochemistry* **235**(1): 73-81.

Marinelli S, Pascucci T, Bernardi G, Puglisi-Allegra S, Mercuri NB (2005). Activation of TRPV1 in the VTA excites dopaminergic neurons and increases chemical-and noxious-induced dopamine release in the nucleus accumbens. *Neuropsychopharmacology* **30**(5): 864-870.

Marowsky A, Burgener J, Falck JR, Fritschy JM, Arand M (2009). Distribution of soluble and microsomal epoxide hydrolase in the mouse brain and its contribution to cerebral epoxyeicosatrienoic acid. *Neuroscience* **163**(2): 646-661.

Martin-Venegas R, Casillas R, Jauregui O, Jose Moreno J (2011). Rapid simultaneous analysis of cyclooxygenase, lipoxygenase and cytochrome P-450 metabolites of arachidonic and linoleic acids using high performance liquid chromatography/mass spectrometry in tandem mode. *Journal of Pharmaceutical and Biomedical Analysis* **56**(5): 976-982.

Marx N, Sukhova GK, Collins T, Libby P, Plutzky J (1999). PPAR alpha activators inhibit cytokine-induced vascular cell adhesion molecule-1 expression in human endothelial cells. *Circulation* **99**(24): 3125-3131.

Masoodi M, Eiden M, Koulman A, Spaner D, Volmer DA (2010). Comprehensive Lipidomics Analysis of Bioactive Lipids in Complex Regulatory Networks.*Analytical Chemistry* **82**(19): 8176-8185.

Masoodi M, Mir AA, Petasis NA, Serhan CN, Nicolaou A (2008). Simultaneous lipidomic analysis of three families of bioactive lipid mediators leukotrienes, resolvins, protectins and related hydroxy-fatty acids by liquid chromatography/electrospray ionisation tandem mass spectrometry. *Rapid Communications in Mass Spectrometry* **22**(2): 75-83.

Matias I, Chen J, De Petrocellis L, Bisogno T, Ligresti A, Fezza F, *et al.* (2004). Prostaglandin ethanolamides (prostamides): In vitro pharmacology and metabolism. *Journal of Pharmacology and Experimental Therapeutics* **309**(2): 745-757.

Matsuda LA, Lolait SJ, Brownstein MJ, Young AC, Bonner TI (1990). Structure of a cannabinoid receptor and functional expression of the cloned CDNA. *Nature* **346**(6284): 561-564.

Matuszewski BK, Constanzer ML, Chavez-Eng CM (2003). Strategies for the assessment of matrix effect in quantitative bioanalytical methods based on HPLC-MS/MS. *Analytical Chemistry* **75**(13): 3019-3030.

Mazzari S, Canella R, Petrelli L, Marcolongo G, Leon A (1996). N-(2-Hydroxyethyl)hexadecanamide is orally active in reducing edema formation and inflammatory hyperalgesia by down-modulating mast cell activation. *European Journal of Pharmacology* **300**(3): 227-236.

Mbvundula EC, Rainsford KD, Bunning RAD (2004). Cannabinoids in pain and inflammation. *Inflammopharmacology* **12**(2): 99-114.

McAdam BF, Mardini IA, Habib A, Burke A, Lawson JA, Kapoor S, *et al.* (2000). Effect of regulated expression of human cyclooxygenase isoforms on eicosanoid and isoeicosanoid production in inflammation. *Journal of Clinical Investigation* **105**(10): 1473-1482.

McMaster MC (2005). LC/MS: A Practical User's Guide, First Edition, Wiley, New Jersey.

Mechoulam R, Benshabat S, Hanus L, Ligumsky M, Kaminski NE, Schatz AR, *et al.* (1995). Identification of an endogenous 2-monoglyceride, present in canine gut, that binds to cannabinoid receptors. *Biochemical Pharmacology* **50**(1): 83-90.

Merskey H (1999). Mechanisms and the classification of pain. *Pain* **82**(3): 319-320.

Meves H (2008). Arachidonic acid and ion channels: an update. *British Journal of Pharmacology* **155**(1): 4-16.

Mezey E, Toth ZE, Cortright DN, Arzubi MK, Krause JE, Elde R, *et al.* (2000). Distribution of mRNA for vanilloid receptor subtype 1 (VR1), and VR1-like immunoreactivity, in the central nervous system of the rat and human. *Proceedings of the National Academy of Sciences of the United States of America***97**(7): 3655-3660.

Michalik L, Wahli W (1999). Peroxisome proliferator-activated receptors: three isotypes for a multitude of functions. *Current Opinion in Biotechnology* **10**(6):564-570.

Millan MJ (2002). Descending control of pain. *Progress in Neurobiology* **66**(6): 355-474.

Millns PJ, Chapman V, Kendall DA (2001). Cannabinoid inhibition of the capsaicin-induced calcium response in rat dorsal root ganglion neurones. *British Journal of Pharmacology* **132**(5): 969-971.

Milton AS, Wendland.S (1971). Effects on body temperature of prostaglandins of A, E and F series on injection into third ventricle of unanaesthetised cats and rabbits. *Journal of Physiology-London* **218**(2): 325-&.

Minami M, Kawasaki H, Samuelsson B, Shimizu T, Suzuki K, Ohno S, *et al.* (1987). Molecular cloning of a CDNA coding for human leukocyte-A4 hydrolase - complete primary structure of an enzyme involved in eicosanoid synthesis. *Journal of Biological Chemistry* **262**(29): 13873-13876.

Minami T, Nakano H, Kobayashi T, Sugimoto Y, Ushikubi F, Ichikawa A, *et al.* (2001). Characterization of EP receptor subtypes responsible for prostaglandin E2-induced pain responses by use of EP1 and EP3 receptor knockout mice. *British Journal of Pharmacology* **133**(3): 438-444.

Minami T, Uda R, Horiguchi S, Ito S, Hyodo M, Hayaishi O (1992). Allodynia evoked by intrathecal administration of prostaglandin-F2-alpha to conscious mice. *Pain* **50**(2): 223-229.

Minuz P, Jiang H, Fava C, Turolo L, Tacconelli S, Ricci M, *et al.* (2008). Altered release of cytochrome p450 metabolites of arachidonic acid in renovascular disease. *Hypertension* **51**(5): 1379-1385.

Mitrirattanakul S, Lopez-Valdes HE, Liang J, Matsuka Y, Mackie K, Faull KF, *et al.* (2007). Bidirectional alterations of hippocampal cannabinoid

1 receptors and their endogenous ligands in a rat model of alcohol withdrawal and dependence. *Alcoholism-Clinical and Experimental Research* **31**(5): 855-867.

Mitrirattanakul S, Ramakul N, Guerrero AV, Matsuka Y, Ono T, Iwase H, *et al.* (2006). Site-specific increases in peripheral cannabinoid receptors and their endogenous ligands in a model of neuropathic pain. *Pain* **126**(1-3): 102-114.

Mitsuhashi T, Ikata T, Morimoto K, Tonai T, Katoh S (1994). Increased production of eicosanoids, TXA2, PGI2 AND LTC4 in experimental spinal cord injuries. *Paraplegia* **32**(8): 524-530.

Mogil JS (2009). Animal models of pain: progress and challenges. *Nature Reviews Neuroscience* **10**(4): 283-294.

Mohapatra DP, Nau C (2005). Regulation of Ca2+-dependent desensitization in the vanilloid receptor TRPV1 by calcineurin and cAMP-dependent protein kinase. *Journal of Biological Chemistry* **280**(14): 13424-13432.

Moncada S, Ferreira SH, Vane JR (1973). Prostaglandins, aspirin-like drugs and oedema of inflammation. *Nature* **246**(5430): 217-218.

Moncada S, Gryglewski R, Bunting S, Vane JR (1976). Enzyme isolated from arteries transforms prostaglandin endoperoxides to an unstable substance that inhibits platelet-aggregration. *Nature* **263**(5579): 663-665.

Monneret G, Gravel S, Diamond M, Rokach J, Powell WS (2001). Prostaglandin D-2 is a potent chemoattractant for human eosinophils that acts via a novel DIP receptor. *Blood* **98**(6): 1942-1948.

Moraes LA, Piqueras L, Bishop-Bailey D (2006). Peroxisome proliferator-activated receptors and inflammation. *Pharmacology & Therapeutics* **110**(3): 371-385.

Moran MM, Xu HX, Clapham DE (2004). TRP ion channels in the nervous system. *Current Opinion in Neurobiology* **14**(3): 362-369.

Moriyama T, Higashi T, Togashi K, Iida T, Segi E, Sugimoto Y, *et al.* (2005). Sensitization of TRPV1 by EP1 and IP reveals peripheral nociceptive mechanism of prostaglandins. *Molecular Pain* **1**.

Morris CJ (2003). Carrageenan-induced paw edema in the rat and mouse. *Methods in molecular biology (Clifton, N.J.)* **225**: 115-121.

Morrison LE (1988). Time-resolved detection of energy transfer - theory and application to immunoassays. *Analytical Biochemistry* **174**(1):101-120.

Muccio GG, Stella N (2008). An optimized GC-MS method detects nanomolar amounts of anandamide in mouse brain. *Analytical Biochemistry* **373**(2): 220-228.

Murata T, Ushikubi F, Matsuoka T, Hirata M, Yamasaki A, Sugimoto Y, *et al.* (1997). Altered pain perception and inflammatory response in mice lacking prostacyclin receptor. *Nature* **388**(6643): 678-682.

Naeini RS, Cahill CM, Ribeiro-da-Silva A, Menard HA, Henry JL (2005). Remodelling of spinal nociceptive mechanisms in an animal model of monoarthritis.*European Journal of Neuroscience* **22**(8): 2005-2015.

Needleman P, Turk J, Jakschik BA, Morrison AR, Lefkowith JB (1986). ARACHIDONIC-ACID METABOLISM. In: (ed)^(eds). *Richardson, C. C.*, edn. p^pp 69-102.

Nelson DR, Koymans L, Kamataki T, Stegeman JJ, Feyereisen R, Waxman DJ, *et al.* (1996). P450 superfamily: Update on new sequences, gene mapping, accession numbers and nomenclature. *Pharmacogenetics* **6**(1): 1-42.

Neugebauer V, Han JS, Adwanikar H, Fu Y, Ji GC (2007). Techniques for assessing knee joint pain in arthritis. *Molecular Pain* **3**: 13.

Neve BP, Corseaux D, Chinetti G, Zawadzki C, Fruchart JC, Duriez P, *et al.* (2001). PPAR alpha agonists inhibit tissue factor expression in human monocytes and macrophages. *Circulation* **103**(2): 207-212.

Niesson WMA (2006). Liquid Chromatography-Mass Spectrometry. Third Edition, Taylor & Francis Group, USA.

Niissalo S, Hukkanen M, Imai S, Tornwall J, Konttinen YT (2002). Neuropeptides in experimental and degenerative arthritis. *Neuroendocrine Immune Basis of the Rheumatic Diseases Ii, Proceedings* **966**: 384-399.

Nithipatikom K, Grall AJ, Holmes BB, Harder DR, Falck JR, Campbell WB (2001). Liquid chromatographic-electrospray ionization-mass spectrometric analysis of cytochrome P450 metabolites of arachidonic acid. *Analytical Biochemistry* **298**(2): 327-336.

Node K, Huo YQ, Ruan XL, Yang BC, Spiecker M, Ley K, *et al.* (1999). Anti-inflammatory properties of cytochrome P450 epoxygenase-derived eicosanoids.*Science* **285**(5431): 1276-1279.

Nugteren DH, Hazelhof E (1973). Isolation and properties of intermediates in prostaglandin synthesis. *Biochimica Et Biophysica Acta* **326**(3):448-461.

O'Sullivan SE, Kendall DA (2010). Cannabinoid activation of peroxisome proliferator-activated receptors: Potential for modulation of inflammatory disease.*Immunobiology* **215**(8): 611-616.

Ochi K, Yoshimoto T, Yamamoto S, Taniguchi K, Miyamoto T (1983). Arachidonate 5-lipoxygenase of guinea pig peritoneal polymorphonuclear leukocytes - activation by adenosine 5-triphosphate. *Journal of Biological Chemistry* **258**(9): 5754-5758.

Okubo M, Yamanaka H, Kobayashi K, Noguchi K (2010). Leukotriene Synthases and the Receptors Induced by Peripheral Nerve Injury in the Spinal Cord Contribute to the Generation of Neuropathic Pain. *Glia* **58**(5): 599-610.

Orange RP, Austen KF (1969). Slow reacting substance of anaphylaxis. *Advances in immunology* **10**: 105-144.

Orita S, Ishikawa T, Miyagi M, Ochiai N, Inoue G, Eguchi Y, *et al.* (2011). Pain-related sensory innervation in monoiodoacetate-induced osteoarthritis in rat knees that gradually develops neuronal injury in addition to inflammatory pain. *Bmc Musculoskeletal Disorders* **12**: 12.

Ott VL, Cambier JC, Kappler J, Marrack P, Swanson BJ (2003). Mast cell-dependent migration of effector CD8(+) T cells through production of leukotriene B-4.*Nature Immunology* **4**(10): 974-981.

Pabreja K, Dua K, Padi SSV (2010). Evaluation of Extemporaneously Manufactured Topical Gels Containing Aceclofenac on Inflammation and Hyperalgesia in Rats. *Current Drug Delivery* **7**(4): 324-328.

Pacher P, Batkai S, Kunos G (2006). The endocannabinoid system as an emerging target of pharmacotherapy. *Pharmacological Reviews* **58**(3): 389-462.

Pagels WR, Sachs RJ, Marnett LJ, Dewitt DL, Day JS, Smith WL (1983). Immunochemical evidence for the involvement of prostaglandin-H-synthase in hydroperoxide-dependent oxidations by ram seminal vesicle microsomes. *Journal of Biological Chemistry* **258**(10): 6517-6523.

Palazzo E, Rossi F, Maione S (2008). Role of TRPV1 receptors in descending modulation of pain. *Molecular and Cellular Endocrinology* **286**(1-2): S79-S83.

Patwardhan AM, Akopian AN, Ruparel NB, Diogenes A, Weintraub ST, Uhlson C, *et al.* (2010a). Heat generates oxidized linoleic acid metabolites that activate TRPV1 and produce pain in rodents. *Journal of Clinical Investigation* **120**(5): 1617-1626.

Patwardhan AM, Akopian AN, Ruparel NB, Diogenes A, Weintraub ST, Uhlson C, *et al.* (2010b). Heat generates oxidized linoleic acid metabolites that activate TRPV1 and produce pain in rodents. *Journal of Clinical Investigation* **120**(5): 1617-1626.

Patwardhan AM, Scotland PE, Akopian AN, Hargreaves KM (2009a). Activation of TRPV1 in the spinal cord by oxidized linoleic acid metabolites contributes to inflammatory hyperalgesia. *Proceedings of the National Academy of Sciences of the United States of America* **106**(44): 18820-18824.

Patwardhan AM, Scotland PE, Akopian AN, Hargreaves KM (2009b). Activation of TRPV1 in the spinal cord by oxidized linoleic acid metabolites contributes to inflammatory hyperalgesia. *Proceedings of the National Academy of Sciences of the United States of America* **106**(44): 18820-18824.

(2008). The therapeutic potential of drugs that target the endogenous cannabinoid system. *21st Congress of the European-College-of-Neuropsychopharmacology*; Aug 30-Sep 03; Barcelona, SPAIN. Elsevier Science Bv. pp S170-S171.

Pertwee RG (2006). The pharmacology of cannabinoid receptors and their ligands: an overview. *International Journal of Obesity* **30**: S13-S18.

Petrosino S, Palazzo E, de Novellis V, Bisogno T, Rossi F, Maione S, *et al.* (2007). Changes in spinal and supraspinal endocannabinoid levels in neuropathic rats. *Neuropharmacology* **52**(2): 415-422.

Phillis JW, Horrocks LA, Farooqui AA (2006). Cyclooxygenases, lipoxygenases, and epoxygenases in CNS: Their role and involvement in neurological disorders.*Brain Research Reviews* **52**(2): 201-243.

Pinto M, Lima D, Tavares I (2007). Neuronal activation at the spinal cord and medullary pain control centers after joint stimulation: A c-fos study in acute and chronic articular inflammation. *Neuroscience* **147**(4): 1076-1089.

Piomelli D (1993). Arachidonic acid in cell signaling. *Current Opinion in Cell Biology* **5**(2): 274-280.

Piomelli D (1994). Eicosanoids in synaptic transmission. *Critical Reviews in Neurobiology* **8**(1-2): 65-83.

Piomelli D, Feinmark SJ, Shapiro E, Schwartz JH (1988). Formation and biological activity of 12-ketoeicosatetraenoic acid in the nervous system of aplysia. *Journal of Biological Chemistry* **263**(32): 16591-16596.

Piper P, Vane J (1971). Release of prostaglandins from lund and other tissues. *Annals of the New York Academy of Sciences* **180**(APR30): 363-&.

Placzek EA, Cooper BR, Placzek AT, Chester JA, Davisson VJ, Barker EL (2010). Lipidomic metabolism analysis of the endogenous cannabinoid anandamide (N-arachidonylethanolamide). *Journal of Pharmaceutical and Biomedical Analysis* **53**(3): 567-575.

Plumb RS, Rainville PD, Potts WB, Johnson KA, Gika E, Wilson ID (2009). Application of Ultra Performance Liquid Chromatography-Mass Spectrometry to Profiling Rat and Dog Bile. *Journal of Proteome Research* **8**(5): 2495-2500.

Plumb RS, Stumpf CL, Gorenstein MV, Castro-Perez JM, Dear GJ, Anthony M, *et al.* (2002). Metabonomics: the use of electrospray mass spectrometry coupled to reversed-phase liquid chromatography shows potential for the screening of rat urine in drug development. *Rapid Communications in Mass Spectrometry***16**(20): 1991-1996.

Pomonis JD, Boulet JM, Gottshall SL, Phillips S, Sellers R, Bunton T, *et al.* (2005). Development and pharmacological characterization of a rat model of osteoarthritis pain. *Pain* **114**(3): 339-346.

Poole CF (2003). New trends in solid-phase extraction. *Trac-Trends in Analytical Chemistry* **22**(6): 362-373.

Prakash C, Shaffer CL, Nedderman A (2007). Analytical strategies for identifying drug metabolites. *Mass Spectrometry Reviews* **26**(3): 340-369.

Prescott ED, Julius D (2003). A modular PIP2 binding site as a determinant of capsaicin receptor sensitivity. *Science* **300**(5623): 1284-1288.

Pritzker KPH (1994). ANIMAL-MODELS FOR OSTEOARTHRITIS - PROCESSES, PROBLEMS AND PROSPECTS. *Annals of the Rheumatic Diseases* **53**(6): 406-420.

Prochazkova M, Zanvit P, Dolezal T, Prokesova L, Krsiak M (2009). Increased Gene Expression and Production of Spinal Cyclooxygenase 1 and 2 during Experimental Osteoarthritis Pain. *Physiological Research* **58**(3): 419-425.

Pulichino AM, Rowland S, Wu T, Clark P, Xu DG, Mathieu MC, *et al.* (2006). Prostacyclin antagonism reduces pain and inflammation in rodent models of hyperalgesia and chronic arthritis. *Journal of Pharmacology and Experimental Therapeutics* **319**(3): 1043-1050.

Puttfarcken PS, Han P, Joshi SK, Neelands TR, Gauvin DM, Baker SJ, *et al.* (2010). A-995662 (R)-8-(4-methyl-5-(4-(trifluoromethyl)phenyl)oxazol-2-ylamino)-1,2,3,4-tetrahydronaphthalen-2-ol , a novel, selective TRPV1 receptor antagonist, reduces spinal release of glutamate and CGRP in a rat knee joint pain model. *Pain* **150**(2): 319-326.

Rainsford KD (2007). Anti-inflammatory drugs in the 21st century. *Subcellular Biochemistry* **42:** 3.

Randall MD, Kendall DA (1998). Endocannabinoids: a new class of vasoactive substances. *Trends in Pharmacological Sciences* **19**(2): 55-58.

Ratnoff OD (1971). Tangled web - interdependence of mechanisms of blood clotting, fibrinolysis, immunity and inflammation. *Thrombosis Et Diathesis Haemorrhagica*: 109-&.

Rea K, Roche M, Finn DP (2007). Supraspinal modulation of pain by cannabinoids: the role of GABA and glutamate. *British Journal of Pharmacology* **152**(5):633-648.

Reinold H, Ahmadi S, Depner UB, Layh B, Heindl C, Hamza M, *et al.* (2005). Spinal inflammatory hyperalgesia is mediated by prostaglandin E receptors of the EP2 subtype. *Journal of Clinical Investigation* **115**(3): 673-679.

Rhodes LE, Gledhill K, Masoodi M, Haylett AK, Brownrigg M, Thody AJ, *et al.* (2009). The sunburn response in human skin is characterized by sequential eicosanoid profiles that may mediate its early and late phases. *Faseb Journal* **23**(11): 3947-3956.

Rice ASC, Farquhar-Smith WP, Nagy I (2002). Endocannabinoids and pain: spinal and peripheral analgesia in inflammation and neuropathy. *Prostaglandins Leukotrienes and Essential Fatty Acids* **66**(2-3): 243-256.

Richardson D, Ortori CA, Chapman V, Kendall DA, Barrett DA (2007). Quantitative profiling of endocannabinoids and related compounds in rat brain using liquid chromatography-tandem electrospray ionization mass spectrometry. *Analytical Biochemistry* **360**(2): 216-226.

Richardson D, Pearson RG, Kurian N, Latif ML, Garle MJ, Barrett DA, *et al.* (2008). Characterisation of the cannabinoid receptor system in synovial tissue and fluid in patients with osteoarthritis and rheumatoid arthritis. *Arthritis Research & Therapy* **10**(2): 14.

Roberts LA, Connor M (2006). TRPV1 antagonists as a potential treatment for hyperalgesia. *Recent patents on CNS drug discovery* **1**(1): 65-76.

Robinson DR, McNaughton PA, Evans ML, Hicks GA (2004). Characterization of the primary spinal afferent innervation of the mouse colon using retrograde labelling. *Neurogastroenterology and Motility* **16**(1): 113-124.

Roman RJ (2002). P-450 metabolites of arachidonic acid in the control of cardiovascular function. *Physiological Reviews* **82**(1): 131-185.

Romanova EV, Lee JE, Kelleher NL, Sweedler JV, Gulley JM (2010). Mass Spectrometry Screening Reveals Peptides Modulated Differentially in the Medial Prefrontal Cortex of Rats with Disparate Initial Sensitivity to Cocaine. *Aaps Journal* **12**(3): 443-454.

Ross RA (2003). Anandamide and vanilloid TRPV1 receptors. *British Journal of Pharmacology* **140**(5): 790-801.

Rossi AG, McCutcheon JC, Roy N, Chilvers ER, Haslett C, Dransfield I (1998). Regulation of macrophage phagocytosis of apoptotic cells by cAMP. *Journal of Immunology* **160**(7): 3562-3568.

Round P, Priestley A, Robinson J (2011). An investigation of the safety and pharmacokinetics of the novel TRPV1 antagonist XEN-D0501 in healthy subjects.*British Journal of Clinical Pharmacology* **72**(6): 921-931.

Rouzer CA, Samuelsson B (1985). On the nature of the 5-lipoxygenase reaction in human leukocytes - enzyme purification and requirement for multiple stimulatory factors. *Proceedings of the National Academy of Sciences of the United States of America* **82**(18): 6040-6044.

Ryan GB, Majno G (1977). Acute inflammation - review. *American Journal of Pathology* **86**(1): 183-276.

Sagar DR, Gaw AG, Okine BN, Woodhams SG, Wong A, Kendall DA, *et al.* (2009). Dynamic regulation of the endocannabinoid system: implications for analgesia. *Molecular Pain* **5**: 59.

Sagar DR, Smith PA, Millns PJ, Smart D, Kendall DA, Chapman V (2004). TRPV1 and CB1 receptor-mediated effects of the endovanilloid/endocannabinoid N-arachidonoyl-dopamine on primary afferent fibre and spinal cord neuronal responses in the rat. *European Journal of Neuroscience* **20**(1): 175-184.

Sagar DR, Staniaszek LE, Okine BN, Woodhams S, Norris LM, Pearson RG, *et al.* (2010). Tonic Modulation of Spinal Hyperexcitability by the Endocannabinoid Receptor System in a Rat Model of Osteoarthritis Pain. *Arthritis and Rheumatism* **62**(12): 3666-3676.

Salvemini D, Wang ZQ, Wyatt PS, Bourdon DM, Marino MH, Manning PT, *et al.* (1996). Nitric oxide: A key mediator in the early and late

phase of carrageenan-induced rat paw inflammation. *British Journal of Pharmacology* **118**(4): 829-838.

Sampath H, Ntambi JM (2011). The role of stearoyl-CoA desaturase in obesity, insulin resistance, and inflammation. *Annals of the New York Academy of Sciences* **1243**(1): 47-53.

Samuelsson B, Dahlen SE, Lindgren JA, Rouzer CA, Serhan CN (1987). Leukotrienes and lipoxins - structures, biosynthesis and biological effects. *Science* **237**(4819): 1171-1176.

Sana TR, Waddell K, Fischer SM (2008). A sample extraction and chromatographic strategy for increasing LC/MS detection coverage of the erythrocyte metabolome. *Journal of Chromatography B-Analytical Technologies in the Biomedical and Life Sciences* **871**(2): 314-321.

Sato Y, Arai N, Negishi A, Ohya K (1997). Expression of cyclooxygenase genes and involvement of endogenous prostaglandin during osteogenesis in the rat tibial bone marrow cavity. *Journal of Medical and Dental Sciences* **44**(4): 81-92.

Saxena PN, Beg MMA, Singhal KC, Ahmad M (1979). Prostaglandin-like activity in the cerebrospinal-fluid of febrile patients. *Indian Journal of Medical Research* **70**(SEP): 495-498.

Scarborough PE, Ma JX, Qu W, Zeldin DC (1999). P450 subfamily CYP2J and their role in the bioactivation of arachidonic acid in extrahepatic tissues. *Drug Metabolism Reviews* **31**(1): 205-234.

Schaible H-G, Schmelz M, Tegeder I (2006). Pathophysiology and treatment of pain in joint disease. *Advanced drug delivery reviews* **58**(2): 323-342.

Schmid HHO, Schmid PC, Natarajan V (1990). N-acylated glycerophospholipids and their derivatives. *Progress in Lipid Research* **29**(1): 1-43.

Schmidt A, Endo N, Rutledge SJ, Vogel R, Shinar D, Rodan GA (1992). Identification of a new member of the steroid-hormone receptor superfamily that is activated by a peroxisome proliferator and faaty acids. *Molecular Endocrinology* **6**(10): 1634-1641.

Schmidt RF (1995). The physiology of pathophysiology of articular pain. *Japanese Journal of Physiology* **45**(SUPPL. 1): S3.

Schnizler K, Shutov LP, Van Kanegan MJ, Merrill MA, Nichols B, McKnight GS, *et al.* (2008). Protein kinase a anchoring via AKAP150 is essential for TRPV1 modulation by forskolin and prostaglandin E(2) in mouse sensory neurons. *Journal of Neuroscience* **28**(19): 4904-4917.

Schuelert N, Johnson MP, Oskins JL, Jassal K, Chambers MG, McDougall JJ (2011). Local application of the endocannabinoid hydrolysis inhibitor URB597 reduces nociception in spontaneous and chemically induced models of osteoarthritis. *Pain* **152**(5): 975-981.

Schuelert N, McDougall JJ (2008). Cannabinoid-mediated antinociception is enhanced in rat osteoarthritic knees. *Arthritis and Rheumatism* **58**(1): 145-153.

Schuelert N, McDougall JJ (2009). Grading of monosodium iodoacetate-induced osteoarthritis reveals a concentration-dependent sensitization of nociceptors in the knee joint of the rat. *Neuroscience Letters* **465**(2): 184-188.

Schumacher HR, Meng Z, Sieck M, Zonay L, Clayburne G, Baker JF, *et al.* (1996). Effect of a nonsteroidal antiinflammatory drug on synovial fluid in osteoarthritis. *Journal of Rheumatology* **23**(10): 1774-1777.

Scott DL, Berry H, Capell H, Coppock J, Daymond T, Doyle DV, *et al.* (2000). The long-term effects of non-steroidal antiinflammatory drugs in osteoarthritis of the knee: a randomized placebo-controlled trial. *Rheumatology* **39**(10): 1095-1101.

Sendobry SM, Cornicelli JA, Welch K, Bocan T, Tait B, Trivedi BK, *et al.* (1997). Attenuation of diet-induced atherosclerosis in rabbits with a highly selective 15-lipoxygenase inhibitor lacking significant antioxidant properties. *British Journal of Pharmacology* **120**(7): 1199-1206.

Serezani CH, Chung J, Ballinger MN, Moore BB, Aronoff DM, Peters-Golden M (2007). Prostaglandin E-2 suppresses bacterial killing in alveolar macrophages by inhibiting NADPH oxidase. *American Journal of Respiratory Cell and Molecular Biology* **37**(5): 562-570.

Serhan CN, Clish CB, Brannon J, Colgan SP, Chiang N, Gronert K (2000). Novel functional sets of lipid-derived mediators with antiinflammatory actions generated from omega-3 fatty acids via cyclooxygenase 2-nonsteroidal antiinflammatory drugs and transcellular processing. *Journal of Experimental Medicine***192**(8): 1197-1204.

Serhan CN, Hamberg M, Samuelsson B (1984). Trihydroxytetraenes - a novel series of compounds formed from arachidonic acid in human leukocytes. *Biochemical and Biophysical Research Communications* **118**(3): 943-949.

Serhan CN, Hong S, Gronert K, Colgan SP, Devchand PR, Mirick G, *et al.* (2002). Resolvins: A family of bioactive products of omega-3 fatty acid transformation circuits initiated by aspirin treatment that counter

proinflammation signals. *Journal of Experimental Medicine* **196**(8): 1025-1037.

Sheskin T, Hanus L, Slager J, Vogel Z, Mechoulam R (1997). Structural requirements for binding of anandamide-type compounds to the brain cannabinoid receptor. *Journal of Medicinal Chemistry* **40**(5): 659-667.

Shimizu T, Yamamoto S, Hayaishi O (1982). Purification of PGH-PGD isomerase from rat brain. *Methods in Enzymology* **86**: 73-77.

Shin J, Cho H, Hwang SW, Jung J, Shin CY, Lee SY, *et al.* (2002). Bradykinin-12-lipoxygenase-VR1 signaling pathway for inflammatory hyperalgesia.*Proceedings of the National Academy of Sciences of the United States of America* **99**(15): 10150-10155.

Silberberg R, Saxton J, Sperling G, McCay C (1952). Degenerative joint disease in syrian hamsters. *Federation Proceedings* **11**(1): 427-427.

Simpson A (1997). The cytochrome P450 4 (CYP4) family. *General Pharmacology* **28**(3): 351-359.

Sipe JC, Arbour N, Gerber A, Beutler E (2005). Reduced endocannabinoid immune modulation by a common cannabinoid 2 (CB2) receptor gene polymorphism: possible risk for autoimmune disorders. *Journal of Leukocyte Biology* **78**(1): 231-238.

Sisk MB, Hausman DB, Martin RJ, Azain MJ (2001). Dietary conjugated linoleic acid reduces adiposity in lean but not obese Zucker rats. *Journal of Nutrition***131**(6): 1668-1674.

Slipetz DM, Oneill GP, Favreau L, Dufresne C, Gallant M, Gareau Y, *et al.* (1995). Activation of the human peripheral cannabinoid receptor results in inhibition of adenylyl cyclase. *Molecular Pharmacology* **48**(2): 352-361.

Smart D, Gunthorpe MJ, Jerman JC, Nasir S, Gray J, Muir AI, *et al.* (2000). The endogenous lipid anandamide is a full agonist at the human vanilloid receptor (hVR1). *British Journal of Pharmacology* **129**(2): 227-230.

Snider NT, Kornilov AM, Kent UM, Hollenberg PF (2007). Anandamide metabolism by human liver and kidney microsomal cytochrome P450 enzymes to form hydroxyeicosatetraenoic and epoxyeicosatrienoic acid ethanolamides. *Journal of Pharmacology and Experimental Therapeutics* **321**(2): 590-597.

Snider NT, Nast JA, Tesmer LA, Hollenberg PF (2009). A Cytochrome P450-Derived Epoxygenated Metabolite of Anandamide Is a Potent

Cannabinoid Receptor 2-Selective Agonist. *Molecular Pharmacology* **75**(4): 965-972.

Sofat N, Beith I, Anilkumar PG, Mitchell P (2011). Recent clinical evidence for the treatment of osteoarthritis: what we have learned. *Reviews on recent clinical trials* **6**(2): 114-126.

Spanbroek R, Hildner M, Kohler A, Muller A, Zintl F, Kuhn H, *et al.* (2001). IL-4 determines eicosanoid formation in dendritic cells by down-regulation of 5-lipoxygenase and up-regulation of 15-lipoxygenase 1 expression. *Proceedings of the National Academy of Sciences of the United States of America* **98**(9):5152-5157.

Staniaszek LE, Norris LM, Kendall DA, Barrett DA, Chapman V (2010). Effects of COX-2 inhibition on spinal nociception: the role of endocannabinoids. *British Journal of Pharmacology* **160**(3): 669-676.

Stark K, Dostalek M, Guengerich FP (2008). Expression and purification of orphan cytochrome P450 4X1 and oxidation of anandamide. *Febs Journal* **275**(14):3706-3717.

Steenland HW, Ko SW, Wu LJ, Zhuo M (2006). Hot receptors in the brain. *Molecular Pain* **2**: 8.

Stein AT, Ufret-Vincenty CA, Hua L, Santana LF, Gordon SE (2006). Phosphoinositide 3-kinase binds to TRPV1 and mediates NGF-stimulated TRPV1 trafficking to the plasma membrane. *Journal of General Physiology* **128**(5): 509-522.

Strehmel N, Hummel J, Erban A, Strassburg K, Kopka J (2008). Retention index thresholds for compound matching in GC-MS metabolite profiling. *Journal of Chromatography B-Analytical Technologies in the Biomedical and Life Sciences* **871**(2): 182-190.

Succar R, Mitchell VA, Vaughan CW (2007). Actions of N-arachidonyl-glycine in a rat inflammatory pain model. *Molecular Pain* **3**: 8.

Sugiura T, Kodaka T, Nakane S, Miyashita T, Kondo S, Suhara Y, *et al.* (1999). Evidence that the cannabinoid CB1 receptor is a 2-arachidonoylglycerol receptor - Structure-activity relationship of 2-arachidonoylglycerol ether-linked analogues, and related compounds. *Journal of Biological Chemistry* **274**(5): 2794-2801.

Sun Y, Alexander SPH, Garle MJ, Gibson CL, Hewitt K, Murphy SP, *et al.* (2007a). Cannabinoid activation of PPAR alpha; a novel neuroprotective mechanism.*British Journal of Pharmacology* **152**(5): 734-743.

Sun Y, Alexander SPH, Kendall DA, Bennett AJ (2006). Cannabinoids and PPAR alpha signalling. *Biochemical Society Transactions* **34:** 1095-1097.

Sun Y, Bennett A (2007b). Cannabinoids: A New Group of Agonists of PPARs. *PPAR Res* **2007:** 23513.

Suzuki R, Dickenson A (2005). Spinal and supraspinal contributions to central sensitization in peripheral neuropathy. *Neurosignals* **14**(4): 175-181.

Svensjo E (1978). Bradykinin and prostaglandin-E1, E2 and F2-alpha-induced macromolecular leakage in hamster cheek pouch. *Prostaglandins and Medicine* **1**(5): 397-410.

Szallasi A, Blumberg PM (1999). Vanilloid (capsaicin) receptors and mechanisms. *Pharmacological Reviews* **51**(2): 159-211.

Tager AM, Luster AD (2003). BLT1 and BLT2: the leukotriene B-4 receptors. *Prostaglandins Leukotrienes and Essential Fatty Acids* **69**(2-3): 123-134.

Takayama K, Garcia-Cardena G, Sukhova GK, Comander J, Gimbrone MA, Libby P (2002). Prostaglandin E-2 suppresses chemokine production in human macrophages through the EP4 receptor. *Journal of Biological Chemistry* **277**(46): 44147-44154.

Takeshita N, Yoshimi E, Hatori C, Kumakura F, Seki N, Shimizu Y (2011). Alleviating Effects of AS1892802, a Rho Kinase Inhibitor, on Osteoarthritic Disorders in Rodents. *Journal of Pharmacological Sciences* **115**(4): 481-489.

Tanaka Y, Ward SL, Smith WL (1987). Immunochemical and kinetic evidence for 2 different prostaglandin-H-prostaglandin E isomerases in sheep vesicular gland microsomes. *Journal of Biological Chemistry* **262**(3): 1374-1381.

Tang CH, Yang RS, Huang TH, Lu DY, Chuang WJ, Huang TF, *et al.* (2006). Ultrasound stimulates cyclooxygenase-2 expression and increases bone formation through integrin, focal adhesion kinase, phosphatidylinositol 3-kinase, and akt pathway in osteoblasts. *Molecular Pharmacology* **69**(6): 2047-2057.

Tang L, Chen Y, Chen ZL, Blumberg PM, Kozikowski AP, Wang ZJ (2007). Antinociceptive pharmacology of N-(4-chlorobenzyl)-N '-(4-hydroxy-3-iodo-5-methoxybenzyl) thiourea, a high-affinity competitive antagonist of the transient receptor potential vanilloid 1 receptor. *Journal of Pharmacology and Experimental Therapeutics* **321**(2): 791-798.

Tapiero H, Ba GN, Couvreur P, Tew KD (2002a). Polyunsaturated fatty acids (PUFA) and eicosanoids in human health and pathologies. *Biomedicine & Pharmacotherapy* **56**(5): 215-222.

Tapiero H, Ba GN, Couvreur P, Tew KD (2002b). Polyunsaturated fatty acids (PUFA) and eicosanoids in human health and pathologies. *Biomedicine & Pharmacotherapy* **56**(5): 215-222.

Theodoridis G, Gika HG, Wilson ID (2008). LC-MS-based methodology for global metabolite profiling in metabonomics/metabolomics. *Trac-Trends in Analytical Chemistry* **27**(3): 251-260.

Thomas A, Hopfgartner G, Giroud C, Staub C (2009). Quantitative and qualitative profiling of endocannabinoids in human plasma using a triple quadrupole linear ion trap mass spectrometer with liquid chromatography. *Rapid Communications in Mass Spectrometry* **23**(5): 629-638.

Thorpe LB, Goldie M, Dolan S (2011). Central and Local Administration of Gingko Biloba Extract EGb 761 (R) Inhibits Thermal Hyperalgesia and Inflammation in the Rat Carrageenan Model. *Anesthesia and Analgesia* **112**(5): 1226-1231.

Tohda C, Sasaki M, Konemura T, Sasamura T, Itoh M, Kuraishi Y (2001). Axonal transport of VR1 capsaicin receptor mRNA in primary afferents and its participation in inflammation-induced increase in capsaicin sensitivity. *Journal of Neurochemistry* **76**(6): 1628-1635.

Tominaga M, Caterina MJ, Malmberg AB, Rosen TA, Gilbert H, Skinner K, *et al.* (1998). The cloned capsaicin receptor integrates multiple pain-producing stimuli.*Neuron* **21**(3): 531-543.

Toth A, Boczan J, Kedei N, Lizanecz E, Bagi Z, Papp Z, *et al.* (2005). Expression and distribution of vanilloid receptor 1 (TRPV1) in the adult rat brain. *Brain research. Molecular brain research* **135**(1-2): 162-168.

Tracey I, Mantyh PW (2007). The cerebral signature and its modulation for pain perception. *Neuron* **55**(3): 377-391.

Trufelli H, Palma P, Famiglini G, Cappiello A (2011). AN Overview of matrix effects in liquid chromatography-mass spectrometry. *Mass Spectrometry Reviews* **30**(3): 491-509.

Ueda N, Yamamoto K, Yamamoto S, Tokunaga T, Shirakawa E, Shinkai H, *et al.* (1995). Lipoxygenase-catalysed oxygenation of arachidonoyl ethanolamide, a cannabinoid receptor agonist. *Biochimica Et Biophysica Acta-Lipids and Lipid Metabolism* **1254**(2): 127-134.

Ueno A, Matsumoto H, Naraba H, Ikeda Y, Ushikubi F, Matsuoka T, *et al.* (2001). Major roles of prostanoid receptors IP and EP3 in

endotoxin-induced enhancement of pain perception. *Biochemical Pharmacology* **62**(2): 157-160.

Ullrich V, Haurand M (1983). Thromboxane synthase as a cytochrome P450 enzyme. *Advances in Prostaglandin Thromboxane and Leukotriene Research***11:** 105-110.

van der Pouw Kraan TC, Boeije LC, Snijders A, Smeenk RJ, Wijdenes J, Aarden LA (1996). Regulation of IL-12 production by human monocytes and the influence of prostaglandin E2. *Annals of the New York Academy of Sciences* **795:** 147-157.

van der Pouw Kraan TC, van Lier RA, Aarden LA (1995). PGE2 and the immune response. A central role for prostaglandin E2 in downregulating the inflammatory immune response. *Molecular medicine today* **1**(2): 61.

van der Stelt M, Trevisani M, Vellani V, De Petrocellis L, Moriello AS, Campi B, *et al.* (2005). Anandamide acts as an intracellular messenger amplifying Ca2+ influx via TRPV1 channels. *Embo Journal* **24**(17): 3026-3037.

Van Sickle MD, Duncan M, Kingsley PJ, Mouihate A, Urbani P, Mackie K, *et al.* (2005). Identification and functional characterization of brainstem cannabinoid CB2 receptors. *Science* **310**(5746): 329-332.

Vanderhoek JY, Bryant RW, Bailey JM (1982). Regulation of leukocyte and platelet lipoxygenases by hydroxyeicosanoids. *Biochemical Pharmacology* **31**(21): 3463-3467.

Vandevoorde S, Jonsson KO, Fowler CJ, Lambert DM (2003). Modifications of the ethanolamine head in N-palmitoylethanolamine: Synthesis and evaluation of new agents interfering with the metabolism of anandamide. *Journal of Medicinal Chemistry* **46**(8): 1440-1448.

Vandevoorde S, Lambert DM (2007). The multiple pathways of endocannabinoid metabolism: A zoom out. *Chemistry & Biodiversity* **4**(8): 1858-1881.

Vay L, Gu CJ, McNaughton PA (2012). The thermo-TRP ion channel family: properties and therapeutic implications. *British Journal of Pharmacology* **165**(4):787-801.

Vellani V, Mapplebeck S, Moriondo A, Davis JB, McNaughton PA (2001). Protein kinase C activation potentiates gating of the vanilloid receptor VR1 by capsaicin, protons, heat and anandamide. *Journal of Physiology-London* **534**(3): 813-825.

Voets T, Droogmans G, Wissenbach U, Janssens A, Flockerzi V, Nilius B (2004). The principle of temperature-dependent gating in cold- and heat-sensitive TRP channels. *Nature* **430**(7001): 748-754.

Walker JM, Huang SM (2002). Endocannabinolds in pain modulation. *Prostaglandins Leukotrienes and Essential Fatty Acids* **66**(2-3): 235-242.

Wang MH, Guan H, Nguyen X, Zand BA, Nasjletti A, Laniado-Schwartzman M (1999). Contribution of cytochrome P-450 4A1 and 4A2 to vascular 20-hydroxyeicosatetraenoic acid synthesis in rat kidneys. *American Journal of Physiology-Renal Physiology* **276**(2): F246-F253.

Wang WH, Liu CH, Sun YM, Lin F, Zhang MM, Wang ZB, *et al.* (2011). Metabolic Profiles of Nonylphenol in Rat Urine. *Chemical Journal of Chinese Universities-Chinese* **32**(10): 2280-2285.

Want EJ, Cravatt BF, Siuzdak G (2005). The expanding role of mass spectrometry in metabolite profiling and characterization. *Chembiochem* **6**(11): 1941-1951.

Weinberg DA, Weston LK, Kaplan JE (1985). Influence of prostaglandin-I2 on fibronectin-mediated phagocytosis in vivo and in vitro. *Journal of Leukocyte Biology* **37**(2): 151-159.

Weksler BB, Coupal CE (1973). Platelet-dependent generation of chemotactic activity in serum. *Journal of Experimental Medicine* **137**(6): 1419-1430.

Wenk MR (2005). The emerging field of lipidomics. *Nature Reviews Drug Discovery* **4**(7): 594-610.

Werz O, Szellas D, Steinhilber D, Radmark O (2002). Arachidonic acid promotes phosphorylation of 5-lipoxygenase at Ser-271 by MAPK-activated protein kinase 2 (MK2). *Journal of Biological Chemistry* **277**(17): 14793-14800.

Wilhelm DL (1973). Mechanisms responsible for increased vascular - permeability in acute inflammation. *Agents and Actions* **3**(5): 297-306.

Williams J, Wood J, Pandarinathan L, Karanian DA, Bahr BA, Vouros P, *et al.* (2007). Quantitative method for the profiling of the endocannabinoid metabolome by LC-atmospheric pressure chemical ionization-MS. *Analytical Chemistry* **79**(15): 5582-5593.

Williams TJ (1979). Prostaglandin-E2, prostaglandin-I2 and the vascular changes of inflammation. *British Journal of Pharmacology* **65**(3): 517-524.

Williams TJ, Jose PJ (1981). Mediation of increased vascular permeability after complement activation - histamine-independent action of rabbit C5A. *Journal of Experimental Medicine* **153**(1): 136-153.

Williams TJ, Morley J (1973). Prostaglandins as potentiators of increased vascular permeability in inflammation. *Nature* **246**(5430): 215-217.

Wilson TA, Nicolosi RJ, Chrysam M, Kritchevsky D (2000). Conjugated linoleic acid reduces early aortic atherosclerosis greater than linoleic acid in hypercholesterolemic hamsters. *Nutrition Research* **20**(12): 1795-1805.

(2003). Mechanisms of central sensitization, neuroimmunology & injury biomechanics in persistent pain: implications for musculoskeletal disorders.*Symposium on perspectives on Musculoskeletal Disorder Causation and Control*; May 21-22; Columus, Ohio. Elsevier Sci Ltd. pp 87-93.

Winter CA, Risley EA, Nuss GW (1962). Carrageenan-induced oedema in hind paw of rat as an assay for anti-inflammatory drugs. *Proceedings of the Society for Experimental Biology and Medicine* **111**(3): 544-&.

Witkamp RF (2005). Genomics and systems biology - how relevant are the developments to veterinary pharmacology, toxicology and therapeutics? *Journal of Veterinary Pharmacology and Therapeutics* **28**(3): 235-245.

Wood JN, Winter J, James IF, Rang HP, Yeats J, Bevan S (1988). Capsaicin-induced ion fluxes in dorsal root ganglion cells in culture. *Journal of Neuroscience* **8**(9): 3208-3220.

Woodward DF, Krauss AHP, Nieves AL, Spada CS (1991). Studies on leukotriene-D4 as an eosinophil chemoattractant. *Drugs under Experimental and Clinical Research* **17**(12): 543-548.

Woolf CJ (2011). Central sensitization: Implications for the diagnosis and treatment of pain. *Pain* **152**(3): S2-S15.

Woolf CJ (2004). Pain: Moving from symptom control toward mechanism-specific pharmacologic management. *Annals of Internal Medicine* **140**(6): 441-451.

Xu RNX, Fan LM, Rieser MJ, El-Shourbagy TA (2007). Recent advances in high-throughput quantitative bioanalysis by LC-MS/MS. *Journal of Pharmaceutical and Biomedical Analysis* **44**(2): 342-355.

Xu XJ, Reichner JS, Mastrofrancesco B, Henry WL, Jr., Albina JE (2008). Prostaglandin E(2) suppresses lipopolysaccharide-stimulated IFN-beta production.*Journal of Immunology* **180**(4): 2125-2131.

Xue LZ, Gyles SL, Wettey FR, Gazi L, Townsend E, Hunter MG, *et al.* (2005). Prostaglandin D-2 causes preferential induction of proinflammatory Th2 cytokine production through an action on chemoattractant receptor-like molecule expressed on Th2 cells. *Journal of Immunology* **175**(10): 6531-6536.

Yang PY, Chan D, Felix E, Madden T, Klein RD, Shureiqi I, *et al.* (2006). Determination of endogenous tissue inflammation profiles by LC/MS/MS: COX- and LOX-derived bioactive lipids. *Prostaglandins Leukotrienes and Essential Fatty Acids* **75**(6): 385-395.

Yoshida Y, Kodai S, Takemura S, Minamiyama Y, Niki E (2008). Simultaneous measurement of F-2-isoprostane, hydroxyoctadecadienoic acid, hydroxyeicosatetraenoic acid, and hydroxycholesterols from physiological samples. *Analytical Biochemistry* **379**(1): 105-115.

Yoshida Y, Niki E (2006). Bio-markers of lipid peroxidation in vivo: Hydroxyoctadecadienoic acid and hydroxycholesterol. *Biofactors* **27**(1-4): 195-202.

Yoshikawa K, Kita Y, Kishimoto K, Shimizu T (2006). Profiling of eicosanoid production in the rat hippocampus during kainic acid-induced seizure - Dual phase regulation and differential involvement of COX-1 and COX-2. *Journal of Biological Chemistry* **281**(21): 14663-14669.

Yoshimi E, Kumakura F, Hatori C, Hamachi E, Iwashita A, Ishii N, *et al.* (2010). Antinociceptive Effects of AS1892802, a Novel Rho Kinase Inhibitor, in Rat Models of Inflammatory and Noninflammatory Arthritis. *Journal of Pharmacology and Experimental Therapeutics* **334**(3): 955-963.

Yu K, Bayona W, Kallen CB, Harding HP, Ravera CP, McMahon G, *et al.* (1995). Differential activation of peroxisome proliferator-activated receptors by eicosanoids. *Journal of Biological Chemistry* **270**(41): 23975-23983.

Yu Y, Correll PH, Vanden Heuvel JP (2002). Conjugated linoleic acid decreases production of pro-inflammatory products in macrophages: evidence for a PPAR gamma-dependent mechanism. *Biochimica Et Biophysica Acta-Molecular and Cell Biology of Lipids* **1581**(3): 89-99.

Yue HF, Jansen SA, Strauss KI, Borenstein MR, Barbe MF, Rossi LJ, *et al.* (2007). A liquid chromatography/mass spectrometric method for simultaneous analysis of arachidonic acid and its endogenous

eicosanoid metabolites prostaglandins, dihydroxyeicosatrienoic acids, hydroxyeicosatetraenoic acids, and epoxyeicosatrienoic acids in rat brain tissue. *Journal of Pharmaceutical and Biomedical Analysis* **43**(3): 1122-1134.

Zhang JH, Pearson T, Matharoo-Ball B, Ortori CA, Warren AY, Khan R, *et al.* (2007a). Quantitative profiling of epoxyeicosatrienoic, hydroxyeicosatetraenoic, and dihydroxyeicosatetraenoic acids in human intrauterine tissues using liquid chromatography/electrospray ionization tandem mass spectrometry. *Analytical Biochemistry* **365**(1): 40-51.

Zhang JH, Pearson T, Matharoo-Ball B, Ortori CA, Warren AY, Khan R, *et al.* (2007b). Quantitative profiling of epoxyeicosatrienoic, hydroxyeicosatetraenoic, and dihydroxyeicosatetraenoic acids in human intrauterine tissues using liquid chromatography/electrospray ionization tandem mass spectrometry. *Analytical Biochemistry* **365**(1): 40-51.

Zhang MY, Gao Y, Btesh J, Kagan N, Kerns E, Samad TA, *et al.* (2010). Simultaneous determination of 2-arachidonoylglycerol, 1-arachidonoylglycerol and arachidonic acid in mouse brain tissue using liquid chromatography/tandem mass spectrometry. *Journal of Mass Spectrometry* **45**(2): 167-177.

Zhang XM, Huang JH, McNaughton PA (2005). NGF rapidly increases membrane expression of TRPV1 heat-gated ion channels. *Embo Journal* **24**(24): 4211-4223.

Zhang XM, McNaughton PA (2006). Why pain gets worse: The mechanism of heat hyperalgesia. *Journal of General Physiology* **128**(5): 491-493.

Zhang XP, Schwarz EM, Young DA, Puzas JE, Rosier RN, O'Keefe RJ (2002). Cyclooxygenase-2 regulates mesenchymal cell differentiation into the osteoblast lineage and is critically involved in bone repair. *Journal of Clinical Investigation* **109**(11): 1405-1415.

Zhang YD, Oltman CL, Lu T, Lee HC, Dellsperger KC, Vanrollins M (2001). EET homologs potently dilate coronary microvessels and activate BKCa channels.*American Journal of Physiology-Heart and Circulatory Physiology* **280**(6): H2430-H2440.

Appendices

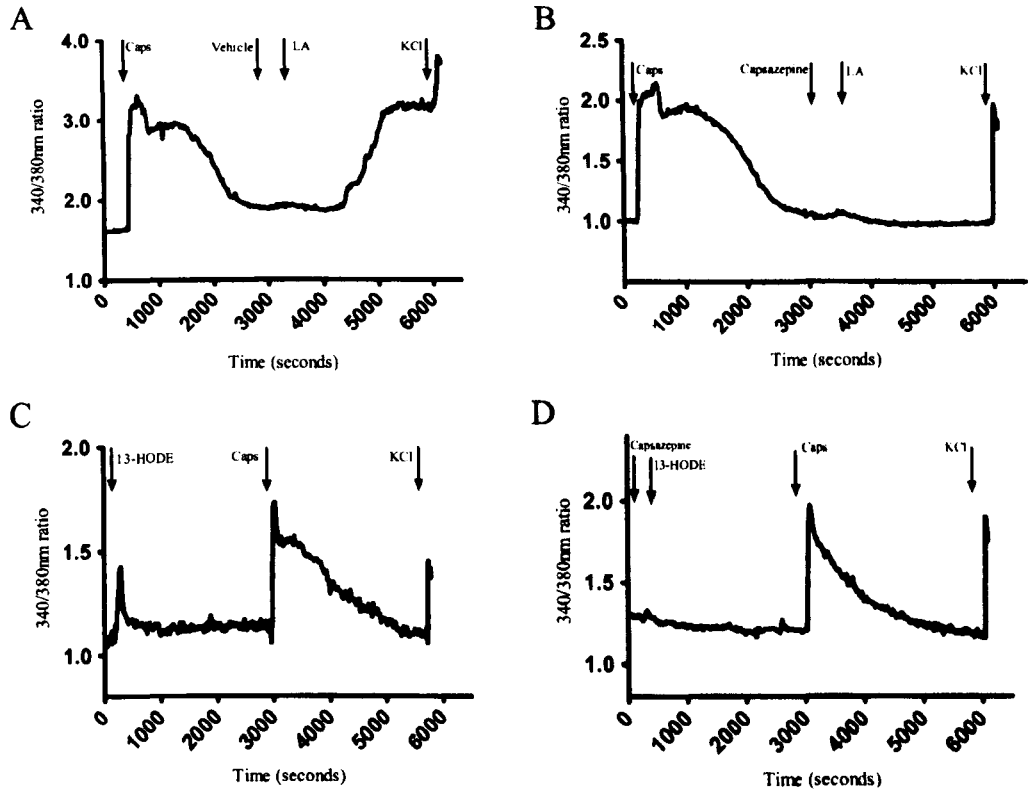

Figure 1: Representative traces illustrating changes in intracellular calcium concentrations (represented by 340:380 nm ratios) in single DRG cells responding to capsaicin, linoleic acid (LA) and 13-HODE. **A:** the cell was exposed for 1 minute to capsaicin (100nm) and for 2 minutes to 1mM LA separated by forty five minutes of wash with buffer. **B**: the cell was exposed to capsaicin (100nm) for 1 minute, and pre-exposed to capsazepine (10μM) for 3 minutes before LA (1mM) was applied. **C**: the cell was exposed for 2 minute to 13-HODE (100μm) and for 1 minute to capsaicin separated by forty five minutes of wash with buffer. **D**: the cell was pre-exposed to capsazepine (10μM) for 3 minutes before 13-HODE (100μm) was applied.

Treatment	Peak response (ΔRU)	Percentage of responding cells	Total number of cells imaged
Vehicle / LA	0.7±0.03	65±7	650
Capsazepine / LA	0.08±0.01***	10±4***	494
Vehicle / 13-HODE	0.2±0.01	68±5	383
Capsazepine / 13-HODE	0.05±0.01###	7±4###	281
Vehicle / 9-HODE	0.3±0.03	55±8	204
Capsazepine / 9-HODE	0.05±0.01†††	10±4††	303

Table 1: Summary of the changes in $[Ca^{2+}]_i$, represented as differences in 340/380 ratios, compared with control values (ΔRU) in DRG cells and the percentage of cells responding following suprafusion of the different treatments. Data (means ± SEM) were analyzed using Student's *t* test (***P<0.001 vs vehicle / LA, ###P<0.001 vs vehicle / 13-HODE, ††P<0.01 vs vehicle / 9-HODE).

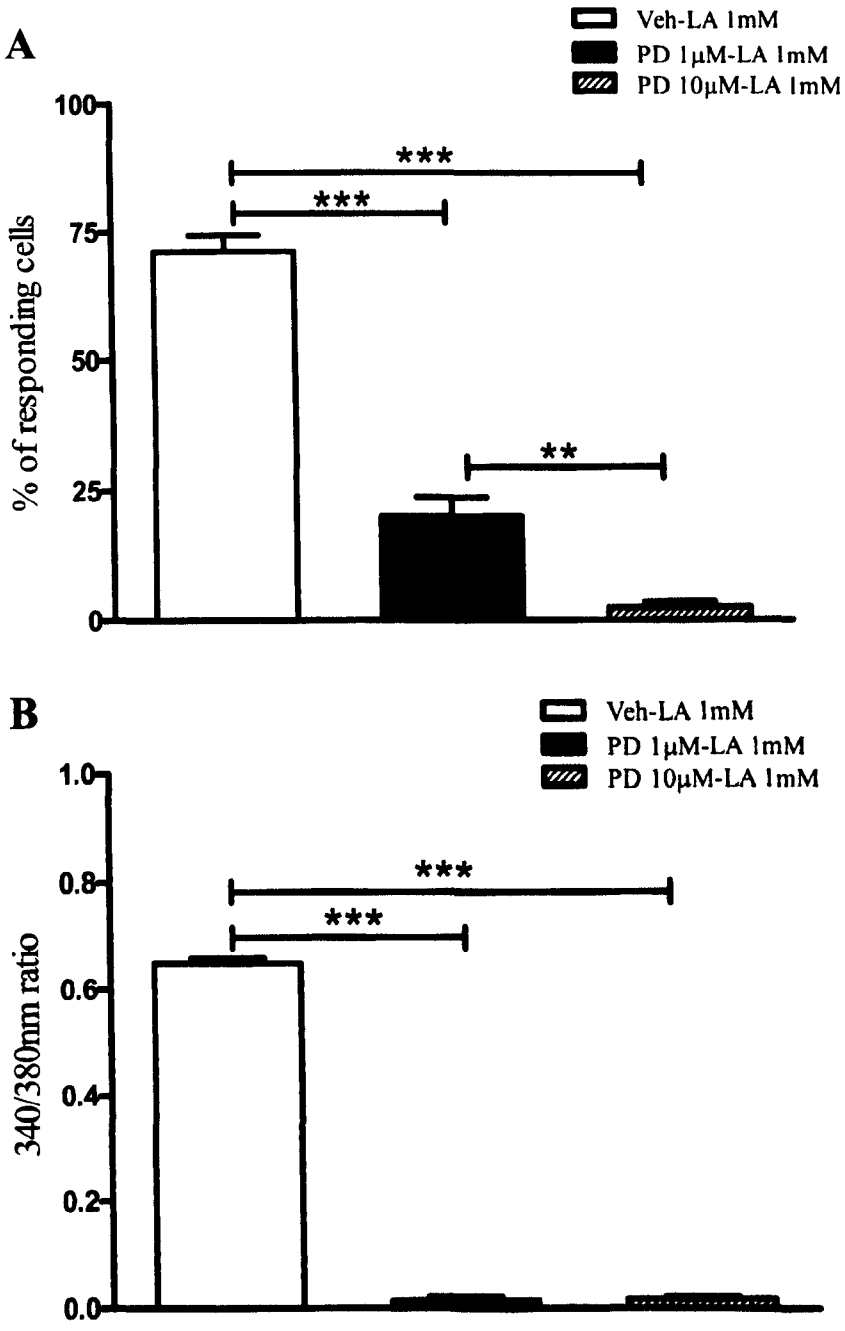

Figure 2. The 15-LOX inhibitor PD146176 significantly decreased the percentage of DRG cells responding to linoleic acid, and reduced linoleic acid-evoked peak responses (B). Statistical analysis with one way ANOVA test followed by Bonferroni *post-hoc:* **P<0.01, ***P<0.001).

Table 2.

Treatment	Paw Circumference (mm)			Paw Volume (3 measurements)								
	Baseline (Pre-Drug or Veh injection)	Second (Pre-Sal or Car injection)	Final (Pre-tissue collection	Baseline (Pre-Drug or Veh injection)-1	Second (Pre-Sal or Car injection)-1	Final (Pre-tissue collection-1	Baseline (Pre-Drug or Veh injection)-2	Second (Pre-Sal or Car injection)-2	Final (Pre-tissue collection-2	Baseline (Pre-Drug or Veh injection)-3	Second (Pre-Sal or Car injection)-3	Final (Pre-tissue collection-3
Veh-Car	26 ±0.2	29 ±0.3	33 ±0.7 ***	1.3 ±0.03	1.6 ±0.01	2.1 ±0.1 ***	1.4 ±0.04	1.6 ±0.01	2.1 ±0.11 ***	1.3 ±0.04	1.6 ±0.02	2.1±0.1 ***
PD-Car	26 ±0.2	28 ±0.3	32 ±1.4 ***	1.3 ±0.02	1.6 ±0.03	1.8 ±0.14 **	1.3 ±0.02	1.6 ±0.02	1.9 ±0.15 **	1.3 ±0.02	1.6 ±0.03	1.8 ±0.13 **
Veh-Sal	26 ±0.3	29 ±0.5	28 ±0.9	1.3 ±0.02	1.6 ±0.03	1.5 ±0.11	1.4 ±0.03	1.6 ±0.01	1.5 ±0.14	1.4±0.02	1.6 ±0.02	1.5 ±0.12
PD-Sal	27 ±0.2	29 ±0.5	28 ±0.8	1.3 ±0.04	1.6 ±0.08	1.4 ±0.04	1.3 ±0.03	1.5 ±0.08	1.4 ±0.04	1.3 ±0.02	1.6 ±0.06	1.3 ±0.04
Naïve	26 ±0.3	26 ±0.3	26 ±0.4	1.3 ±0.02	1.3 ±0.04	1.3 ±0.04	1.3 ±0.04	1.3 ±0.05	1.3 ±0.03	1.3 ±0.02	1.3 ±0.04	1.3 ±0.03

Table 2. Intraplantar injection of 2% carrageenan significantly altered hindpaw circumference and hindpaw volume in vehicle-carrageenan (Veh-Car) and PD 146176-carrageenan (PD-Car) groups in the ipsilateral hindpaw compared to control at this four hour timepoint; however, PD 146176 treatment did not significantly alter carrageenan-induced increases in hindpaw circumference or hindpaw volume in these rats (n=6). Data were analysed using a one-way Anova with Bonferoni *post hoc* test, ***P<0.001, **P<0.01. Data are expressed as mean ± SEM of ipsilateral hindpaws (n=6).

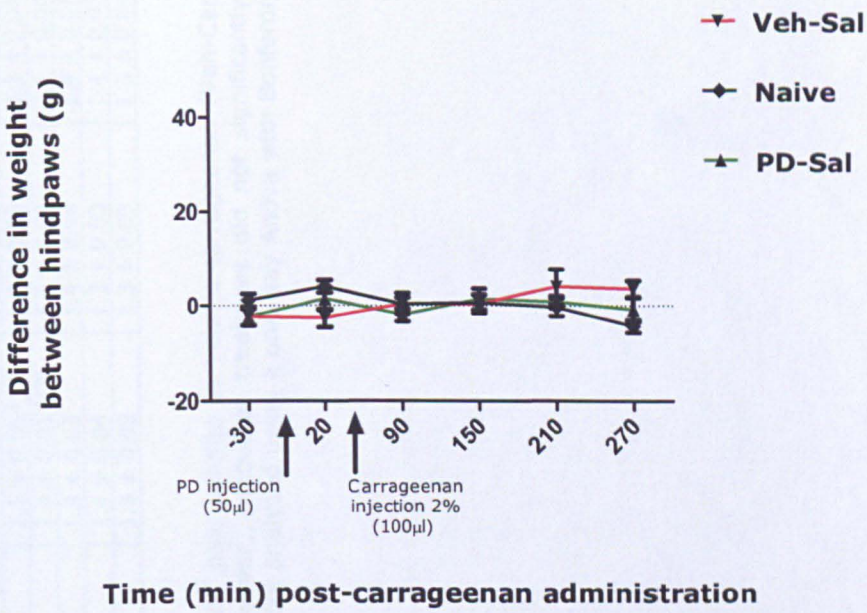

Figure 3. Rats treated with PD 146176 followed by saline (PD-Sal) did not show any changes in weight bearing, which was comparable to the naïve and vehicle-saline (Veh-Sal) treated groups (n=6).

Table 3.

Treatment	Paw Circumference (mm)		Paw Volume (3 measurements)					
	Baseline (Pre-injection)	Final (Pre-tissue collection	Baseline (Pre-injection)-1	Final (Pre-tissue collection-1	Baseline (Pre-injection)-2	Final (Pre-tissue collection-2	Baseline (Pre-injection)-3	Final (Pre-tissue collection-3
Veh-Car	26 ± 0.2	35 ± 0.4***	1.3 ± 0.03	2.1 ± 0.04***	1.4 ± 0.04	2.1 ± 0.05***	1.4 ± 0.03	2.1 ± 0.06***
AB-Car	26 ± 0.2	34 ± 1.1***	1.4 ± 0.02	2.0 ± 0.08***	1.3 ± 0.03	2.0 ± 0.05***	1.4 ± 0.03	2.1 ± 0.08***
Veh-Sal	26 ± 0.2	27 ± 0.2	1.3 ± 0.03	1.4 ± 0.04	1.3 ± 0.04	1.4 ± 0.03	1.4 ± 0.04	1.4 ± 0.05
AB-Sal	27 ± 0.4	27 ± 0.3	1.3 ± 0.03	1.4 ± 0.04	1.3 ± 0.03	1.4 ± 0.04	1.3 ± 0.03	1.4 ± 0.02
Naïve	27 ± 0.3	26 ± 0.3	1.3 ± 0.04	1.3 ± 0.04	1.4 ± 0.05	1.3 ± 0.03	1.3 ± 0.03	1.3 ± 0.04

Table 3. Intraplantar injection of 2% carrageenan significantly altered paw circumference and paw volume in vehicle-carrageenan (Veh-Car) and antibodies-carrageenan (AB-Car) groups in the ipsilateral hindpaw compared to control; however, antibodies treatment did not significantly alter carrageenan-induced increases in paw circumference or paw volume in these same rats. Data were analysed using a one-way Anova with Bonferoni *post hoc* test, ***P<0.001. Data are expressed as mean ± SEM of ipsilateral hindpaws (n=6).

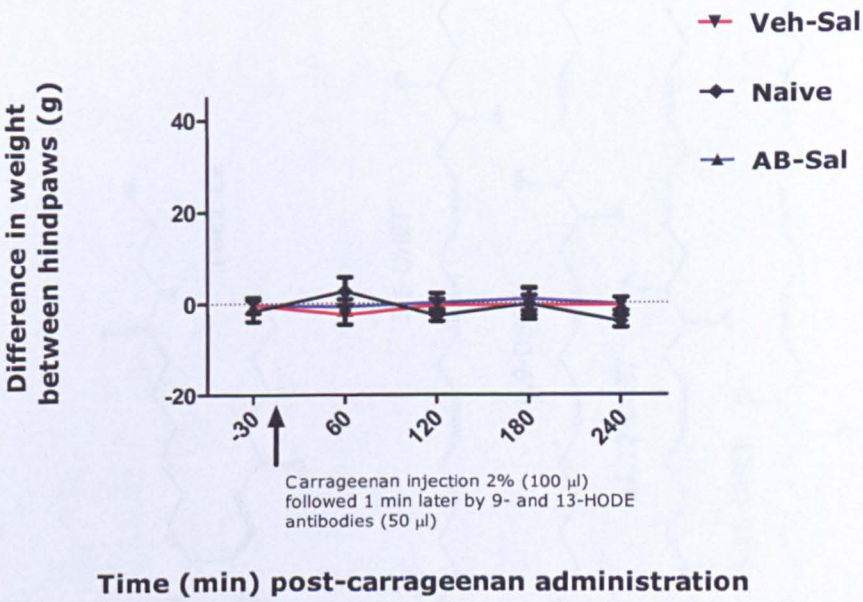

Figure 4. Rats injected with 9- and 13-HODE antibodies followed by saline (AB-Sal) did not show any changes in weight bearing, which was comparable to the naïve and vehicle-saline (Veh-Sal) treated groups (n=6).

Table 4.

	Contralateral		
	Knee Joint	DRGs (L3-L5)	Spinal Cord
PGD2/PGE2	27 ± 5	142 ± 28	24 ± 5
TXB2	7 ± 1	155 ± 36	42 ± 10
13-HODE	40 ± 6	64 ± 19	3 ± 1
9-HODE	13 ± 2	69 ± 16	2 ± 1
13-oxoODE	1 ± 0.1	ND	ND
9-oxoODE	1 ± 0.1	ND	ND
15-HETE	5 ± 1	17 ± 4	4 ± 1
11-HETE	3 ± 0.3	32 ± 8	14 ± 1
12-HETE	10 ± 2	210 ± 59	18 ± 7
8-HETE	1 ± 0.2	BLOQ	BLOQ
5-HETE	1 ± 0.1	9 ± 3	BLOQ
LA	440 ± 41	261 ± 58	142 ± 53
AA	43 ± 3	271 ± 66	134 ± 38
AEA	2 ±0.1	13 ± 3	8 ± 1
2-AG	0.7 ± 0.03	2 ± 1	23 ± 4
PEA	6 ± 1	307 ± 140	147 ± 50
OEA	4 ± 0.3	89 ± 28	144 ± 18

Table 4. Levels of lipids measured per g wet weight tissue in the contralateral knee joint, DRGs and spinal cord (n=8). Values are expressed as mean ± SEM in pmol/g for all tissues except AA, which is expressed in nmol/g. BLOQ = below limit of quantification.

Chemical Structures 1

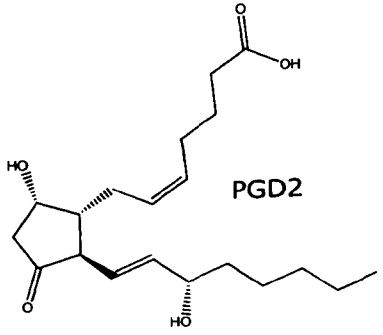

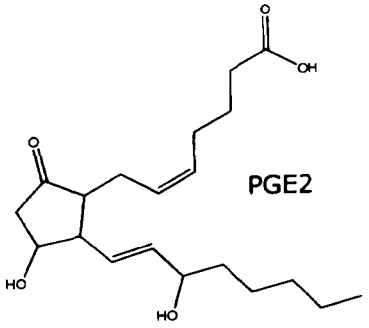

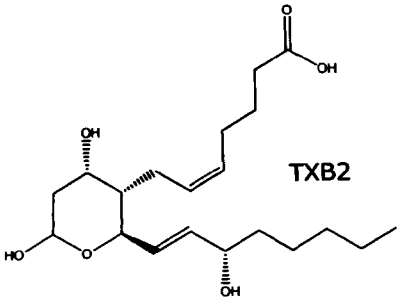

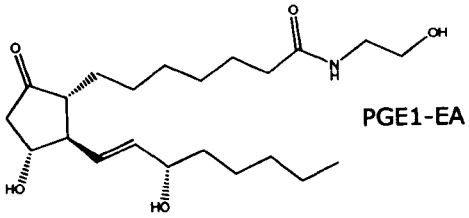

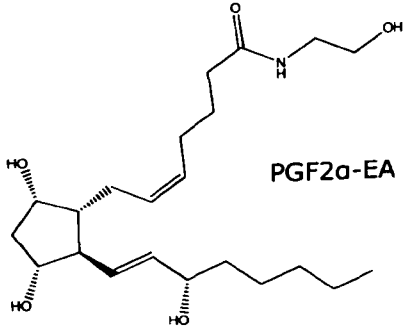

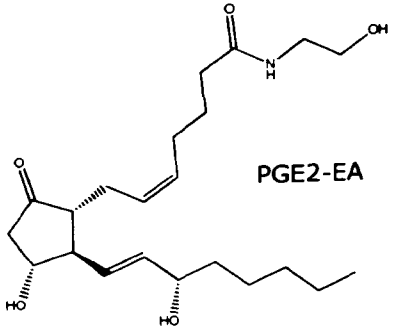

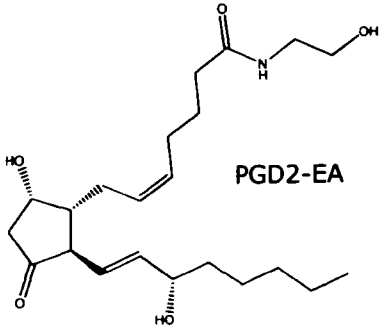

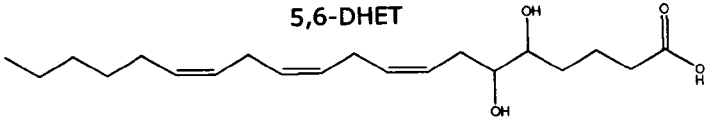

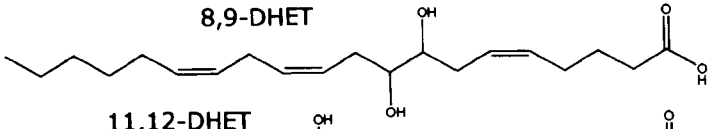

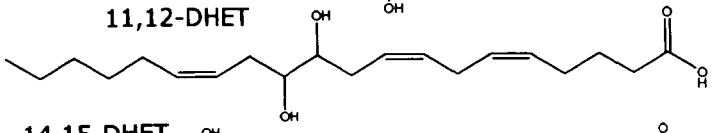

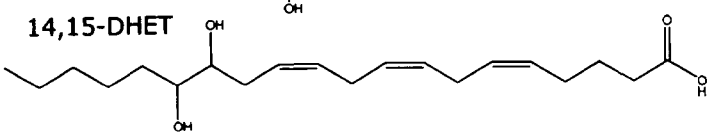

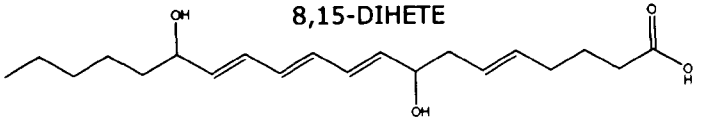

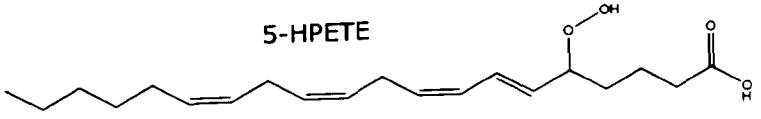

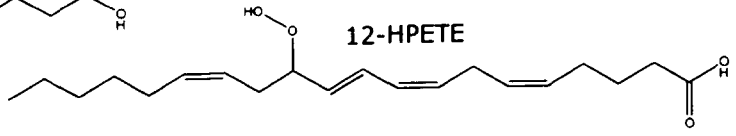

Chemical Structures 2

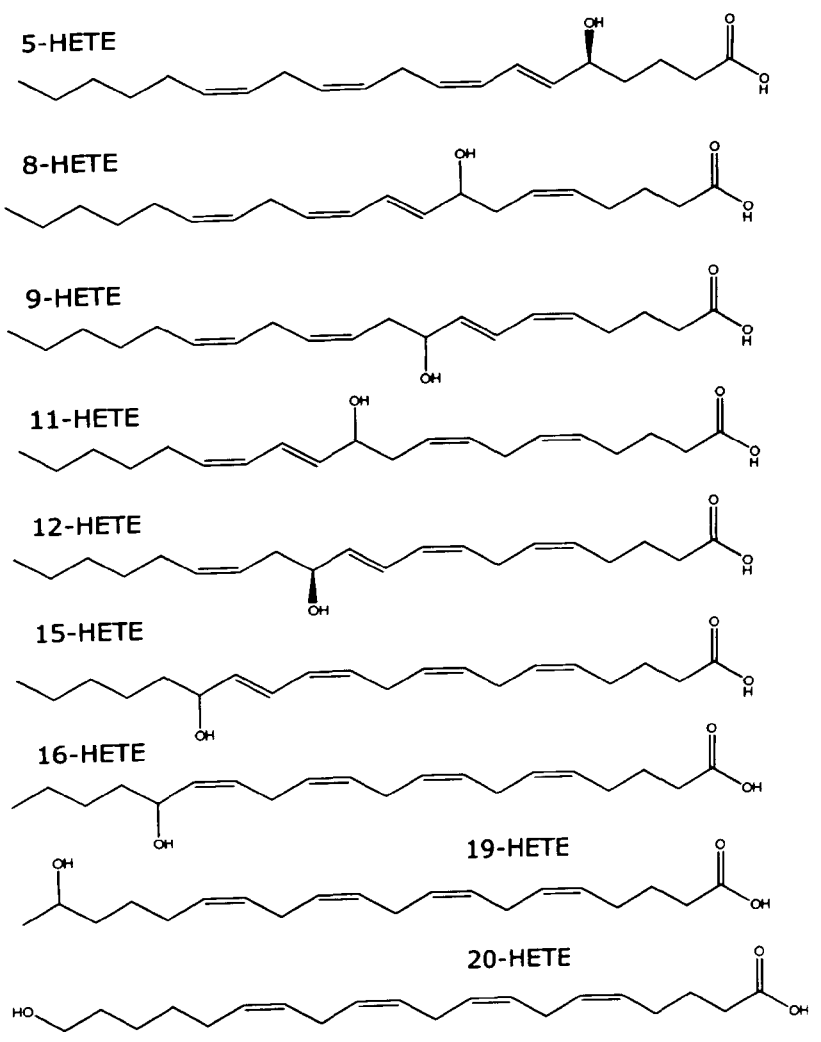

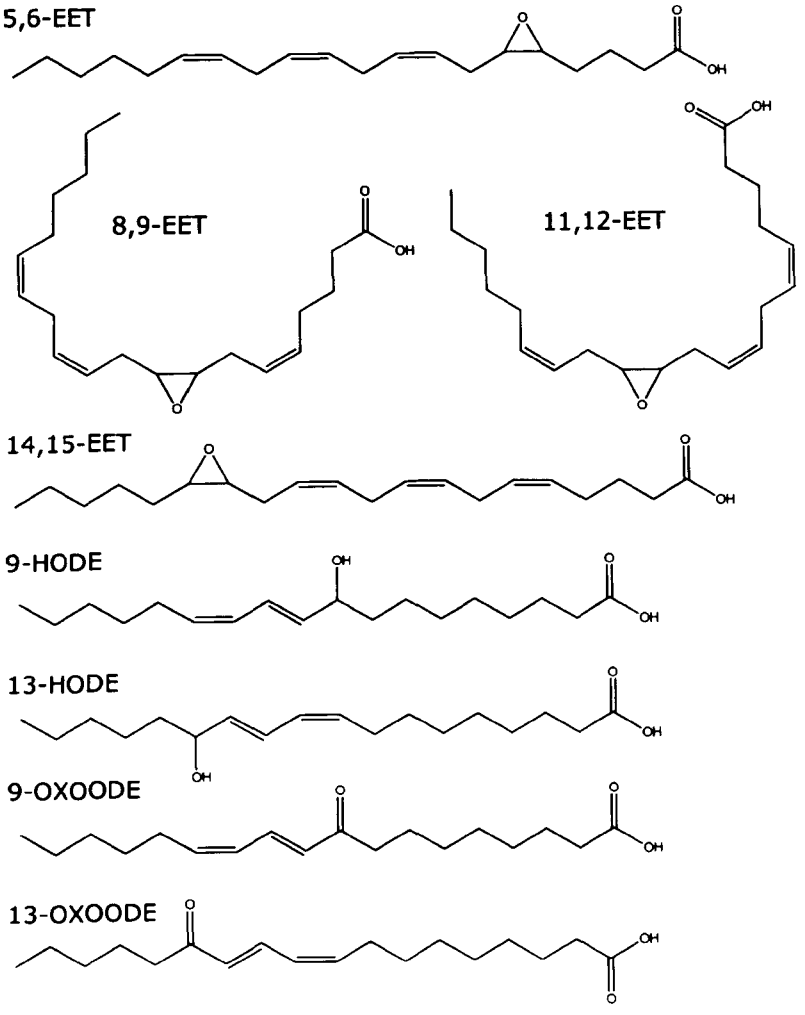

Chemical Structures 3